



**Molecular transitions regulating ryanodine receptor channel  
gating; potential target for therapeutic intervention in heart failure  
and arrhythmia**

**Julia Griffiths**

**Submitted in accordance with the requirements for the degree of Doctor of  
Philosophy.**

**School of Medicine**

**September 2011**





**Molecular transitions regulating ryanodine receptor channel  
gating; potential target for therapeutic intervention in heart failure  
and arrhythmia**

**Julia Griffiths**

**Submitted in accordance with the requirements for the degree of Doctor of  
Philosophy.**

**School of Medicine**

**September 2011**

UMI Number: U517372

All rights reserved

INFORMATION TO ALL USERS

The quality of this reproduction is dependent upon the quality of the copy submitted.

In the unlikely event that the author did not send a complete manuscript and there are missing pages, these will be noted. Also, if material had to be removed, a note will indicate the deletion.



UMI U517372

Published by ProQuest LLC 2013. Copyright in the Dissertation held by the Author.  
Microform Edition © ProQuest LLC.

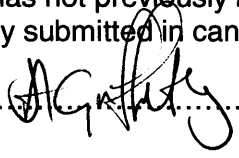
All rights reserved. This work is protected against  
unauthorized copying under Title 17, United States Code.



ProQuest LLC  
789 East Eisenhower Parkway  
P.O. Box 1346  
Ann Arbor, MI 48106-1346

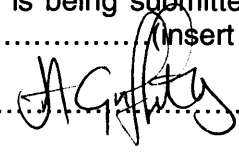
**DECLARATION**

This work has not previously been accepted in substance for any degree and is not concurrently submitted in candidature for any degree.

Signed .....  ..... (candidate)      Date ..... 25/11/11 .....

**STATEMENT 1**

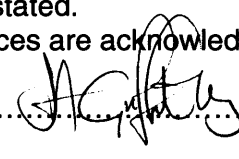
This thesis is being submitted in partial fulfillment of the requirements for the degree of ..... (insert MCh, MD, MPhil, PhD etc, as appropriate)

Signed .....  ..... (candidate)      Date ..... 25/11/11 .....

**STATEMENT 2**

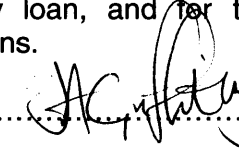
This thesis is the result of my own independent work/investigation, except where otherwise stated.

Other sources are acknowledged by explicit references.

Signed .....  ..... (candidate)      Date ..... 25/11/11 .....

**STATEMENT 3**

I hereby give consent for my thesis, if accepted, to be available for photocopying and for inter-library loan, and for the title and summary to be made available to outside organisations.

Signed .....  ..... (candidate)      Date ..... 25/11/11 .....

**STATEMENT 4: PREVIOUSLY APPROVED BAR ON ACCESS**

I hereby give consent for my thesis, if accepted, to be available for photocopying and for inter-library loans **after expiry of a bar on access previously approved by the Graduate Development Committee.**

Signed ..... (candidate)      Date .....

---

## **SUMMARY**

Aberrant calcium handling in cardiomyocytes, linked to ryanodine receptor (RyR) dysfunction, causes cardiac arrhythmias underlying catecholaminergic polymorphic ventricular tachycardia (CPVT) and heart failure. CPVT links to point mutations in specific domains of the cardiac ryanodine receptor (RyR2). Similar mutational clusters in RyR1 (skeletal muscle) cause malignant hyperthermia and central core disease suggesting common mechanisms of dysfunction underlying cardiac and skeletal muscle pathologies, leading to the domain interaction hypothesis. Peptides complimentary to N-terminus and central domain mutational clusters activate RyR by disrupting interaction. RyR1/2 is regulated by calcium, ATP, magnesium, phosphorylation and the accessory protein FKBP12/12.6. Previous work, on RyR1/2 modulation, assessing phosphorylation in relation to FKBP12/12.6 stabilisation of channel activity, indicates convergent regulation involving control of domain interaction sites by phosphorylation, FKBP12/12.6 and other modulators. This study used a central domain peptide (DP4) and its mutant form (DP4M) to investigate the relationship between FKBP12, phosphorylation, and other modulators to identify this region of convergent regulation. Native RyR1 channels, stripped of endogenous FKBP12 and phosphorylated or dephosphorylated, were shown, by [<sup>3</sup>H]ryanodine binding, to be fully functional and to be activated by calcium and ATP. FKBP12 and magnesium were each shown to inhibit channel activity, and phosphorylation reversed magnesium inhibition. DP4, peptide, synthesised from two sources, activated RyR1 2-fold in the presence of  $\mu\text{M}$  calcium, less than the activity observed with ATP. Magnesium and FKBP12 inhibited RyR1 activation by DP4. In contrast to previous studies, DP4M was not an inactive control peptide. To investigate this discrepancy, recombinant GST-tagged (R-)DP4M and (R-)DP4 were generated and neither showed an activatory effect. However, once cleaved of GST, the R-DP4 was as potent as synthetic DP4 at 10  $\mu\text{M}$ . Experiments with RyR2 demonstrated similar results for calcium and ATP activation with inhibition by FKBP12.6. The RyR2 central domain peptide (DPc10) has been cloned and the protein produced.

---

## CONTENTS

<b>SUMMARY</b> .....	<b>i</b>
<b>CONTENTS</b> .....	<b>ii</b>
<b>List of Figures</b> .....	<b>vi</b>
<b>List of Tables</b> .....	<b>ix</b>
<b>Abbreviations</b> .....	<b>x</b>
<b>CHAPTER 1; General Introduction</b> .....	<b>2</b>
1.1 What is the ryanodine receptor? .....	3
1.2 Excitation- contraction coupling in muscle.....	4
1.3 Compartmentalisation .....	5
1.4 RyR macromolecular complex .....	7
1.5 Calcium induced calcium release.....	8
1.6 Calcium homeostasis.....	9
1.7 Regulation of ECC by adrenergic drive (Flight or fight response) .....	10
1.8 Calcium/calmodulin-dependent protein kinase II (CaMKII).....	12
1.9 Ryanodine receptor dysfunction in skeletal muscle and cardiac diseases.....	13
1.9.1 Calcium and arrhythmias in Heart Failure.....	14
1.9.2 Catecholaminergic polymorphic ventricular tachycardia .....	16
1.9.3 Drug therapy for CPVT .....	17
1.9.4 Malignant Hyperthermia .....	19
1.10 Molecular Mechanisms of RyR2 dysfunction.....	20
1.10.1 Phosphorylation.....	20
1.10.2 Redox effects .....	22
1.10.3 Cytosolic and luminal calcium sensitivity .....	23
1.10.4 Channel inter-domain interaction .....	24
1.11 Modulation of the RyR .....	26
1.11.1 Calcium, ATP and Magnesium .....	26
1.11.2 Accessory protein modulation.....	28
1.12 RyR structure and function.....	30
1.13 Previous work and the context of this project .....	32
1.14 Aims and hypothesis of this study .....	35
<b>CHAPTER 2; General Materials and Methods</b> .....	<b>37</b>
2.1 Molecular Biology .....	37
2.1.1 Analysis of DNA products.....	37
2.1.2 Cloning of DNA.....	38

---

2.1.3 Quikchange® XL Site-Directed Mutagenesis.....	50
2.2.1 Protein analysis by SDS-Polyacrylamide gel electrophoresis (PAGE) .....	52
2.2.2 GST-tagged recombinant protein production .....	57
2.2.3 Affinity Purification of GST-tagged proteins .....	60
2.2.4 Gel Filtration.....	62
2.2.5 Protein purification using Vivapure Ion Exchange Spin Columns (Sartorius). ..	63
2.2.6 Protein quantification using Bicinchoninic Acid (BCA) (Micro BCA Protein Assay Kit, Pierce) .....	63
2.3 [ <sup>3</sup> H]Ryanodine binding.....	63
2.3.1 Free Calcium Buffers.....	64
2.3.2 [ <sup>3</sup> H]Ryanodine binding protocol .....	65
2.4 Health and Safety .....	66
2.5 Statistical analysis .....	66
<b>CHAPTER 3; Preparation of functional RyR channels from native tissue.....</b>	<b>68</b>
3.1 Introduction.....	68
3.2 Methods and Materials.....	69
3.2.1 RyR extraction and purification from native tissue .....	69
3.2.2 RyR purification by ion exchange chromatography.....	72
3.2.3 SDS-PAGE analysis of purified RyR protein.....	73
3.2.4 Phosphorylation and de-phosphorylation of RyR protein .....	73
3.3 Results.....	75
3.3.1 RyR1 solubilisation and purification by anion exchange .....	75
3.3.2 RyR2 solubilisation and purification by anion exchange .....	78
3.4 Discussion .....	82
<b>CHAPTER 4; Physiological modulators of RyR1 activity.....</b>	<b>85</b>
4.1 Introduction.....	85
4.2 Results.....	91
4.2.1 RyR1 dose response to free calcium .....	91
4.2.2 RyR1 and dose response to ATP addition .....	92
4.2.3 FKBP12 protein production and purification.....	94
4.2.3 Effect of physiological inhibitors on activators of RyR1 .....	97
4.3 Discussion .....	102
<b>CHAPTER 5; Production and purification of activatory domain peptides of RyR1 .....</b>	<b>106</b>
5.1 Introduction.....	106
5.3 Results.....	109
5.3.1 PCR cloning of DP4 into pGEX-6P1.....	109



5.3.2 Insertion of the R2458C point mutation.....	113
5.3.3 Optimisation of Recombinant Protein Expression .....	115
5.3.4 Purification of GST-DP4WT and GST-DP4M.....	118
5.3.5 Purification of peptides R-DP4WT and R-DP4M.....	119
5.4 Discussion .....	124
5.4.1 Purification of recombinant peptide.....	125
<b>CHAPTER 6; Peptide and pharmacological regulation of RyR1 .....</b>	<b>128</b>
6.1 Introduction.....	128
6.2 Results.....	132
6.2.1 Effect of synthetic DP4WT and DP4M peptides on RyR1 [ <sup>3</sup> H]ryanodine binding .....	132
6.2.2 Effect of inhibitors of RyR1 activity on DP4WT activation of the channel .....	134
6.2.3 Effect of the original Ikemoto DP4WT peptide .....	136
6.2.4 Effect of recombinant peptides in comparison to the original Ikemoto peptide.....	138
6.2.5 Peptide interaction with FKBP12 protein.....	139
6.2.6 Pharmacological modulation of RyR1 .....	140
6.3 Discussion .....	141
<b>CHAPTER 7; Modulation of RyR2 .....</b>	<b>149</b>
7.1 Introduction.....	149
7.2 Results.....	152
7.2.1 Physiological modulators of RyR2 .....	152
7.2.2 Cloning, production and purification of FKBP12.6.....	155
7.2.3 FKBP12.6 effect on RyR2 [ <sup>3</sup> H]ryanodine binding .....	162
7.2.4 Cloning of DPc10 into pGEX-6P-1 and optimisation of protein expression. ....	162
7.3 Discussion .....	168
<b>CHAPTER 8; Discussion .....</b>	<b>171</b>
8.1 The domain interaction hypothesis.....	171
8.2 Mode of action of DP4/ DPc10.....	173
8.3 Purified RyR preparations.....	175
8.4 RyR1 as a surrogate for RyR2 .....	178
8.5 Do the findings using DP4 peptide support our hypothesis of convergent regulation? .....	180
8.6 Further work.....	182
8.7 Conclusion.....	183
<b>REFERENCES.....</b>	<b>185</b>
<b>PUBLICATIONS .....</b>	<b>211</b>

---

<b>APPENDIX .....</b>	<b>213</b>
<b>Acknowledgements.....</b>	<b>223</b>

---

## List of Figures

<b>CHAPTER 1; General Introduction .....</b>	<b>2</b>
Figure 1.1 Electron micrograph showing a central t-tubule in a triad junction section.....	3
Figure 1.2 Structure of a skeletal myocyte.....	6
Figure 1.3 Structural representation of a section through a myocyte.....	7
Figure 1.4 RyR2 as a scaffolding protein .....	8
Figure 1.5 Calcium transport in ventricular myocytes.....	9
Figure 1.6 $\beta$ -adrenergic receptor activation.....	11
Figure 1.7 The proposed mode of action of PKA in stress-induced arrhythmia in patients with CPVT and HF mutations.....	16
Figure 1.8 Mutational clusters on N-, C- and central domains of RyR1 and RyR2.....	20
Figure 1.9 Inter-domain interaction hypothesis. ....	26
Figure 1.10 Primary sequence and 3D structure of RyR1 with potential ligand binding sites.....	31
Figure 1.11 Structural representation of the similar structures of A) RyR1 and B) RyR2. ....	32
Figure 1.12 Convergent regulation hypothesis.....	34
<b>CHAPTER 2; General Materials and Methods .....</b>	<b>37</b>
Figure 2.1 Representation of primer design .....	39
Figure 2.2 The multiple cloning site of pGEX-6P-1 vector .....	44
Figure 2.3 Quikchange® mutagenesis.....	51
Figure 2.4 The ECL detection process.....	56
Figure 2.5 pGEX-6P-1 plasmid map .....	58
Figure 2.6 3C cleavage of recombinant protein for removal of the glutathione sepharose tag. ....	62
<b>CHAPTER 3; Preparation of functional RyR channels from native tissue .....</b>	<b>68</b>
Figure 3.1 Flow chart describing the protocol for preparation of SR membrane preparations from skeletal or cardiac muscle.....	71
Figure 3.2 Flow diagram showing the steps involved in solubilisation of SR microsomes to extract functional RyR protein.....	72
Figure 3.3 Solubilisation of RyR1 SR microsomes using Triton and CHAPS detergents. ....	76
Figure 3.4 RyR1 purification by anion exchange chromatography .....	77
Figure 3.5 RyR2 purification by anion exchange chromatography .....	79
Figure 3.6 RyR1 phosphorylation time course western blot .....	81
<b>CHAPTER 4; Physiological modulators of RyR1 activity.....</b>	<b>85</b>

---

Figure 4.1 RyR1 biphasic response to free calcium (pCa), demonstrated by [ <sup>3</sup> H] ryanodine binding .....	91
Figure 4.2 Effect of ATP on RyR1 [ <sup>3</sup> H] ryanodine binding. ....	93
Figure 4.3 FKBP12 cleavage with 3C protease and purification by gel filtration chromatography.....	95
Figure 4.4 FKBP12 further affinity purification, confirmation by western blot and quantification. ....	96
Figure 4.5 Effect of FKBP12 on RyR1 [ <sup>3</sup> H]Ryanodine binding.....	97
Figure 4.6 Effect of FKBP12 inhibition on ATP activation of RyR1 [ <sup>3</sup> H] ryanodine binding .....	98
Figure 4.7 Effect of KCl concentration on magnesium inhibition of RyR1 [ <sup>3</sup> H]ryanodine binding.....	100
Figure 4.8 Effect of magnesium inhibition on RyR1 [ <sup>3</sup> H]Ryanodine binding in the presence of PKA phosphorylation and FKBP12. ....	101
<b>CHAPTER 5; Production and purification of activatory domain peptides of RyR1 .....</b>	<b>106</b>
Figure 5.1 Structural model of DP4 achieved using NMR. ....	108
Figure 5.2 DP4 and DP4M forward and reverse primer design .....	110
Figure 5.3 Cloning of DP4 into pGEX-6P-1 .....	111
Figure 5.4 Sequencing of DP4-pGEX-6P-1.....	112
Figure 5.5 DP4-pGEX-6P-1 Quick change mutagenesis to insert the R2458C mutation. ....	114
Figure 5.6 Sequencing of DP4M-pGEX-6P-1 .....	115
Figure 5.7 Induction of GST-DP4WT/DP4M protein.....	116
Figure 5.8 Induction of GST-DP4WT/DP4M protein.....	117
Figure 5.9 UV quantification estimate of concentrated protein. ....	119
Figure 5.10 R-DP4WT and R-DP4M proteomic analysis using ExPASy Protparam software.....	121
Figure 5.11 Cleavage of GST-DP4WT and GST-DP4M.....	122
Figure 5.12 R-DP4WT purification using ion exchange.....	123
Figure 5.13 R-DP4WT purification analysis.....	124
<b>CHAPTER 6; Peptide and pharmacological regulation of RyR1 .....</b>	<b>128</b>
Figure 6.1 Structures of A) Diltiazem and B) K201 .....	132
Figure 6.2 Effect of synthetic DP4WT peptide on RyR1 [ <sup>3</sup> H]ryanodine binding .....	133
Figure 6.3 Effect of synthetic DP4WT activation on RyR1 [ <sup>3</sup> H]ryanodine binding in the presence of Mg <sup>2+</sup> .....	134
Figure 6.4 Effect of synthetic DP4WT activation on RyR1 [ <sup>3</sup> H]ryanodine binding in the presence of FKBP12.....	135
Figure 6.5 Effect of IK-DP4WT peptide on RyR1 [ <sup>3</sup> H]ryanodine binding.....	136

---

Figure 6.6 Effect of IK-DP4WT peptide activation on RyR1 [ <sup>3</sup> H]ryanodine binding in the presence of magnesium and FKBP12.....	137
Figure 6.7 Effect of recombinant GST-DP4WT/M on RyR1 [ <sup>3</sup> H]ryanodine binding. ....	138
Figure 6.8 Effect of the recombinant DP4WT peptide on RyR1 [ <sup>3</sup> H]ryanodine binding compared with IK-DP4WT peptide.....	139
Figure 6.9 GST-DP4WT pull down assay for FKBP12 .....	140
Figure 6.10 Effect of Diltiazem on RyR1 [ <sup>3</sup> H]ryanodine binding.....	141
<b>CHAPTER 7; Modulation of RyR2.....</b>	<b>149</b>
Figure 7.1 RyR2 biphasic response to varying free calcium (pCa).....	153
Figure 7.2 Effect of ATP on RyR2 [ <sup>3</sup> H]ryanodine binding. ....	154
Figure 7.3 FKBP12.6 forward and reverse primer design.....	156
Figure 7.4 Cloning of FKBP12.6 by PCR and preparation for ligation into pGEX-6P-1 vector.....	157
Figure 7.5 Screening for positive FKBP12.6-pGEX-6P-1 transformed TOP10 colonies .....	158
Figure 7.6 Sequencing of FKBP12.6-pGEX-6P-1.....	159
Figure 7.7 FKBP12.6 expression, GST affinity purification and cleavage of the GST tag .....	160
Figure 7.8 Quantification of purified cleaved FKBP12.6 and FKBP12.6-GST and western blotting .....	161
Figure 7.9 Effect of FKBP12.6 on RyR2 [ <sup>3</sup> H]ryanodine binding. ....	162
Figure 7.10 DPc10 forward and reverse primer design .....	165
Figure 7.11 DPc10 cloning into pGEX-6P-1 .....	166
Figure 7.12 Sequencing of DPc10-pGEX-6P-1.....	167
Figure 7.13 DPc10-GST expression optimisation.....	168

---

**List of Tables**

<b>CHAPTER 2; General Materials and Methods .....</b>	<b>37</b>
Table 2.1 Standard PCR reaction mix.....	40
Table 2.2 Extended PCR cycle .....	41
Table 2.3 Standard Restriction digest recipe.....	43
Table 2.4 Standard Ligation recipe .....	45
Table 2.5 Colony screen PCR reaction recipe .....	46
Table 2.6 PCR cycle used .....	47
Table 2.7 BIG DYE sequencing PCR reaction recipe.....	49
Table 2.8 Standard sequencing PCR cycle.....	50
Table 2.9 PCR reaction mix for site-directed mutagenesis.....	52
Table 2.10 PCR cycle for site-directed mutagenesis .....	52
Table 2.11 Acrylamide gel composition.....	54
Table 2.12; Free Calcium Buffers .....	65
Table 2.13 Standard <sup>3</sup> [H]Ryanodine binding assay mix.....	66
<b>CHAPTER 3; Preparation of functional RyR channels from native tissue .....</b>	<b>68</b>
Table 3.1 Standard assay mix for phosphorylation and de-phosphorylation using 200 μl purified RyR preparation .....	74

---

### **Abbreviations**

A <sub>260</sub>	absorbance at 260 nm
A <sub>280</sub>	absorbance at 280 nm
Ab	antibody
AEBSF	4-(2-Aminoethyl) benzenesulfonyl fluoride hydrochloride
ATP	adenosine-5'-triphosphate
β-AR	Beta-adrenergic receptor
ARVD	arrhythmogenic right ventricular dysplasia
bp	base pair
BCA	bicinchoninic acid
BSA	bovine serum albumin
CaM	calmodulin
CaMKII	calcium/calmodulin dependent kinase II
cAMP	cyclic adenosine monophosphate
CCD	central core disease
cDNA	complementary DNA
CHAPS	3-[(3-cholamidopropyl)dimethylammonio]-2-hydroxy-1-propanesulfonate
CICR	calcium induced calcium release
CPVT	catecholaminergic polymorphic ventricular tachycardia
CSQ	calsequestrin
CV	Carvedilol
DAD	delayed after depolarisation
dATP	deoxyadenosine 5'-triphosphate
dCTP	deoxycytosine 5'-triphosphate
dH <sub>2</sub> O	deionised water
dGTP	deoxyguanine 5'-triphosphate
DMSO	dimethylsulphoxide
DNA	deoxyribonucleic acid

---

dNTP	deonucleotide triphosphates
DP4	domain peptide 4
DPc10	central domain peptide 10
DTT	1,4-dithiothreitol
dTTP	deoxythymine triphosphate
ECC	excitation- contraction coupling
<i>E.coli</i>	<i>Escherischia coli</i>
EDTA	ethylenediaminetetraacetic acid
EGTA	ethylene glycol-bis-( $\beta$ -amino ether) N,N,N',N'-tetraacetic acid
EtOH	ethanol
FKBP12/12.6	FK506 binding protein 12/12.6
FPLC	fast protein liquid chromatography
FRET	Fluorescence resonance energy transfer
GST	glutathione sepharose transferase
HCl	hydrochloric acid
HF	heart failure
ICD	implantable cardioverter defibrillation
IPTG	isopropyl $\beta$ -D-1-thiogalactopyranoside
Kb	kilobase
KCl	potassium chloride
kDa	kilodaltons
KO	knockout mutant
LB	Luria-Bertani media
LCC	L-type calcium channel
M	mutant
MCS	multiple cloning site
MH	malignant hyperthermia
NaOH	sodium hydroxide
NCX	sodium-calcium exchanger



---

OD	optical density
PBS	phosphate buffered saline
pCa	inverse log of free calcium
PCR	polymerase chain reaction
pI	isoelectric point
PIPES	piperazine-N,N'-bis(2-ethanesulfonic acid)
PKA	protein kinase A
PLB	phospholamban
PP1	protein phosphatase 1
PVDF	polyvinylidene fluoride
RNA	ribonucleic acid
ROS	reactive oxygen species
rpm	revolutions per minute
RyR	ryanodine receptor
hRyR	human ryanodine receptor
rRyR	rabbit ryanodine receptor
SCD	sudden cardiac death
SDS	sodium dodecyl sulfate
SDS-PAGE	sodium dodecyl sulfate polyacrylamide gel electrophoresis
SERCA	sarco/endoplasmic reticulum Ca <sup>2+</sup> -ATPase
SOICR	store overload induced calcium release
SPR	surface plasmon resonance
SR	sarcoplasmic reticulum
<i>Taq</i>	<i>Thermus aquaticus</i>
TBS	tris buffered saline
TEA	tetraethylammonium
UV	Ultraviolet
WT	wildtype

## **Chapter 1; Introduction**

**CHAPTER 1: General Introduction**

Aberrant calcium handling in skeletal myocytes, manifesting as the condition malignant hyperthermia (MH), results in patients responding to volatile anaesthetics with skeletal muscle rigidity, tachycardia, and rising blood pressure which may eventually lead to death if not treated quickly (MacLennan and Phillips 1992). A number of mutations have identified the ryanodine receptor type 1 gene (*RyR1*) as the causal gene for this condition and also central core disease (CCD), which is a congenital myopathy (MacLennan, Duff et al. 1990; McCarthy, Healy et al. 1990; Zhang, Chen et al. 1993). CCD symptoms involve hypotonia (decreased muscle tone) and muscle weakness that is present in infancy and leads to a delay in achieving motor milestones. Patients with CCD are at high risk of suffering MH during anaesthesia (Zhang, Chen et al. 1993). *RyR1* mutations in MH/CCD have been found to result in abnormal calcium channel gating that alters the channels ability to inactivate and hence induces potentially fatal arrhythmia (Denborough 1998).

In 2001, the first report of a disease linked mutation in *RyR2* was published (Priori, Napolitano et al. 2001). Many more have been discovered since, in analogous regions to those in *RyR1* found to cause MH/CCD (Marks, Priori et al. 2002). In *RyR2* these mutations manifest as arrhythmogenic right ventricular dysplasia (ARVD) or catecholaminergic polymorphic ventricular tachycardia (CPVT) (Priori, Napolitano et al. 2001). CPVT patients exhibit no abnormal phenotype at rest, however, may suffer lethal arrhythmia triggered by physical or emotional stress (Priori, Napolitano et al. 2002).

The pathological role of CPVT-linked *RyR2* mutations has been evaluated and shown to result in similar channel hyperactivity to that seen in MH. The nature of the arrhythmias common to CPVT and MH are also a common feature of heart failure (HF) (Yano, Yamamoto et al. 2005) and thus modulation of *RyR1/2* functionality has been the subject of extensive medical research since the discovery that this calcium channel is a crucial factor in cardiac disease and sudden cardiac death (SCD) (Phrommintikul and Chattipakorn 2006).

### **1.1 What is the ryanodine receptor?**

The RyR was first discovered in 1985 by Fleischer et al. when the plant alkaloid ryanodine, used commonly as an insecticide as it lead to irreversible muscle contractures, was suspected of influencing the calcium handling of contractile cells (Fleischer, Ogunbunmi et al. 1985). At the time of discovery little was known about the mechanism involved in calcium release from the cellular calcium store, the sarcoplasmic reticulum (SR) in the process of muscle contraction. Ryanodine at nM concentrations was found to block the ability of ruthenium red to inhibit calcium release and was able to stabilise and maintain calcium release from the SR, using purified fractions of SR from rabbit skeletal muscle (twitch muscle). These were analysed and radiolabelled [ $^3\text{H}$ ]ryanodine used to isolate the binding region to the terminal cisternae of the SR. Further work by this group lead to the identification of the 'ryanodine receptor' as a calcium release channel and designated the 'foot structure', which could be seen in electron microscopy sections of skeletal muscle, located across the triad junction, as the protein through which the calcium signal passed (Figure 1.1). The foot structure was noted to respond directly to the signal from transverse tubules and to cause the release of calcium from the junctional face membrane of the SR (Inui, Saito et al. 1987).

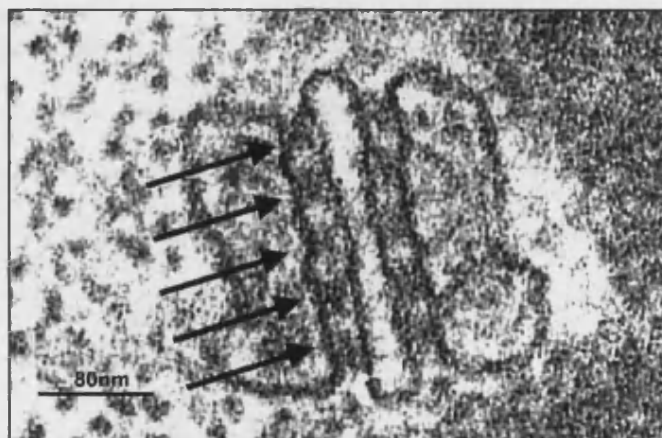


**Figure 1.1** Electron micrograph showing a central t-tubule in a triad junction section. The tubule is flanked on either side by a terminal cisternae element of the SR. Arrows indicate the electron dense junctional feet spanning the junctional gap (Franzini.C 1970).

The RyR was first purified from the SR by Makoto Inui using a CHAPS detergent supplemented with phospholipid to solubilise the membrane and was visualized using electron microscopy (Inui, Saito et al. 1987). The size of the RyR polypeptide was estimated by northern blot analysis to be about 550 kilodaltons (kDa) (Marks, Tempst et al. 1989), but the mass of the receptor was found to be  $2.3 \pm 0.3$  megadaltons using scanning electron microscopy of unstained receptors, making it the largest channel known (Fleischer 2008). Once the full amino acid sequence became available for skeletal muscle RyR, the size was confirmed as 565.233 kDa (Takeshima, Nishimura et al. 1989). This difference was reconciled by the suggestion that dividing 565,000 into 2.3 million meant that the RyR existed as a homotetramer, consisting of four identical subunits. Further evidence for the existence of the RyR homotetramer was found by Lai et al in 1988 who successfully purified the receptor from native tissue using sucrose density gradient centrifugation and used zwitterionic detergent to generate RyR monomers (Lai, Erickson et al. 1988). The RyR from the heart was also purified and the mass found to be similar to that for skeletal muscle (Otsu, Willard et al. 1990).

Three different isoforms of the RyR have been cloned. These have been designated as skeletal (RyR1) (Takeshima, Nishimura et al. 1989), cardiac (RyR2) (Otsu, Willard et al. 1990; Tunwell, Wickenden et al. 1996) and brain (RyR3) (Jeyakumar, Copello et al. 1998), although combinations of different isoforms do exist in specific tissue, these are the tissues from which the isotypes were originally cloned. The amino acid sequences of all three isoforms share a high degree of sequence homology (66-70%). Major variations occur in three regions known as divergent regions 1, 2 and 3. ~90% of the RyR polypeptide chain forms the cytoplasmic domain that modulates channel function. The remaining 10% of the channel sequence (C-terminal region) forms the transmembrane and pore regions (Sorrentino and Volpe 1993).

## **1.2 Excitation- contraction coupling in muscle**

Excitation-contraction coupling (ECC) is the process by which an electrical excitation of a contractile cell (myocyte) results in a physical movement of the muscle tissue (Bers 2002). This is a particularly important cycle when considering cardiac muscle, which results in the rhythmical contraction of the heart to propel blood around the body. Calcium is an essential messenger in

ECC as it is the direct activator of the myofillaments, actin and myosin, which cause the cellular contraction (Bers 2004)

### **1.3 Compartmentalisation**

Skeletal and cardiac myocytes have a highly organised and typical intracellular architecture. This organisation is vitally important to the process of ECC (Bers 2004). The mammalian skeletal muscle fibre (myofibre) consists of hundreds of myofibrils which extend the full length of the myofibre (possibly many centimetres long and ~100 µm diameter). Myofibrils consist of linear arrays of sarcomeres, the fundamental units of muscle contraction. Thick myosin filaments slide between thin filaments, which consist of actin and regulatory subunits such as troponin or tropomyosin, to result in the shortening of the sarcomere during muscular contraction (Fleischer 2008). In spite of the large size of the myofibre, the depolarization is rapidly transferred longitudinally along the full length of the fibre, as well as transversely along the transverse tubules, to within the muscle fibre. Transverse tubules are invaginations of the plasma membrane (sarcolemma) and are associated with the SR, forming a network system (Brette and Orchard 2003). The transverse tubules are junctionally associated with the terminal cisternae of the SR to form an intracellular junction or triad junction (Saito, Seiler et al. 1984). The 'foot' region of the RyR sits between these two membranes, with its transmembrane region passing through the SR membrane so that the luminal portion is immersed in the cellular calcium store (Franzini-Armstrong, Protasi et al. 1999). Skeletal muscle contraction does not require external calcium for activation (depolarisation induced calcium release), however the cardiac muscle of the heart is dependent on calcium influx via the voltage gated L-type calcium channel (LCC) in the sarcolemma to trigger further calcium release from the SR (calcium induced calcium release- CICR) via RyR2, a term first proposed by Fabiato et al in 1979 (Fabiato and Fabiato 1979). Skeletal muscle RyR(1) is mechanically linked to the LCC, via allosteric interaction, meaning that activation of the LCC opens the RyR directly (Cheng, Altafaj et al. 2005).

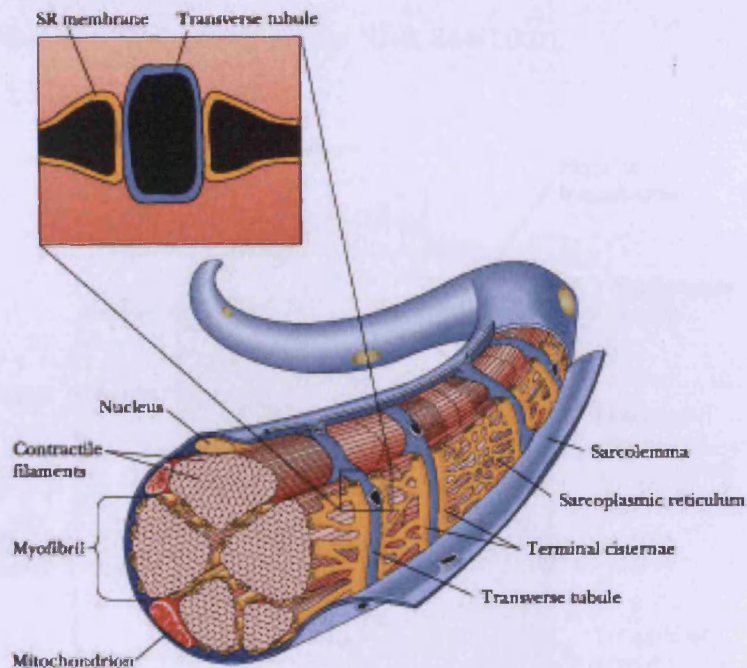


**Figure 1.2 Structure of a skeletal myocyte.** T-tubules enable the sarcolemma to connect to the ends of each myofibril. Inset: Structure of the 'foot' region (Garrett and Grisham 1998).

Cardiac myocytes are smaller in size than skeletal myocytes, about 10-20  $\mu\text{m}$  in diameter and ~100  $\mu\text{m}$  long. In heart tissue, the cardiomyocytes are connected to one another at their longitudinal ends by junctions referred to as intercalated discs. The signal for depolarisation is transferred from one cardiomyocyte to another via gap junctions, in the intercalated discs. This assembly enables the action potential to pass from one cardiomyocyte to another, resulting in one signal being effective over long distances. In mammalian skeletal muscle, the triads are found at the junction between the A and the I band of the sarcomere (Figure 1.2B), whereas cardiomyocytes form diads rather than triads between the t-tubules and the SR at the Z lines, which are the borders which separate and link sarcomeres within a myocyte (Fleischer 2008).

Cardiomyocytes obtain their energy from mitochondrial oxidative phosphorylation. Mitochondria make up approximately 35% of the total cell mass of the myocyte. They are also known to have the capacity to bind and take up large amounts of cytosolic calcium and therefore play a role in the

buffering of cytosolic calcium, helping to protect the myocyte from the potential arrhythmogenic effects of calcium overload (Walker and Spinale 1999; Bers 2002).

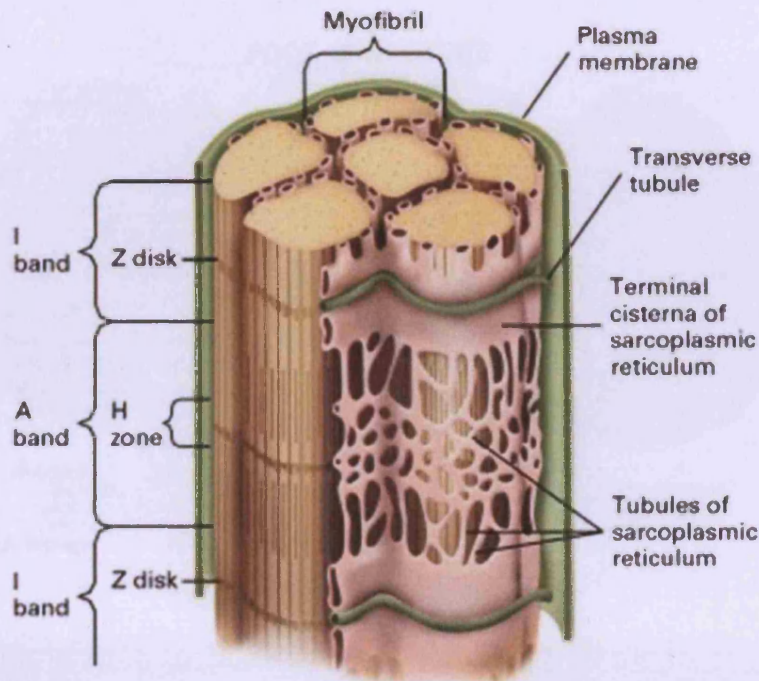


**Figure 1.3 Structural representation of a section through a myocyte.** The invaginations from the plasma membrane form the t-tubules. These enter the myofibrils at the Z-disks, connecting the terminal cisternae of the SR, forming the triad junctions. The SR tubules, which store calcium, form a network over the A band (Lodish, Berk et al. 2000).

#### **1.4 RyR macromolecular complex**

RyRs form 2D arrays at the terminal cisternae of the junctional SR with clusters of up to 100 molecules in each array (Franzini-Armstrong, Protasi et al. 1999). These form a couplon together with the LCC and sodium/calcium exchange protein (NCX) (Stern, Song et al. 1999) and this functional calcium release unit may actually be centred on up to 10 neighbouring RyR molecules at any one junction (Cheng, Lederer et al. 1993). RyR has an important role as a scaffolding protein, producing a huge macromolecular complex with many regulatory proteins. It associates with FK506 binding protein (FKBP12/12.6), protein kinase A (PKA), protein phosphatases 1 (PP1) and 2A (PP2A), calmodulin, calmodulin kinase II (CaMKII) and the phosphodiesterase PDE4D3. Junctin and triadin anchor calsequestrin and bind to the luminal side of RyR2. PKA and PP1 and 2A are



bound to the RyR through anchoring proteins. The spatial association of the RyR with the LCC and its modulatory proteins form a key functional unit in cardiac ECC (Bers 2004).

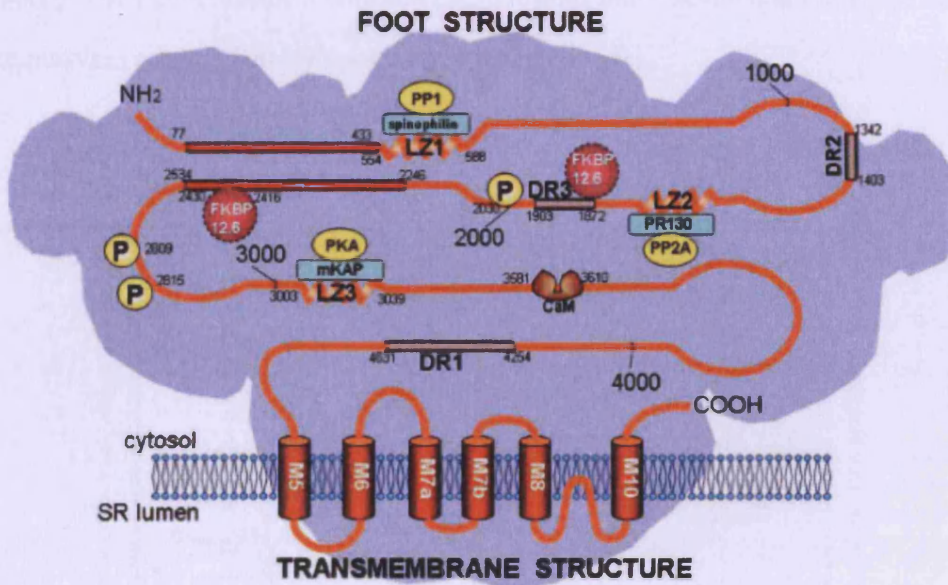


**Figure 1.4 RyR2 as a scaffolding protein.** The primary polypeptide chain of RyR2 is shown with its associated satellite proteins. On the cytoplasmic region, calmodulin, FKBP12.6, PKA, phosphatase 1 and phosphatase 2A are shown to bind. Junctin and triadin bind to the interluminal region, where they anchor calsequestrin to the RyR molecule in a calcium-dependent manner. The three major non-homologous (divergent) regions are indicated, DR1, DR2, DR3 (Yano 2008).

### 1.5 Calcium induced calcium release

During the cardiac action potential, calcium enters the myocyte through the voltage-gated LCC situated in the T-tubules of the sarcolemma at the cell surface. A small amount of 'trigger' calcium, approximately 10% of that required for contraction of the myofilaments, passes across the diadic cleft to the RyR2 where calcium entry triggers the opening of RyR2 and additional calcium is released from the SR calcium store, the process of CICR (Fabiato and Fabiato 1979). The combination of calcium influx and release raises the free intracellular calcium concentration from 100 nM to about 1  $\mu$ M, allowing calcium to bind to the myofilament protein troponin C, which then switches on the contractile machinery (Bers 2002). Relaxation, during which calcium dissociates from troponin C, occurs because calcium release from the SR ceases. Calcium is transported out of

the cytosol and the SR calcium ATPase (SERCA) sequesters calcium back into the SR calcium store. The sarcolemmal NCX removes calcium from the cytosol to the extracellular space, as does the SERCA, but to a lesser extent. The mitochondrial calcium uniport can also take up calcium (Bers 2002). The perfect balance between calcium influx and calcium efflux must be maintained in order to maintain calcium homeostasis for a regular heart rate.

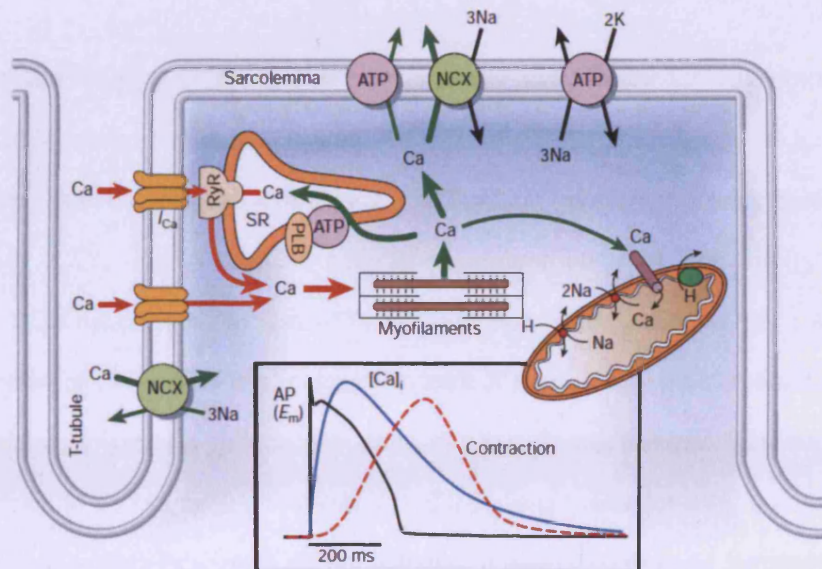


**Figure 1.5 Calcium transport in ventricular myocytes.** Calcium entry via LCCs (yellow) results in calcium release from the SR through RyR. This rise in intracellular calcium causes cellular contraction through myofilament activation. Relaxation is achieved through the reduction of cytosolic calcium via calcium-ATPase and NCX on the cell membrane, along with the SERCA and mitochondrial calcium uniport. Inset: Cardiac action potential (AP), intracellular calcium concentration ( $[Ca]_i$ ) and myocyte contraction (Bers 2002).

### 1.6 Calcium homeostasis

High SR calcium content means that more calcium is available for release and therefore the fraction of total SR calcium released in response to the inward 'trigger' calcium is also increased. High SR (luminal) calcium has a stimulatory effect on the RyR, and hence increases the RyR open probability. This enhanced sensitivity of the RyR means that when the SR calcium content is high, a process often termed 'spontaneous SR calcium release' or calcium 'leak' may occur. This is the basis of aftercontractions, transient inward currents and delayed after depolarisations (DADs)

which can trigger arrhythmia. RyR2 must close to maintain the fidelity of the heart beat but the underlying mechanisms leading to closure have been difficult to ascertain, primarily because of the many factors affecting calcium currents within the cell (Bers 2002). However likely causes of RyR2 closure include decreased luminal calcium, detection of high calcium in the dyadic cleft and potential inherent properties of the RyR acting to modify channel gating, as discussed in section 1.10.

When the calcium content of the SR is comparatively low, the inward calcium trigger may be unable to elicit SR calcium release (Bassani, Yuan et al. 1995). This assists calcium reuptake into the SR upon its relative depletion. A reduction in SR calcium release enables greater calcium influx through inward LCCs, due to reduced calcium-dependent inhibition, and through a shift in the action of the NCX away from calcium efflux. A reduction, even locally, in SR calcium load may result in inhibition of CICR. The total calcium content of the SR may be increased as a result of a rise in the calcium influx or a reduction in calcium efflux. It may also be achieved through more efficient SR calcium uptake as a direct result of  $\beta$ -adrenergic receptor ( $\beta$ -AR) stimulation, greater frequency of stimulation, increased action potential duration and raised intracellular calcium or sodium (Bers 2002).

### **1.7 Regulation of ECC by adrenergic drive (Flight or fight response)**

Physical or emotional stresses result in activation of the  $\beta$ -AR/PKA signalling pathway.  $\beta$ -AR stimulation results in both a positive inotropic and a positive lusitropic response. Inotropy is the measure of the strength of muscular contraction and an increase is associated with faster contractile events. Lusitropy, the measure of muscular relaxation, is increased to return the myocyte to a ground state enabling further contractions. Stimulation of  $\beta$ -AR, on the surface of the myocyte (Figure 1.4), by norepinephrine or epinephrine (Epi/Norepi) results in activation of the receptor-coupled G-protein ( $\alpha$ ,  $\beta$  and  $\gamma$  complex) and subsequent release of the GTP-bound  $G_s$  subunit. This subunit binds to and activates adenylyl cyclase (AC), which in turn produces the PKA activator cyclic adenosine monophosphate (cAMP). The now active PKA is able to phosphorylate many of the ECC-related proteins including phospholamban (PLB), LCC ( $I_{Ca}$ ), troponin I, myosin binding protein C and RyR (Bers 2002).

Phosphorylation of PLB and troponin I mediates the positive lusitropic response, with phosphorylated PLB, the more dominant effector of lusitropy, increasing calcium re-uptake, and phosphorylated troponin I accelerating calcium dissociation from the myofilaments (Li, Desantiago et al. 2000).

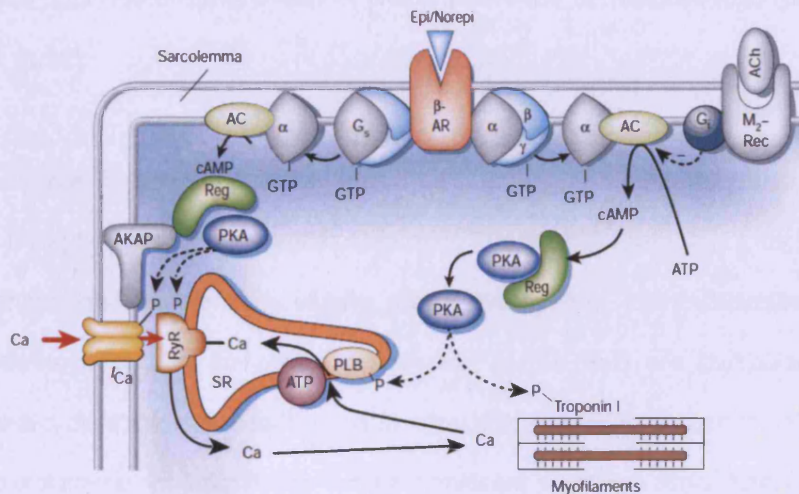


**Figure 1.6 β-adrenergic receptor activation.** Stimulation of β-AR by epi/norepinephrine results in an increase in the developed contractions (Inotropy) and an acceleration of relaxation (Lusitropy). This change is brought about through cAMP-mediated PKA activation (Bers 2002).

The increase in both the inward calcium trigger, due to phosphorylation of the LCC, and the availability of calcium within the SR, due to phosphorylated PLB-mediated calcium re-uptake, results in much larger calcium transients resulting from a given inward calcium trigger. These larger calcium transients provide the positive inotropic response, greatly outweighing the negative inotropic response provided by the accelerated calcium dissociation from the myofilaments via phosphorylated troponin I (Kentish, McCloskey et al. 2001).

PKA has also been shown to modulate the open probability of RyRs, although there is a great deal of controversy surrounding the extent and nature of this modulation. It has been proposed that chronic PKA hyperphosphorylation of RyR2 can result in incomplete channel closure and a calcium 'leak' during diastole, which causes depletion of the SR calcium store and reduced calcium release upon receptor activation. Marx et al have found that PKA phosphorylation enhanced the steady-

state open probability of single RyRs in bilayers, and suggested this to be a result of FKBP12.6 dissociation from RyR2 (Marx, Reiken et al. 2000). They attributed the reduced SR calcium, as seen in HF, to the finding that RyRs were hyperphosphorylated. However, alternative experimental models involving permeabilised myocytes have shown no change in resting SR calcium leak in relation to PKA-dependent RyR2 phosphorylation where the SR calcium load remained stable (Li, Kranias et al. 2002).

SR calcium release, in response to the inward calcium trigger signal, may also be altered by the level of RyR phosphorylation, but results concerning this are disparate, and thus the level of control exerted by phosphorylation remains elusive (Song, Wang et al. 2001; Ginsburg and Bers 2005). The finer details of calcium handling with respect to the RyR are particularly challenging to measure in intact cells, because both a rise in intracellular calcium and an increase in SR calcium uptake make isolation of intrinsic RyR effects a significant challenge (Bers 2002).

Local signalling, assisted by the macromolecular complex of the RyR, is also important in the  $\beta$ -adrenergic cascade. LCC form an assembly with  $\beta$ -AR, G-proteins, AC, PKA and PP2A and the close physical proximity of these proteins may be functionally essential to enable rapid cellular signalling (Bers and Ziolo 2001; Marx, Reiken et al. 2001).

Catecholaminergic stimulation of the heart as part of the sympathetic nervous system activation during stress (fight or flight response) has been linked to PKA phosphorylation of RyR2 at S2808 (Wehrens, Lehnart et al. 2006) and S2030 (Xiao, Jiang et al. 2005; Xiao, Tian et al. 2007). The relative importance of these two sites with regard to the role of RyR regulation during ECC, and particularly in pathology (Jiang, Lokuta et al. 2002; Xiao, Sutherland et al. 2004; Xiao, Tian et al. 2007), is disputed.

### **1.8 Calcium/calmodulin-dependent protein kinase II (CaMKII)**

The RyR complex also associates with CaMKII, potentially through mutual binding to calcineurin (Wehrens, Lehnart et al. 2004), although the specific interacting site of CamKII with RyR has not yet been identified. CaMKII phosphorylation has been suggested to increase single channel RyR2

open probability but to a smaller extent than PKA phosphorylation (Wehrens, Lehnart et al. 2004). Mutagenesis studies have confirmed S2814 as a CaMKII site (Marx, Reiken et al. 2001), although there are potentially more sites for this kinase, as discussed in section 1.10.1. CaMKII is activated by increased levels of calcium or calmodulin, for example when intracellular calcium is increased upon  $\beta$ -AR regulation (Zhang, Khoo et al. 2005). This kinase features three subunits featuring three key domains. The association domain directs assembly, the regulatory domain controls enzyme activation and auto-inhibition and the catalytic domain performs the kinase function of CaMKII. Upon binding of calcium or calmodulin, the kinase undergoes a conformational change whereby the regulatory domain inhibition of the kinase domain is relieved (Hudmon and Schulman 2002; Rosenberg, Deindl et al. 2005). This enables enzyme activation, however, in sustained calcium or calmodulin presence, the enzyme is able to self phosphorylate at a site which prevents reassociation of the regulatory domain with the kinase region, preventing autoinhibition. This self phosphorylation results in calcium/calmodulin independent activity and enables CaMKII to sustain its kinase activity which may result in excessive phosphorylation coincident with disease pathology (Hudmon and Schulman 2002).

### **1.9 Ryanodine receptor dysfunction in skeletal muscle and cardiac diseases**

The involvement of RyR in cardiac disease has been recognised by its association with arrhythmogenesis in HF, ventricular outflow tract tachycardia and CPVT. This arrhythmia is defined as DADs, or 'triggered arrhythmia' which may be fatal and hence result in SCD.

Waves of calcium release have been shown to activate DADs. Calcium waves occur during diastole, if calcium release from the SR occurs in the absence of an inward calcium trigger. Diastolic calcium release activates NCX, which depolarises the cell and the resulting inward current can trigger a DAD (Scoote and Williams 2002; Pogwizd and Bers 2004). The initial cause for this SR calcium release, or leak, is an overloaded SR store, which occurs due to an imbalance between calcium entry into the cell and efflux out of the cell (Trafford, Diaz et al. 2001). Increased SR calcium content increases the open probability of the RyR and decreases the threshold for calcium release (Cheng, Lederer et al. 1996), enhancing the likelihood of a calcium wave and hence arrhythmia.

Experimental models with myocytes have used caffeine, in addition to a  $\beta$ -adrenergic stimulant, to increase RyR open probability, which results in initial production of calcium waves, and DADs, which become progressively smaller and then disappear. It has been observed that before adding the caffeine, the calcium content of the SR is constant from beat to beat, suggesting a perfect balance between influx and efflux. However, the waves of calcium efflux generated by caffeine result in a net loss of calcium, meaning that there is an overall decline in SR calcium compared with the control. At the end of a calcium wave, the decrease in SR content has been shown to be equal to the amount of calcium removed during that wave, indicating an inability to replenish the calcium store (Venetucci, Trafford et al. 2007).

The idea of an SR calcium store threshold, which must be overcome before calcium efflux from the SR will occur, has been backed by many experiments, and has resulted in the term store overload induced calcium release (SOICR) (Jiang, Wang et al. 2005). This threshold for calcium release has been attributed to the properties of the RyR, where an increased open potential of the RyR decreases the threshold for calcium release (Xiao, Tian et al. 2007). Conversely, decreasing the open probability of the RyR with tetracaine, a channel blocker, increases the threshold for calcium release (Venetucci, Trafford et al. 2006). In addition to this, DADs are known to be prevented by ryanodine, which is a specific blocker of the open state RyR (Song and Belardinelli 1994).

### **1.9.1 Calcium and arrhythmias in Heart Failure**

Persistent pathological stress on the heart, such as HF, results in long term compensation and remodelling of cardiac ECC as SR calcium content is reduced, and intracellular free calcium increases. Reduced calcium pumping by SERCA and increased SR calcium leak via RyR2 result in this reduced SR calcium content and raised intracellular calcium, hence there is a loss of calcium homeostasis. There is good evidence that DADs contribute significantly to many ventricular arrhythmias seen in HF (Pogwizd and Bers 2004). A study on a small group of patients with dilated cardiomyopathy suggested that arrhythmias are caused by a focal mechanism involving triggered activity and DADs (Pogwizd, McKenzie et al. 1998).

A paradox exists in HF, where decreased SR calcium content (resulting in smaller contractions) is observed, yet an increased prevalence of arrhythmia (linked to SR calcium overload) is also apparent. A potential explanation for this is that the threshold for SR calcium release is reduced as a consequence of HF, which may be due to a change in the properties of RyR. It has been reported that RyR2 becomes excessively phosphorylated (hyperphosphorylated) in HF, which may result in dissociation of the stabilising protein FKBP12.6 from RyR2 and lead to reduced threshold for SR calcium (Marx, Reiken et al. 2000; Wehrens, Lehnart et al. 2006).

Spontaneous calcium release has been shown to be increased in rats with HF, suggesting a reduced threshold for SOICR (Obayashi, Xiao et al. 2006). This is consistent with the finding of increased sensitivity to luminal calcium in single RyR2 channels isolated from failing canine hearts (Li and Chen 2001). The Chen group hypothesize that RyR2 sensitivity to luminal calcium is the primary determinant of SOICR threshold and that PKA phosphorylation (due to  $\beta$ -AR stimulation) of RyR2 reduces the threshold for SOICR (Figure 1.7). This elicits no calcium leak in normal cells, because this reduced SOICR threshold is still higher than the increased SR calcium store level. However, in abnormal (HF) SR, the threshold for SOICR is already reduced, due to cellular remodelling over time, so that during stressful conditions, the PKA phosphorylation of PLB activating SERCA results in abrupt overloading of the SR with calcium. Hence DADs occur and triggered arrhythmia (Xiao, Tian et al. 2007). Treatment by  $\beta$ -AR antagonists ( $\beta$ -blockers) is able to restore the SR calcium level as they prevent the stress-related PKA phosphorylation response.



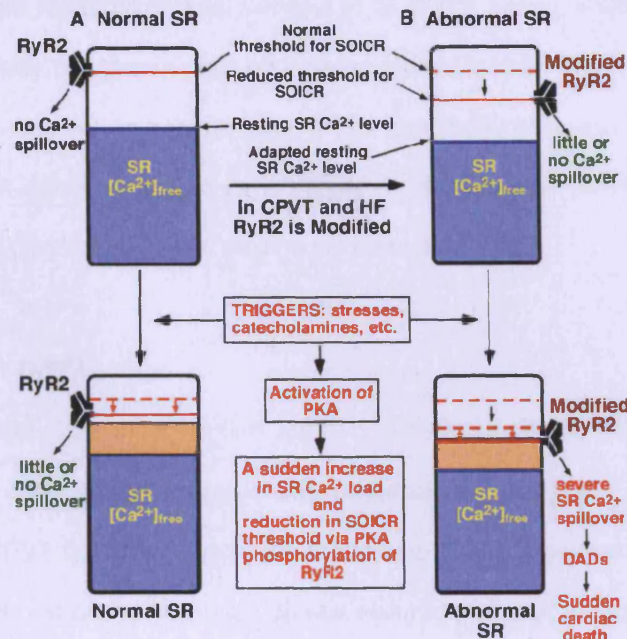


**Figure 1.7** The proposed mode of action of PKA in stress-induced arrhythmia in patients with CPVT and HF mutations. As explained in section 1.9.1 (Xiao, Tian et al. 2007).

Ventricular outflow tract tachycardia accounts for ~70% of all ventricular tachycardias in patients with structural heart disease. It is caused by abnormalities in metabolism of cAMP (the main intracellular messenger of  $\beta$ -AR stimulation), this generates cellular calcium overload and thence, by the same mechanism as described, DADs (Eisner, Kashimura et al. 2009).

### 1.9.2 Catecholaminergic polymorphic ventricular tachycardia

CPVT is an inherited syndrome, characterised by ventricular tachycardias, linked to DADs, developing under conditions of physical or emotional stress, when circulating catecholamines (such as adrenaline) are increased (Leenhardt, Lucet et al. 1995), hence the  $\beta$ -AR pathway is activated. CPVT was first associated with mutations in RyR2, which is an autosomal dominant form of the disease (Priori, Napolitano et al. 2001). There is no structural manifestation of the disease and patients have a normal resting sinus rhythm and electrocardiogram. More recently, a recessive form has been described, in which the underlying mutations occur in the SR calcium buffer-calsequestrin (CSQ) (George, Higgs et al. 2003; Wehrens, Lehnart et al. 2003). Work on isolated

RyRs has shown that the probability they are open at low cytosolic calcium concentrations is greater than for wildtype RyRs (Wehrens, Lehnart et al. 2003) (Jiang, Xiao et al. 2004) and that DADs are also more likely to occur in cells expressing mutant forms of RyR or CSQ (Liu, Colombi et al. 2006). That this condition is only unveiled under conditions of stress places direct focus on the importance of PKA phosphorylation as a trigger for the resultant arrhythmias, therefore the mechanism involved in CPVT arrhythmia may be linked to that of HF.

### **1.9.3 Drug therapy for CPVT**

$\beta$ -blockers were the first therapeutic option for CPVT because of the link between stress and arrhythmic symptoms. Initial clinical observations suggested this drug was effective in preventing arrhythmic events in CPVT patients (Leenhardt, Lucet et al. 1995), however, longer term follow up studies have suggested cardiac arrhythmias do still occur in patients, and one study has reported mortality rates in CPVT patients as high as 19%, for those using  $\beta$ -blocker therapy (Sumitomo, Harada et al. 2003). Implantable cardioverter defibrillator therapy (ICD) has been used as an alternative for patients not responsive to  $\beta$ -blockers, this device delivers a small series of shocks upon detection of arrhythmia, but death has been shown to occur despite the device being in place in a few documented cases (Uwais, Michael et al. 2006).

The experimental drug K201, a derivative of the benzothiazepine class of voltage-gated channel blockers, has been proposed to stabilise the binding of FKBP12.6 to RyR2 and hence result in normalised channel function (Yano, Kobayashi et al. 2002; Wehrens, Lehnart et al. 2004). However, the validity of FKBP12.6 dissociation linked to CPVT has been questioned, with some studies suggesting the mode of action of K201 is independent of FKBP12.6 (Hunt 2007; Blayney, Jones et al. 2010). One knock in mouse model has shown that mutations in the N-terminal and central RyR domains, regions where CPVT mutations reside, result in defective domain interactions which result in channel destabilisation (see domain interaction hypothesis section 1.10.3). The effect of these mutations can be corrected by the K201 drug (Tateishi, Yano et al. 2009). Previous studies in this group have shown K201 to stabilise RyR2 in [<sup>3</sup>H]ryanodine binding studies, in spite of an absence of FKBP12.6 as RyR channels were stripped of FKBP12.6 prior to the experiment. In parallel surface plasmon resonance (SPR) experiments assessing the binding

affinity of FKBP12.6 for RyR2, the affinity was found to be reduced in the presence of K201. The lack of an additive effect seen in the [<sup>3</sup>H]ryanodine binding studies has led to the suggestion of a common site of regulation for both K201 and FKBP12.6 (Blayney, Jones et al. 2010).

K201 has also been shown to have an inhibitory effect on the SERCA, suggesting there may be more than one site of action for the drug (Loughrey, Otani et al. 2007), indeed, K201 lacks specificity for the RyR2 channel, so its beneficial effects may be a result of this broader range of action.

Some studies have provided evidence against the use of K201 as an anti-arrhythmic drug. In one knock in mouse model featuring a CPVT mutation, K201 had no protective effect on catecholamine-induced DADs (Liu, Colombi et al. 2006). A more recent study has also suggested that the effects of K201 may only be beneficial to certain mutations, given that aberrant domain-domain interaction incurred by a mutation in the I-domain was not corrected by K201 (Tateishi, Yano et al. 2009).

Another drug from the same family as K201, S107 is thought to have higher specificity for RyR2 as it prevented arrhythmias in an alternative knock in mouse CPVT model, also by apparently encouraging FKBP12.6 binding (Lehnart, Mongillo et al. 2008). This drug has shown promising results so far in experiments, however has not been fully tested as yet (Bellinger, Reiken et al. 2009).

Some studies have suggested Verapamil to be a suitable alternative treatment option for CPVT. This has already been used in combination with  $\beta$ -blockers to treat CPVT (Rafael, Jonathan et al. 2007). Verapamil is classed as an LCC blocker, therefore effects seen are considered to be indirectly linked to RyR2 due to a reduction in the trigger calcium during an action potential. In spite of this, the drug has actually been shown to bind directly to the RyR2 channel, reducing open probability (Valdivia, Valdivia et al. 1990). In cases where the combination of Verapamil and  $\beta$ -blockers are ineffective, the anaesthetic Flecainide has been proposed as an alternative. This drug is a cardiac sodium channel antagonist, which is now also thought to block RyR2 (Watanabe,

Chopra et al. 2009). Single channel experiments have demonstrated the ability of Flecainide to increase the frequency of closing events, and in a CSQ mutant model of CPVT, it decreased the frequency of arrhythmogenic calcium waves without altering the SR calcium load, suggesting this drug does not act by altering the balance of SR calcium flux. This drug has also been shown to induce a subconductance channel state of the RyR, which occurs when the channel is open, implying a direct physical blocking mechanism of action (Hilliard, Steele et al. 2010). The effects of Flecainide need to be further investigated, partly due to its non-specific mode of action, and also because of potential pro-arrhythmic effects in HF patients with ventricular tachycardia (Echt, Liebson et al. 1991). This drug has also been withdrawn from one study, due to increased loss of consciousness in CPVT patients (Sumitomo, Harada et al. 2003).

Dantrolene is another candidate drug for CPVT treatment. This drug is commonly used to treat MH, and binds at a site in the N-terminus region of the RyR1, but is known to also bind to RyR2. Dantrolene has been shown to stabilise channel domain interaction in one model of HF, using isolated SR and cardiomyocytes from either normal or rapidly paced dogs treated with CPVT mimicking domain peptides capable of disrupting natural domain interaction (Kobayashi, Yano et al. 2009). It has also recently been used in fluorescence resonance energy transfer (FRET) studies assessing labelled N-terminal and central domain interaction which generated FRET on mutual interaction. Dantrolene was shown to stabilise the RyR2 domain in the presence of activatory peptides, restoring 'zipping' between subunits and thus generating FRET (Liu, Wang et al. 2010).

#### **1.9.4 Malignant Hyperthermia**

MH and CCD are disorders linked to the skeletal muscle isoform (RyR1). MH mutations cluster into three distinct regions or 'hot-spots' of the coding sequence, corresponding to those in RyR2 linked to CPVT. Thus it has been suggested that these C-terminal, N-terminal and central domains may represent modulatory regions, proposed to interact and stabilise channel function (Yamamoto, El-Hayek et al. 2000). MH mutations were identified a decade earlier than those causing CPVT in RyR2 (MacLennan, Duff et al. 1990) but the corresponding nature of MH triggered by anaesthetics and of DADs triggered by stress in CPVT leads to the belief of many groups that these mutational clusters are related to a common mechanism of RyR regulation and pathology (Yamamoto, El-

Hayek et al. 2000). An abundance of disease-linked RyR1 and RyR2 mutations have been recognised to date, these include over 120 substitutions, one insertion, one deletion and two genomic rearrangements, resulting in deletion of an entire exon (Thomas, Maxwell et al. 2010). Figure 1.8 demonstrates the analogous mutation clusters in the two RyR isoforms.

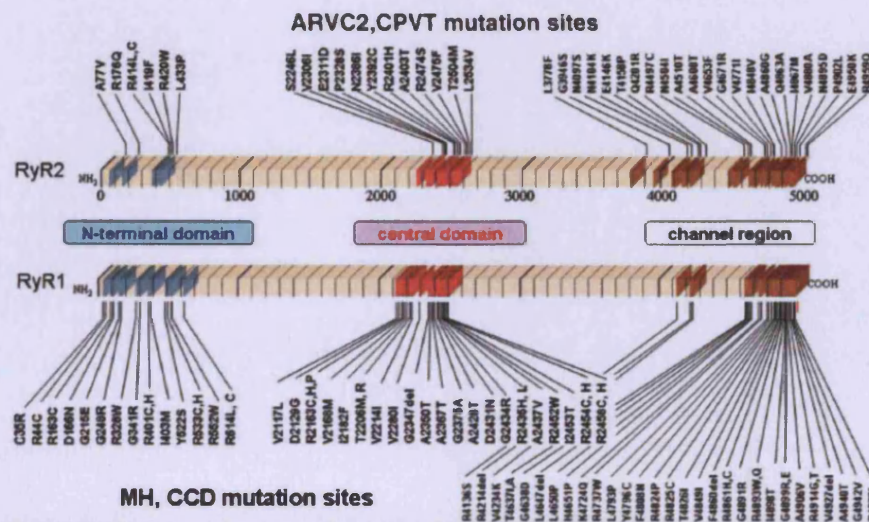


**Figure 1.8** Mutational clusters on N-, C- and central domains of RyR1 and RyR2. The high correlation of mutation sites that cause the isoform-specific diseases is shown (Yano 2008).

## 1.10 Molecular Mechanisms of RyR2 dysfunction

### 1.10.1 Phosphorylation

Consequences of RyR2 phosphorylation have not yet been well established and remain controversial in terms of the site of action and the exact kinases involved in channel modulation pertinent to disease and aberrant RyR function. There are two main kinases suggested to be involved; PKA, which is immediately highlighted by its direct upregulation as a result of  $\beta$ -AR stimulation (Bers 2002) and CaMKII, (Currie, Loughrey et al. 2004) (Grimm and Brown 2010). PKA dependent phosphorylation at S2808 has been proposed by one group as increasing the open probability of RyR2 and to result in channel destabilisation. This has been attributed to dissociation of the FK506 binding protein FKBP12.6 from the RyR2 (Marx, Reiken et al. 2000). However, CaMKII has also been proposed to phosphorylate at this same serine residue, and S2815, with no increased RyR open probability or evidence of subconductance states (Witcher, Kovacs et al.

1991; Wehrens, Lehnart et al. 2003). Insertion of a permanently phosphorylated mutation at the site in question was then found to increase open probability coincident with FKBP12.6 dissociation, suggesting an alternative kinase may be acting on this site. RyR2 channels featuring recombinantly expressed mutations were then shown by this group to have reduced affinity for FKBP12.6 following PKA phosphorylation, suggesting this kinase to be the most important (Wehrens, Lehnart et al. 2003).

An alternative site for PKA phosphorylation at S2030 has been proposed and this site was shown to be phosphorylated after  $\beta$ -AR stimulation of rat cardiac myocytes but not before, whereas the S2808 site remained unchanged (Xiao, Tian et al. 2007). It was proposed that phosphorylation at S2808 did not affect FKBP12.6 binding and that FKBP12.6 dissociation was not concurrent with mutant RyR2 dysfunction. Single channel studies have also implicated S2030 mutants as reducing the activating effect of PKA, where S2808 had no effect, adding to the idea that this may be the more relevant site of phosphorylation (Xiao, Tian et al. 2007). In addition to this, RyR2 phosphorylation at both sites was suggested to be unchanged in failing and non-failing canine hearts, placing the hyperphosphorylation theory into question (Wehrens, Lehnart et al. 2006). Knock in mouse models of CPVT have further complicated the phosphorylation story. Two of three models studied have shown similar wildtype (WT) and mutant RyR2-FKBP12.6 interaction and S2808 phosphorylation both before and after  $\beta$ -AR stimulation (Kannankeril, Mitchell et al. 2006; Liu, Colombi et al. 2006; Fernandez-Velasco, Rueda et al. 2009). A more recent model then showed dramatic differences in the WT and mutant, suggesting the effect of mutations may be more complicated than originally thought and there may be specific mechanisms linked to mutant heterogeneity (Thomas, George et al. 2004; Lehnart, Mongillo et al. 2008).

It has been suggested that the hyperphosphorylation observed in HF may actually be due to CaMKII, hence the discrepancies in experimental findings linked to PKA phosphorylation (Xiao, Tian et al. 2007).

Wehrens et al have found another site of CaMKII phosphorylation at S2814 (Wehrens, Lehnart et al. 2004) and CaMKII activation has been increasingly related to sympathetic adrenergic drive, with

other possible sites of action suggested in the literature (Rodriguez, Bhogal et al. 2003). S2814 phosphorylation of RyR has been shown to potently activate the channel and evidence suggests that abnormal phosphorylation by CaMKII may be a key factor in aberrant RyR function (Ai, Curran et al. 2005; Ferrero, Said et al. 2007). It may be the case that PKA and CaMKII activity are not independent of one another, and that PKA activation, due to  $\beta$ -AR stimulation, and thus increased calcium transients, may then affect activation of CaMKII (Ferrero, Said et al. 2007). Alternatively, there may be PKA independent activation of CaMKII via a cAMP-activated protein named Epac. CaMKII activation via Epac has been shown to result in S2814 phosphorylation and this protein has also been linked to increased SR calcium leak in adult rat cardiomyocytes in the presence of phosphorylation by CaMKII (Pereira, MÃ©trich et al. 2007). As yet, little is known of the importance of CaMKII linked with CPVT and further research is required to elucidate the exact mechanism for activation and the effect of this kinase.

In addition to these findings, work within this group has shown a reduced affinity of RyR2 for FKBP12.6 caused by PKA phosphorylation of isolated RyR channels, which was not translated into increased open probability of channels in [<sup>3</sup>H]ryanodine binding (Blayney, Jones et al. 2010). This finding points to a conformational change of RyR incurred by PKA phosphorylation at a level difficult to detect in many experimental models, which would explain the lack of PKA effect suggested by several groups.

### **1.10.2 Redox effects**

Catecholamine induction stimulates the release of reactive oxygen species (ROS) which may have an effect on mutant RyR2 function in patients exhibiting heightened sensitivity to these (Zhang, Kimura et al. 2005). Oxidative stress is measured as the number of free thiols, or reduced cysteine residues present on the RyR. Redox modification of RyR2 has been linked to calcium leak from the SR in HF, even though the level of redox sensitivity of FKBP12.6 bound to RyR2 remained unchanged in WT and mutant channels (Zhang, Kimura et al. 2005; Mochizuki, Yano et al. 2007; Zissimofolilos, Thomas et al. 2009). Carvedilol (CV) is a  $\beta$ -blocker with an antioxidant effect, which was shown to prevent HF in dogs subjected to chronic pacing. CV treated failing hearts have shown heightened free thiol levels compared with untreated failing hearts, suggesting this drug

may be valid for restoring normal RyR2 oxidation levels in mutant channels. An oxidative agent SIN-1 was able to reduce the number of free thiols of RyR2, but when added in conjunction with CV, free thiols were increased. This suggests that the stabilising effect of CV can be attributed to its prevention of RyR2 oxidation. CV was also shown to reduce calcium leak triggered by SIN-1, however, the addition of the DPc10 domain peptide, proposed to disrupt interdomain interaction of RyR2, completely abolished this CV effect. This would suggest that benefits of CV link to restoration of the defective domain interaction proposed in failing cardiomyocytes by reducing the oxidative stress level of RyR2 (Mochizuki, Yano et al. 2007).

CaMKII activation has also been linked to oxidation, implying that stabilising effects of CV may also be linked to reduced phosphorylation levels. Oxidation of methionine residues in the regulatory domain of CaMKII induces sustained kinase activity in the absence of calcium or calmodulin, and it is suggested that oxidation can directly modify the autoinhibitory region of CaMKII, in a mechanism analogous to autophosphorylation which enables this calcium/calmodulin independent activity (Erickson, Joiner et al. 2008).

### **1.10.3 Cytosolic and luminal calcium sensitivity**

As calcium is the primary agonist of RyR2, it makes sense that fluctuations in calcium concentration will directly affect channel functionality. Recent mouse models have placed focus on increased calcium sensitivity as a common feature of mutant dysfunction. This is reflected in an increased level of [<sup>3</sup>H]ryanodine binding, and increased spark frequency in permeabilised myocytes (Fernandez-Velasco, Rueda et al. 2009).

As mentioned previously, low doses of caffeine result in DADs in cardiomyocytes in the presence of  $\beta$ -AR stimulation due to increased calcium sensitivity, suggesting a direct link to arrhythmia (Venetucci, Trafford et al. 2006). It is well known that RyR is regulated by calcium at both a luminal and a cytosolic site and increased luminal (SR) calcium sensitivity has been reported for most of the characterised CPVT mutants (Jiang, Xiao et al. 2004; Jiang, Wang et al. 2005). Some of these mutants exhibit diastolic leak, with an increased open probability at sub-activatory trigger (cytosolic) calcium levels compared to WT channels, in the absence of any phosphorylation treatment (Jiang,



Xiao et al. 2004). However, other mutants have reduced sensitivity to trigger calcium and subsequent CICR, suggesting that these mutations affect deactivation of the channel, rather than activation (Thomas, Lai et al. 2005).

The recessive form of CPVT, linked to a cardiac CSQ mutation, has been shown to result in aberrant luminal calcium sensitivity (Viatchenko-Karpinski, Terentyev et al. 2004). CSQ is an RyR accessory protein which has a low affinity for calcium and therefore may serve to monitor and buffer luminal calcium levels to maintain homeostasis (Mitchell, Simmerman et al. 1988). Calcium release from the SR has been shown to rise at a faster rate as calcium concentration within the SR increases. This would correlate with potential saturation of SR buffering proteins, such as CSQ (Shannon, Ginsburg et al. 2000). Certain CSQ mutations have been suggested to modify the calcium buffering or the RyR2 interaction ability of CSQ. Interactions with other accessory proteins, such as triadin are also altered in CSQ mutants but have not been tested in the RyR2 CPVT mutants. Triadin may act in complex with CSQ, along with junctin, another luminal protein (Györke, Hester et al. 2004). Mouse models suggest that all types of disease-linked CSQ mutant affect the ability to restore RyR2 calcium release to its normal state, thus preventing aberrant calcium release which may cause arrhythmia. CSQ knock-out mice have also shown increased SR volume, demonstrating a possible compensation for its loss (Knollmann, Chopra et al. 2006).

There may also be a link between luminal calcium activation and phosphorylation, as mentioned earlier, so that PKA only stimulates channel open probability in the presence of luminal activation (SR calcium beyond threshold level) (Xiao, Tian et al. 2007). The specific effects of luminal or cytosolic calcium are difficult to determine

#### **1.10.4 Channel inter-domain interaction**

Peptide studies have shown that interacting domains of RyR1 and RyR2 can be disrupted by single base mutations specific to MH (RyR1) or CPVT (RyR2), leading to channel instability and diastolic leak, indicating that these interactions are essential to channel closure and may be involved in a conformational change which is implicated in RyR calcium release (Yamamoto and Ikemoto 2002; Yang, Ikemoto et al. 2006). Domain peptides corresponding to portions of the N-terminal (590-639)

and central domain (2460-2495) (Dpc10) of RyR2 have been shown to enhance [<sup>3</sup>H]ryanodine binding to cardiac SR preparations suggesting an increased open probability. Increased calcium release from the SR has also been shown in the presence of these peptides, with increased sensitivity to both luminal and cytosolic calcium evident in permeabilised cardiomyocytes, suggesting a replication of mechanisms involved in CPVT (Yang, Ikemoto et al. 2006). These findings have led to the interdomain interaction hypothesis by the Ikemoto group. They suggest that competitive binding of central domain peptide to the N-terminal of the channel, and conversely, binding of the N-terminal domain peptide to the central domain of the channel, disrupt the natural intramolecular interactions that would normally stabilise the channel in its resting state. Introduction of a CPVT mutation (R2474S) into the central domain peptide was shown to eliminate the activating effect, indicating that the mutation was sufficient to disturb interaction with the N-terminus and thus disrupt channel regulation. It was therefore proposed that defective interaction between these two domains, caused by a single point mutation, could represent a mechanism underlying RyR dysfunction in arrhythmia (Yamamoto and Ikemoto 2002).

Use of peptides has been extended to other RyR2 domains and cross linking studies have confirmed the region of peptide binding on the RyR1 isoform as being between the N-terminus and central domains (Hamada, Bannister et al. 2007). The DPc10 equivalent for RyR1 is DP4, the mutant of which features an MH specific mutation of the central domain. The DP4 peptide has been shown to activate RyR1 in a similar fashion to DPc10 in RyR2 studies (Yamamoto, El-Hayek et al. 2000), which are discussed in more detail in chapter 6. One group has used a fluorescence quench study to assess potential disruption of domain interaction in the presence of peptides from three different regions of RyR2, including DPc10. A quenching molecule only had access to the fluorescent label if the bound domain regions were unzipped (Tateishi, Yano et al. 2009). All three peptides were thus shown to disrupt inter-domain interaction and to increase SR calcium leak, as well as increasing ryanodine binding of SR vesicles. It would seem that the level of instability induced by these peptides may be variable however, given that one peptide used in the previously mentioned study, corresponding to the I-domain of RyR2 and proposed to bind to the transmembrane cytoplasmic loop (George, Jundi et al. 2004), did not exhibit a reversible effect on wash out (Tateishi, Yano et al. 2009). This suggests that mutations in this region do not result in

the same outcome with regard to RyR dysfunction even though they would appear to induce conformational and calcium release instability, in accordance with alternative peptide studies (George, Jundi et al. 2004). This heterogeneity in response has implications for drug therapy, where a single solution may not be valid and the therapy may need to be suited more specifically to the individual case (Thomas, Maxwell et al. 2010).

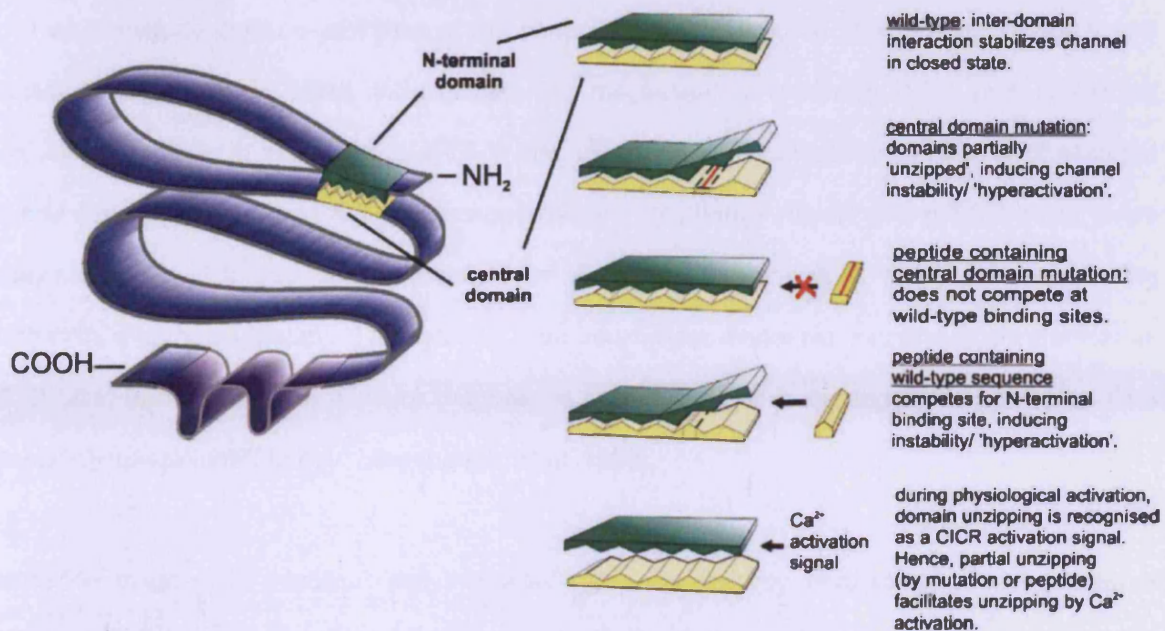


**Figure 1.9 Inter-domain interaction hypothesis.** Shows the presented theory that complex folding brings the N-terminal and central domain together allowing them to bind, regulating the RyR channel state. The mode of action of the wild-type and mutant peptides is also indicated (Yang, Ikemoto et al. 2006).

## 1.11 Modulation of the RyR

### 1.11.1 Calcium, ATP and Magnesium

Calcium is the key modulator of the RyR channel, and it is now well known from single channel and ryanodine binding experiments that RyR open probability shows a biphasic response to cytoplasmic calcium concentrations, with a threshold for activation at nM range of free calcium and maximal activation at  $\mu\text{M}$  free calcium. This activation then declines as free calcium rises until maximal inhibition occurs at 1 mM free calcium (RyR1) and  $\sim 10$  mM free calcium (RyR2).

(Nagasaki and Kasai 1983) (Kirino, Osakabe et al. 1983) (Meissner, Rousseau et al. 1988) (Lai, Misra et al. 1989; Mickelson, Litterer et al. 1990) However, maximal activation of the channel is only obtained in the presence of ~1 mM ATP (Xu, Mann et al. 1996; Kermode, Williams et al. 1998) and it has been widely reported that magnesium at mM concentrations will completely inhibit the open probability of the channel. Magnesium and ATP are therefore also key regulators of the RyR channel and it is generally believed that magnesium competes with calcium for the activating sites (A-site), or that magnesium can bind to low-affinity, inhibitory, non ion-selective sites (I-site) that can also mediate calcium inhibition of the channel (Kirino, Osakabe et al. 1983; Nagasaki and Kasai 1983; Meissner 1986) Intracellular free magnesium is normally 0.5-1 mM in cardiac myocytes, however at physiological ATP- 5 mM, magnesium only modestly inhibits RyR2 gating at 2 mM concentration. Since ATP and magnesium do not change rapidly during ECC these levels may set the physiological calcium sensitivity of the RyR (Xu, Mann et al. 1996). However, during ischemia, a common feature of tachycardia, free intracellular magnesium increases several fold as ATP falls, because ATP is a major magnesium buffer, this has been suggested to reduce RyR sensitivity to calcium (Murphy, Steenbergen et al. 1989).

Reduced magnesium inhibition and increased calcium sensitivity were found in MH (Meissner 2002). It has been reported that ATP can open the RyR from skeletal muscle even under conditions where almost no free calcium is present. (Dias, Szegedi et al. 2006) The biphasic response to calcium may be explained by the presence of activating calcium sites on RyR with a high calcium affinity, as well as low affinity, inhibitory calcium binding sites. Dias et al show a total of eight nucleotide binding sites are located on RyR1 from skeletal muscle and they propose that ATP binding at all eight sites on the RyR tetramer stabilizes an open channel conformation or primes the channel for opening events, while binding of ATP to only four of the sites correlates to closed channel conditions, suggesting there may conformational change of RyR linked to ATP binding (Dias, Szegedi et al. 2006). Magnesium and ATP binding site locations are not yet known.

### **1.11.2 Accessory protein modulation**

#### ***FK506 binding protein***

As previously mentioned, dissociation of the FK506 binding protein FKBP12.6 from RyR2 has been implicated in HF and RyR2 linked arrhythmias (Marx, Reiken et al. 2000; Yano, Ono et al. 2000). Although the cause of this dissociation has been the subject of much controversy, it is known that FKBP12.6 dissociation results in excess calcium release from the SR (McCall, Li et al. 1996). It has also been shown by our group that FKBP12.6 reduces ryanodine binding by approximately 50%, suggesting a reduction in RyR2 open probability, and a reduced affinity for the channel in its open conformation (Blayney, Jones et al. 2010). FKBP12.6 has been suggested to coordinate the opening of neighbouring RyR2 channels, from single channel studies (Marx, Gaburjakova et al. 2001). Although it is established that one FKBP12.6 binds to each subunit of RyR2, it is unknown exactly where this protein binds (Meissner 2002). The RyR1 equivalent, from the same family, is named FKBP12 and has been suggested to have similar stabilising effects on this RyR1 isoform (Avila, Lee et al. 2003).

#### ***Calsequestrin***

The role of CSQ as a luminal regulatory protein has already been discussed in section 1.10.2. It has been suggested that CSQ communicates with the RyR through interaction with triadin and junctin, although there is evidence that CSQ may be able to bind RyR in their absence as well (Herzog, Szegedi et al. 2000). Binding of calcium by CSQ causes a major conformational change in the molecule (Mitchell, Simmerman et al. 1988) however CSQ also possesses a similar affinity for magnesium (Ikemoto, Nagy et al. 1974) and there is no known active transport of magnesium across the SR membrane therefore CSQ is an important modulator of luminal magnesium concentrations. The effect of luminal magnesium concentration on RyR is little known, but a recent study assessing sheep RyR2 in lipid bilayers, proposes that luminal magnesium does in fact play a key role in RyR2 calcium release by inhibiting at activatory calcium concentrations (Laver and Honen 2008).

***Triadin and Junctin***

Triadin and junctin, which have luminal and transmembrane regions (Zhang, Kelley et al. 1997) and are found in many tissues where they are thought to have ubiquitous roles in calcium signalling. CSQ knockout mice have been shown to have suppressed expression of junctin and triadin but the roles of these proteins in mediating regulation of the RyR by CSQ and the response to luminal calcium have not been established. Overexpression of triadin has been correlated with a predisposition to arrhythmia in cardiomyocytes (Terentyev, Cala et al. 2005) and junctin overexpression has been associated with a reduced SR calcium load (Kirchhefer, Hanske et al. 2006).

***Sorcin***

The calcium binding protein sorcin has been shown to bind to RyR2 with high affinity, inhibiting the channels activity (Farrell 2004). Shown to reduce the calcium transient amplitude without affecting that of the inward calcium trigger signal, this modulator appears to inhibit the 'gain' of calcium signalling usually observed in ECC. Sorcin has been localised to the dyadic cleft and, although the site of interaction has not been established, it has been linked with the LCC (Meyers, Pickel et al. 1995; Meyers, Puri et al. 1998). Whether directly, or indirectly, through association with the LCC, the depressive effect of sorcin on RyR activity has been shown to be relieved by PKA phosphorylation (Lokuta, Meyers et al. 1997; Farrell, Antaramian et al. 2003).

***Calmodulin***

Calmodulin (CaM) binds to both RyR1 and RyR2 in a 1:1 stoichiometry at a high affinity binding site (Rodney, Williams et al. 2000). CaM inhibits RyR2 at all calcium concentrations, but only inhibits RyR1 at the  $\mu\text{M}$  concentrations of calcium associated with muscle contraction (Tripathy, Xu et al. 1995; Balshaw, Xu et al. 2001). CaM binds to RyR between residues 3630-3637 and may be involved in calcium-RyR binding during ECC as its association enhances channel opening and closing (Balshaw, Xu et al. 2001).

### **1.12 RyR structure and function**

RyR is a homotetramer with a central calcium pore and each subunit has a molecular mass of ~560 kDa, making RyR the largest known calcium channel protein with a total molecular mass of >2000 kDa. (Lai, Erickson et al. 1988)

Given the enormous size of the RyR homotetramer and its inherent stability, this protein is suitable for image analysis by cryo-electron microscopy and electron density maps of the molecule have been produced at 14 Å (Samsó and Wagenknecht 1998; Serysheva, Hamilton et al. 2005) and 30 Å (Radermacher, Rao et al. 1994). From these maps, a tetragonal structure, with a large cytoplasmic region and a transmembrane stalk, has been observed (Figure 1.10).

Sequence analysis has shown that 20% of the C-terminus is made up of hydrophobic helical regions. These are likely transmembrane domains (Takeshima, Nishimura et al. 1989). A substantial section of these domains share a high homology with the potassium channel pore loop. As this channel has been crystallised (Jiang, Lee et al. 2002), comparisons have been drawn between the two channels in an attempt to hypothesise the likely configuration of the RyR calcium pore (Welch, Rheault et al. 2004).

According to topology models, RyR1 and RyR2 are subjected to a conformational change involving domain rearrangements in the transition from the open to closed conductive state. The binding of FKBP12.6 has also been shown to induce a conformational change in RyR2 (Serysheva, Schatz et al. 1999; Sharma, Jeyakumar et al. 2006). Through domain mapping studies, it has been suggested that the N-terminus and the central domains, both sites of CPVT-causing mutations, are situated at the corners ('clamp' regions) of the RyR homotetramer within close proximity of one another (Liu, Zhang et al. 2001; Liu, Wang et al. 2005).

That so many domains, from various regions of the RyR primary sequence, have been mapped to this 'clamp' region, indicates the possibility of convoluted folding, in the tertiary structure, bringing together otherwise distant domains (Blayney and Lai 2009).

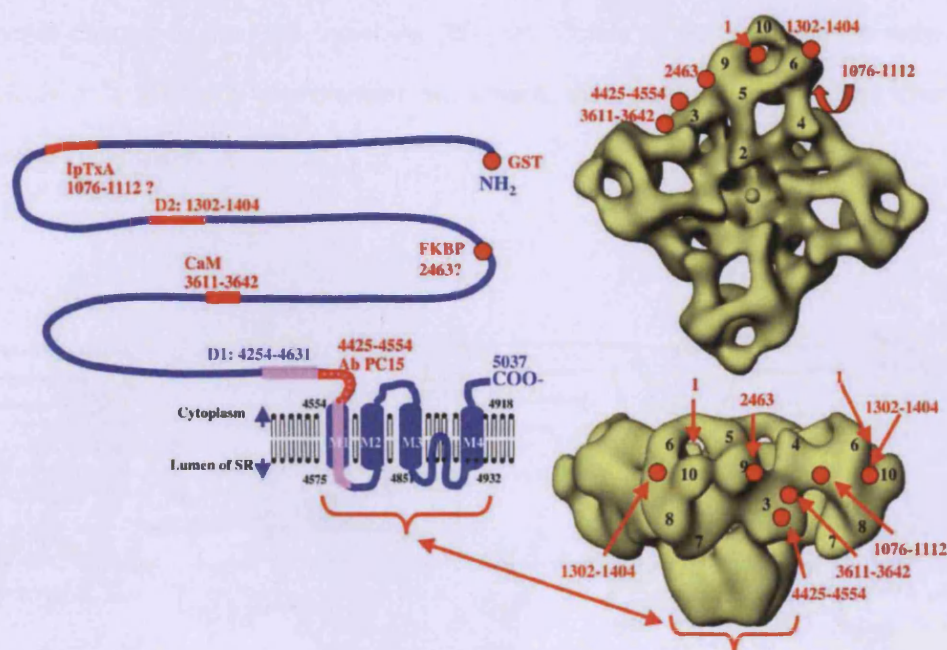


**Figure 1.10 Primary sequence and 3D structure of RyR1 with potential ligand binding sites.** Left: Primary polypeptide structure showing the proposed transmembrane domains. Putative ligand binding regions are indicated (red). Right: Solid body representation (Top: Cytoplasmic view. Bottom: Side view) showing sequence specific markers (red). Arrow indicates transmembrane region correlation (Radermacher, Rao et al. 1994).

In 2009 the first successful crystallisation of the N-terminal portion of RyR1 was achieved (Amador, Liu et al. 2009). The structure of the first 217 amino acids (N-terminus) were obtained and shown to be highly homologous between RyR1 and RyR2 in further studies by Van Petegem et al (Lobo and Van Petegem 2009). Both studies demonstrated that the N terminal region of the RyR adopts a  $\beta$ -trefoil structure, not dissimilar to that of the IP3 receptor (Figure 1.11). This fold is found among proteins with very distinct functions but likely has a key role in regulatory mechanisms in the IP3 receptor family. The  $\beta$ -trefoil is flanked by an alpha-helix (Lobo and Van Petegem 2009).

Three MH associated mutations in the RyR1 sequence were found to have no adverse affect on the global stability or fold of RyR, yet Van Petegem et al crystallised two RyR2 disease mutants which apparently caused distinct local changes in the surface of the protein and significant changes in RyR thermal stability (Lobo and Van Petegem 2009). These studies further add to the idea that



there may be mutation-specific effects on calcium-handling and that these are linked to conformational change in the RyR molecule (Blayney, Jones et al. 2010), which may occur at different levels in a hierarchy of molecular movement, thus some mutation-linked changes are more dramatic than others.

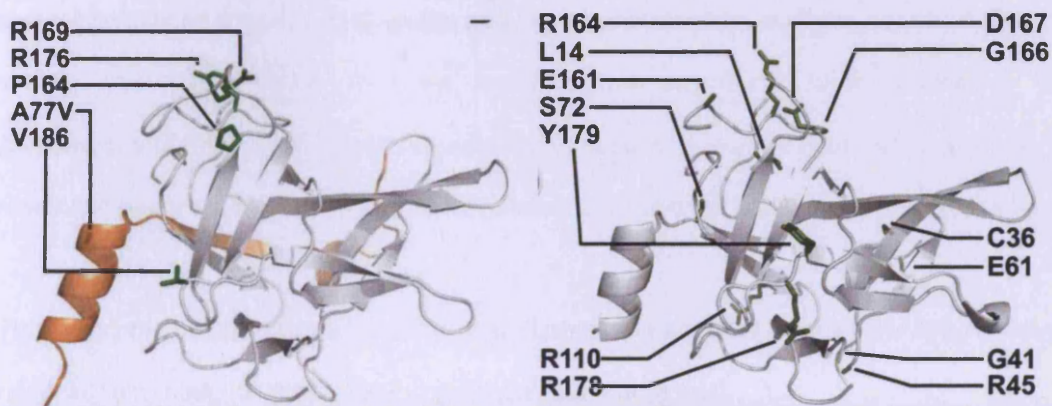


**Figure 1.11 Structural representation of the similar structures of A) RyR1 and B) RyR2.** Disease positions are highlighted (Green) and, from a severe form of CPVT, a deletion (orange) of exon 3 (Lobo and Van Petegem 2009).

### 1.13 Previous work and the context of this project

Recent research has provided valuable clues toward RyR structure and is slowly helping us to elucidate functionality of the RyR channel and offer insights into its dysfunction. It is clear however, that there are still many pieces of the RyR jigsaw unsolved, such as the key regions of the channel involved in stabilisation and modulation. The binding sites for many of the key modulators of RyR activity, such as calcium, ATP, magnesium, or the protein modulators such as FKBP12/12.6 or calmodulin are unknown. Some phosphorylation sites have been identified for PKA and CaMKII but there is controversy over their relative importance in both normal regulation and their contribution to pathology. The point mutation clusters associated with MH and CPVT in RyR1 and RyR2 respectively have suggested two pairs of interacting domains which may be critical to regulation of RyR channel gating; the N-terminus with the central domain (Yamamoto, El-Hayek et al. 2000) and the I-domain with the transmembrane cytoplasmic loops (George, Jundi et al. 2004).

Previous work done by this group has centred on the interaction of RyR1/2 with FKBP12/12.6 which had been highlighted by the suggestion that hyperphosphorylation of RyR, associated with HF, dissociates these modulatory proteins rendering the RyR leaky. The relationship between RyR1/2, FKBP12/12.6 and phosphorylation of RyR had been untested in normal physiological conditions. In cells, or by using SR preparations, the factors modulating RyR function are numerous and themselves subject to environmental influence. Our unique approach is to study these interactions in isolation from the cellular environment by purifying native RyR1 (from rabbit skeletal muscle) or RyR2 (from pig heart). In this way it has been possible to strip these preparations of FKBP12/12.6 and regulate RyR phosphorylation by PKA and to examine their inter-relationship (Jones, Reynolds et al. 2005; Jones, D'Cruz et al. 2007; Blayney, Jones et al. 2010) .

This work, the components of which are described more fully in each of the chapter introductions, has lead to a model of 'convergent regulation', see figure 1.12.

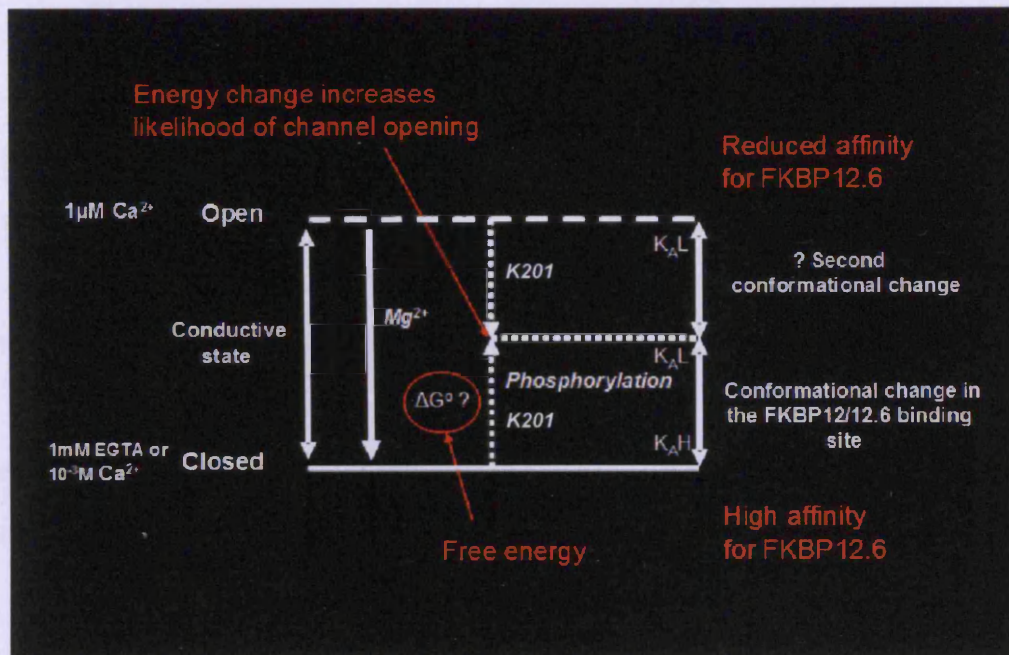


**Figure 1.12 Convergent regulation hypothesis.** The diagram above illustrates the findings from previous studies by this group on the kinetics of binding of FKBP12/12.6 to RyR1/2 and the influence of PKA phosphorylation.

Using [ $^3\text{H}$ ]ryanodine binding to determine the open state it was found that the RyR1 channel was closed in the presence of EGTA (which lowers the calcium to  $<p\text{Ca}8$ ) and in 1 mM calcium. The channel could be opened by 1  $\mu\text{M}$  calcium, shown by the upward arrow on the left. Thus the open/closed conductive state could be manipulated by changing the calcium buffer. Using buffers containing RyR modulators which either opened or closed the channel the affinity of RyR1 for FKBP12 was determined using SPR (Biacore) to measure the kinetics of interaction (Jones, Reynolds et al. 2005).

Initial experiments using physiological or pharmacological activators of the RyR- calcium, ATP, caffeine and the inhibitors calcium (1 mM), EGTA or ruthenium red, showed that the transition from the closed to the open state altered the affinity of RyR1 for FKBP12, such that the affinity was reduced four-fold when the channel was open (Jones, Reynolds et al. 2005). PKA phosphorylation was able to reduce the affinity of RyR1/2 for FKBP12/12.6 whilst the channel was in the closed state. Ryanodine binding studies also showed that the stabilising drug K201 could reduce the affinity for FKBP12/12.6. [ $^3\text{H}$ ]ryanodine binding showed that the biphasic response to calcium was not influenced by phosphorylation but K201 reduced activity.

It was proposed that phosphorylation can cause a conformational change which poises the channel ready to open by reducing the inhibition by FKBP12/12.6. K201 also causes the same conformational change but can stabilise the proposed transition state. This mechanism may underlie the 'flight or fight' response and poise the RyR molecule to open and close faster during sympathetic upregulation of ECC. Phosphorylation in our studies and others has been shown to reverse the effects of magnesium inhibition and the masking and unmasking of a magnesium inhibition site would be consistent with our data (Blayney, Jones et al. 2010).

### **1.14 Aims and hypothesis of this study**

As outlined above, circumstantial evidence points to a series of interactions that are linked to a conformational change in RyR2, which masks a magnesium inhibition site and reduces the affinity for FKBP12.6 in response to PKA phosphorylation. The experimental drug K201 appears to influence the same pathway. The peptide probes DP4 and DPc10, which are derived from central domain sequence of RyR1 and RyR2, respectively, can activate RyR1/2 in a manner postulated to disrupt the N-terminus/central domain interaction by causing a conformational change. Key to the domain interaction hypothesis was that DP4 or DPc10 with an MH or CPVT mutation respectively in the sequence (DP4M or DPc10M) were inactive, caused no conformational change and did not increase the open probability of the channel.

Identification of this region of convergent regulation is the intention of this work.

The PKA-mediated conformational change of RyR1/2, reducing the affinity for FKBP12/12.6, observed in previous studies, has been hypothesised to involve the central domain. Use of the peptide probes, DP4 and DPc10, should be able to confirm this if they alter the affinity of RyR1/2 for FKBP12/12.6 in a similar way to phosphorylation.

The intention was to carry out preliminary experiments for proof of concept using [<sup>3</sup>H]ryanodine binding to establish the effect of the DP4 wildtype and mutant domain peptides on the open/closed activity of RyR1 due to the relative low abundance of RyR2 that can be purified from native tissue. This will enable further experiments on the affinity for FKBP12 using SPR technology to measure the kinetics of interaction in the presence of DP4. Key experiments would then be performed using RyR2, FKBP12.6 and DPc10.

**Chapter 2; General materials and  
methods**

## **CHAPTER 2: General Materials and Methods**

Unless otherwise stated, all chemicals were obtained from Sigma-Aldrich (Dorset, UK) and Fisher Scientific (Leicestershire, UK), solutions were made in dH<sub>2</sub>O and stored at 4°C and standard experimental protocols were based on those given in 'Short protocols in Molecular Biology', Ausobel et al 2002 and 'Molecular Cloning: a lab manual' by Sambrook and Russell, 2001.

### **2.1 Molecular Biology**

Aseptic technique was employed throughout and all surfaces swabbed with 70% v/v methanol before and after use. Sterile flow hoods were used for pouring plates and all culture inoculation steps. Sterile plasticware (culture tubes, universals, centrifuge tubes, petri dishes, spreaders and loops) were obtained from Fisher Scientific. All non-sterile apparatus was washed in detergent free water and autoclaved at 135°C, 4 bar pressure for 90 minutes. All media was autoclaved in the same manner before use. Restriction enzymes and their respective buffers were obtained from New England Biolabs (NEB, Hertfordshire, UK) and Promega, (Hampshire, UK) unless otherwise stated. Filter sterilisation was performed using 0.2 µm filters (Sartorius, Aubagne, France). Antibiotics (Ampicillin and Chloramphenicol) were purchased from Formedium (Norfolk, UK)

#### **2.1.1 Analysis of DNA products**

##### **2.1.1.1 Agarose Gel Electrophoresis**

DNA Loading Buffer (2x stock): TAE (2x), glycerol 50% v/v, Orange G 0.25% w/v. Glycerol provides the necessary weight to sink the DNA into the gel wells, whilst the orange G dye enables visualisation of the dye front as it migrates through the gel.

Ethidium bromide (EtBr): Stock concentration 10 mg/ml Added at 1 µl/50 ml agarose. EtBr, the most commonly used nucleic acid stain for agarose gel electrophoresis, increases in fluorescence 25-fold upon intercalating double-stranded DNA. As a result destaining the background is usually not required.

Tris/acetate EDTA (TAE) buffer: 50x stock made-up and diluted to give Tris/acetate 40 mM, EDTA 1 mM, pH 7.4 (with glacial acetic acid).

Agarose gels were made by dissolving a w/v percentage of agarose in 1xTAE buffer by boiling in a microwave. Agarose was cooled to ~ 50°C before addition of 0.1 µg/ml EtBr and pouring into gel casting trays (Biorad or Hoeffer) with a comb to create loading wells and assembled as per manufacturers' instructions. Once the gel had set the tray was placed into an electrophoresis tank. 5 µl of sample mixed with 5 µl of 2x DNA loading buffer was pipetted into each well. A DNA ladder (Hyperladder (Bioline, London, UK) or NEB) of a suitable kb range was run alongside the samples. This was used to estimate the size of the DNA sample, from the distance run by the marker bands of known size, and its concentration, by comparison with the brightness of the bands, which contained known quantities of marker DNA. The lid was placed on the electrophoresis tank and a voltage of 80 V (small gel) or 120 V (large gel) was applied until the orange dye front, which migrates coincident with DNA of ~50 base pairs (bp), had migrated approximately three quarters of the length of the gel. The gel was then removed from the tank and viewed by exposure to UV light, using a XRS Gel Doc system and Quantity One software (Bio-Rad, Hertfordshire, UK).

#### **2.1.1.2 Quantification of DNA by spectrophotometry**

Peak absorption of DNA is at  $A_{260}$  and this wavelength was used to determine the quantity of DNA in an unknown sample by using the constant that 50 ng/µl of DNA has an absorption of 1. Using a quartz cuvette of pathlength 1 cm and volume 100 µl, a x100 – x25 dilution with dH<sub>2</sub>O of the DNA preparation was scanned from  $A_{200}$ - $A_{400}$ . The  $A_{260}$  was used to calculate the DNA concentration. The ratio of  $A_{260}/A_{280}$  gave an indication of its purity with respect to contaminating protein (which has a maximum absorbance at  $A_{280}$ ). A ratio of >2.0 indicated good purity, which was valuable when DNA had been extracted from bacterial lysates.

### **2.1.2 Cloning of DNA**

#### **2.1.2.1 Oligonucleotide primers**

All primers were ordered from Sigma. These were supplied as lyophilised pellets which were reconstituted with sterile dH<sub>2</sub>O to give a 100 µM stock solution and solution of 10 µM was prepared by dilution with sterile dH<sub>2</sub>O for PCR amplification. These solutions were stored at -20°C. Two gene specific primers were designed for each clone required, using the full

nucleotide sequences published in GenBank. Restriction sites, compatible with the vector multiple cloning site, were inserted immediately before the first nucleotide of the desired forward sequence and immediately before a stop codon in the reverse sequence. Primers were generally of 30 bp in length with a 50-60% GC content which was adjusted by calculating the number of individual nucleotides comprising the restriction site and compatible forward or reverse sequence of the primer. Any deficit was balanced within a nucleotide clamp 5' to the restriction site (Figure 2.1). The primer pairs used to create specific DNA clones are given in the relevant chapters.

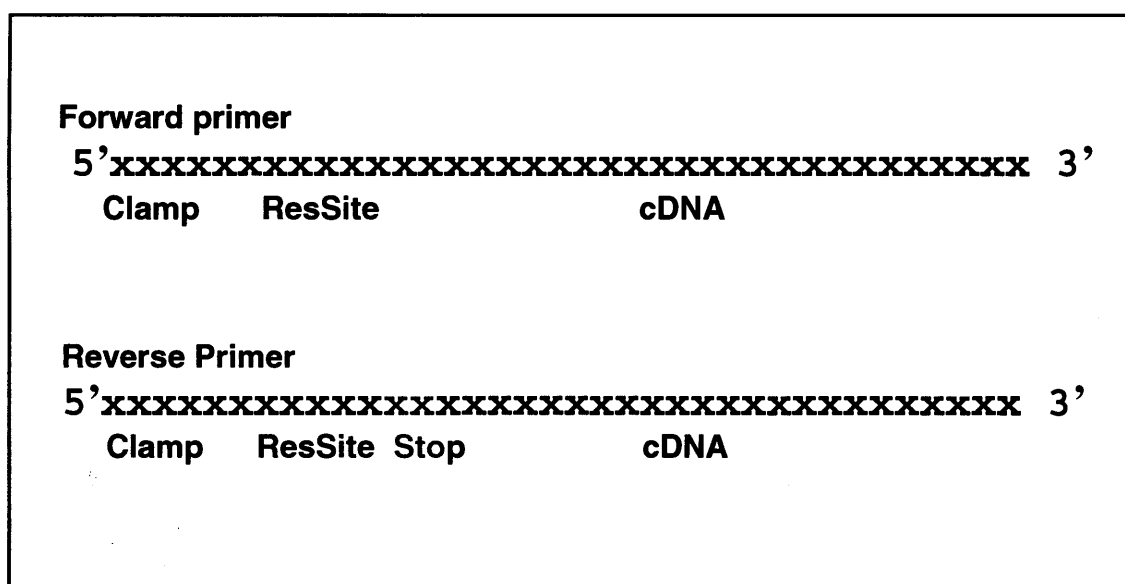


**Figure 2.1 Representation of primer design**

### 2.1.2.2 Polymerase Chain Reaction (PCR)

Phusion High-Fidelity DNA Polymerase (Finnzymes, Massachusetts, USA): This is a highly accurate thermostable polymerase. A double-strand DNA binding domain, fused with a polymerase, increases processivity 10-fold, reduces extension times, provides greater amplification yield and enables long templates to be copied more rapidly. Supplied as 2 units/ $\mu$ l stock. Storage at  $-20^{\circ}\text{C}$ , in buffer Tris/HCl 20 mM, KCl 100 mM, DTT 1 mM, EDTA 0.1 mM, BSA 200  $\mu\text{g}/\text{ml}$ , Glycerol 50%, Tween-20 0.5%, Nonidet P40 0.5%, pH 7.4 at  $25^{\circ}\text{C}$ .

Phusion HF buffer: Contains  $\text{MgCl}_2$  7.5 mM

Deoxynucleotide mix (Sigma): Contains 10 mM each of Ultrapure dATP, dCTP, dGTP and TTP sodium salts in high molecular biology grade water. Stored at  $-20^{\circ}\text{C}$ .



Molecular biology grade dH<sub>2</sub>O (Sigma): DNase, RNase and protease free. 0.1 µm filter sterilised.

**Table 2.1 Standard PCR reaction mix**

Reagent	Final	
	Concentration	Volume (µl)
Phusion DNA Polymerase	1 Unit	0.5
Phusion HF Buffer (5x)	1x	10
dNTPs (10 mM)	200 µM	1
DNA template (2 ng/ µl)	40 pg	1
Forward Primer (10 µM)	0.2 µM	1
Reverse Primer (10 µM)	0.2 µM	1
dH <sub>2</sub> O (molecular biology grade)		35.5
	<b>TOTAL</b>	<b>50</b>

A two-step 'extended' PCR programme was used (Table 2.2). The first five cycles were at a high annealing temperature to encourage specific binding of primers to their complementary sequence and provide a stock of specific template DNA for the clone required. The annealing temperature was then lowered for the final 38 cycles as non-specific binding to the original template (outside of the region to be cloned) would be overwhelmed by the concentration of specific DNA cloned in the first five cycles.

**Table 2.2 Extended PCR cycle**

Step	Temperature (°C)	Time	No. Cycles
Denaturation	95	5 min	1
Denaturation	95	30 sec	10
Annealing	65	10 sec	10
Extension	72	15 sec/kb	10
Denaturation	95	30 sec	42
Annealing	55	15 sec/kb	42
Extension	72	2 min	42
Extension	72	10 min	1

PCR reactions were set up as shown above (Table 2.1) and placed into a thermocycler (GeneAmp PCR system 9700, Applied Biosystems, California, USA) using the extended PCR program.

### 2.1.2.3 PCR clean-up

Two methods were used for PCR clean-up. Three of the constructs cloned were small ~133 bp and the size limit of the extraction medium was critical to the removal of primers, nucleotides, enzymes, salts, and other impurities from the cloned DNA samples.

Gel extraction kit (Qiagen, West Sussex, UK): Enables removal of primers, nucleotides, enzymes, agarose and EtBr from DNA. The size limit to extract and purify DNA was 70 bp which made this the method of choice for small DNA constructs. PCR products were run on an agarose gel. Using a UV lamp for detection, bands containing the correct sized PCR product were excised and weighed. A specific volume, relative to gel weight, of Qiagen buffer QG was then added and incubated at 50°C until all agarose was dissolved. 1 gel volume of isopropanol was added and the mixture applied to a 'QIAquick' column and centrifuged for 1 minute at 10,000 g to bind DNA to the silica-gel membrane of the column. The eluate was disposed of the DNA washed with another 0.5 ml of buffer QG to remove all residual traces of agarose. The DNA was then washed in a buffer containing ethanol and the remainder of the protocol was the

same as for the PCR purification using the QIAquick column. DNA was eluted into a small volume of elution buffer to finish.

PCR clean-up kit (Qiagen): 100 bp – 10 kb. 5 volumes of a high salt buffer were added to the PCR mixture which was then passed through the membrane by centrifugation at 10,000 *g* for 1 minute. Nucleic acids adsorb to the silica-gel membrane in buffer containing chaotropic salts which reduce the negative charge of the DNA to enable stronger interaction with the column membrane. The DNA was washed in 0.75 ml ethanol buffer and the column was centrifuged for 1 minute. The eluate was discarded and a second centrifugation was used to remove all residual traces of ethanol which may interfere with DNA elution. The DNA was then eluted in a small volume of low salt buffer in a final centrifugation step for 1 minute, which increases the repulsion between the membrane and the DNA.

#### **2.1.2.4 Ethanol precipitation**

Where PCR fragments were too small for PCR purification, ethanol precipitation was used instead. This involved addition of 1/10<sup>th</sup> DNA mixture volume of sodium acetate to the DNA mix. In the presence of ethanol, which reduces the polarity of the solution, DNA phosphate groups form stable ionic bonds with any positively charged ions available (Na<sup>+</sup>) and the DNA precipitates out of solution. The mixture was incubated on dry ice with 3x total volume of 100% ethanol for 30 minutes, then centrifuged at 13,000 *g* for 10 minutes. The supernatant was carefully removed and the pellet washed with 70% ethanol. Following a second spin for 1 minute and removal of supernatant, the pellet was resuspended in a small volume of water.

#### **2.1.2.5 Restriction digest**

Following DNA clean-up the PCR products were subjected to a restriction digest to prepare them for insertion into the pGEX 6P-1 cloning vector.

BamH1 enzyme (NEB): Recognition site; 5'...GGATTC...3' 3'...CCTAGG...5'

20,000 units per ml concentration (One unit is defined as the amount of enzyme required to digest 1 µg of λ DNA in 1 hour at 37°C in a total reaction volume of 50 µl.)

EcoR1 enzyme (NEB): Recognition site; 5'...GAATTC...3' 3'...CTTAAG...5'

Enzymes are stored in 50% glycerol at -20°C and are sourced from Ecolab

EcoR1 buffer (10x) (NEB): Tris-HCl 100 mM, NaCl 50 mM, MgCl<sub>2</sub> 10 mM, Triton X-100 0.025%, pH 7.5 at 25°C

BSA (100x) (NEB): 100 µg/ml

Both restriction enzymes have 100% efficiency in the EcoR1 buffer, which enabled a double digest reaction to be performed. BSA is required by BamH1 and provides additional protein which helps to stabilise this enzyme and balance any negative effects arising as a result of enzyme interaction with solid surfaces and/or the air-liquid interface. To ensure glycerol levels were not too high in the mixture, which could result in 'star' activity (non-fidelity to the restriction sequence resulting in non-specific cuts) by the restriction enzymes the glycerol must be no more than 2% of the total volume. 1 µl of each enzyme is sufficient for a total reaction volume up to 100 µl.

**Table 2.3 Standard Restriction digest recipe**

Reagent	Concentration	Volume (µl)
Undigested DNA	5 µg	10
Eco R1 enzyme	20 units	1
Bam H1 enzyme	20 units	1
Eco R1 buffer (10x)	1x	2.5
BSA (100x)	1x	0.25
dH <sub>2</sub> O	41%	10.25
<b>TOTAL</b>		<b>25</b>

Following restriction digest (Table 2.3) the cut product was cleaned up by either gel extraction or PCR clean-up. The final elution step was into 30 µl of dH<sub>2</sub>O. 5 µl was run on an agarose gel to visualise, assess the quality and estimate the concentration of the DNA.

The cloning vector pGEX-6P-1 was also cut by the EcoR1 and BamH1 restriction enzymes to prepare it for ligation with the cloned and cut DNA fragments (Figure 2.2).

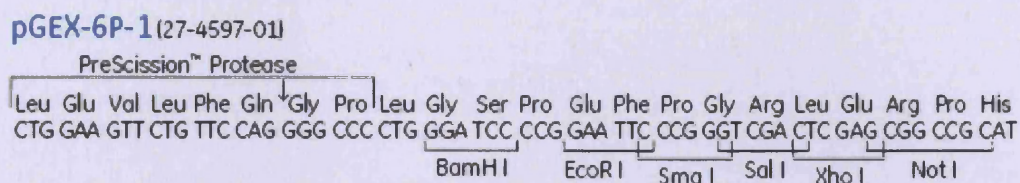


**Figure 2.2** The multiple cloning site of pGEX-6P-1 vector showing the protease cleavage site and BamHI and EcoRI restriction sites (GE Healthcare, UK).

### 2.1.2.6 Ligation

T4 Ligase buffer (10x): Tris-HCl 50 mM, MgCl<sub>2</sub> 10 mM, ATP 1 mM, DTT 10 mM, pH 7.5 at 25°C.

T4 Ligase (NEB): Catalyzes the formation of a phosphodiester bond between juxtaposed 5' phosphate and 3' hydroxyl termini in duplex DNA or RNA. This enzyme will join blunt end and cohesive end termini as well as repair single stranded nicks in duplex DNA, RNA or DNA/RNA hybrids. Recombinantly sourced, purified from *E.coli*. 12,000 units/mg. (One unit is defined as the amount of enzyme required to give 50% ligation of HindIII fragments of λ DNA in a total reaction volume of 20 μl in 30 minutes at 16°C in 1X T4 DNA Ligase Reaction Buffer).

#### Standard Ligation protocol

For efficient ligation, a ratio of insert to vector of approximately 10:1 is required.

To calculate this for each given insert, the number of ng per kb of vector is first calculated (e.g. 100 ng/4.9 kb = 20.41 ng/kb). The number of ng insert needed for a 1:1 ratio is calculated by multiplying this value by the size of the insert in kb (e.g. for an insert of size 1 kb; 1 x 20.41 = 20.41 ng insert is required)

To get the 10:1 ratio, this value is multiplied by 10.

The following table (2.4) provides the amounts of each reagent used in the ligation experiments

**Table 2.4 Standard Ligation recipe**

Reagent	Stock concentration	Final concentration	Volume
Insert (X kb)	Y ng/μl	Z ng/μl	V
Vector pGEX 6P-1 (4.9 kb)	100 ng/μl	20 ng/μl	1 μl
T4 DNA Ligase	7x	~1x	2 μl
T4 Buffer	10x	1x	2 μl
dH <sub>2</sub> O	-	-	Up to 20 μl
		<b>Total</b>	<b>20 μl</b>

X = Length of insert (kb)

Y = Stock concentration of insert (ng/μl)

Z = (10X x (100/4.9))/20

V = 20/(Y/Z)

### 2.1.2.7 Transformation

TOP10 *E.Coli* chemically competent cells: Suitable for cloning unmethylated DNA from PCR amplifications.

Super Optimal Broth with Catabolite repression (SOC) media, filter sterilised: Bacto-tryptone 2% w/v, yeast extract 0.5% w/v, NaCl 10 mM, KCl 2.5 mM, MgCl<sub>2</sub> 10 mM, glucose 20 mM, dH<sub>2</sub>O, pH 7.0. Stored at -20°C. Nutrient rich bacterial growth medium, results in higher transformation efficiency of plasmids (Sun 2009).

Lysogeny Broth (LB) media (broth): Tryptone 10 g/L, Yeast Extract 5 g/L, NaCl 5 g/L, dH<sub>2</sub>O. Autoclaved as described previously. For LB agar, 15 g/L agar was added. LB Agar was cooled to 50°C before adding relevant antibiotics and pouring into petri dishes to set.

Ampicillin, filter sterilised: 100 mg/ml stock made up in dH<sub>2</sub>O. Ampicillin is a broad-spectrum β-lactam antibiotic. It is able to disrupt cell wall synthesis, acting as an inhibitor of transpeptidase, in certain Gram-positive and Gram-negative bacteria.

Chloramphenicol, filter sterilised: 40 mg/ml stock made up in EtOH. This is a broad spectrum antibiotic, effective against a wide variety of Gram-positive and Gram-negative bacteria. It inhibits bacterial protein synthesis.

50 µl chemically competent bacteria were gently thawed on ice before adding 1-5 µl of ligation mix in a microcentrifuge tube. The mixture was incubated on ice for 30 minutes and then subjected to a 45 second heat shock in a 42°C water bath. The microcentrifuge tube was placed back on ice for 2 minutes and 1 ml of room temperature SOC media was added. The culture was incubated for 1 hour at 37°C in an Innova 4300 shaker (New Brunswick Scientific, Hertfordshire, UK) at 225 rpm. 150 µl of the cell mixture grown in the SOC media was plated onto a pre-warmed LB agar plate containing Ampicillin at 100 µg/ml. Plates were incubated for 16-18 hours at 37°C. Colonies were screened for plasmid containing the insert either by preparing DNA using a mini prep kit, or by colony screening.

### 2.1.2.8 Colony PCR

GoTaq® Green Master Mix (Promega): Contains GoTaq® Green polymerase in 2x reaction buffer with dNTPs (400 µM) and MgCl<sub>2</sub> (3 mM). Enables the PCR reaction to be directly loaded onto an agarose gel as the reaction buffer increases sample density, serving as a loading dye.

**Table 2.5 Colony screen PCR reaction recipe**

Reagent	Concentration	Volume (µl)
GoTaq Green Master mix (2x)	1x	12.5
Forward primer	0.1-1 µM	x
Reverse primer	0.1-1 µM	x
DNA template/ bacteria	<250 ng	x
dH <sub>2</sub> O (molecular biology grade)		to 25 µl

**Table 2.6 PCR cycle used**

Step	Temperature (°C)	Time	No. Cycles
Denaturation	95	2 min	1
Denaturation	95	1 min	
Annealing	50	30 sec	30
Extension	72	1 min/ kb insert	
Extension	72	5 min	1

Defined colonies were selected for screening for vector containing the insert by scraping a small sample of a single colony with a sterile pipette tip and adding this to the GoTaq reaction mixture within a PCR tube by repeatedly pipetting up and down to disperse the cells. The PCR cycle incorporates an initial boiling step to enable cell lysis and DNA dispersal within the PCR mixture. Taq polymerase has a relatively low specificity but as there will be no template for the polymerase to bind to in negative colonies, any positive PCR reaction will indicate potential positively transformed colonies, which can be further analysed by mini-prep and sequencing.

### 2.1.2.9 Plasmid purification

Resuspension solution: Tris-HCl 50 mM (pH 7.5), EDTA 10 mM, RNase A 100 µg/ ml

Lysis solution: NaOH 0.2 M, SDS 1%

Neutralization solution: Guanidine hydrochloride 4.09 M, Potassium acetate 0.759 M, Glacial acetic acid 2.12 M, pH 4.2.

Column wash solution: Potassium acetate 162.8 mM, Tris-HCl 22.6 mM pH 7.5, EDTA 0.109 mM, pH 8.0

Mini-prep kit (Promega): Wizard Plus SV Minipreps DNA Purification System: For small scale isolation of plasmid DNA. Defined colonies were selected for screening of vector-containing insert by picking a small colony with a sterile pipette tip and adding this to 5-10 ml LB media containing Ampicillin and growing overnight (Innova shaker, 37°C). Bacteria were then pelleted at 3000 g in an Avanti centrifuge for 5 minutes. The media was discarded and the pellet resuspended in 250 µl resuspension solution. 250 µl cell lysis solution was added. This contains SDS to solubilise the phospholipid and protein components of the cell membrane, leading to



lysis and release of DNA. NaOH denatures chromosomal and plasmid DNA. Alkaline protease (10 µl) is added after lysis to inactivate endonucleases and other proteins released during bacterial lysis. The lysate was then neutralised by addition of potassium acetate in neutralization buffer (350 µl). The high salt concentration precipitates chromosomal DNA and proteins, as well as cellular debris but the plasmid DNA remains in solution. Precipitants were pelleted by centrifugation at 14,000 rpm for 20 minutes. The supernatant, containing plasmid DNA, was passed through a collection tube. The DNA, bound to the matrix, was washed twice with wash solution containing ethanol to remove any residual cell constituents, first with 750 µl, then with 250 µl after another centrifugation for 1 minute. A centrifugation is used to remove the second wash buffer, a further spin removes any residual ethanol that may prevent resolubilisation of DNA in elution buffer. The purified DNA was eluted in 40 µl of dH<sub>2</sub>O. 5 µl was screened for insert by performing a double digest, in a 20 µl reaction, with Bam H1 and EcoR1 enzymes as above. 5 µl of the digest was then analysed by agarose gel electrophoresis. If the cleaved fragment of insert DNA was required for future ligation then the band was extracted using the gel extraction kit (Qiagen).

Plasmid maxi-prep, Qiagen: For large scale (up to 100 µg) isolation of plasmid DNA. The principles behind this protocol are the same as for plasmid mini-prep, but a starting culture of approximately 200 ml was used to generate the DNA. Bacteria were harvested at 6000 g for 15 minutes at 4°C, then resuspended in 10 ml resuspension buffer. 10 ml lysis buffer was then added and the sample gently agitated for 5 minutes to encourage cell breakage without shearing of genomic DNA. A neutralization buffer (10 ml) was added and mixed immediately, again by gentle inverting, followed by incubation on ice for 20 minutes to enhance precipitation. The sample was then centrifuged at 20,000 g for 30 minutes at 4°C and the supernatant was applied to a 10 ml QIAGEN column to bind DNA by gravity flow. The column was washed with 2 x 30 ml wash buffer containing ethanol, followed by elution with 15 ml water or specific elution buffer. DNA was then precipitated by addition of 10.5 ml room temperature isopropanol. This was mixed and centrifuged immediately at 15,000 g for 30 minutes at 4°C. The supernatant was carefully discarded and the DNA pellet washed in 5 ml of room temperature 70 % ethanol,

followed by another centrifugation, for 10 minutes. The supernatant was removed and the pellet air dried. DNA was then redissolved in 400  $\mu$ l molecular grade water.

### 2.1.2.10 Sequencing

ABI prism BIG-DYE<sup>®</sup> terminator sequencing dNTPs: Incorporation of uniquely labelled BIG-DYE dNTPs during the PCR cycle results in termination of the DNA extension. A successful PCR will contain truncated amplicons at all possible lengths. This sample is then passed through a gel-filled capillary tube, with a charge applied across it as in standard electrophoresis, where DNA migrates towards a positive charge such that smaller fragments move fastest. Simultaneous recording of the dNTP fluorescence passing through the capillary provides a read-out of the incorporated base at each length, as each of the four dNTPs is labelled with a different coloured dye. Hence a full sequence can be obtained for the PCR product.

DyeEx 2.0 Spin kit (Qiagen): Unincorporated dye terminators following the sequencing PCR reaction (above), are retained in a gel matrix to prevent interference during the sequencing read. A column containing the gel matrix is vortexed and centrifuged at 3000 rpm for 3 minutes to remove the storage buffer. The PCR reaction mixture is pipetted onto the surface of the gel. Subsequent centrifugation (3 minutes) passes the sample through the gel matrix and the clean sample can be sequenced directly.

**Table 2.7 BIG DYE sequencing PCR reaction recipe**

Reagent	Concentration	Volume (ul)
ABI BIG DYE <sup>®</sup> terminator sequencing kit (7x)	1x	2
Sequencing primer	10 $\mu$ M	2
DNA template	2 ng / $\mu$ l	2
dH <sub>2</sub> O (molecular biology grade)		14

**Table 2.8 Standard sequencing PCR cycle**

Step	Temperature (°C)	Time	No. Cycles
Denaturation	95	3 min	1
Denaturation	95	30 sec	32
Annealing	50	15 sec	32
Extension	60	4 min	32
Extension	60	10 min	1

Mini-prep plasmid preparations were sequenced using the above protocol to confirm correct plasmid insert sequence. Samples were sent to CBS Cardiff University for sequencing in an ABI Prism 377 sequencer.

### 2.1.3 Quikchange<sup>®</sup> XL Site-Directed Mutagenesis

Primers, designed to be complementary to a region of intended mutation, except for the specific bases in which the mutation is desired, are used in a PCR reaction to produce modified DNA amplicons. Quikchange<sup>®</sup> enables point mutations, changes in amino acids, or deletions/insertions of amino acids using a thermal cycling technique in combination with Dpn1 restriction digest. As Dpn1 is specific to methylated and hemi-methylated DNA, it will only digest the non-mutated parental DNA template but does not digest the mutant-synthesized DNA. The system uses Pfu Ultra-High Fidelity DNA polymerase. Two primers, both containing the desired mutation, cover the area where the mutation is to be made.

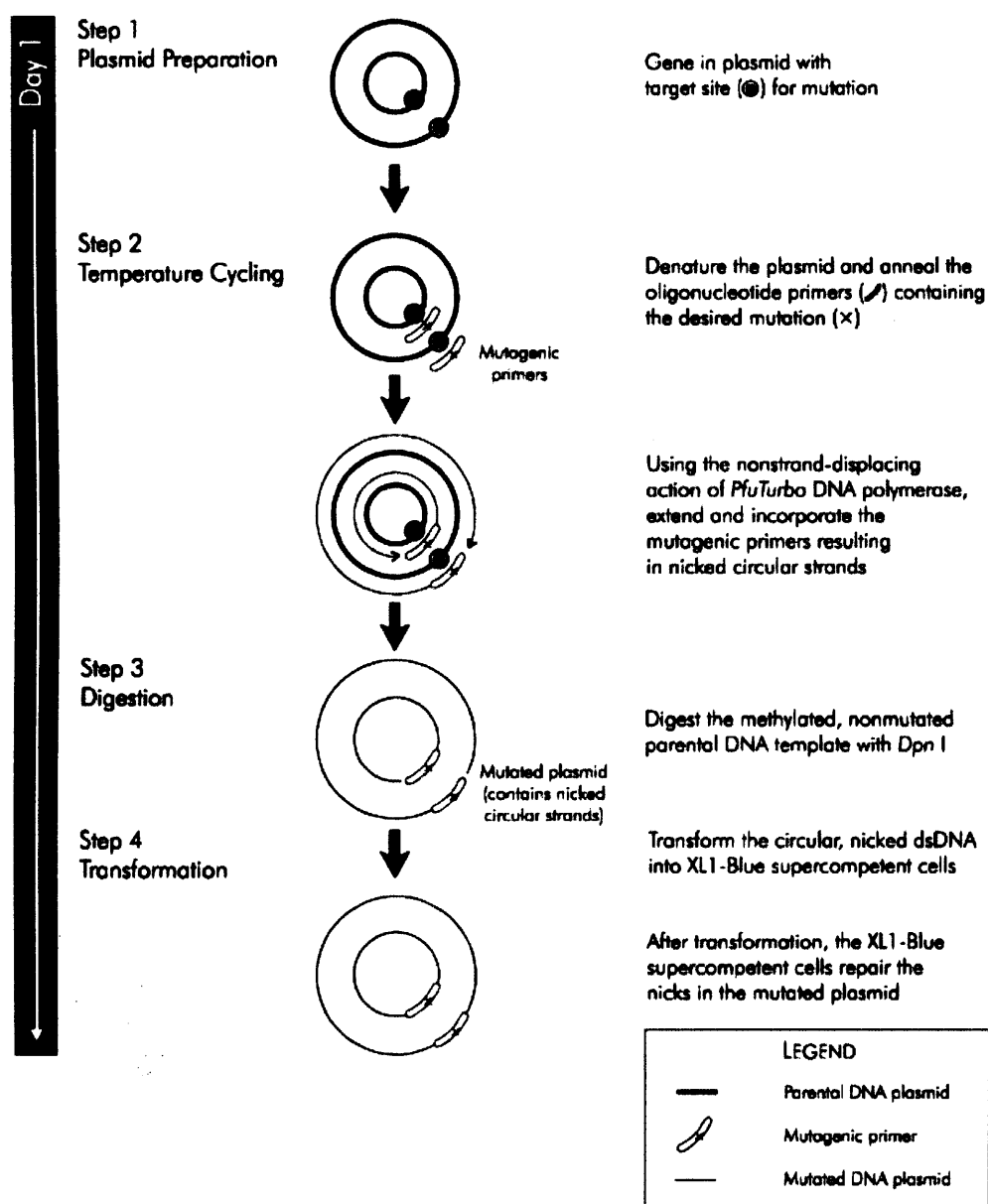


**Figure 2.3 Quikchange® mutagenesis as shown in the manufacturers' manual.**

The protocol for site-directed mutagenesis was found to be more efficient when modified slightly. The manufacturer recommends addition of 1  $\mu$ l Dpn1 enzyme to the PCR reaction for 1 hour to digest parental DNA, however, 1.5  $\mu$ l enzyme with a 2 hour incubation gave positive results, where the recommended protocol did not.

**Table 2.9 PCR reaction mix for site-directed mutagenesis (Polymerase is added after the mixture is made up to 50  $\mu$ l).**

Reagent	Concentration	Volume ( $\mu$ l)
reaction buffer (10x)	1x	500%
dsDNA template	10 ng	X
mutant primer 1	125 ng	X
mutant primer 2	125 ng	X
dNTP mix		1
Quiksolution		3
dH <sub>2</sub> O		Up to 50 $\mu$ l
<i>PfuTurbo</i> DNA polymerase	2.5 units	1

**Table 2.10 PCR cycle for site-directed mutagenesis**

Step	Temperature ( $^{\circ}$ C)	Time	No. cycles
Denaturation	95	1 min	1
Denaturation	95	50 sec	
Annealing	60	50 sec	18
Extension	68	1 min/kb plasmid	
Extension	68	7 min	1

## **2.2 Protein production and biochemistry**

### **2.2.1 Protein analysis by SDS-Polyacrylamide gel electrophoresis (PAGE)**

SDS Sample buffer with bromophenol blue: Tris 1M, SDS 20% w/v, glycerol 6 ml, EDTA 100 mM, dH<sub>2</sub>O to total volume of 20 ml, pH 6.8, a small spatula of Bromophenol blue was added and when dissolved the solution was filtered through a micropore 0.22  $\mu$ m filter and stored at room temperature, DTT was added at 50 mg/ml buffer immediately prior to use. The SDS (an anionic detergent) and DTT (which reduces thiol groups and disrupts cysteine bridges) both

contribute to the disruption of the tertiary and secondary structure of proteins. In addition the SDS binds to the protein (a process aided by heating the sample with the loading buffer) and gives each protein a uniform negative charge.

SDS running buffer: Tris 15 g/L, Glycine 72 g/L, SDS 5 g/L, (5x stock), store at room temperature and dilute for use

1.5 M Tris/HCl (separating gel) buffer: Tris 1.5 M, dH<sub>2</sub>O, pH 8.8, stored at 4°C

0.5M Tris/HCl (stacking gel) buffer: Tris 0.5 M, dH<sub>2</sub>O, pH 6.8, stored at 4°C.

40% Acrylamide/Bis solution 19:1 ratio (Biorad): Polyacrylamide gels form as a result of crosslinking between acrylamide and bis-acrylamide.

Ammonium persulphate: 50 mg in 0.5 ml dH<sub>2</sub>O.

TEMED: Increases the rate of production of free radicals from persulphate. These free radicals increase the rate of polymerisation of acrylamide by reacting with and radicalising unpolymerised acrylamide. This reactive acrylamide then reacts with other acrylamide molecules creating crosslinks which in turn creates a gel matrix.

PBS buffer 1X: NaCl 137 mM, KCl 2.7 mM, Na<sub>2</sub>HPO<sub>4</sub> 4.3 mM, KH<sub>2</sub>PO<sub>4</sub> 1.47 mM pH7.4 (prepared as a 10X stock and diluted prior to use).

Protein stain: SimplyBlue™ SafeStain – coomassie based (Invitrogen, Paisley, UK).

Protein MW Markers: Kaleidoscope prestained MW range, 7–200 kDa (Biorad), Wide range MW markers, 7–200 kDa (Sigma) or ColourPlus prestained markers, Biorad range, 7–175 kDa (NEB).

Transfer buffer: Tris 48 mM, Glycine 39 mM, SDS 3.75 ml of 10% solution, 20% methanol (exclude methanol for RyR transfer), dH<sub>2</sub>O, stored at 4°C

Blotting buffer: (Tris-buffered saline - TBS): Tris 200 mM, NaCl 1.37 M, dH<sub>2</sub>O, pH 7.4, stored at room temperature as 10x stock, diluted prior to use, allowing for addition of 1 ml Tween-20 per 500 ml buffer, re-pH to 7.4. BSA 5% w/v or non-fat milk powder 5% w/v (dependent upon the primary antibody) were added for all but the last two washes of the Western blot procedure (see below). These proteins are present to block non-specific binding of low affinity proteins and prevent non-specific binding of antibodies to the polyvinylidene fluoride (PVDF) membrane

Proteins can be separated on the basis of their molecular size by electrophoresis (Laemmli 1970). The gels are formed from acrylamide and *bis* acrylamide which are cross-linked in the presence of TEMED and ammonium persulphate (see above).

**Table 2.11 Acrylamide gel composition**

Reagent	Final proportion (separating gel)	Final proportion (stacking gel)
bis- acrylamide	x %	2.50%
Tris pH 6.8 (pH 8.8 for stack)	25% v/v	25% v/v
SDS 10% w/v	0.5% v/v	0.5% v/v
Ammonium persulphate 10% w/v	0.5% v/v	0.5% v/v
TEMED	0.05% v/v	0.05% v/v
dH <sub>2</sub> O	Up to 30 ml	Up to 30 ml

X is dependent on the percentage of acrylamide required according to the size of the proteins to be run – the larger the protein the smaller the percentage gel. The lower percentage and pH of the stacking gel concentrates the proteins into a tight band at the interface with the separating gel. As the proteins move through the latter their progress and resolution is dependent upon their mass.

SDS-PAGE mini-gel tanks and plates were supplied by Biorad and assembled following the manufacturers' protocol. The appropriate percentage separating gel was poured and a layer of water applied over the top. When the gel was set the water layer was removed by absorption using a paper towel. The stacking gel and comb (0.75 mm), used to create loading wells, were then added. When set, the gel containing plates were clamped into the electrode assembly and placed in a running tank which was filled with 1x SDS running buffer. 20 µl protein samples were boiled with 10 µl of 3x SDS loading buffer for 1 minute. Cooled samples were then loaded into the gel wells using a Gilson pipette and Biorad gel tips for precision loading. Protein standards were run in one lane. A charge of 80 V was placed across the chamber until the dye front had passed through the stack of the gel. The voltage was then increased to 200 V until the

dye front (Bromophenol blue) was at the bottom of the gel. The gel was removed from the tank and either stained with Coomassie or used for Western Blotting (see below).

### **2.2.1.1 Coomassie Staining**

The gel was transferred to a flat container and washed in dH<sub>2</sub>O for 20 minutes, with 2 changes of water, to remove SDS from the gel. 10 ml of coomassie stain was then added to the gel and incubated until significant bands were visible – usually 1 hour to overnight. The gel was then washed in dH<sub>2</sub>O until all the background stain had disappeared.

### **2.2.1.2 Western Blotting**

#### Antibodies (Ab)s

Anti-phosphoserine 16B4, mouse monoclonal (Sigma), used at x200 dilution

Anti-RyR1 (2142), 'in house' rabbit polyclonal raised against a peptide to rRyR1 aa 830-835 (used at x1000),

Anti-RyR2 (1093), 'in house' rabbit polyclonal raised against peptide to hRyR2 4459-4478 (used at x1000),

Anti-FKBP (12/12.6), goat polyclonal (Santa Cruz Biotechnologies), used at x250

Anti-GST (103T), 'in house' rabbit polyclonal raised against recombinant GST used at x10000.

Anti-mouse secondary, HRP conjugate (Pierce), used at x5000 dilution

Anti-rabbit secondary, HRP conjugate (Sigma), used at x10000 dilution.

Anti-goat secondary, HRP conjugate, (Pierce), used at x5000 dilution

PVDF membrane, Immobilon-P (Millipore, Watford, UK): 0.45 µm pore size. Prepared before use by soaking in methanol for 1 minute.

ECL reagents (Amersham, Buckinghamshire, UK): Enables chemiluminescent detection of antibody binding using horse-radish peroxidase (HRP). HRP conjugated secondary antibody bound to the PVDF membrane surface reacts with water in the detection reagent. This oxidises luminal, also in the reagents, to generate enhanced chemiluminescence. The ECL reagents are mixed in a 1:1 ratio to activate the oxidation reaction and any light emitted is detected on ECL hyperfilm upon exposure in a dark room.



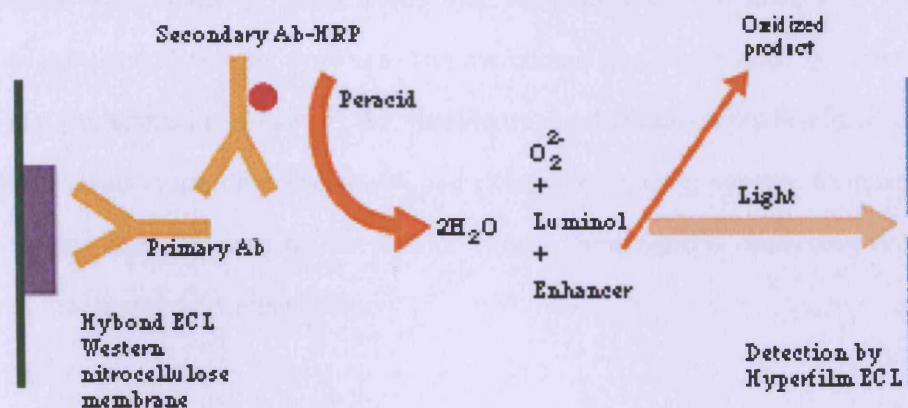


**Figure 2.4** The ECL detection process from the GE Healthcare website.

Following SDS-PAGE the run gel is soaked in transfer buffer for 20 minutes. The PVDF membrane was washed for 30 seconds in methanol to prime before also soaking in transfer buffer, along with 6 sheets of blotting paper. The gel, membrane and blotting paper were then assembled on the bottom plate (anode) of a semi dry blotter (Trans-blot SD, semi-dry transfer cell, Biorad) in the following order; blotting paper x 3, PVDF membrane, gel, blotting paper x 3. Each layer was gently rolled onto the next using a plastic pipette as a 'rolling pin' to remove air bubbles, which would have inhibited transfer. After assembly, the lid of the semi-dry-blotter containing the cathode plate was placed on top. The transfer was run for 30 minutes at 400 mA for small MW proteins and up to 4 hours for those of very high MW (see individual chapters). The blotting stack was disassembled. Kaleidoscope markers were normally run on SDS-PAGE gels destined for Western Blot and the transfer of these was a good test of efficiency. The membrane was normally marked with a biro to indicate the marker bands as these would often fade during the antibody incubation stages. The membrane was placed in blotting buffer with the appropriate BSA or milk powder addition, to prevent non-specific binding, for 1 hour at room temperature or overnight at 4°C. At room temperature the primary Ab at the given dilution was then added for 1 hour. This was followed by 3 consecutive 10 minute washes with blotting buffer. The HRP conjugated secondary Ab was then added at the appropriate dilution for 1 hour. Finally the membrane was washed once with blotting buffer (10 minutes) and twice with TBS-Tween buffer minus the BSA or milk powder.

For detection of the specific protein bands ECL reagents were combined in a 1:1 ratio and washed over the membrane for 1 minute. The membrane was then placed in a cassette with a sheet of film (Amersham Hyperfilm<sup>TM</sup>, GE Healthcare) for 1 minute in the first instance. The film was then removed in the dark and developed (X-ograph Imaging system, Compact X4). The membrane was then exposed to the film for varying time periods depending on the signal strength of the developed 1 minute film.

### 2.2.2 GST-tagged recombinant protein production

Salt buffers for protein purification and washes: NaCl 1 M / 300 mM / 50 mM, Tris 20 mM, EDTA 2 mM, DTT 2 mM (added before use), pH 7.5

Rosetta<sup>TM</sup> *E.coli*: These are bacteria engineered to expressing eukaryotic codons rarely used by *E.coli*. Rosetta provide tRNAs for these codons on a compatible chloramphenicol-resistant plasmid. Rosetta originate from the BL21 strain of *E. coli* and thereby also lack two key proteases which would otherwise contribute to the degradation of expressed proteins.

Isopropyl  $\beta$ -D-1-thiogalactopyranoside (IPTG): 100 mM stock in dH<sub>2</sub>O, filter sterilised, stored at -20°C, diluted 1:1000 for use. IPTG is a non-metabolisable analogue of lactose and remains at constant concentration when added to bacterial culture. It is used with bacterial expression vectors (such as pGEX-6P-1 see below) where the *lac* operon drives plasmid protein production.

Glutathione sepharose 4B affinity chromatography medium (GE Healthcare): 60% slurry in 20% ethanol, washed to remove ethanol before use. This has an affinity for GST and other glutathione binding proteins. Total binding capacity is 10 mg recombinant GST/ml medium.

Reduced glutathione solution: Reduced glutathione (Sigma) 10 mM was dissolved in Tris/HCl 50 mM, pH 8.0. The solution was made immediately before use.

Lysozyme: Catalyzes hydrolysis of bacterial cell walls (From Egg white 50000 units/mg, Merck-Chemicals, Nottingham, UK).

Benzonase, purity grade II (> 90%),Merck: pH 8.0, specific activity  $\geq 1.0E+06$  units/mg, high speed activity, genetically engineered endonuclease for degrading DNA and RNA.

Vivaspin 3,000 kDa cut-off column (Sartorius): the appropriate buffer was washed through membrane before use to remove membrane preservatives and prime the membrane for use.

### 2.2.2.1 The pGEX expression vector system

The glutathione S-Transferase (GST) Gene Fusion System was developed by GE Healthcare. The pGEX series of vectors are all characterised by the inclusion of a GST 'tag' C-terminus to the multiple cloning site and separated from it by a protease cleavage site. For our studies we have used pGEX-6P-1 (see Figure 2.4). Expression in *E. coli* produces a fusion protein which can be affinity purified from bacterial lysate by high affinity binding to glutathione sepharose 4B beads. If required, the fused protein can be removed from the beads by the addition of a reduced glutathione solution. Alternatively the precision protease site can be used to cleave the cloned protein from the GST tag using 3C protease, which is derived from human Rhinovirus and is itself cloned into a pGEX vector. This enables the 3C protease and the cleaved GST moiety to remain attached to the beads and the recombinant protein is liberated into solution for further purification. As well as the role in affinity purification, the GST tag can be used to track expression using an Anti GST Ab, it also aids solubility of the recombinant protein. pGEX vectors all contain a *lacI<sup>q</sup>* expression operon and expression can be induced by IPTG (see above) which combines with the *lac* repressor protein and de-inhibits transcription (Jacob and Monod 1961). pGEX vectors also carry an ampicillin resistance gene which is used for selection of colonies carrying the plasmid as these will grow in ampicillin containing medium.

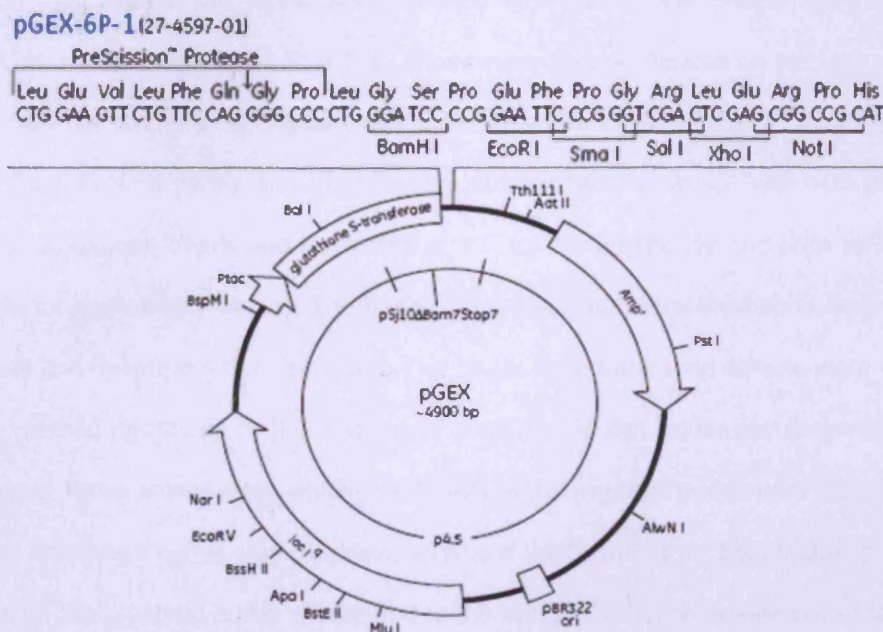


**Figure 2.5 pGEX-6P-1 plasmid map** The glutathione sepharose transferase (GST) tag region is highlighted, along with the Amp resistance gene and the *lac* operon (From the GE Healthcare website).

### 2.2.2.2 Optimisation of protein expression in Rosetta

Rosetta bacteria were transformed with 2  $\mu$ l of protein plasmid construct (mini-prep or maxi-prep -known from sequencing to contain plasmid with the correctly cloned DNA) following the standard protocol and plated for selection on LB agar plates containing both Ampicillin and Chloramphenicol. A single colony was inoculated into 4 x 10 ml starter cultures for 16-18 hours (37°C, Innova shaker). These four clonal cultures were then combined and added to 1 litre LB broth containing only Ampicillin antibiotic as Chloramphenicol can reduce protein synthesis efficiency. The culture was incubated at 37°C in a shaking incubator (Innova shaker). Growth was tracked with a spectrophotometer at  $\lambda$ 600 nm, using a 1 cm plastic cuvette and uninoculated culture medium as the blank, until an optical density at  $A_{600}$  of ~0.6 was obtained. At this point the temperature was reduced to either 25°C or 30°C for 30 min to acclimatise the culture to the protein growth temperature. A 50 ml sample of the culture was decanted following which 1 ml of IPTG was added to induce protein production. The culture continued for a total of four hours at either 25°C or 30°C, with 50 ml samples taken every hour. The 50 ml samples were pelleted in a centrifuge tube at 7000 *g* for 15 minutes, the supernatant was discarded and the pellet frozen at -20°C.

To liberate and assess the recombinant protein expression, the pellets were thawed and resuspended in 2 ml of 50 mM salt buffer. These were then sonicated on ice in 3 x 15 second bursts to lyse the bacteria. The lysate was centrifuged at 15,000 *g* for 10 minutes to remove unbroken bacteria and debris and the resultant supernatant combined with 100  $\mu$ l of washed Glutathione sepharose beads and incubated at 4°C for 1 hour (beads and prep split between 2 eppendorfs for each time sample). The bead and protein mix were then spun down at 1,000 *g* for 1 minute and the supernatant removed. The beads from each time sample were recombined and were washed rigorously by the addition of 1 ml of 1 M salt buffer and re-centrifuged. This was repeated three times, after which the beads were washed twice more with 50 mM salt buffer. The final wash buffer was removed leaving a total volume (of beads plus buffer) of 100  $\mu$ l. 50  $\mu$ l of 3x SDS loading buffer was added to the sample, which was then boiled for 1 minute. 20  $\mu$ l samples were then loaded and run on pairs of SDS-PAGE gels, one of which was

analysed by Coomassie staining, and the other by Western Blot to determine optimal induction time for protein production.

### **2.2.2.3 Making glycerol stocks of transformed Rosetta cells**

A small scale culture (50 ml) was started from a colony, from a transformation of sequenced mini prep or maxiprep plasmid, grown on a selective ampicillin and chloramphenicol agar plate. The culture was grown overnight, the bacteria spun down and the media removed. 5 ml of SOC medium was combined with 5 ml of glycerol and 10  $\mu$ l each of concentrated ampicillin and chloramphenicol antibiotics were added. The 10 ml mixture was filter sterilised and added to the bacterial pellet, which was resuspended by vortexing. 1 ml aliquots were pipetted into sterile tubes and stored frozen at  $-80^{\circ}\text{C}$ . Whenever more protein was required, a sterile loop was stabbed into the glycerol stock and spread on a selective plate to grow fresh colonies.

### **2.2.3 Affinity Purification of GST-tagged proteins**

Once optimal growth conditions were ascertained, large scale cultures were grown (1- 2 litres) and harvested in 1 litre buckets. Once spun down to harvest cells, pellets were resuspended in 25 ml PBS / 1 litre pellet and stored frozen at  $-20^{\circ}\text{C}$ .

Frozen bacterial pellets were thawed and lysozyme (20 mg/pellet from 1 litre of culture plus 1  $\mu$ l of DNAase (Benzonase) were added. The suspension was rolled for 4 hours at  $4^{\circ}\text{C}$  to start cell wall lysis. The cells were then passed through the French press four times to lyse the cells completely under high pressure. The cell debris was then pelleted at 15,000  $g$  for 10 minutes (Beckman Coulter Avanti at  $4^{\circ}\text{C}$ ) and the resultant supernatant combined with 0.5 ml bed volume washed glutathione sepharose beads (per 1 litre culture). Beads and supernatant were incubated at  $4^{\circ}\text{C}$  over night. Beads and supernatant were then centrifuged at 500 rpm for 5 minutes in the Allegra bench top centrifuge at  $4^{\circ}\text{C}$ . The supernatant was discarded and the beads were washed with 3 x 25 ml 1 M salt buffer, followed by 1 x 25 ml 50 mM salt buffer.

### **2.2.3.1 GST-tagged protein liberation**

The procedure was scaled according to the initial culture size. For every 1 ml of beads a bed volume of 5 ml of reduced glutathione solution was used. Beads were rolled with the solution at 4°C for 4 hours. The beads and solution were transferred to a gravity feed column and the eluate collected. The beads were washed twice more with 5 ml of glutathione solution and the eluates combined. For small volumes (<200 µl) the beads were centrifuged at 1000 g for 2 minutes and the supernatant collected. This was followed by two further 10 minute incubations with glutathione solution each followed by centrifugation, after which all the supernatants were combined. The combined supernatants were concentrated down to ~2 ml using Vivaspin centrifugal concentrators (Sartorius).

### **2.2.3.1 3C cleavage of recombinant GST protein**

3C protease was produced in Rosetta *E. Coli* from a pGEX-3X vector, following the same protocol as standard GST-tagged proteins. This was stored as a harvested pellet at -20°C. When the cleavage of a recombinant protein from the 3C moiety was required, the pellet from 1 litre of culture was processed and combined with 1 ml of GST-beads, which were rigorously washed using the methods described above. For cleavage of the required recombinant protein from the GST tag, the GST-3C beads were mixed with those from the affinity purification of the GST-recombinant protein, in a ratio of 1:6. 2 bed volumes of cleavage buffer were used and the beads tumbled together at 4°C overnight. The beads and solution were transferred to a gravity-feed column and the eluate collected. The beads were washed with 2 bed volumes of cleavage buffer and the eluates combined. The eluates were concentrated to 2 ml using a centrifugal concentrator.

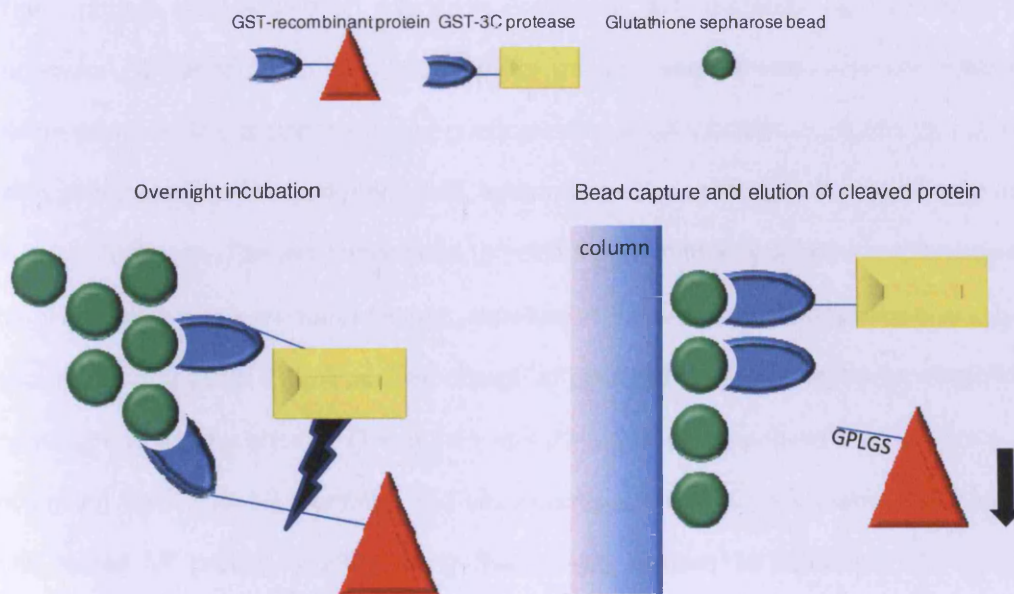


**Figure 2.6 3C cleavage of recombinant protein for removal of the glutathione sepharose tag.** The first stage involves incubation of GST-tagged 3C protease and the GST tagged recombinant protein with GST beads separately to enable binding. Subsequent wash steps eliminate non-specifically bound proteins. Both sets of protein bound to beads are then combined and incubated overnight to enable cleavage to occur. Beads are then captured on a column along with the GST-tagged 3C and any cleaved GST moiety. Cleaved protein is eluted with a small GPLGS tag intact.

### 2.2.4 Gel Filtration

Gel filtration using Fast Protein Liquid Chromatography (FPLC), AKTA Prime FPLC, GE Healthcare) was used to purify cleaved recombinant protein further. 2 ml of concentrated protein was injected onto a S75 gel filtration column using a 2 ml sample loop. The column was pre-equilibrated with Tris/HCl 20 mM, NaCl 300 mM, 2 mM DTT (added on the day of the experiment). Flow rate was 0.4 ml/minute. 1 ml fractions were collected and the protein content analysed by SDS PAGE and Western Blot. The peak fractions containing the purified protein were combined, re-concentrated with a centrifugal concentrator if necessary, aliquoted and stored at -20 °C.

### **2.2.5 Protein purification using Vivapure Ion Exchange Spin Columns (Sartorius).**

Where protein was lacking an extinction coefficient, and therefore not amenable to FPLC purification, which relies on UV absorption for tracking and generally involves relatively large elution volumes, this protocol enabled purification of small volumes of protein by ion exchange using centrifugation. Charged molecules, such as proteins, adsorb to the membrane surface of an opposite charge. The isoelectric point (pI) of the protein to be purified must be known, as this the pH at which it has a neutral charge, therefore this determines whether there is a positive or negative charge at pH 7.0. A positive charge at pH 7.0 required a negatively charged column membrane to enable binding. The protein was then eluted by applying small volumes (2 ml) of increasing NaCl buffer separately, and centrifuging the column each time. Each sample was then tested for protein quantity using BCA assay (below) to determine the optimum salt concentration for protein elution. This could then be used in future purifications of this protein.

### **2.2.6 Protein quantification using Bicinchoninic Acid (BCA) (Micro BCA Protein Assay Kit, Pierce)**

The basis of the BCA assay is the biuret reaction, which is the formation of a cuprous ion ( $\text{Cu}^+$ ) from ( $\text{Cu}^{2+}$ ) when it chelates with peptide bonds at alkaline pH to form a blue coloured complex. BCA then interacts with the  $\text{Cu}^+$  produced to form a copper complex with a strong violet coloured absorbance at  $A_{562}$ . This latter reaction is about 100-fold more sensitive than the biuret reaction and the assay is capable of detecting protein in the 0.5-20  $\mu\text{g}/\text{ml}$  range. BSA standards were used to produce a standard curve and the assay was set up in 96 well, flat bottomed plastic plates with a total volume of 200  $\mu\text{l}$  in each well of which 25  $\mu\text{l}$  was sample or standard, 75  $\mu\text{l}$   $\text{dH}_2\text{O}$  and 100  $\mu\text{l}$  Reagents A, B and C, mixed in the proportions 25:24:1, as per the Pierce protocol. The colour was developed by incubation at  $60^\circ\text{C}$  for 1 hour and the absorbance at  $A_{562}$  determined using a plate reader (Multiskan EX, MTX Lab Systems, Virginia, USA) and Genesis software.

### **2.3 [ $^3\text{H}$ ]Ryanodine binding**

Hot ryanodine mix: Radiolabelled Ryanodine (Perkin Elmer) Concentration 0.1 mCi/ml + cold ryanodine at equivalent concentrations in low salt buffer A (section 3.2.1) (Activity; 100 Ci



/mmol) to provide 5 nM of each in the final assay concentration. Combining labelled with equivalent unlabelled ryanodine meant that the labelled ryanodine spread further in experiments while ensuring saturation of all potential ryanodine binding sites.

Cold ryanodine (Polysciences Inc): 1.5 mM dissolved in dH<sub>2</sub>O. Ryanodine is a poisonous plant alkaloid with extremely high affinity to the ryanodine receptor.

Diltiazem: A non-dihydropyridine member of the group of drugs known as benzothiazepines, which are a class of calcium channel blockers of the same family as the K201 anti-arrhythmic drug. It is a potent vasodilator.

Dimethyl Sulfoxide (DMSO): Miscible in a wide range of organic solvents including water.

FK506 monohydrate (Sigma): 1 mM solution made up in DMSO. Stored at -20°C. Interacts with FKBP12/12.6.

Binding wash buffer: Tris 25 mM, KCl 200 mM, dH<sub>2</sub>O, pH 8.0, stored at 4°C

Scintisafe Liquid Scintillation Cocktail (Fisher): 50% efficiency for Tritium. A petroleum hydrocarbon based gelling cocktail for aqueous samples. Liberates tritium into solution to enable the radioactivity to be counted.

20 mm Glass fibre membranes GFF (Whatman): Soaked in binding buffer before use

### **2.3.1 Free Calcium Buffers**

Stock buffer: PIPES 20 mM, CHAPS 0.05% w/v, KCl 2 M (high salt)/300 mM (low salt), dH<sub>2</sub>O, pH 7.4

Stock EGTA: 200 mM, dissolved in a small volume of 10 M NaCl and diluted into stock buffer (above), pH 7.4, serial dilutions in the stock buffer provide 20 mM final concentration. EGTA has a much higher affinity for calcium ions than magnesium ions and is useful for making buffer solutions that resemble the environment inside living cells, where the calcium ions are often at least a thousand fold less concentrated than magnesium.

Stock CaCl<sub>2</sub>: 100 mM of dihydrate in stock buffer (above)

**Table 2.12; Free Calcium Buffers**

Free Ca <sup>2+</sup> Conc (uM)	20 mM EGTA	Ca <sup>2+</sup> stock- high salt (ml)	Ca <sup>2+</sup> stock- low salt (ml)	Total volume
1.00E-08	10 ml	2.65 of 100 mM	0.32 of 10 mM	100 ml
1.00E-07	10 ml	1.21 of 100 mM	1.28 of 10 mM	100 ml
5.00E-07	10 ml	1.76 of 10 mM	1.80 of 10 mM	100 ml
1.00E-06	10 ml	1.88 of 10 mM	1.88 of 10 mM	100 ml
5.00E-06	10 ml	1.98 of 10 mM	1.98 of 10 mM	100 ml
1.00E-05	10 ml	2.01 of 10 mM	2.01 of 10 mM	100 ml
1.00E-04	10 ml	2.20 of 10 mM	2.20 of 10 mM	100 ml
1.00E-03	10 ml	4.00 of 10 mM	4.00 of 10 mM	100 ml

\*values were calculated using the Maxchelator programme to calculate total calcium required with the following constants: assay temp 37°C, pH 7.4, ionic strength 1 M for high salt and 0.15 M for low salt, EGTA- Ca<sup>2+</sup> dissociation constant: 10.98 from <http://www.stanford.edu/~cpatton/xlsconstants.htm> on 04/03/2011.

### 2.3.2 <sup>3</sup>[H]Ryanodine binding protocol

Assays were set up as below to a total reaction volume of 300 µl and in duplicate for each condition type. Ryanodine coupled to radioactive tritium was used to measure the amount of ryanodine bound. Buffer A was added to make up the total volume in each case and the assays were then incubated in a 37°C water bath for 90 minutes.

Pre-soaked Whatman GFF membranes were then placed on columns of a vacuum manifold (Hoeffler). A vacuum was obtained using a Heto Master Jet pump. One full assay was pipetted into 5 ml wash buffer on top of the membrane. The membranes were then washed 2x with 5 ml ice cold binding wash buffer to stop the reaction and to wash away any un-bound radioactive ryanodine. Membranes were removed from the manifold and placed in a scintillation vial with 5 ml Scintisafe liquid scintillation cocktail before counting radioactivity on the scintillation counter (counts per minute) (Packard Tricarb 2100TR Liquid Scintillation Analyser). This process was repeated for all assay samples.

**Table 2.13 Standard  $^3\text{H}$ Ryanodine binding assay mix**

<b>Addition</b>	<b>Volume (<math>\mu\text{l}</math>)</b>
RyR preparation	50
Calcium buffer	150
Hot ryanodine mix	10
RyR modulator	X
Buffer A	to 300

X denotes the volume of RyR modulator added depending on stock concentration and desired final concentration. Control assays were set up per each experiment with 10  $\mu\text{l}$  cold ryanodine added (3 mM stock) and with no RyR preparation added to detect non specific binding to the membranes used. A 10  $\mu\text{l}$  sample of the hot ryanodine mix was also added directly to 5 ml scintillation fluid for each experiment to measure the total radioactivity counts per assay.

#### **2.4 Health and Safety**

All work done for this investigation was carried out using aseptic technique and all chemicals were handled in accordance with COSHH and local college safety regulations. All bacterial waste was disinfected with Actichlor (Adams Healthcare, Yorkshire, UK) at 1000 ppm available chlorine (1 tablet/1 litre of waste) prior to disposal.

#### **2.5 Statistical analysis**

All data are presented as mean values with the standard error of the mean. As most experiments were paired, the student's paired t-test was used to determine statistical significance, with a value of  $p < 0.05$  considered significant. Where unpaired data were compared, an unpaired t-test has been used and this is indicated in the figure legend.

**Chapter 3; Preparation of functional  
RyR channels from native tissue**

## **CHAPTER 3; Preparation of functional RyR channels from native tissue**

### **3.1 Introduction**

The RyR complex was first isolated from rabbit skeletal muscle SR fraction in 1988 by Lai et al. (Lai, Erickson et al. 1988) CHAPS zwitterionic detergent was used to solubilise RyR protein from the SR membrane by creating proteolipids within which the RyR homotetramer is relatively stable (Lai et al 1988). Addition of Triton X-100 was reported to selectively remove calcium-ATPase, an abundant protein of SR membranes and potential contaminant of RyR preparations.

The solubilised protein was applied to sucrose density gradients to separate the RyR protein (2,200 kDa) from other solubilised membrane proteins, for example calcium-ATPase (100 kDa), or calsequestrin (66 kDa), on the basis of size. The RyR protein, moving more rapidly than its smaller companions, could be characterised and isolated from the lower fractions.

Sucrose gradient preparations give a relatively pure RyR samples but the high sucrose and NaCl concentrations used restrict their use in certain experimental procedures, for example protein-protein interaction studies. Exchanging the sucrose buffer, using dialysis, results in a considerable loss of RyR protein, possibly due to aggregation and precipitation. These issues were explored when SPR experiments for RyR1/2 and FKBP12/12.6 interaction studies were designed (Jones, Reynolds et al. 2005; Jones, D'Cruz et al. 2007; Blayney, Jones et al. 2010).

An alternative protocol, using FPLC and anion exchange, was employed to purify and exchange the buffer in one step, taking the CHAPs concentration down to 0.05%, instead of 0.5%, as present in sucrose gradients. In this protocol the final NaCl concentration was ~300 mM, so the sample only required a 2x dilution before experimental application. Sucrose was eliminated from the purification method and a faster protocol resulted in extraction of RyR from a microsomal preparation in ~4.5 hours, greatly reducing the likelihood of loss of channel functionality for experiments.

This chapter outlines the purification methods for extraction of functional RyR1 and RyR2 protein from rabbit skeletal and pig heart tissue respectively. The preparations were stripped of endogenous FKBP12/12.6 and dephosphorylated or phosphorylated so that modulators of activity could be controlled and compared.

## **3.2 Methods and Materials**

### **3.2.1 RyR extraction and purification from native tissue**

RyR1 was extracted from rabbit skeletal muscle and RyR2 from pig hearts. Male New Zealand White rabbits (2-2.5 kg) were sacrificed with sodium pentobarbitone according to university guidelines and pig hearts were obtained from an abattoir. This investigation conforms to the Guide for the Care and Use of Laboratory Animals published by the US National Institutes of Health (NIH publication number 85-23, revised 1966).

NB/ Where protease inhibitors were used, they were made-up and added immediately prior to use.

Homogenisation buffer: PIPES (Disodium Salt) 10 mM, Sucrose 0.3 M, EDTA 0.5 mM (dissolved in 10 M NaOH), dH<sub>2</sub>O, pH 7.4, stored at 4°C (+protease inhibitors)

Resuspension buffer: KCl 0.6 M, PIPES 10 mM, dH<sub>2</sub>O, pH 7.1, stored at 4°C (+protease inhibitors)

Protease Inhibitor cocktail: Benzamidine hydrochloride 0.8 mM, Iodoacetamide 1 mM, AEBSF 0.2 mM, DTT 2 mM, dH<sub>2</sub>O (dilute 1:100 for use). Benzamidine is a reversible competitive inhibitor of trypsin, trypsin-like enzymes and serine proteases. Iodoacetamide is able to bind covalently with cysteine, so disulfide bonds cannot form. AEBSF/FLUKA is a water soluble, irreversible serine protease inhibitor. DTT is an unusually strong reducing agent, owing to its high conformational propensity to form a six membered ring with an internal disulfide bond.

Solubilisation buffer: PIPES 10 mM, EGTA 100 µM, CaCl<sub>2</sub> 150 µM, dH<sub>2</sub>O, pH 7.1, stored at 4°C.

Triton buffer: 1 g Triton X-100 per 100 ml solubilisation buffer, stored at 4°C. Triton X-100 is a commonly used non-ionic detergent for solubilising membrane proteins during isolation of membrane-protein complexes. This stage selectively removes the calcium-ATPase from the SR membrane complex.

CHAPS buffer: PIPES 10 mM, NaCl 1 M, CHAPS (Roche) 1.2% w/v, phosphatidylcholine (from soybean) 1% w/v, EGTA 100  $\mu$ M, CaCl<sub>2</sub> 150  $\mu$ M, dH<sub>2</sub>O, pH 7.1, stored at 4°C. CHAPS is a zwitterionic detergent for solubilisation of membrane proteins (which are often insoluble in aqueous solution due to their natively hydrophobic cellular environment).

No salt buffer (Buffer A): CHAPS 0.05%, PIPES 20 mM, EGTA 100  $\mu$ M, CaCl<sub>2</sub> 150  $\mu$ M, dH<sub>2</sub>O, pH 7.1, de-gassed and stored at 4°C (+protease inhibitors).

High salt buffer (Buffer B): Same as Buffer A with NaCl 1 M, dH<sub>2</sub>O, pH 7.1, de-gassed and stored at 4°C (+protease inhibitors).

Low salt buffer (Buffer A/B): 1 part Buffer B + 7 parts Buffer A to give 125 mM NaCl, degassed and stored at 4°C (+protease inhibitors).

FK506 monohydrate (Sigma): 1 mM solution made up in DMSO. Stored at -20°C. FK506 is able to form a complex with FKBP12/12.6, preventing these proteins binding to their RyR binding sites.

Figures 3.1 and 3.2 outline the procedures used for extraction of RyR from native tissue.

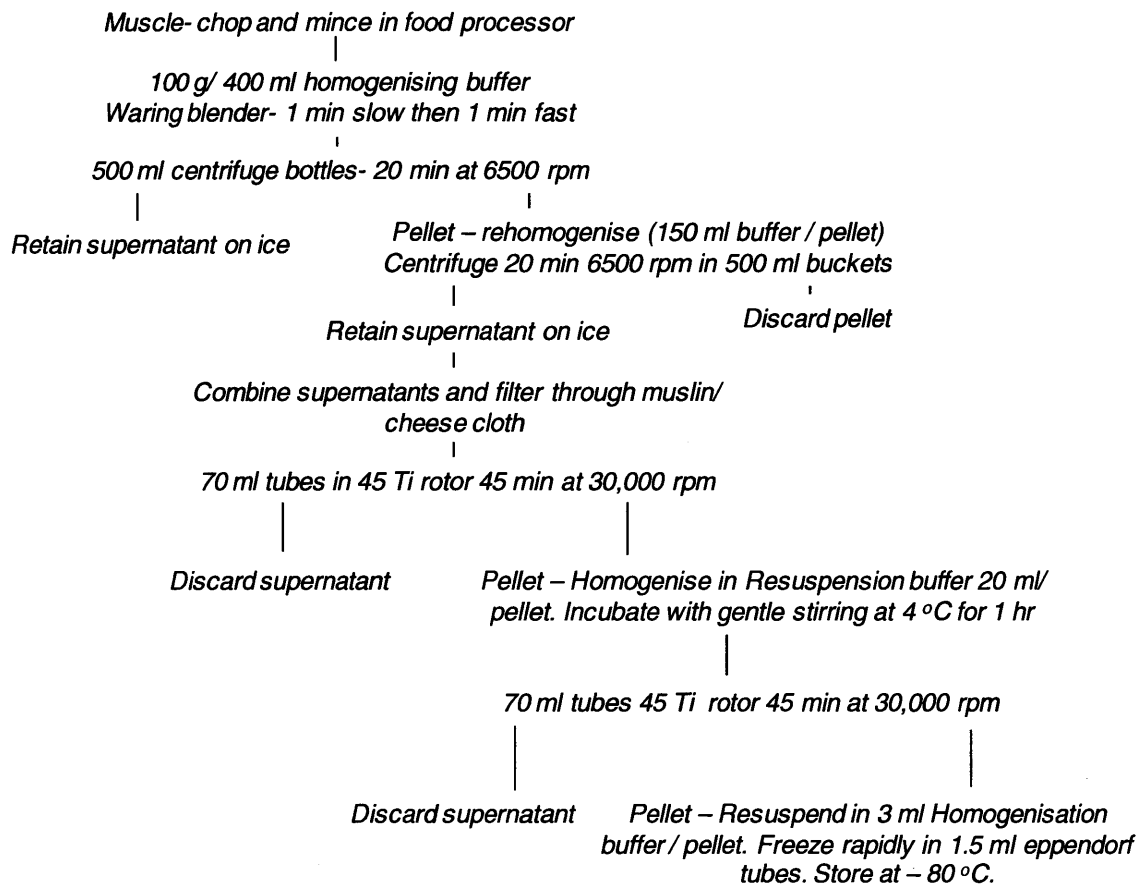


**Figure 3.1** Flow chart describing the protocol for preparation of SR membrane preparations from skeletal or cardiac muscle. Standard procedure typically involved preparation of ~500 g rabbit skeletal muscle or ~500 g pig hearts to obtain  $n=1$ .



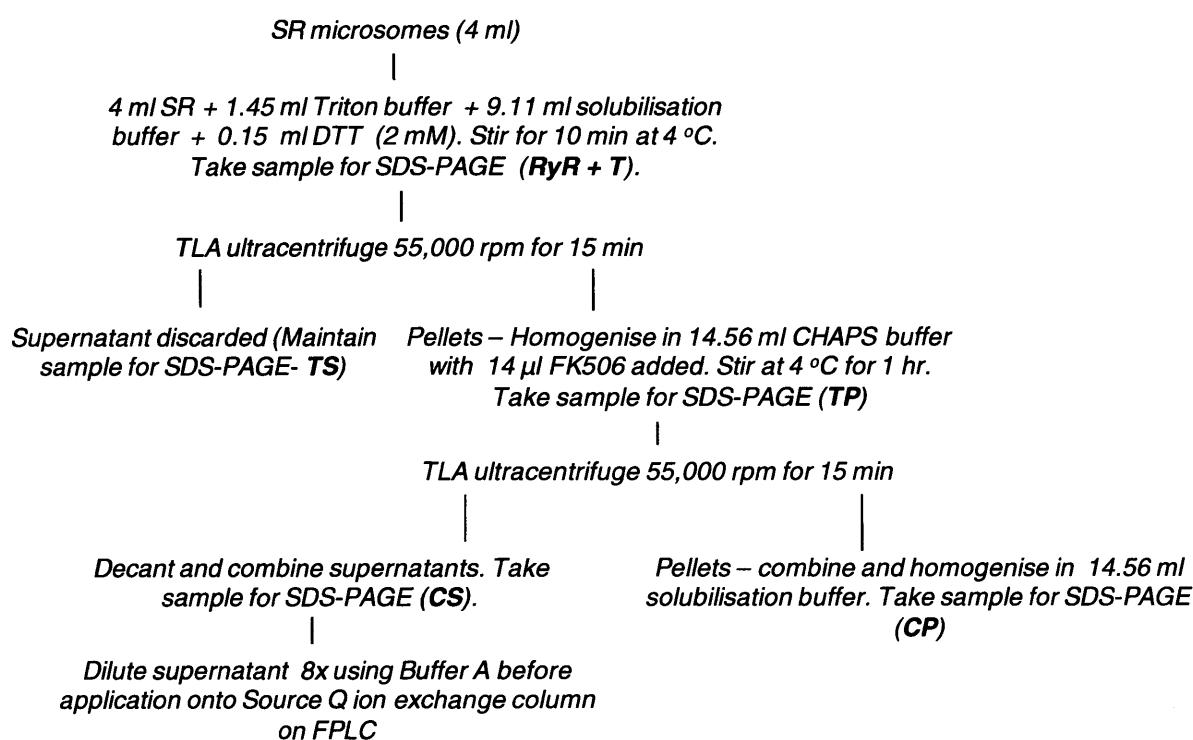


**Figure 3.2** Flow diagram showing the steps involved in solubilisation of SR microsomes to extract functional RyR protein. Values shown are specific to a 4 ml starting volume of SR microsomes (typically 25 mg/ml). FK506 (1  $\mu$ M) was added to remove endogenous FKBP protein as shown previously (Blayney, Zissimopoulos et al. 2004). Samples were taken at each stage for analysis by SDS-PAGE and named as shown, where T corresponds to triton and C to CHAPS, S for supernatant and P for pellet at the respective stages.

### 3.2.2 RyR purification by ion exchange chromatography

Ion exchange chromatography separates ions and polar molecules, such as proteins, based on their charge. Charged molecules are retained on a column due to ionic interactions with functional groups displayed on the column. The ionic concentration of a solution passed over the column surface can be altered to elute the retained analyte. In cation exchange chromatography, a sodium salt gradient is used, where the increased availability of positively charged sodium ions will displace the positively charged functional group, binding to the negatively charged analyte and allowing it to be collected. When used for protein purification, UV absorbance at  $A_{280}$  is used to track the protein displacement and provide a measurement of peak elution times and quantities. Proteins with a low isoelectric point (pI), the pH at which their

charge is zero, will elute at higher salt concentrations, as they bind more strongly to the column, requiring a greater concentration of sodium ions to displace them.

1 ml bed volume of Source Q anion exchange media was loaded into a column and washed with 10 ml degassed dH<sub>2</sub>O before priming with 10 ml 100% NaCl buffer (buffer B). This media was reused 3 times before changing. The column used provided a positive charge to enable binding of RyR which, at pH 7.4, has a negative charge.

Supernatant containing the solubilised RyR protein was diluted down 8x in volume with buffer A to bring the salt concentration down from 1 M to 125 mM, as RyR would not bind to the column in 1 M NaCl. The preparation was then passed through the anion exchange column using the FPLC (AKTA prime) before elution by application of a salt gradient. The standard protocol for elution of RyR1 involved applying a low salt 'step' (A/B buffer ~ 20% NaCl) to elute the less tightly bound proteins. A gradient was then applied to elute the remaining proteins from the column in as small a volume as possible without compromising on resolution.

RyR2 had a different program to RyR1 as the protein has previously been found to bind less tightly to the column, therefore a 50% NaCl step was used to remove the RyR2 in a small volume (1-3ml) in preference to a gradient to prevent the protein being too dilute for further use.

### **3.2.3 SDS-PAGE analysis of purified RyR protein**

FPLC fractions and solubilisation samples were analysed on 5.5 % SDS-PAGE gels made up using Tris-HCl buffers. The rest of the protocol was completed as per section 2.2.1.

### **3.2.4 Phosphorylation and de-phosphorylation of RyR protein**

Protein Kinase A (PKA) active subunit, Bovine heart: Dissolved in buffer A/B to give 1 active unit/  $\mu$ l. Stored at -20°C in 5  $\mu$ l aliquots. PKA is a serine/ threonine protein kinase.

Protein Phosphatase 1 (PP1): (New England Biolabs), thawed, spun down and stored at -80°C in 2  $\mu$ l aliquots (5 units) Isolated from a source of Ecolab. Releases phosphate groups from protein serine/ threonine/ tyrosine residues. Manganese dependent.

Manganese Chloride (MnCl<sub>2</sub>): 1 mM stock (New England Biolabs), thawed, spun down and stored at -80°C in 44 µl aliquots

Mg/ATP: MgCl<sub>2</sub> 300 µM, ATP 300 µM, dissolved in buffer A/B. Stored at -20°C in 10 µl aliquots.

**Table 3.1 Standard assay mix for phosphorylation and de-phosphorylation using 200 µl purified RyR preparation**

Phosphorylation	Dephosphorylation
200 µl RyR	200 µl RyR
2 µl Mg/ATP	22 µl MnCl <sub>2</sub>
5 µl PKA (5 units)	1 µl PP1 (2.5 units)
16 µl buffer A/B	
Total 223 µl	

The RyR protein to be used in the experiment was divided, with half subjected to phosphorylation by adding Protein Kinase A (PKA), along with Mg/ATP (to provide the phosphate) and buffer A/B, and then incubating on the bench at room temperature for 1 hour. The other half of the protein mix was de-phosphorylated. De-phosphorylation involved incubation for 1 hour with Protein Phosphatase 1 (PP1) and Manganese Chloride (Table 3.1). To confirm efficiency of the phosphorylation and de-phosphorylation protocols, 20 µl samples were taken at 15 minute intervals during the 1 hour incubation period, boiled with 10 µl of 3xSDS-loading buffer for 1 minute and run on 5.5% SDS-PAGE gels along with 20 µl RyR sample for control purposes (section 2.2.1). Western blotting was then carried out using BSA to block instead of Marvel milk as the phosphoserines in the milk interact with the anti-phosphoserine antibody used. The remainder of the protocol was followed as standard (see section 2.2.1.2) with anti-phosphoserine antibody 16B4 (Sigma) alongside an anti-RyR 1093 antibody to determine whether the 1 hour incubation period was sufficient to enable full phosphorylation or de-phosphorylation of the ryanodine receptor. For secondary antibodies see section 2.2.1.2.

### **3.3 Results**

#### **3.3.1 RyR1 solubilisation and purification by anion exchange**

Figure 3.3 shows an increased proportion of RyR1 compared with other SR proteins in sample CS (Figure 3.2) which was loaded onto the FPLC. Contractile protein (~200 kDa) and Ca ATPase (~100 kDa) are still in high abundance but a large quantity of both are present in the triton supernatant (lane 4), which is discarded. This suggests triton is useful for dislodging some SR membrane proteins without removing RyR, as a first step in solubilisation. The triton pellet (Lane 3) was treated with CHAPs and high salt to solubilise the RyR, further cleaning the preparation. Following the FPLC anion exchange, RyR1 was cleaner still. This step enables the detergent concentration to be reduced and although there is still contamination of Ca-ATPase, this protein doesn't bind ryanodine or the FKBP12 used in SPR experiments. Therefore this contaminant protein is not likely to participate in the interactions which are part of this study. The RyR was found to elute over several fractions as the A/B buffer ratio approached 30% (~300 mM NaCl) (black trace line on chromatogram, figure 3.4 A), peaking at fraction 19, as shown by SDS-PAGE analysis (Figure 3.4 B/C). Insertion of a step at ~10% ionic conductivity eluted some of the lower ionic strength proteins (shown by blue line peak on chromatogram), but these are not visible on the SDS-PAGE gel due to the low resolution of smaller sized proteins on 5.5% gels. The quantity of RyR1 eluted was sufficient for [<sup>3</sup>H]ryanodine binding and due to the nature of the [<sup>3</sup>H]ryanodine binding experiments, further purification was not necessary. Fractions containing the highest level of RyR were pooled for experiments. From analysis of the SDS-PAGE gels and the chromatogram, it can be seen that CSQ elutes at a similar ionic strength to the RyR and peaks just before RyR on the trace. These two proteins have proved difficult to separate but generally the RyR peak fraction contains a lower proportion of this contaminating protein. RyR1 has a theoretical pI of 5.1, and is negatively charged at pH 7.0. CSQ has a pI of ~3.6, therefore would possess a similar charge to RyR at the conditions used for ion exchange (pH 7.4), this would explain the overlapping elution profiles, and the fact that calsequestrin elutes a little later than RyR, due to its slightly stronger charge.

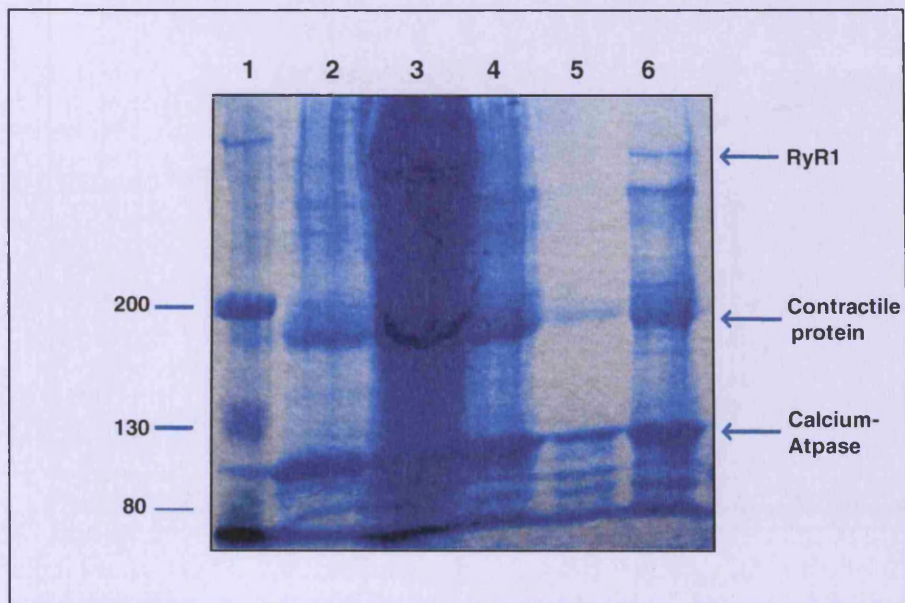


**Figure 3.3 Solubilisation of RyR1 SR microsomes using Triton and CHAPS detergents.** Samples were taken as shown in figure 3.2 and passed through buffer exchange columns (Biorad) to reduce the salt level. Samples were then run on a 5.5 % SDS-PAGE gel. Lane 1, Kaleidoscope protein size marker, sizes are shown on the left in kilodaltons (kDa). Lane 2, sample RyR+T. Lane 3, sample TP. Lane 4, sample TS. Lane 5, sample CP. Lane 6, sample CS. RyR protein is indicated on the gel.

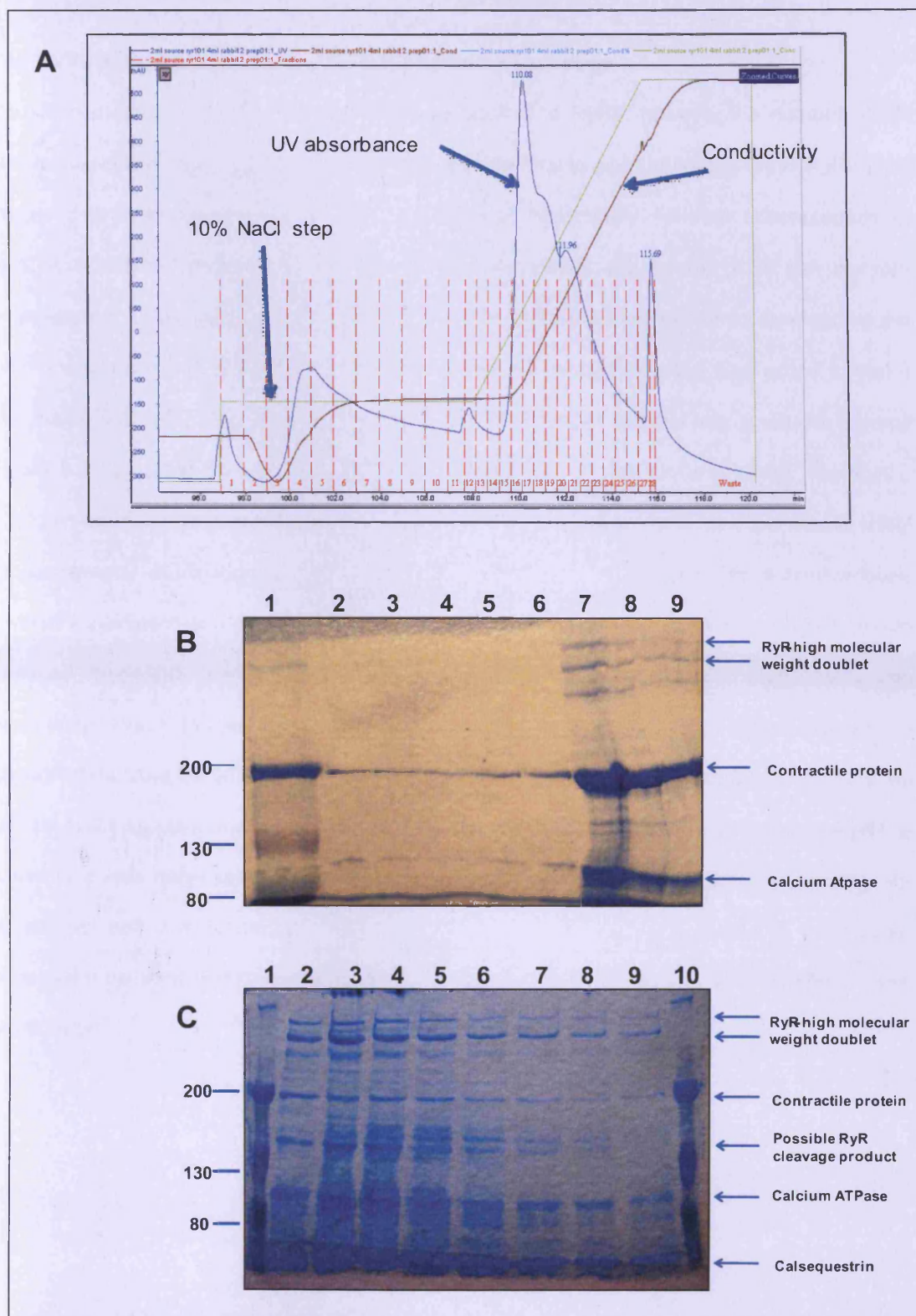


**Figure 3.4 RyR1 purification by anion exchange chromatography**

**A)** RyR1 elution chromatogram. Following solubilisation RyR preparation was passed over ion exchange resin in 125 mM NaCl on an AKTA Prime FPLC. A 20% salt step was used to elute the majority of weakly bound proteins so that the RyR could be eluted in as small a volume as possible along a continuous salt gradient. Green line shows salt gradient program, black line is actual salt conductivity and blue line is UV absorbance.

**B)** and **C)** 1 ml samples of eluate were collected and analysed on 5.5% SDS-PAGE gels. Lane 1, Kaleidoscope protein size markers, sizes are shown on the left (kDa). Gel B, Lanes 2-9 correspond to fractions 10-17. Gel C, Lanes 2-9 correspond to fractions 18-25. RyR protein is indicated on both gels, as well as Calcium ATPase and CSQ proteins. RyR is shown to peak in fraction 19.

### 3.3.2 RyR2 solubilisation and purification by anion exchange

The same protocol for RyR1 solubilisation was applied to RyR2, however the number of SR samples processed was typically doubled from 4 ml to 8 ml to account for the lower RyR2 yield compared to RyR1, buffer volumes were also adjusted accordingly. Although concentrations of RyR2 in microsomal preparations may be 10x lower than RyR1, the number of SR samples was not increased 10 fold due to volume limitations of the anion exchange column. Overloading the column would result in a decreased resolution. The FPLC program used also varied in that a 50% NaCl (500 mM) step was used to elute the RyR2 more sharply into a smaller volume (Figure 3.5 A), rather than allowing it to elute slowly over a continuous gradient (like RyR1) which has been shown to result in eluate that has too low a yield of RyR2 for experiments. Initial chromatography purification of RyR2 was done using a 1 ml column with a narrow bore, however experimentation with a wider bore column showed an increased yield of RyR2, due to increased resolution, therefore this was used in proceeding purifications. RyR2 yield was consistently found to be lower than that of RyR1, and always on the threshold for experimentation but the SDS-PAGE gel (Figure 3.5B) shows one of the better runs obtained. As 500 mM NaCl was required to elute RyR2, rather than the 300 mM NaCl used to elute RyR1, a dilution step was necessary before this sample was used in further experiments to control for the relative salt concentrations. RyR was found to stick to membranes of commercial concentrator columns and therefore experiments with this isoform were somewhat limited in this investigation.

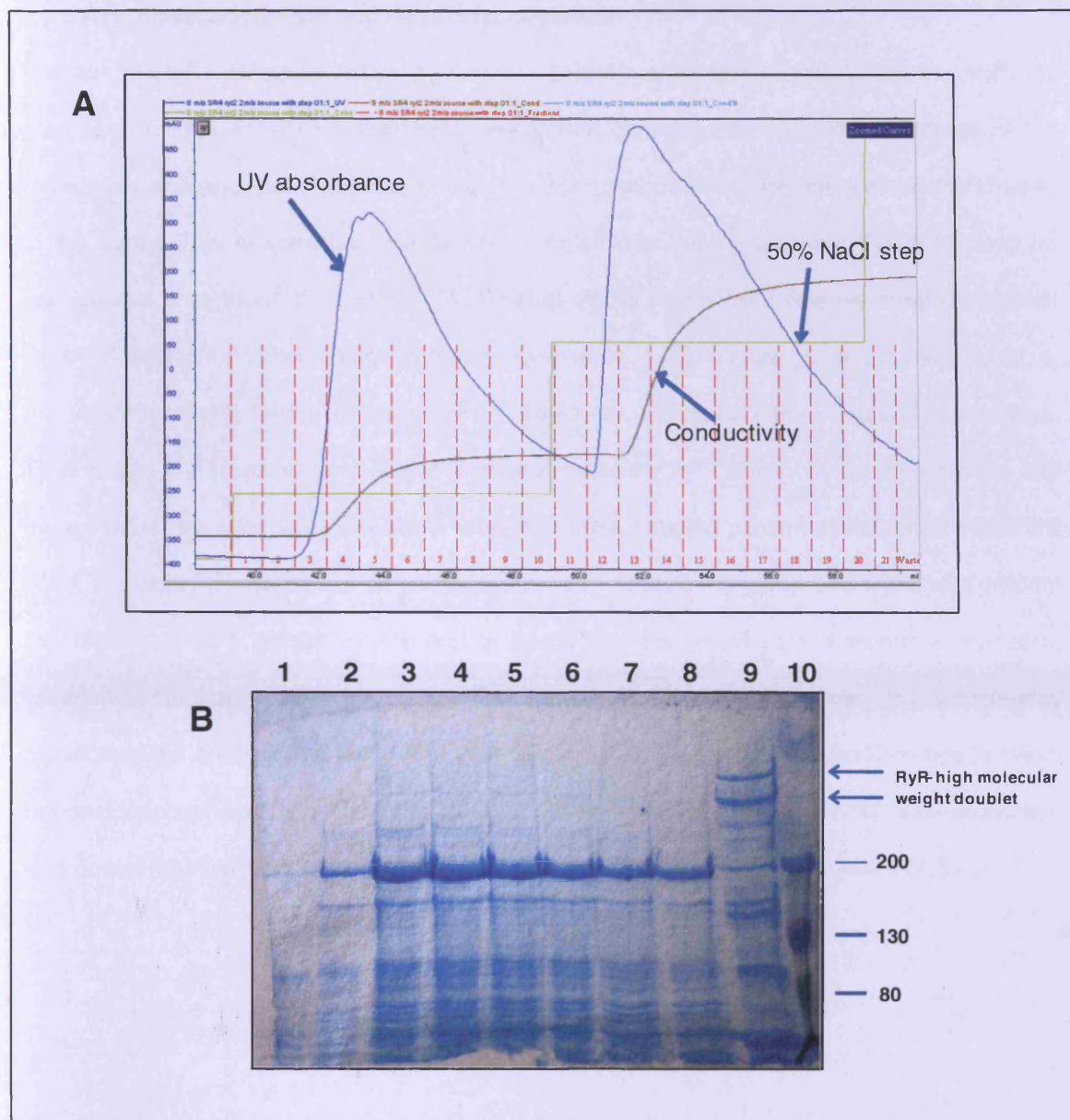


**Figure 3.5 RyR2 purification by anion exchange chromatography**

**A)** RyR2 elution chromatogram. Following solubilisation RyR2 preparation was passed over ion exchange resin in 125 mM NaCl on an AKTA Prime FPLC. A 20% salt step was used to elute the majority of weakly bound proteins and then a 50% NaCl step was used to elute the RyR2 specifically. The 50% salt step ensures the protein is all eluted into as small a volume as possible. Green line shows salt gradient program, black line is actual salt conductivity and blue line is UV absorbance.

**B)** 1 ml samples of eluate were collected and analysed on 5.5% SDS-PAGE gels. Lanes 1-8 correspond to fractions 10-17, RyR peaks at fraction 13. Lane 9, RyR1 sample run as a control marker. RyR bands are highlighted. Lane 10, Kaleidoscope protein size markers, sizes are shown on the right in (kDa).



### 3.3.3 RyR phosphorylation and de-phosphorylation

Analysis of RyR1 phosphorylation by western blotting using an anti-phosphoserine antibody showed that PKA activity on the RyR1 preparation continued for the full 90 minutes of the experiment and also that there was substantial endogenous phosphorylation of the RyR1 used in this study. This is quite unusual for RyR1 which has been previously shown to have no endogenous phosphorylation (Jones, D'Cruz et al. 2007). Therefore it was necessary to strip all RyR1 of phosphorylation using protein phosphatase 1 (PP1), as done by Blayney et al previously for RyR2 before experiments to provide an adequate control baseline for assays. Time course A in figure 3.6 shows that after 40 minutes the PP1 activity seemed to stabilise and though there was substantial decline in phosphoserine-detected phosphorylation, there was still some remaining. However, as all preparations were treated the same and there was evident stabilisation of PP1 activity by the end of treatment, this would have ensured a consistent baseline at the start of all experiments. The degree of phosphorylation was also considerably higher than the endogenous level after PKA treatment so there was a large difference between the de-phosphorylated and phosphorylated RyR1 for experiments. The RyR2 phosphorylation time course was very difficult to obtain due to the low yield problems mentioned in 4.3.2.

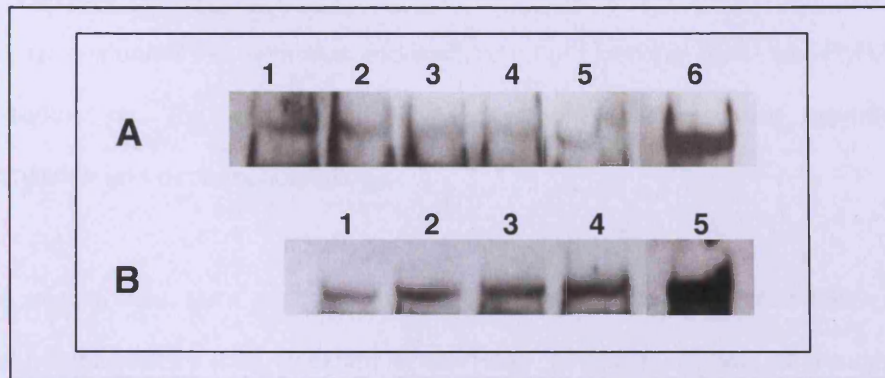


**Figure 3.6 RyR1 phosphorylation time course western blot**

**A)** RyR1 dephosphorylation. Purified RyR1 preparation was incubated with Protein Phosphatase 1 as per table 3.1 for a total of 90 minutes, samples were taken at  $t=0$ , 20, 40, 60 and 90 minutes and boiled with SDS loading buffer to stop enzyme activity. Samples were then run on a 5.5% SDS-PAGE gel, transferred to a nitrocellulose membrane and blotted with an anti-phosphoserine antibody. Lanes 1-5, 0-90 minutes. Lane 6, RyR1 control blotted with anti-RyR1 antibody ( $n=1$ ).

**B)** RyR1 phosphorylation. Purified RyR1 preparation was incubated with Protein Kinase A for a total of 90 minutes, samples were taken at  $t=0$ , 30, 60 and 90 minutes and boiled with SDS loading buffer to stop enzyme activity. Samples were then run on a 5.5% SDS-PAGE gel as for the dephosphorylation and subjected to the same antibodies. Lanes 1-4, 0-90 minutes. Lane 5, RyR1 control ( $n=1$ ).

### **3.4 Discussion**

This chapter evaluated the extraction and purification of functional RyR1 and RyR2 from native animal tissue and the preparation of this protein for subsequent experiments using phosphorylation and dephosphorylation.

RyR SR microsomes were successfully extracted from the native tissue following protocols previously employed by (Lai, Erickson et al. 1988). However, instead of a sucrose gradient purification stage, to prepare 'heavy SR', which has been shown to enrich the junctional SR where the RyR is predominant, a KCl step was added to solubilise contaminating contractile protein. It could have been advantageous to use sucrose density gradients as part of the microsomal purification step but this technique is suitable for preparations from small animals (e.g. rats or mice), however for preparations of microsomes from pig hearts or rabbit skeletal muscle with 500 g of starting tissue this would have proved an unwieldy step. SR microsomes were treated with a combination of detergents (Triton X-100 and CHAPS), and the lipid phosphatidylcholine to solubilise RyR for use in experiments. This protocol also allowed for the addition of FK506 to strip the RyR1/2 of endogenous FKBP12/12.6 and their removal during subsequent purification steps (Jones, Reynolds et al. 2005) FPLC purification of RyR using anion exchange gave a consistent and sufficient yield of RyR1.

RyR2 purification efficiency seemed to vary between different heart preparations which may mean that there was some fluctuation in the efficiency of the RyR2 extraction from the microsomal preparation. Solubilisation buffers were found to vary in their RyR purification efficacy if the supplier of CHAPS varied and the source of the phosphatidylcholine (egg yolk rather than soy bean) changed. But these changes were noted early in the investigation and amended accordingly. Modification of the standard RyR1 protocol by use of a wider bore FPLC column and sharp elution at 50% NaCl was shown to yield sufficient RyR2 in some instances, but was not reliably consistent. Three usable purified RyR2 preparations were obtained from one batch of pig hearts. The following batch processed did not provide sufficient purified RyR2 from the microsomes to use in further experiments, the reasons for this can only be speculative. Pig hearts were handed to us immediately after slaughter at the abattoir and appeared to be of

consistent size. However, the abattoir is a small one and we cannot be certain that each batch of pigs is of the same breed or age, this may have been an important variable. The RyR2 level within the microsomal preparations also appeared to be low, meaning that detecting even this protein by western blot was a challenge. Given that the solubilisation procedure is unlikely to result in 100% extraction of RyR, the starting material needs to be very RyR rich to account for any loss during solubilisation and subsequent purification stages, if the starting material is variable and sometimes poor, then this would explain the consistent problem. Although the RyR2 phosphorylation time course western blot could not be obtained due to the low yield of this protein, the enzymes have been shown to work for RyR1 and there is no reason why they should have reduced efficacy for the RyR2 preparation used. Figure 3.6 shows the RyR1 phosphorylation for  $n=1$ , however this experiment was performed merely as confirmation of results obtained previously on a different batch of rabbit preparations (Blayney, Jones et al. 2010), to test that the protocol was still valid in this instance. Ideally the blot should be repeated in the presence of a loading control to ensure protein amount is not variable across the time course western blot. It should be noted however that all lanes were loaded from the same RyR1 and enzyme stock, therefore variability in protein quantity should be minimal.

The amount of endogenous RyR1 phosphorylation changed over the course of the study. In the early experiments no endogenous phosphorylation was detected. Skeletal muscle for microsomal preparation was sourced from rabbits which were used after sacrifice, and subsequent removal of vascular material, by another group. The experimenter changed, and higher background levels of phosphorylated RyR1 were noted. As a result, for all the work in this thesis, the protocol was changed and PP1 was then used to dephosphorylate preparations, and PKA to phosphorylate them, for matched experiments (see future chapters).

**Chapter 4; Physiological modulators  
of RyR1 activity**

## **CHAPTER 4; Physiological modulators of RyR1 activity**

### **4.1 Introduction**

RyR activity is subject to regulation by a large number of biochemical and protein modulators. It is also directly modified by protein kinase phosphorylation and redox potential. The relationship between FKBP12/12.6 and PKA phosphorylation of RyR channels has been previously assessed by this group as these two modulators have been linked to the pathology of CPVT and RyR1/RyR2 dysfunction (Blayney, Jones et al. 2010). This investigation aims to put these changes in the context of the domain interaction hypothesis. The intention was to look at domain peptide modulation of the same RyR preparations used in previous studies of our group (Jones, Reynolds et al. 2005; Blayney, Jones et al. 2010) and to study peptide interaction with other channel modulators including calcium, FKBP12, magnesium and ATP.

FKBP12, a *cis-trans* peptidyl-prolyl isomerase, was first identified by its copurification with the RyR1 (Collins 1991) and is now well documented as a potent and important regulator of RyR1 function. Single channel bilayer studies have demonstrated its ability to stabilise and inhibit channel activity and thus reduce open probability (Brillantes, Ondrias et al. 1994). FKBP12 has greatest affinity for the RyR channel in its closed state, but retains a high affinity for the channel in the open state, as shown in recent work by our group (Jones, Reynolds et al. 2005). Four FKBP12 molecules can bind to an RyR homotetramer, with one binding per subunit (Jayaraman, Brillantes et al. 1992), however to date the region of FKBP12 binding to RyR1 has yet to be elucidated. Electron cryomicroscopy and three-dimensional reconstruction have shown these four FKBP12 molecules to bind close to the N-terminus of the RyR (Wagenknecht, Radermacher et al. 1997). The site of FKBP12 binding to RyR was originally thought to be in the central domain around a leucine-proline motif at site 2407-2520 (Cameron, Nucifora et al. 1997), which corresponds to the proposed site of binding on the inositol (1,4,5) tris phosphate receptor. Mutations in this area were shown to decrease FKBP12 binding (Gaburjakova, Gaburjakova et al. 2001) and in the context of this study, this proposed binding region is within the DP4 peptide. Topology studies then suggested that the central domain cluster (2246-2534) mapped to the N terminus region, which alleviated the likelihood of the FKBP12 binding site for RyR1 being in this region of the central domain (Wagenknecht, Radermacher et al. 1997).

Hence precise definition of the FKBP12 binding site has not yet been determined, and further structural analysis is required.

FK506 is able to inhibit interaction of FKBP12 with RyR by binding to the FKBP12 molecule at its binding site (Chelu, Danila et al. 2004). FK506 was found to increase channel open probability in single bilayer studies and sub-conductance states were reported in some instances, suggesting that inter subunit interactions of RyR occur which may be stabilised by the binding of FKBP12 (Brillantes, Ondrias et al. 1994). FKBP12 may also play a role in coupled gating of RyRs, given its ability to coordinate channel opening in bilayer studies. The location of the proposed FKBP12 binding site is distinct from the region of RyR-RyR interaction, suggesting it is able to exert an effect via allosteric modification of the neighbouring channels (Marx, Gaburjakova et al. 2001).

Loss of FKBP12 from RyR1, linked to aberrant calcium handling in skeletal myocytes, has been attributed to hyperphosphorylation of RyR1 by one group. Wehrens et al have shown defective function of RyR1 channels in HF skeletal muscle, analogous to those in RyR2 channels in failing myocardium. This manifested as PKA hyperphosphorylation and depletion of FKBP12, as well as a gain of function channel defect, and has been proposed as a key factor in the limited exercise capacity seen in patients with RyR2-linked cardiomyopathies (Wehrens, Lehnart et al. 2005). The pertinence of RyR1 in cardiac ECC was originally suggested by the finding that FKBP12 null mice showed no apparent defect in the skeletal muscle, yet were shown to exhibit severe developmental cardiac defects. Therefore it seems there is an important physiological link between RyR1 and RyR2 modulation. The anti-arrhythmic drug K201 (JTV519) has been shown to increase skeletal muscle function, possibly by enhancing FKBP12 binding (Wehrens, Lehnart et al. 2005). Another drug, S107, which is a calcium channel stabiliser, has been proposed to preserve the binding of FKBP12 to RyR1 and was shown to increase the exercise capacity of WT mice, but not FKBP12 K/O mice, suggesting a mode of function involving interaction with FKBP12 (Bellinger, Reiken et al. 2008).

Biacore technology has been used by (Jones, Reynolds et al. 2005) to measure the equilibrium binding kinetics of interaction between RyR1 and FKBP12. It was shown that the affinity of solubilised RyR1 for FKBP12 is lower for the open channel than for the closed, this was also true for RyR2 (Jones, Reynolds et al. 2005; Blayney, Jones et al. 2010). PKA phosphorylation was found to shift the affinity of the closed channel for FKBP12/12.6 to the lower affinity of the open channel, however, the affinity for the open channel remained high. It was concluded that this shift in affinity was part of the normal 'fight or flight' response mechanism, linked to  $\beta$ -AR stimulation of PKA phosphorylation. The data was suggested to demonstrate a change in RyR conformation caused by PKA phosphorylation, possibly a molecular movement towards a state which favours the open/closed transition. (Jones, Lai et al. 2006). A similar mechanism was suggested in single channel studies (Valdivia, Kaplan et al. 1995).

Calcium is known to be the main modulator of the RyR1 channel and the biphasic dose response, with maximal activation occurring at micromolar free calcium, in the absence of other regulatory ligands, has been well documented in the literature. Such a curve suggests that the calcium release channel possesses high-affinity activating and low-affinity inhibitory calcium binding sites (Meissner, Lai et al. 1990). In single channel studies, the channels open probability ( $P_o$ ) was close to zero with nanomolar free calcium on the *cis* (SR cytoplasmic) side of the bilayer. Addition of micromolar calcium to the *cis* chamber activated the channel and induced rapid channel openings and closings. The presence of millimolar calcium in the *cis* chamber resulted in channel inactivation (Meissner 2002). Ryanodine binding studies have also shown a bimodal regulation of the RyR by calcium (Meissner, Lai et al. 1990) (Meissner review 1994).

CICR has been found to be greatly potentiated by relatively high (mM) levels of ATP and optimal channel activation has been found in the presence of  $\mu$ M calcium and mM ATP. Bull et al. have demonstrated that *cis*-ATP addition of 3 mM decreased the threshold for calcium activation, increased maximal open probability and shifted channel inhibition to higher calcium in single channel bilayer studies (Bull, Finkelstein et al. 2007). However, it is likely that magnesium-ATP, rather than free ATP, is a major physiological regulator of the RyR channel because most of the ATP in cells is complexed with magnesium (Meissner 2002).



Conversely, cytoplasmic magnesium has consistently been found to inhibit the RyR channel, suggesting RyR1 activation is strongly inhibited by magnesium under physiological conditions in resting muscle. Magnesium is a permeant cation of the RyR and likely inhibits the channel by a dual mechanism involving competing with calcium for the calcium activation site (H-site) and also binding to the low affinity calcium inhibitory site (I-site) (Meissner and Henderson 1987). It has been suggested that the physical activation of RyR1 by the LCC may reverse the magnesium block and thus permit activation by ATP and calcium (Lamb and Stephenson 1991). Further to this, a study was carried out with peptides impeding the region of interaction between the LCC and RyR1 (C-region), showing a decreased sensitivity of the RyR for magnesium inhibition and suggesting the LCC may be the key determinate of magnesium control if it reduces the magnesium affinity of the regulatory sites on RyR1 (Haarmann, Dulhunty et al. 2005).

Caffeine has been reportedly unable to induce maximal calcium release from the SR at physiological magnesium levels suggesting activators of the RyR must first overcome magnesium inhibition before calcium release can occur. Thus magnesium may serve to stabilise CICR between periods of activation (Lamb, Cellini et al. 2001). Assessment of MH susceptible porcine muscle has shown a decreased sensitivity to magnesium inhibition and another group have shown this to be a common feature in human MH (Laver, Baynes et al. 1997; Duke, Hopkins et al. 2002).

One study has tested the effect of the anaesthetic halothane on magnesium inhibition, given that volatile anaesthetics, such as halothane, are the key trigger of MH. The results suggest that halothane induced calcium release from the SR in skeletal muscle is strongly reduced in the presence of physiological magnesium concentrations, however, when this level is reduced, halothane induced a marked efflux of calcium from the SR and resultant calcium waves. Given the reported reduction in magnesium inhibition evident in MH patients, this finding may be highly significant (Duke, Hopkins et al. 2003).

Bull et al. have shown inhibition of [<sup>3</sup>H]ryanodine binding in the presence of 1 mM magnesium on RyR from the rat brain cortex (Bull, Finkelstein et al. 2007) and single channel studies have suggested that luminal calcium may influence RyR1 gating by an indirect mechanism involving reduction of the affinity of the cytosolic calcium activation site for magnesium. This would be explained by an allosteric, non-competitive effect, suggesting conformational change to mask/un-mask the magnesium binding site (Laver, O'Neill et al. 2004).

The idea of a conformational change is also supported by studies assessing the effects of phosphorylation on magnesium inhibition. Phosphorylation has been shown to overcome the magnesium inhibition (Hain, Onoue et al. 1995; Uehara, Yasukochi et al. 2002), as has the central domain peptide (DP4) (Yamamoto, El-Hayek et al. 2000), suggesting central domain involvement as a potential regulator of a magnesium binding site. Given that PKA phosphorylation was also reported to modify the channels affinity for FKBP12 while remaining in a closed state, this suggests the same conformational change may mask the magnesium binding site prior to channel opening (Blayney, Jones et al. 2010). This idea is also supported by a fluorescence quench study (Yamamoto and Ikemoto 2002).

ATP has been shown to overcome magnesium inhibition on isolated RyR1 from rabbit skeletal muscle (Jóna, Szegedi et al. 2001) and in one study carried out (Dias, Szegedi et al. 2006) 8 ATP binding sites per one RyR homotetramer were proposed, with 2 different types of ATP site per each RyR monomer, this has also been suggested by ligand binding functional studies (Laver, Lenz et al. 2001). Biphasic activation of RyR in response to increasing concentrations of ATP has implied different classes of ATP binding sites (Jóna, Szegedi et al. 2001) but the study by Dias et al. links this to magnesium inhibition. This work suggests that in the presence of activating calcium and inhibitory magnesium, all 8 ATP sites are available and occupied, but at inhibitory calcium concentrations, in addition to inhibitory magnesium concentrations, only 4 of these sites are occupied, in spite of high ATP concentration. Dias et al propose that occupation of all 8 ATP binding sites links to an open or 'opening' channel. This work ties in with a theory of conformational change of the RyR caused by the presence or absence of calcium or magnesium, which may be the cause of varied accessibility of ATP binding, resulting in maximal

binding of either 4 or 8 ATP molecules. Binding ATP may then stabilise the open or closed conformation (Dias, Szegedi et al. 2006). Alternatively, the opening or closing events may be the result of conformational changes caused by ATP binding. The group hypothesizes that binding of 4 ATP sites per RyR tetramer is most likely linked to closure of the channel and hence increased channel stability.

In spite of the above evidence suggesting that both FKBP binding and ATP binding to RyR may result in a conformational change, modifying the propensity for an open or closed channel, few studies have combined FKBP12 with magnesium and ATP to determine their combined effect. This is of particular interest in the context of this project, which aims to identify the possible region of convergent regulation of the RyR as put forward by Blayney et al. (Blayney, Jones et al. 2010).

Before domain peptides could be included in experiments, it was necessary to determine the effect of these physiological modulators individually and in combination. In order to assess the functionality of the channels prepared for this investigation, they were first assessed for their dose response to free calcium concentrations. The calcium concentration found to maximally open the channel then served as the chosen concentration at which the effects of other RyR channel modulators were assessed. The fact that the control channel was already open meant that both inhibitors and activators could exhibit their effects.

The aim of this chapter is to assess the effects of physiological modulators shown previously to modify channel gating, on isolated RyR1 channels. Modulators were examined both individually, and in addition to one another. This chapter will first look at activators of the RyR1, that is calcium and ATP and then analyse the effects of the physiological inhibitors; FKBP12 and magnesium on ryanodine binding of RyR1. The FKBP12 protein for this study was produced and purified in house from a ready-made construct (ref to methods). This chapter will provide baseline data for the subsequent studies using [<sup>3</sup>H]ryanodine binding to examine the effects of inhibitory peptides (Chapter 6).

## 4.2 Results

### 4.2.1 RyR1 dose response to free calcium

Ryanodine binding demonstrated that solubilised RyR1 channels exhibited the standard calcium biphasic dose response (Figure 4.1). For the calcium buffers used in this study, it would seem pCa4 opened the channel maximally. Therefore this calcium concentration was used to provide the 100% control in the experimental model. Assays were carried out on both PKA phosphorylated and PP1 dephosphorylated RyR and no significant difference was found in these conditions. Blayney et al. have documented previously that phosphorylation effects are rarely seen in [<sup>3</sup>H]ryanodine binding assays, but differences are sometimes unmasked using a more sensitive technique SPR (Biacore) kinetic analysis (Jones, Lai et al. 2006).

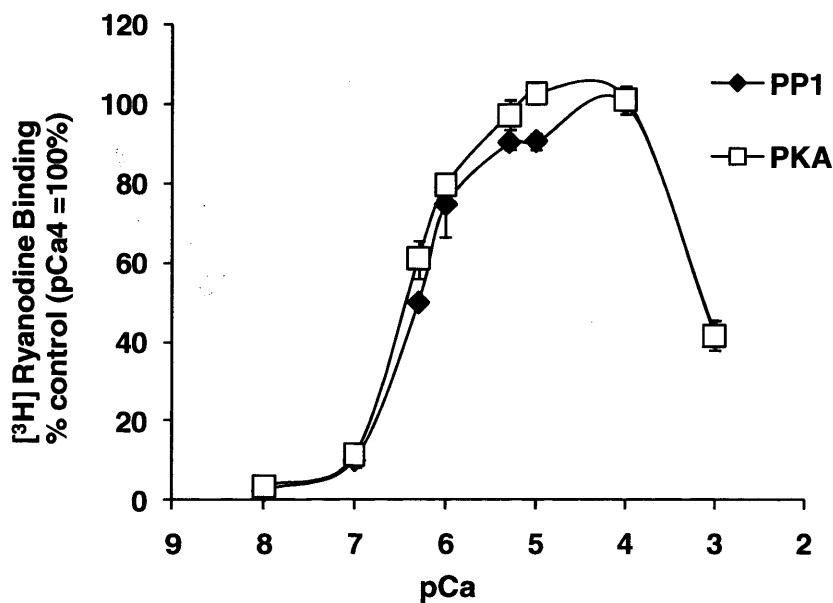


**Figure 4.1 RyR1 biphasic response to free calcium (pCa), demonstrated by [<sup>3</sup>H] ryanodine binding**  
Each point represents the mean of 3 RyR1 preparations. (pCa 4 is taken as 100%). Bars show standard error.

#### 4.2.2 RyR1 and dose response to ATP addition

ATP was shown to activate the channel over and above that at pCa4 (Figure 4.2A), suggesting full opening of the channel only occurs in the presence of both calcium and ATP. 2.5 mM ATP increased ryanodine binding maximally and it was then observed that increasing the ATP concentration further actually reduced [<sup>3</sup>H]ryanodine binding. The effect of ATP on the free calcium dose response curve showed a significant activation across all concentrations (Figure 4.2B). There were no differences between phosphorylated and dephosphorylated preparations.

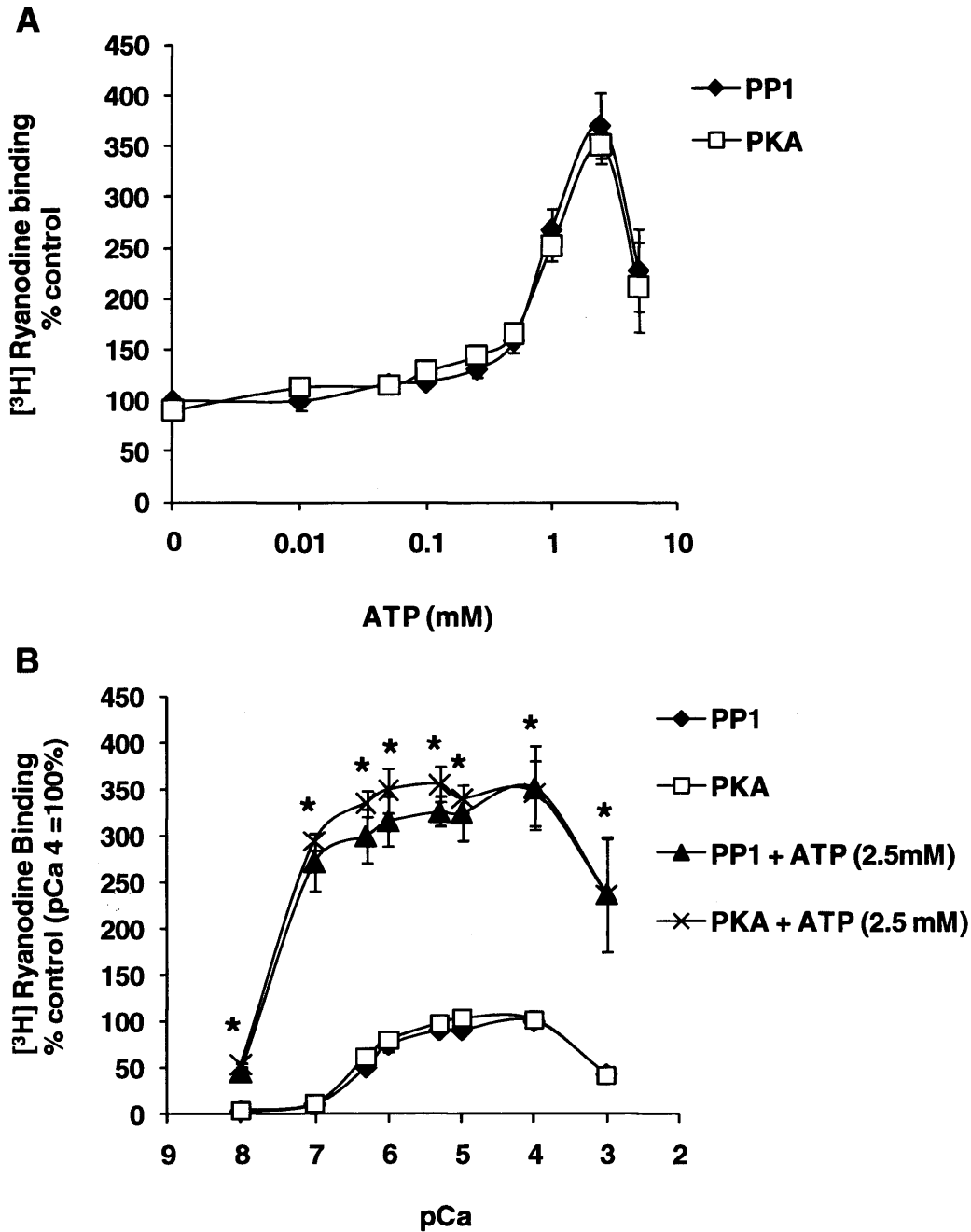


**Figure 4.2 Effect of ATP on RyR1 [<sup>3</sup>H] ryanodine binding. A) ATP dose response. Each point represents the mean of 6 RyR1 preparations. B) ATP effect on binding across the calcium biphasic response. Calcium response is shown in the presence and absence of 2.5 mM ATP. Each point represents the mean of 3 RyR1 preparations. (\*) indicates a significant difference ( $p < 0.05$ , students paired t-test) from the equivalent value on the calcium dose response without ATP addition. (Binding in pCa4 is taken as 100%). Bars show standard error.**

### 4.2.3 FKBP12 protein production and purification

To determine the effects of the protein modulator FKBP12, this was first prepared as a recombinant protein. FKBP12 had previously been cloned into pGEX-6P-1. FKBP12-GST protein was successfully grown in Rosetta and induced at 30°C for 3 hours. Following incubation of bacterial lysate colonies containing the FKBP12-GST protein with glutathione sepharose beads, samples were shown to contain sufficient quantities of FKBP12 by SDS-PAGE. 3C protease cleavage was effective, as shown by the lower band on the gel, however separation of the cleaved protein eluate and the beads showed there to be a large amount of residual uncleaved 3C and GST (Figure 4.3A). Gel filtration chromatography separates proteins based on their size and so this was used with a view to separate the protein contaminants from the cleaved FKBP12 protein. An S75 column was used but although FKBP12 was eluted in later fractions, there was considerable overlapping contamination. Figure 4.3B clearly shows contamination of FKBP12 protein which has been eluted along fractions 1-8. The chromatogram UV trace shows the protein eluting on the shoulder of the UV peak (Figure 4.3C), insufficiently resolved from 3C and GST. As the chromatography separation was incomplete, more glutathione sepharose beads were added back to the protein mixture to remove the GST-tagged 3C and cleaved GST by further affinity purification. Glutathione sepharose beads have a limited capacity so it was possible that with the large quantity of FKBP12-GST protein produced, the beads on the first affinity purification step were saturated. This was effective and figure 4.4 shows the clean protein eluted from the beads. Protein identity was confirmed by western blot analysis using an anti-FKBP12 specific antibody and protein quantity was estimated by running dilutions of FKBP12 alongside known quantities of BSA control (Approximately 4 mg/ml).

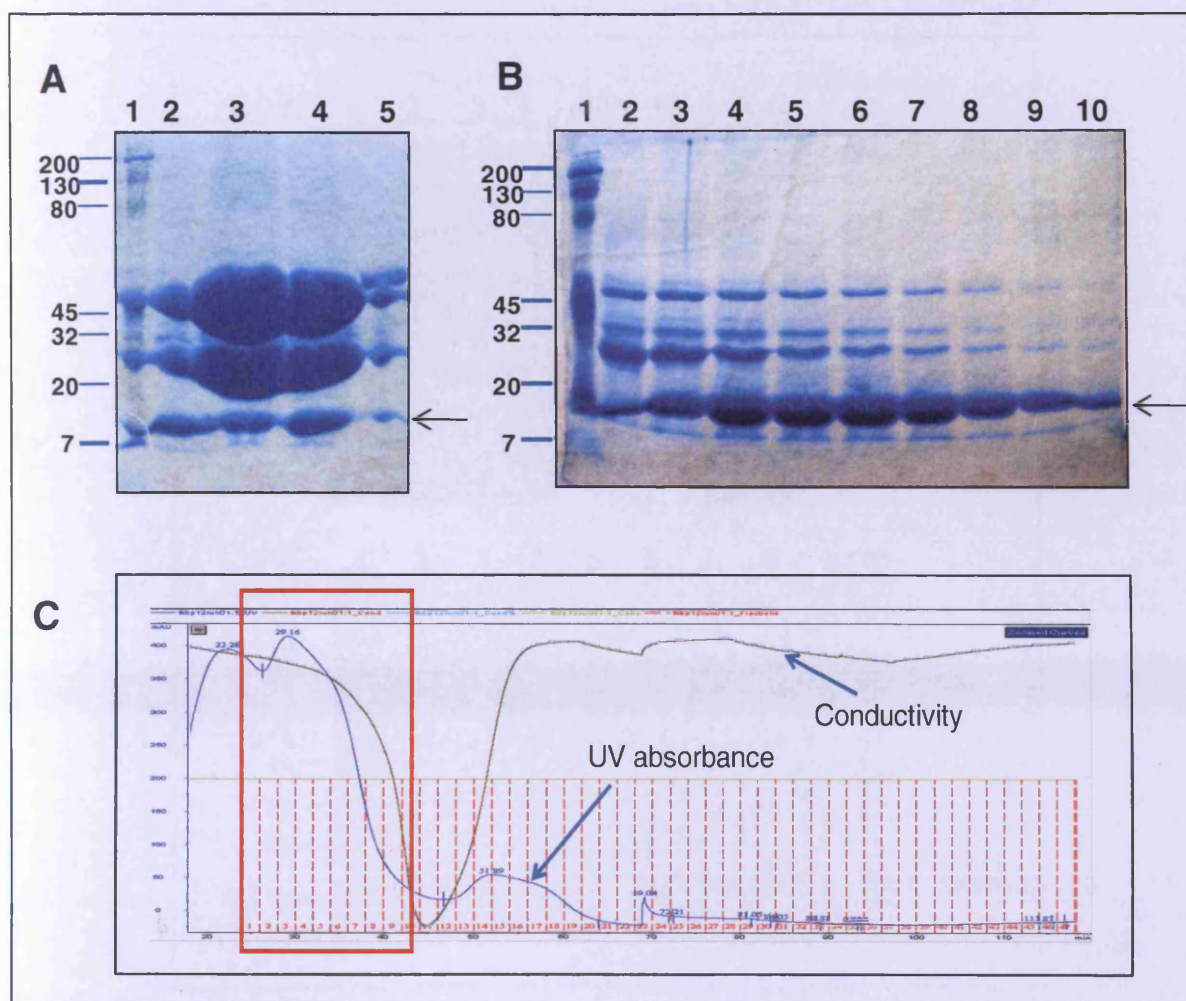


**Figure 4.3 FKBP12 cleavage with 3C protease and purification by gel filtration chromatography**

**A)** Samples were collected before and after cleavage of FKBP12-GST with 3C protease and analysed by running on an 18% SDS-PAGE gel. Lane 1, Kaleidoscope protein size marker, sizes are indicated on the left (kDa). Lane 2, mixture of cleaved FKBP12 (12 kDa), GST (26 kDa) and 3C-GST (48 kDa) following overnight incubation and prior to separation. Lanes 3 and 4, eluate containing cleaved FKBP12 after filtration of the GST beads and contaminating GST and 3C-GST. Lane 5, washed beads showing GST and 3C-GST and some residual cleaved FKBP12 due to inefficient washing. Arrow indicates FKBP12.

**B)** Gel filtration chromatography was used to further purify the cleaved FKBP12. Eluate was collected in 1 ml fractions and samples from each fraction were separated on a 15% SDS-PAGE gel for analysis. Lane 1, Kaleidoscope protein size marker, sizes are shown on the left (kDa). Lanes 2-10 correspond to fractions 1 to 9 on the FPLC trace (highlighted in red). FKBP12 elution peaks across fractions 3, 4 and 5. Arrow indicates FKBP12.

**C)** FPLC trace showing the elution profile for FKBP12 from an S75 gel filtration column. The blue line represents UV absorbance, smaller proteins are eluted last. The black line represents salt conductivity.



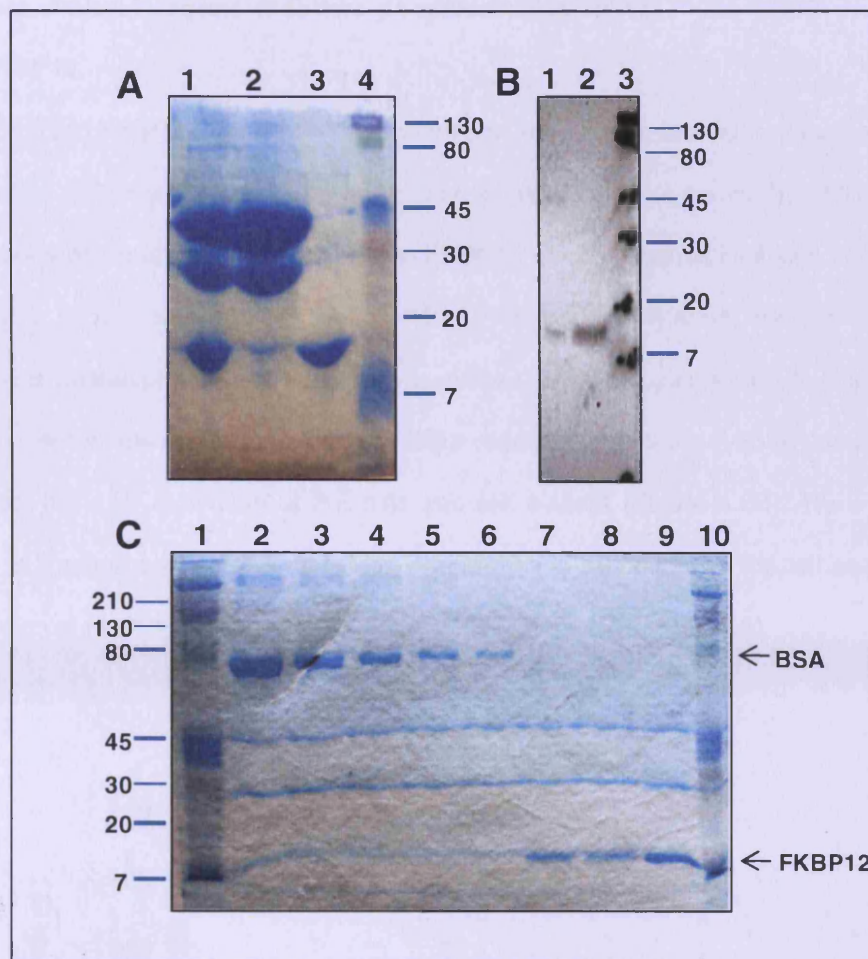


**Figure 4.4 FKBP12 further affinity purification, confirmation by western blot and quantification.**

**A)** FKBP12 eluate was incubated for a second time with GST beads. Samples were taken and separated on a 15% SDS-PAGE gel for analysis. Lane 1, mixture of cleaved FKBP12 (12 kDa), GST (26 kDa) and 3C-GST (48 kDa) following overnight incubation and prior to separation. Lane 2, washed beads showing GST and 3C-GST and very little residual FKBP12 protein. Lane 3, FKBP12 eluate showing very little contaminating protein. Lane 4, Kaleidoscope protein size marker, sizes are shown on the right (kDa).

**B)** FKBP12 was transferred to a nitrocellulose membrane and blotted with an FKBP12 specific antibody to confirm presence of the correct protein. Lane 1, FKBP12 preparation diluted 10x. Lane 2, neat FKBP12. Lane 3, protein size markers, sizes are shown on the right (kDa).

**C)** Bovine serum albumin (BSA) standards were run alongside FKBP12 recombinant protein to provide an estimate of quantification. Samples were run on a 15% SDS-PAGE gel. Lanes 1 and 10, Kaleidoscope protein size marker, sizes are given on the left (kDa). Lanes 2-6, serial dilutions of BSA (66 kDa); 2, 20 μg, 3, 10 μg, 4, 5 μg, 5, 2.5 μg, 6, 1.25 μg. Lane 7, Cleaved FKBP12 (12 kDa) 1:10 diluted. Lane 8, FKBP12 1:20 diluted. Lane 9, FKBP12 1:50 diluted.

### 4.2.3 Effect of physiological inhibitors on activators of RyR1

#### 4.2.3.1 FKBP12

The recombinant FKBP12 generated in this chapter was shown to inhibit ryanodine binding by approximately 50% (Figure 4.5). The specificity of this result was shown by addition of FK506 control protein which effectively inhibited the FKBP12 effect. Maximal inhibition of [<sup>3</sup>H]ryanodine binding was shown with 1 μM of FKBP12. PKA phosphorylation showed no difference compared to dephosphorylated preparations. When FKBP12 was added in the presence of varying concentrations of ATP there was a slight reduction in binding (~25%) compared with the ATP control but ATP activation at 2.5 mM was still evident (Figure 4.6B). The FKBP12 dose response in the presence of 2.5 mM ATP was shown to be shifted to the left so that a higher concentration of FKBP12 was required to see 50% inhibition (Figure 4.6A).

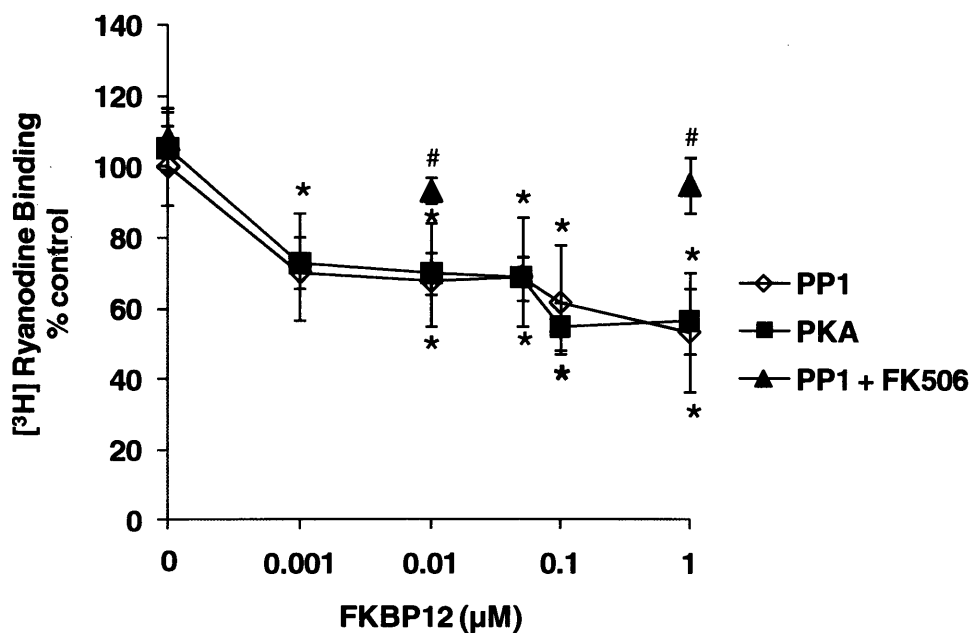


**Figure 4.5 Effect of FKBP12 on RyR1 [<sup>3</sup>H]Ryanodine binding. FKBP12 dose response.** Each point represents the mean of 7 RyR1 preparations. (\*) indicates a significant difference from the control value ( $p < 0.05$ , students paired t-test) without FKBP12 addition. There was no significant difference between PP1 and PKA treatments. (Binding in pCa4 is taken as 100%). 10 μM FK506 was added as a control for specificity. (#) indicates a significant difference ( $p < 0.05$ , students paired t-test) from the equivalent value without FK506 addition. Bars show standard error.

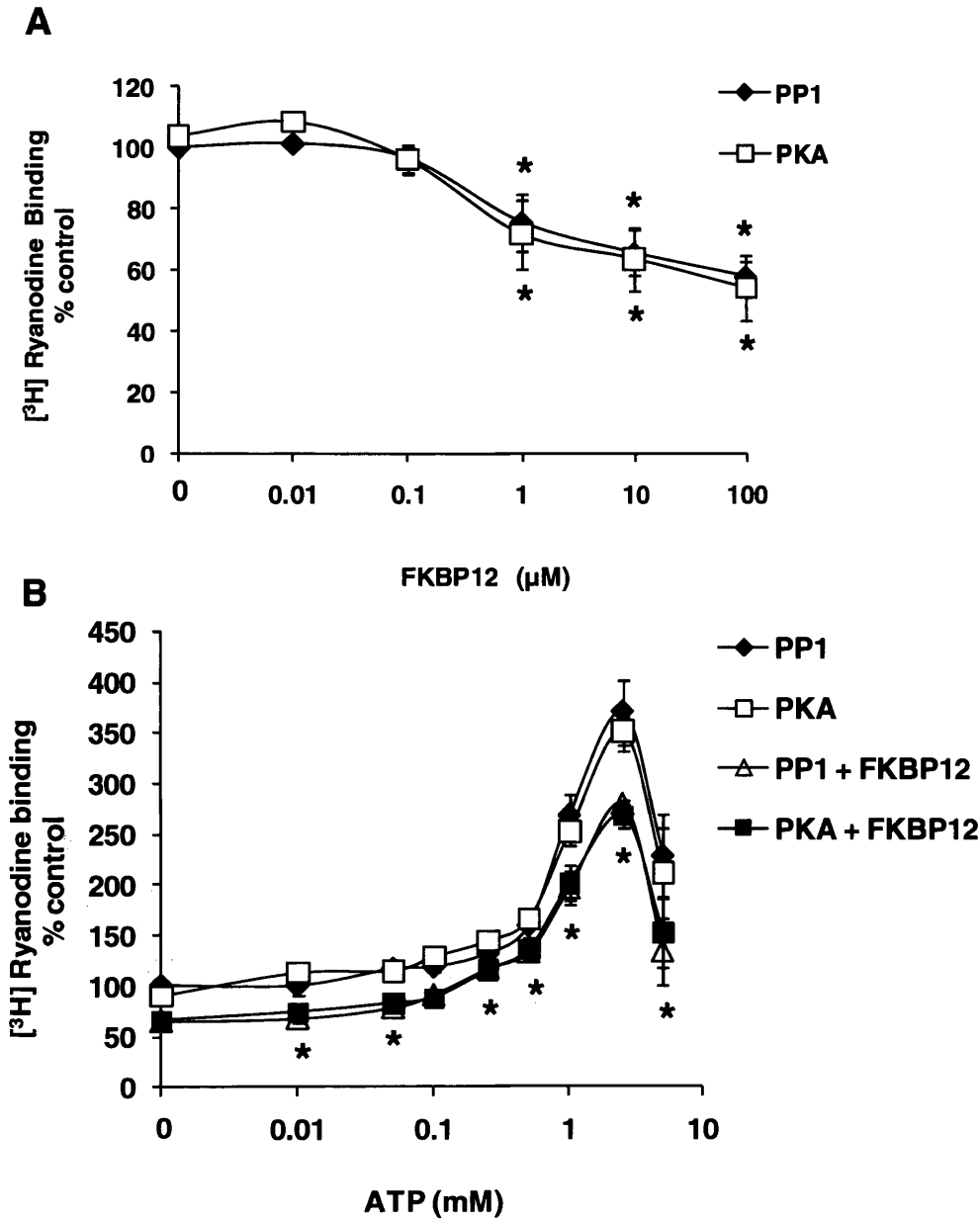


**Figure 4.6 Effect of FKBP12 inhibition on ATP activation of RyR1  $[^3\text{H}]$  ryanodine binding**  
**A)** FKBP12 dose response in the presence of 2.5 mM ATP. Each point represents the mean of 5 RyR1 preparations. (\*) indicates a significant difference ( $p < 0.05$ , students paired t-test) from the control value with no FKBP12 addition. (Binding in pCa4 calcium with 2.5 mM ATP is taken as 100%). There was no significant difference between PP1 and PKA treatments. **B)** ATP dose response is shown in the presence and absence of 10  $\mu\text{M}$  FKBP12. Each point represents the mean of 6 RyR1 preparations. (\*) indicates a significant difference ( $p < 0.05$ , students paired t-test) from the corresponding values of the ATP dose response without FKBP12 addition. (Binding in pCa4 is taken as 100%). Bars show standard error.

#### 4.2.3.2 Magnesium

Magnesium inhibition of RyR has also been reported in previous studies and high ionic strength was reported to mask the magnesium effect (Padua, Nagy et al. 1994). In this study, ryanodine binding assays were originally designed with 1 M KCl in the assay buffer as this has been found to enhance binding, however, as shown in Figure 4.7A, Magnesium inhibition at this KCl concentration was not as dramatic as shown previously in the literature. When the KCl concentration was reduced to 150 mM, a strong magnesium effect was seen (Figure 4.7B) 150 mM KCl was then used in all magnesium binding experiments and earlier experiments repeated where necessary to ensure a fair comparison. Magnesium and FKBP12 effects have not been combined in a single experiment previous to this investigation and it was found that the magnesium inhibition was further enhanced by the presence of FKBP12. Even when magnesium was present at 1 mM, FKBP12 was able to reduce binding further by approximately 50%.

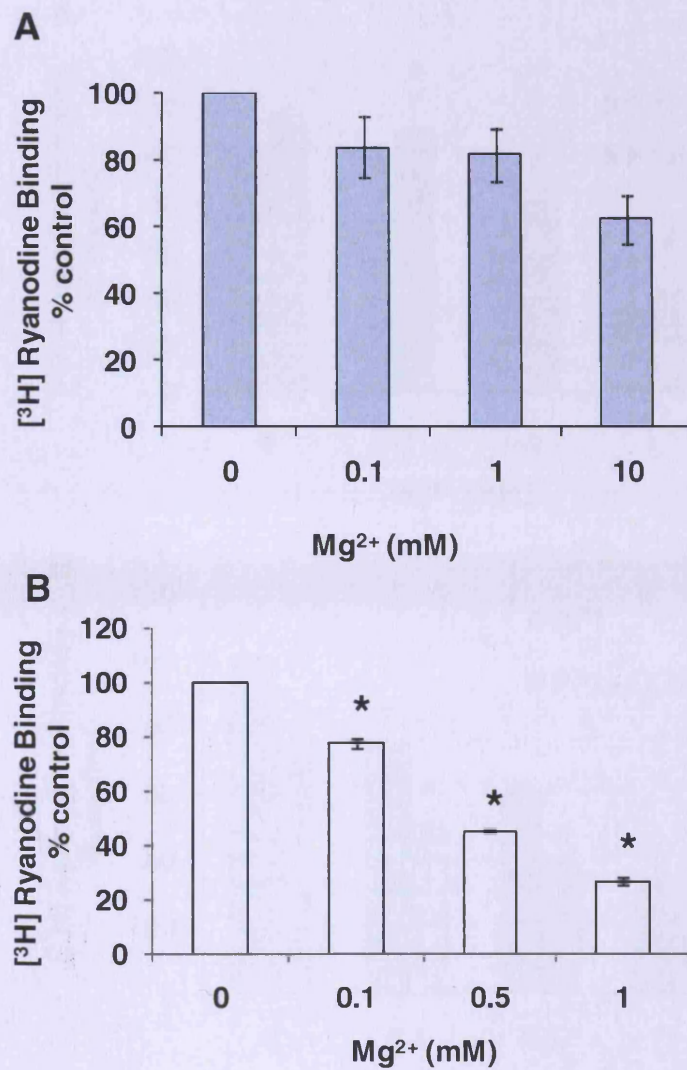


**Figure 4.7 Effect of KCl concentration on magnesium inhibition of RyR1  $[^3\text{H}]$ ryanodine binding**

**A)** Magnesium dose response in 1 M KCl. Each bar represents the mean of 5 RyR1 preparations. **B)** Magnesium dose response in the presence of 150 mM KCl. Each bar represents the mean of 6 RyR1 preparations. (\*) indicates a significant difference ( $p < 0.05$ , students paired t-test) from the control value with no  $\text{Mg}^{2+}$  addition. (Binding in  $p\text{Ca}4$  is taken as 100%). Bars show standard error.

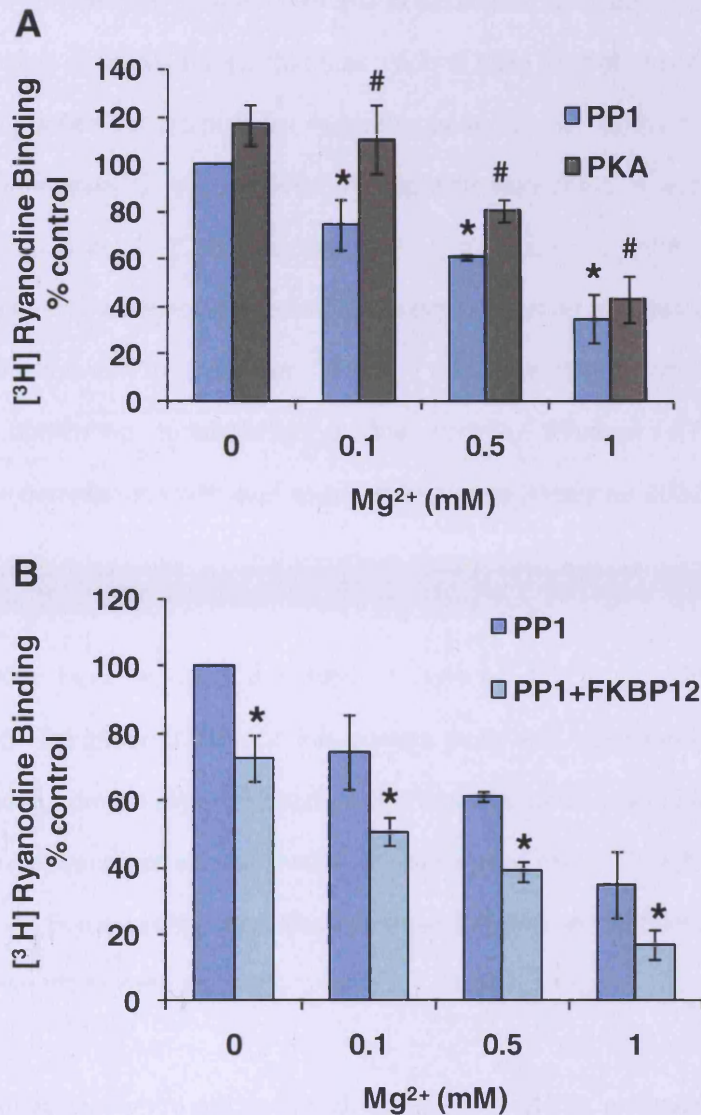


**Figure 4.8** Effect of magnesium inhibition on RyR1 [<sup>3</sup>H]Ryanodine binding in the presence of PKA phosphorylation and FKBP12.

**A)** Magnesium dose response is shown in the presence and absence of PKA phosphorylation. Each point represents the mean of 6 RyR1 preparations. (\*) indicates a significant difference ( $p < 0.05$ , students paired t-test) from the control value with no magnesium addition. (#) indicates a significant difference ( $p < 0.05$ , students t-test) from the magnesium effect in the absence of PKA. **B)** Magnesium dose response is shown in the presence and absence of 10  $\mu$ M FKBP12. Each point represents the mean of 6 RyR1 preparations. (\*) indicates a significant difference ( $p < 0.05$ , students paired t-test) from the control value without magnesium addition. (Binding in pCa4 is taken as 100%). Bars show standard error.

### **4.3 Discussion**

This chapter examined the effects of known physiological activators and inhibitors of RyR on ryanodine binding of native RyR1 channels purified from animal tissue. FKBP12 protein was produced and purified successfully for experiments and shown to exert inhibition on ryanodine binding. Channel opening was reduced by approximately 50%, in accordance with previous studies (Jones, Lai et al. 2006). Purified RyR1 was shown to exhibit the well documented biphasic response to calcium, with maximal binding occurring at pCa4 (100  $\mu$ M), and channel inhibition at nM and mM free calcium. ATP (2.5 mM) was able to increase binding by ~4 fold consistently, confirming functionality of the protein. Maximal ATP activation at mM concentrations corresponds with studies by other groups (Meissner 2002; Bull, Finkelstein et al. 2007).

Previous studies have reported activation of RyR by ATP that is independent of calcium (Meissner and Henderson 1987). In this current study the magnitude of binding at pCa7 is greatly increased from an almost closed level of binding, to approximately 75% of the maximal opening in the presence of calcium and ATP, suggesting that ATP enhances the sensitivity of RyR for calcium. Some binding was also observed at pCa8, in the presence of ATP, where nM levels of calcium alone were shown to completely inhibit binding.

ATP activation was shown to reduce the proportion of FKBP12 inhibition at 10  $\mu$ M, but at lower ATP concentrations the FKBP12 effect was closer to 50%, the level seen in the absence of ATP. This suggests that the maximal opening of the RyR channel incurred by 2.5 mM ATP and calcium makes the channel less susceptible to stabilisation by FKBP12. This finding correlates with previous SPR studies carried out within this group, documenting a reduced affinity of RyR1 for FKBP12 in the presence of ATP (Jones, Reynolds et al. 2005). It may therefore be the case that ATP induces a further conformational change to maximally open the RyR channel, which masks the FKBP12 binding site.

Magnesium inhibition however, was shown to be consistently enhanced by the presence of FKBP12, suggesting full channel stabilisation only occurs in the presence of both  $\mu$ M FKBP12

and mM magnesium and that they have an additive effect. This finding would point to FKBP12 and magnesium acting at independent sites, and a possible unmasking of the magnesium binding site(s) by FKBP12, enabling maximal inhibition. Maximal magnesium inhibition was shown at 1 mM, consistent with previous findings, however this was only observed in low salt binding conditions, as shown in figure 4.7. It has been reported previously that an increase in ionic strength enhances channel sensitivity to calcium, ATP and magnesium (Meissner 2002), however a paper by (Murayama, Kurebayashi et al. 1998) lead to an assessment of magnesium effect in high (1 M KCl) and low/endogenous (150 mM KCl) salt conditions (Padua, Nagy et al. 1994; Murayama and Ogawa 1996). The lower ionic strength was found to greatly enhance the magnesium inhibition, thus this condition was used for all subsequent experiments, with earlier experiments repeated to enable a fair comparison.

Phosphorylation was able to partially overcome magnesium inhibition, as documented previously (Mayrleitner, Chandler et al. 1995). Magnesium inhibition is still evident, but consistently reduced in the phosphorylated preparations. This has been interpreted as a conformational change which may mask a magnesium binding site (Blayney, Jones et al. 2010). Had time permitted, it would have been interesting to test the effect of phosphorylation on the combined channel inhibition of magnesium and FKBP12. Although it has been shown previously that phosphorylation is able to reduce channel affinity for FKBP12, using SPR and Biacore for kinetic analysis, no differences between phosphorylated and dephosphorylated preparations could be observed in [<sup>3</sup>H]ryanodine binding experiments (Blayney, Jones et al. 2010). The phosphorylation status of the RyR preparations was not monitored over the time frame of the experiments in this investigation, however a previous assessment of phosphorylation on similarly prepared RyR was carried out after a 5 hour SPR experiment, and shown to remain unchanged (Blayney, Jones et al. 2010).

The effect of magnesium inhibition on ATP activation was not tested and would require the careful titration of ATP and magnesium, which form a complex, to control the level of 'free' magnesium concentration (Laver 2005). It has been reported that adenine nucleotides reduce the sensitivity of RyR to magnesium inhibition (Meissner and Henderson 1987) but others found



no evidence of this in their study using AMPPCP, a nonhydrolyzable ATP analogue (Murayama, Kurebayashi et al. 2000).

Some of these studies have been performed by other groups using SR preparations and the isolated native RyR1 channels in this investigation have generally shown the same responses as previously documented. These results provide a positive indication that the isolated channels have retained key functional characteristics.

**Chapter 5; Production and  
purification of activatory domain  
peptides of RyR1**

---

**CHAPTER 5: Production and purification of activatory domain peptides of RyR1****5.1 Introduction**

The use of domain peptides originated from experiments to test the domain interaction hypothesis when it was first proposed (Yamamoto, El-Hayek et al. 2000). This hypothesis originated from a number of key observations. Topology studies had shown that there were discernable differences in electron density arising from changes in RyR channel architecture when comparing the open (calcium and ATP analogue) and closed (EGTA) conformations of the channel. These included the clamp (corner regions), a rotation of the transmembrane region and a decrease in size of the central channel pore region (Orlova, Serysheva et al. 1996). The MH mutations in RyR1, of which only a few were known at the time, were clustered in the N-terminus and central domain portions of the RyR1 protein sequence. Previous cross-linking studies (Wu, Aghdasi et al. 1997) had shown these central and N terminus regions to interact. Studies of SR vesicles or RyR1 channels containing MH mutations demonstrated hypersensitivity to activation. Furthermore, an Ab to an MH mutation site (G341) activated RyR and lowered the threshold for CICR and a peptide containing G341 was shown, using overlay assays, to bind to RyR1 regions 3010-3225 and 799-1172 suggesting subdomain interactions (Zorzato, Menegazzi et al. 1996).

A number of domain peptides to both the N-terminus and central domain regions have been tested previously, of these the most potent activatory peptide was DP4 (L<sup>2442</sup> to P<sup>2277</sup>), which increased <sup>3</sup>[H]ryanodine binding to skeletal muscle microsomes ~3 fold. It was proposed that this is able to insinuate into the protein structure and compete with the endogenous central domain interaction, which stabilises the closed state of the channel. This causes activation by domain 'unzipping'. The fact that the DP4M peptide (with the MH R2458C mutation) did not activate RyR was taken as evidence that this mutation altered the peptide structure so that it could not bind to the N-terminus. Thus, in MH patients, a fault in the stabilising N-terminus and central domain interaction might account for the hypersensitivity of RyR and contribute to the underlying pathology (Yamamoto, El-Hayek et al. 2000; Lamb, Posterino et al. 2001).

Further studies with DP4 peptide containing other MH mutations R2452W, R2545C and R2458H showed that the R2452W mutation, in particular, increased activity by ~2 fold and all showed some activatory activity at 100  $\mu$ M although this was least for R2458C (Bannister, Hamada et al. 2007). Thus, the R to C mutation was found to have the most severe reduction in the DP4 activatory effect. The authors considered that the majority of mutations falling into the most severe class involve arginine residues, suggesting interaction is governed by electrostatic forces and that mutations classed as modest generally involved hydrophobic residues. Antibodies produced against peptides including DP4 (central domain) and DP1 N-terminus (590D-C609) showed a dose-dependent activation of SR [ $^3$ H]ryanodine binding and increased the sensitivity of SR calcium release to a highly specific activator of RyR, polylysine, further supporting the domain interaction hypothesis (Kobayashi, Yamamoto et al. 2004).

NMR analysis clearly indicated that DP4 has a defined 3D structure that is characterized by a helix 1-loop (turn)-helix 2. Since DP4 retained several important functional properties ascribable to its corresponding *in vivo* domain, it was suggested that the structure of the Leu-Pro region of RyR1, to which DP4 corresponds, has a similar or identical structure and critical residues appeared to be located in a particular area in the helix-loop region (Bannister, Hamada et al. 2007). Experiments involving domain peptides carried out by the Ikemoto group are based on the underlying assumption that peptides are capable of mimicking native conformations in the *in vitro* solution.

Thus one of the central beliefs of the domain interaction hypothesis is activation of RyR by a homologous activatory domain peptide, by binding to an endogenous partner domain and thereby disrupting a closed and stable RyR conformation. The inability of an MH-, or CPVT-containing mutant peptide to mimic the WT gives credence to the destabilising effect of a critically placed point mutation and provides a compelling mechanism for a 'leaky' RyR underlying the disease phenotype (Yamamoto, El-Hayek et al. 2000; Yamamoto and Ikemoto 2002). This was the rationale for using DP4 (and DPc10- see chapter 7) to identify the potential region of conformational change linked to reduced FKBP12/12.6 affinity for RyR1/2 elicited by

phosphorylation. The central domain is considered to be a likely candidate for this proposed region of co-ordinated regulation (Blayney, Jones et al. 2010).

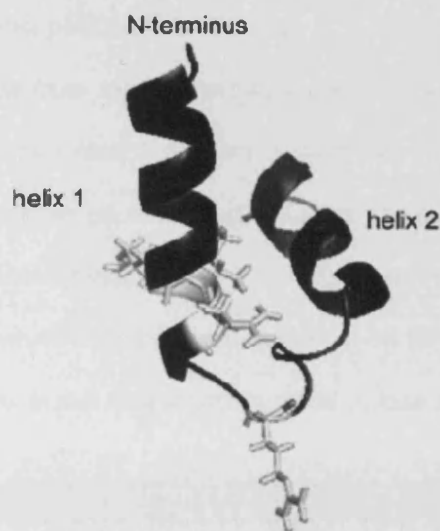


**Figure 5.1 Structural model of DP4 achieved using NMR.** MH mutation residues are labelled white with side chains and cluster close to the C-terminal end of helix 1 and at the N-terminal of the loop connecting helix 1 and helix 2 (Bannister, Hamada et al. 2007).

Functional experiments in this investigation;  $^3\text{[H]}$  ryanodine binding using synthetic peptides purchased from Severn Biotech (Worcestershire, UK), yielded significant activation of RyR1 (see chapter 6). However, the mutant peptide (DP4M) was as active as the WT. 5 mg of DP4WT peptide was received as a gift from the Ikemoto group (IK-DP4WT), which gave very similar results to the DP4WT purchased. Unfortunately we were unable to obtain any of the mutant peptide from the same source. The expense of a further purchase of peptides for comparison from a different commercial supplier prompted exploration into a novel avenue for producing the peptides as a bacterial recombinant protein. Producing and purifying the peptides 'in-house' may actually be beneficial, although time consuming, because the peptides ordered from elsewhere are lyophilised and subjected to harsh chemicals during synthesis which could alter the properties of the protein.

This chapter outlines the protocols involved in production and purification of DP4WT and DP4M recombinant peptides.

### **5.3 Results**

#### **5.3.1 PCR cloning of DP4 into pGEX-6P1.**

DP4 was created by cloning from rRyR1 template using DP4 forward and reverse primers designed with BamH1 and EcoR1 restriction sites (Figure 5.2 A and B). The PCR amplicon was shown to run at the correct size on a 3% agarose gel (section 2.1.1.1) and was then gel extracted (section 2.1.2.3). Gel extraction was found to be more effective for removal of PCR reagents for the DP4 amplicon of 133 bp, because the cut-off for PCR clean-up resin is 100 bp, close to the size of this piece, and it was found to result in loss of yield (Figure 5.3A). Both the DP4 insert (Figure 5.3B) and pGEX-6P-1 vector (Figure 5.3C) were cut with BamH1 and EcoR1 restriction enzymes in order to prepare them for ligation. Gels B and C confirm a reduction in size of the DP4 amplicon and linearization of pGEX-6P-1 respectively. The digested DP4 was gel extracted again to remove residual enzymes and buffers, and a small sample run on a gel to gain an estimation of quantity for ligation. The cut insert was ligated into the compatible cut vector's multiple cloning site using a 5:1 ratio of insert to vector (as described in section 2.1.2.6). Following transformation colonies were screened by diagnostic colony PCR using the pGEX forward primer and the DP4 reverse primer. The pGEX primer increases the expected amplicon size by 100 bp and of the 10 colonies screened, two were shown to generate PCR product (Figure 5.3D). These colonies were then 'miniprep'd (section 2.1.2.9) and the resultant plasmid preparations sequenced using the BIG DYE sequencing kit (section 2.1.2.10). The electropherogram and alignment using the BLAST 'align two sequences' software (Figure 5.4) confirmed the correct insert was in frame within the pGEX-6P-1 vector. The 3C protease site is indicated in-frame with the BamH1 restriction site. The codon for R2458 is shown and the stop codon and EcoR1 site are correct.

**A**

clamp BamH1 rRyR1 cDNA  
 DP4 F (5' - 3') TATATGGATCCCTGATCCAAGCCGGCAAGG

clamp EcoR1 Stop r RyR1 cDNA  
 DP4 R (5' - 3') CTATCGAATTCTCAGGGGATCTGCAGCGGG

**B**

Peptide name	Gene of Interest	Genebank Accession Number	Size of Amplicon (bp)
DP4WT	rRyR1	X15750	133

**C**

DP4M F (5' - 3') TCCGCGCCATCCTTTGCTCCCTCGTGCCCC

DP4M R (5' - 3') GGGGCACGAGGGAGCAAAGGATGGCGCGGA

**Figure 5.2 DP4 and DP4M forward and reverse primer design**

**A)** DP4WT forward and reverse primer sequences. The stop codon on the reverse primer is highlighted in red. Restriction endonuclease sites were incorporated as shown. GC content is approximately 50%.

**B)** Table demonstrating average primer annealing temperatures- designed to be similar for forward and reverse primers to increase PCR efficiency. Gene sequence was obtained from published GenBank sequence, the accession number for which is provided.

**C)** DP4M forward and reverse primer sequence used in site-directed mutagenesis. The pink highlighted area shows the region incorporating the base change mutation.

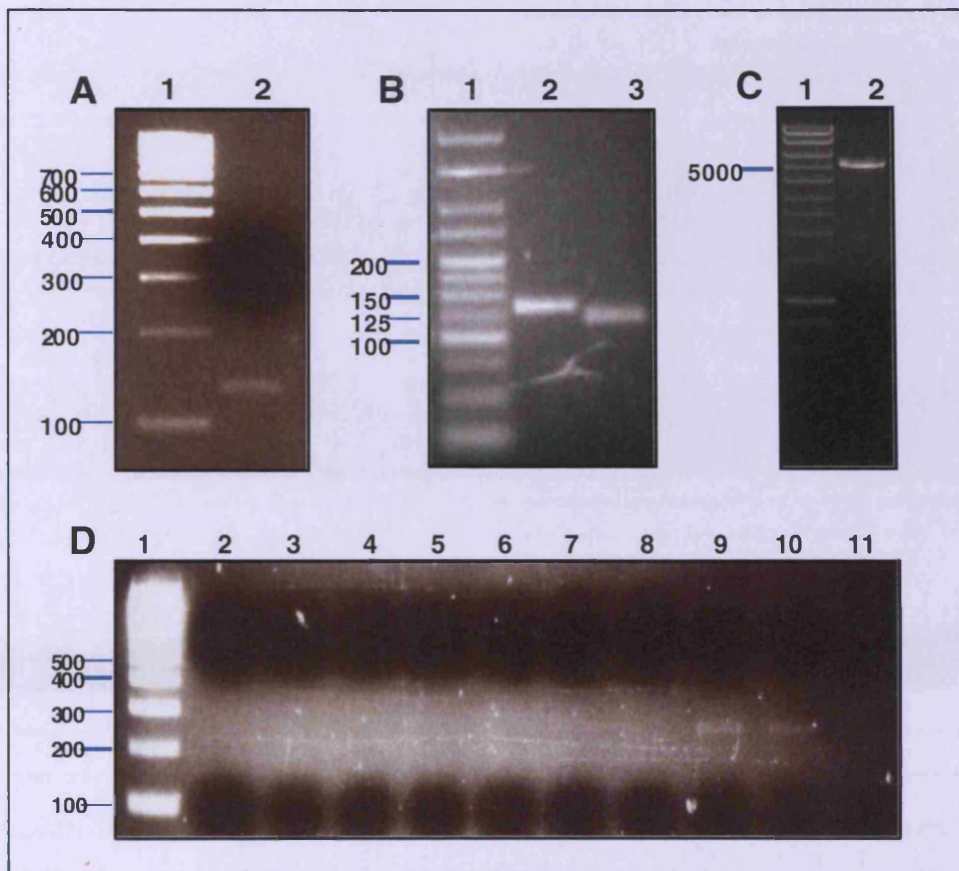


**Figure 5.3 Cloning of DP4 into pGEX-6P-1**

**A)** DP4 sequence was amplified from RyR1 template using PCR with primers DP4F and DP4M and the product was run on a 3% (w/v) TAE agarose gel (section 2.1.1.1) Lane 1, 1 Kb DNA marker, sizes are shown on the left (bp). Lane 2, DP4 PCR synthesized DNA product running at 133 Bp.

**B)** DP4 PCR amplicon was gel extracted and subjected to a double digest with BamH1 and EcoR1 restriction endonucleases. The products were separated on a 3% TAE agarose gel. Lane 1, hyperladder V DNA marker, sizes are shown on the left in base pairs (bp). Lane 2, undigested gel extracted DP4 PCR product. Lane 3, digested gel extracted DP4 product.

**C)** pGEX-6P-1 vector was prepared for ligation by EcoR1 and BamH1 double digest and treatment with protein phosphatase. Product was run on a 1% (w/v) TAE agarose gel. Lane 1, 10 Kb DNA size marker, the 5000 bp marker is indicated on the left. Lane 2, pGEX-6P-1 digested vector.

**D)** Of the colonies that grew on LB agar with Ampicillin following transformation, 10 were selected and subjected to a colony PCR screen (section 2.1.2.8) using the pGEX forward primer and the DP4 reverse primer. PCR products were separated on 3% w/v TAE agarose by gel electrophoresis. Lane 1, 1 Kb DNA marker with sizes shown on the left in base pairs (bp). Lanes 1-8 and 11 show colony PCRs with no insert. Lanes 9 and 10 show positive colony PCR amplicons.



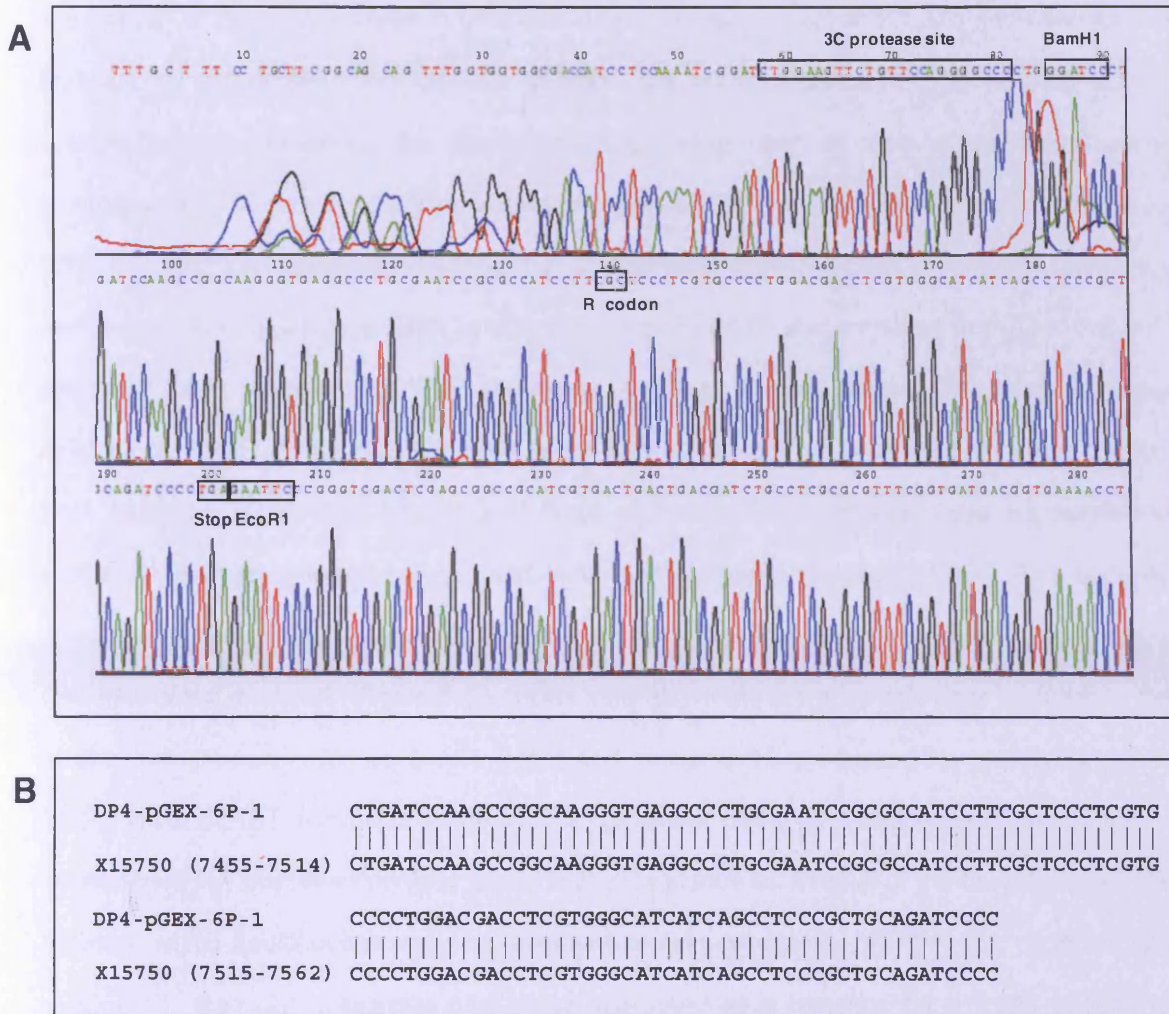


**Figure 5.4 Sequencing of DP4-pGEX-6P-1**

**A)** Electropherogram sequencing result. BamH1 and EcoR1 restriction sites are highlighted which flank the DP4 sequence. C-protease cleavage site is shown to be present and in frame. The R-codon is the site where the DP4M mutation would occur and is shown to be in the wildtype format. There is a stop codon immediately before the EcoR1 restriction site.

**B)** Sequence identity is confirmed by a BLAST sequence alignment with RyR1 sequence from the GenBank database (Accession number X15750) showing 100% match.

### 5.3.2 Insertion of the R2458C point mutation

A maxiprep of the DP4 wildtype in pGEX-6P-1 was prepared (section 2.1.2.9) and used as the template for site-directed mutagenesis to insert the point mutation R2458C (section 2.1.3). Specific primers containing the desired mutation were used as part of the QuikChange mutagenesis kit (Figure 5.2 C). The protocol involves a PCR cycle to generate mutant sequence from the wildtype template, followed by an enzyme (Dpn1) digest process to eliminate methylated parental wildtype DNA (which was synthesised by and extracted from Top10 *E.coli*, section 2.1.2.7), whereas the PCR produced DNA was not methylated. This step therefore selected for the PCR synthesised DNA which should contain the point mutation. The treated DNA was then transformed into XLGold *E.coli* and plated onto LB agar plates supplemented with ampicillin and chloramphenicol and incubated overnight (section 2.1.2.7). Five colonies grew and minipreps were prepared for each of them. The DNA was sequenced to confirm the presence of the mutation. Figure 5.5A shows insertion of the correct single base mutation in the electropherogram, as well as a fully intact and in frame 3C protease site, and BamH1 and EcoR1 sites. BLAST alignment confirmed the remainder of the DP4 sequence remained intact. To eliminate any possible misreads in the vector sequence as a result of the QuikChange PCR reaction, which could compromise subsequent protein expression, DP4M was recloned into pGEX-6P-1. One of the positive mini preps was used as a template for a PCR reaction to generate DP4M. This was run on a 1% gel and extracted. The product was then cut using a BamH1 and Eco R1 double digest (Figure 5.5B) and ligated into similarly cut fresh pGEX-6P-1 as described above for ligation of the DP4WT.

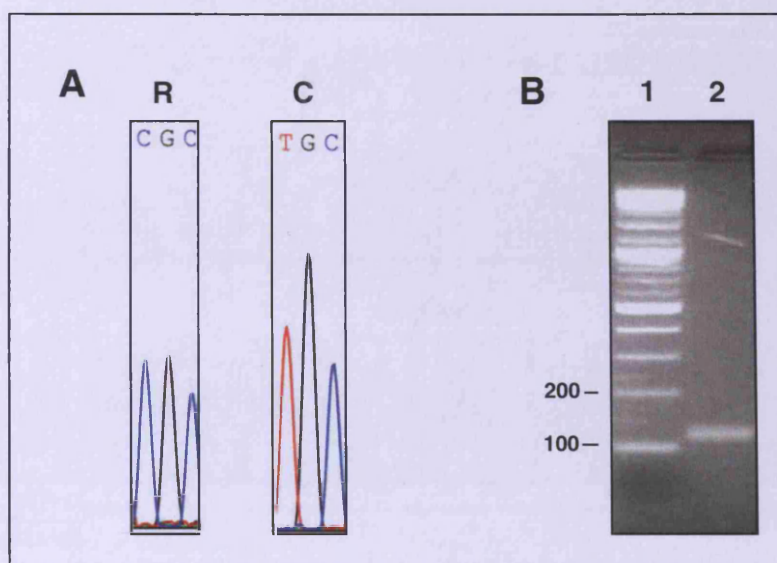


**Figure 5.5 DP4-pGEX-6P-1 Quick change mutagenesis to insert the R2458C mutation.**

**A)** Sample of the sequencing electropherogram result showing the codon change from R (DP4WT) **CGC** to C (DP4M) **TGC**

**B)** Colonies grown on selective agar following quick change mutagenesis (section 2.1.3) were screened by colony PCR and a maxiprep was generated from a positive DP4M containing colony. The DP4M insert was then excised from maxiprep vector using BamH1 and EcoR1 enzymes and was subsequently ligated into freshly cut pGEX-6P-1. Digested DP4M product was run on a 3% (w/v) TAE agarose gel by gel electrophoresis. Lane 1, DNA size marker, sizes are shown on the left in base pairs (bp). Lane 2, digested DP4M.

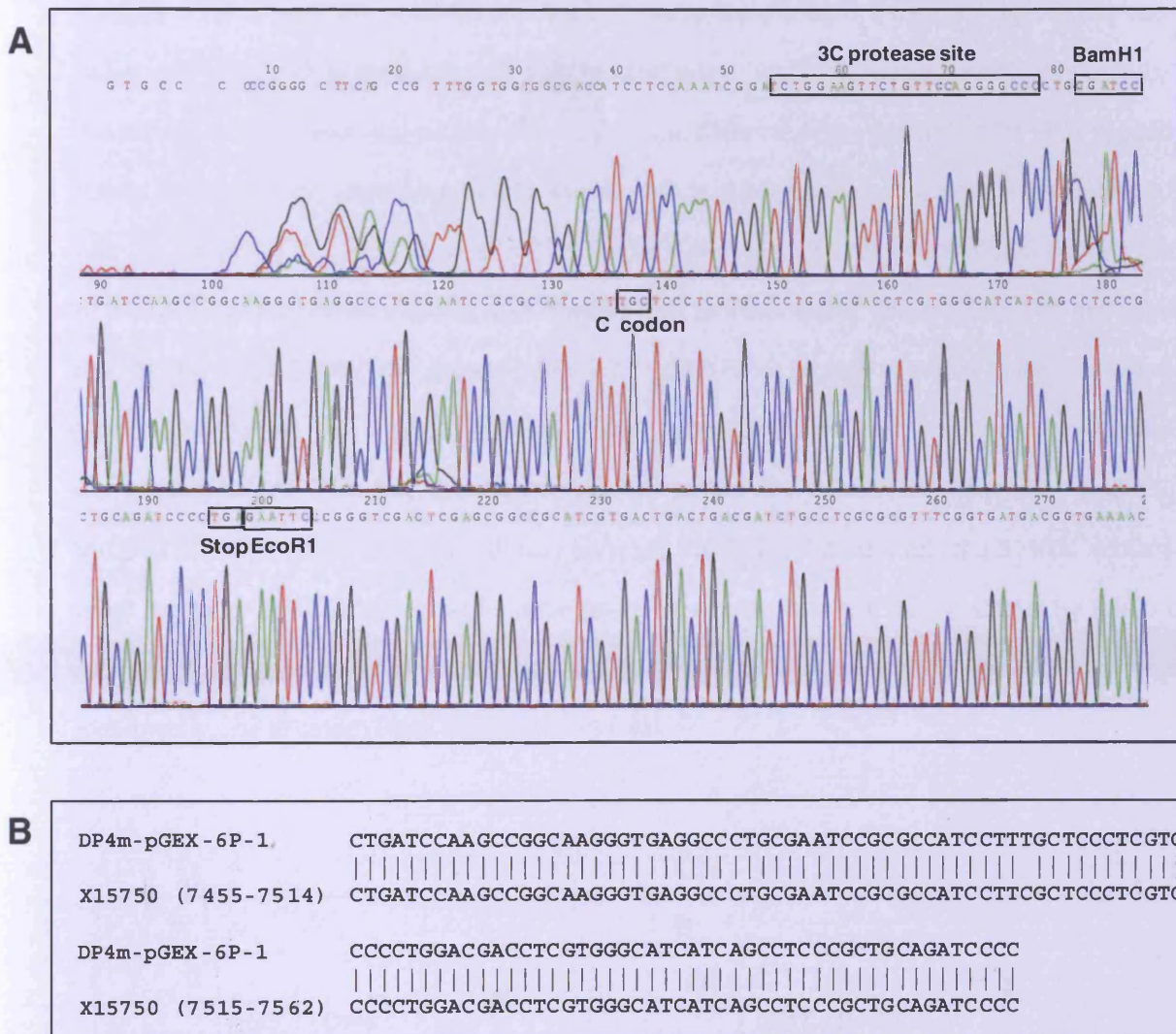


**Figure 5.6 Sequencing of DP4M-pGEX-6P-1**

**A)** Electropherogram sequencing result. BamHI and EcoR1 restriction sites are highlighted which flank the DP4M sequence. The C-protease cleavage site is shown to be present and in frame. The C-codon is the site where the DP4M mutation was inserted and is shown to be TGC rather than CGC. There is a stop codon immediately before the EcoR1 restriction site.

**B)** Sequence identity is confirmed by a BLAST sequence alignment with RyR1 sequence from the GenBank database showing 100% match with the exception of the mutated base.

### 5.3.3 Optimisation of Recombinant Protein Expression

The DP4WT and DP4M vector clones were transformed into *E.coli* Rosetta strain (section 2.2.2) for protein expression. 1 litre cultures were seeded with 20 ml of overnight starter culture and grown at 37°C. Their OD was tracked at  $A_{600}$  every 30 minutes and once the OD reached 0.6 the temperature of the incubator was reduced to either 30°C or 25°C, depending on the chosen induction temperature, over 30 minutes (Figure 5.8). At this point a 50 ml sample was harvested

( $t_{\text{induction}} = 0$  hour) and the pellet frozen. IPTG (final concentration 0.1 mM) (section 2.2.2) was added and further 50 ml samples were pelleted and frozen (at  $-20^{\circ}\text{C}$ ) every hour for 4 hours. The pellets were thawed and protein expression was determined by capture of the GST-tagged protein on glutathione sepharose beads (section 2.2.3). After washing, the protein was released from the beads by the addition of 3x SDS sample buffer and 5  $\mu\text{l}$  loaded onto SDS PAGE gels for analysis by Coomassie staining and Western Blot (section 2.2.1), (Figure 5.8). The expected size of the GST-DP4WT/M protein was 30.7 kDa. The protein markers used for these experiments do not give a good estimate of the protein size and they tend to run higher than their expected MW. This has been noticed for a number of proteins (see figures 7.7 and 7.8) and GST/DP4M runs consistently half way between the 23 kDa (green) and the 30 kDa markers on all the gels. Both  $30^{\circ}\text{C}$  and  $25^{\circ}\text{C}$  gave good expression and this was maximal by 3 hours with very little expression of protein pre-induction ( $t=0$ ). The presence of the GST tag was confirmed by the Western Blots using anti-GST Ab.

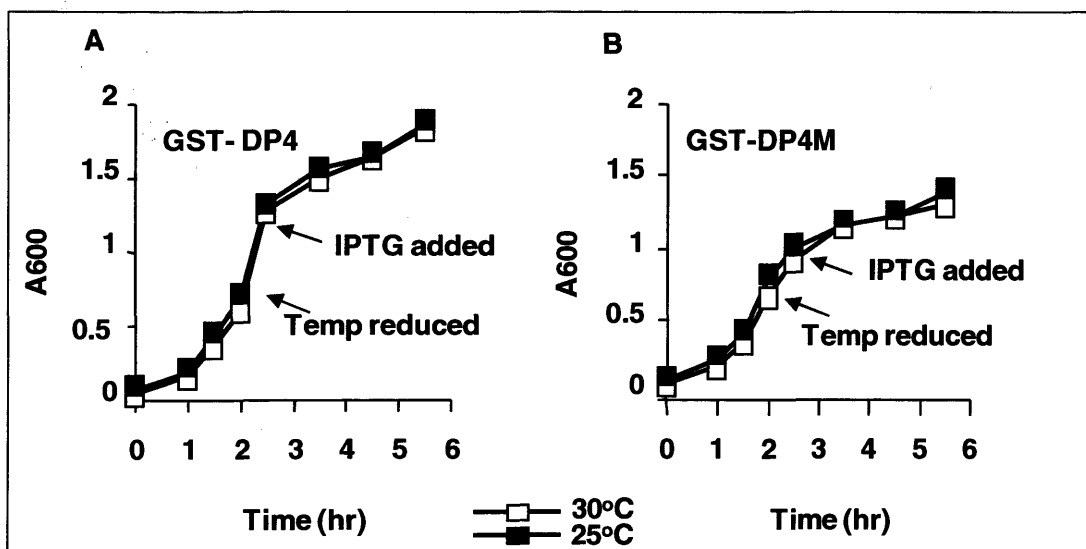


**Figure 5.7 Induction of GST-DP4WT/DP4M protein**

The time course of bacterial growth was plotted by taking  $OD_{600}$  absorbance readings on a UV spectrophotometer every 30 minutes from the start of incubation at  $37^{\circ}\text{C}$  until the end of protein expression after induction with IPTG as indicated for A) GST-DP4WT and B) GST-DP4M.

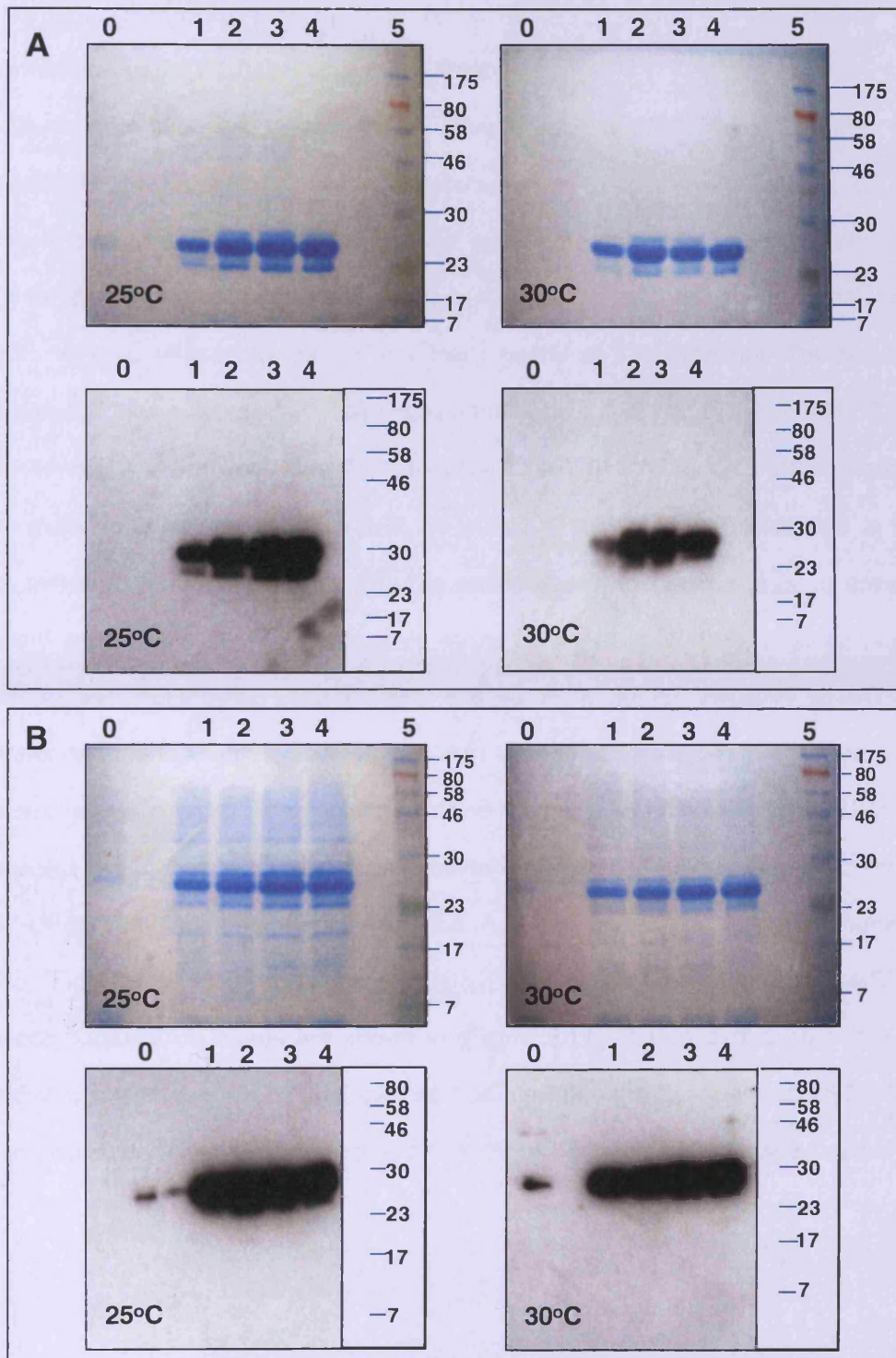


**Figure 5.8 Induction of GST-DP4WT/DP4M protein**

Protein expression was monitored from the time of IPTG addition ( $t=0$ ) until  $t=5$  hours by taking 50 ml samples of culture at hourly intervals. Samples from each hour were separated on a 15% SDS-PAGE gel and samples were also transferred to nitrocellulose membranes for blotting with anti-GST antibody to confirm expression of the correct protein. This protocol was repeated at both 30°C and 25°C to see if temperature difference resulted in increased yield.

**A)** DP4 expression optimisation. Lanes 0-4 in all images correspond to  $t=0,1,2,3$  and 4 hours of induction respectively. Lane 5, Kaleidoscope protein size marker, sizes are shown on the right (kDa). Upper images are SDS-PAGE gels, lower images are western blots.

**B)** DP4M expression optimisation. Lanes 0-4 in all images correspond to  $t=0,1,2,3$  and 4 hours of induction respectively. Lane 5, Kaleidoscope protein size marker, sizes are shown on the right (kDa). Upper images are SDS-PAGE gels, lower images are western blots.

### 5.3.4 Purification of GST-DP4WT and GST-DP4M

1 litre cultures were harvested and the pellets stored frozen at  $-20^{\circ}\text{C}$ . The pellets were thawed and treated with lysozyme and DNAase (Benzonase) for 4 hours at  $4^{\circ}\text{C}$  (section 2.2.3). The lysates were then subject to three 30 second cycles of sonication before centrifugation at  $10,000\ g$  for 20 minutes to remove cell debris and unbroken bacteria. The supernatants were mixed with washed glutathione beads and rolled gently at  $4^{\circ}\text{C}$  overnight. The beads were washed with 10x their volume of 20 mM Tris/HCl buffer pH 8.0, 2 mM EDTA, 2 mM DTT plus 1 M NaCl followed by a similar wash with 50 mM NaCl. GST-DP4WT or GST-DP4M were eluted from the glutathione beads by rolling with 10 ml of 10 mM reduced glutathione in 50 mM Tris/HCL buffer pH 8.0 for 2 hours at  $4^{\circ}\text{C}$ . The beads were transferred to a 20 ml column and the eluate drained and kept. The beads were washed with a further 10 ml of glutathione buffer and both eluates combined. Eluates were applied to a 20 ml Vivaspin 10,000 MWCO concentrator and the total eluate was reduced in volume to  $\sim 1$  ml. To remove the glutathione, a diafiltration cup was placed in the concentrator and filled with 15 ml of 20 mM PIPES buffer pH 7.1 containing 150 mM NaCl. This diafiltration step was repeated. The protein concentration of the GST-DP4WT/M was determined from the  $A_{280}$  and calculated using the amino acid sequence, (Figure 5.9). Coomassie stained SDS PAGE of the GST-DP4WT and GST-DP4M preparations captured on beads are shown in (Figure 5.11) The concentration of the protein was continued to achieve  $\sim 15$  mg/ml so that a x5 dilution into the assay of GST-DP4WT/M effects on [ $^3\text{H}$ ]ryanodine binding would give a final concentration of  $100\ \mu\text{M}$  (see chapter 6)

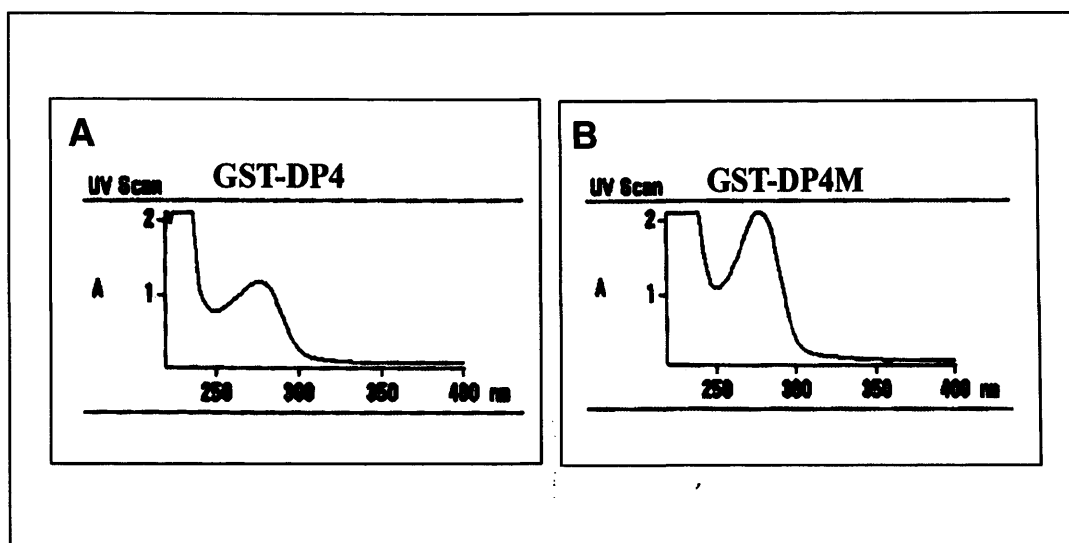


**Figure 5.9 UV quantification estimate of concentrated protein.**

The protein peak is at  $A_{280}$ . The flat extinction between 300 and 400 nm shows minimal light scattering indicating that the protein is free from aggregation. **A)** GST-DP4WT and **B)** GST-DP4M.

### 5.3.5 Purification of peptides R-DP4WT and R-DP4M

Recombinant (R-) peptides were prepared by removal of the GST tag from affinity purified GST-DP4WT or GST-DP4M via the 3C cleavage site. A pellet from a 1 litre culture of GST-3C protease was subjected to the same lysis, affinity capture, and wash protocol as the GST-DP4WT/M bead capture (section 2.2.3.1). 3C beads and GST-DP4WT or GST-DP4M were mixed in a ratio of 1:6 and rolled overnight at 4°C in 10 ml of 20 mM Tris/HCl pH 8.0, 2 mM EDTA and 2 mM DTT buffer. The beads were transferred to a column and drained free of eluate. They were washed with a further 10 ml of cleavage buffer. The cleavage is illustrated in Figure 5.11. The theoretical pI of R-DP4WT was ~8.6 and hence the protein was positively charged at pH 7.0. Capture after cleavage was therefore attempted using a 20 ml Vivapure IEX S (which is negatively charged) centrifugal spin column (20 ml –maxi M) with a capacity of 15-20 mg protein. The final volume of eluate containing the cleaved peptide was 27.5 ml in pH 8.0 buffer. For successful capture on the spin column the pH was reduced to 7.0 by adding an equal volume of 20 mM MES buffer pH 6.0 - total volume 55 ml. This was passed through the Vivapure column 15 ml at a time using the Allegra centrifuge – 500 g (1475 rpm). The column was washed twice with 20 mM PIPES buffer pH 7.0. The peptide was eluted in 2 ml steps of increasing NaCl concentration in PIPES buffer, (0, 50, 150, 300, 400 and 500 mM) keeping the



eluate for BCA protein assay, which quantifies protein based on peptide bonds (Figure 5.12). R-DP4M purification using this technique has not yet been tested as the discovery that this protein has a negative charge at pH 7.0 means an alternative, positively charged Vivapure column is needed for this stage.

To prepare a larger batch of R-DP4WT, this was captured onto GST beads and washed and cleaved as described above. The pH was adjusted to 7.0 and the cleaved peptide captured using the Vivapure protocol. The peptide was eluted from the resin by 2 ml of 300 mM NaCl in 20 mM PIPES pH 7.0. This was allowed to drain through slowly for 30 minutes before a final spin at 500 *g* to complete the process. The peptide was concentrated using a 3000 MWCO Vivaspin concentrator to give a final concentration, which was measured by BCA assay as 0.257 mg/ml (450  $\mu$ l). The final product was run on an SDS PAGE gel to see if bands of contaminating protein could be detected. None were evident (Figure 5.13).

**A**

Amino acid composition:		
Ala (A)	3	7.3%
Arg (R)	3	7.3%
Asn (N)	0	0.0%
Asp (D)	2	4.9%
Cys (C)	0	0.0%
Gln (Q)	2	4.9%
Glu (E)	1	2.4%
Gly (G)	5	12.2%
His (H)	0	0.0%
Ile (I)	6	14.6%
Leu (L)	9	22.0%
Lys (K)	1	2.4%
Met (M)	0	0.0%
Phe (F)	0	0.0%
Pro (P)	4	9.8%
Ser (S)	3	7.3%
Thr (T)	0	0.0%
Trp (W)	0	0.0%
Tyr (Y)	0	0.0%
Val (V)	2	4.9%
Pyl (O)	0	0.0%
Sec (U)	0	0.0%

**B**

Peptide name	Molecular weight (Da)	Theoretical pI
R-DP4WT	4274.1	8.74
R-DP4M	4221.1	6.11

**Figure 5.10 R-DP4WT and R-DP4M proteomic analysis using ExPASy ProtParam software.**

**A)** The amino acid composition for R-DP4WT is shown to be lacking any phenylalanine or tryptophan residues, and therefore has no extinction coefficient for analysis.

**B)** Highlights the dramatic change in the isoelectric point of the peptide on insertion of the R – C mutation, meaning that the charge of the wildtype at pH 7.0 will be positive, and the mutant negative.

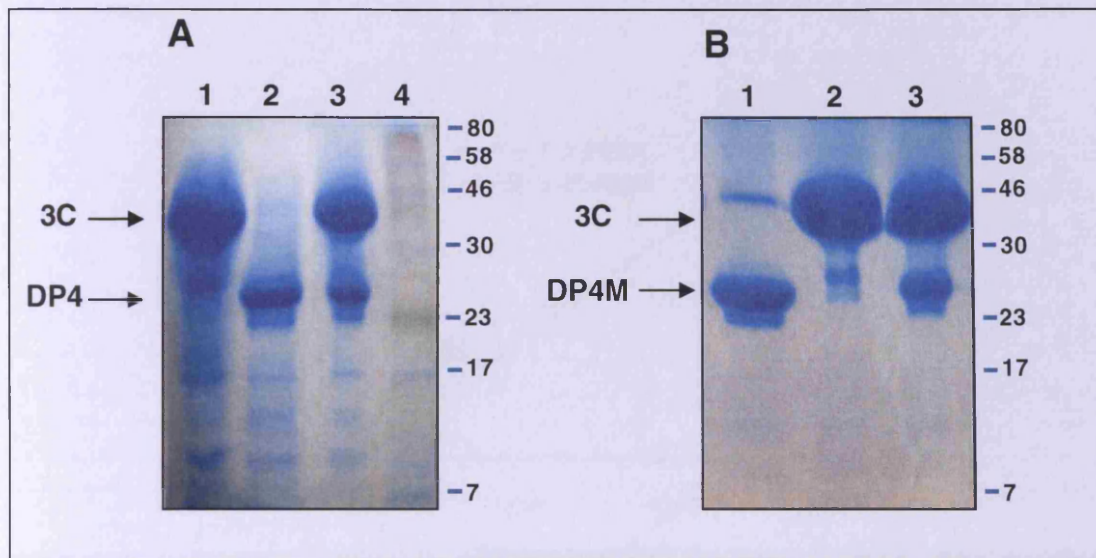


**Figure 5.11 Cleavage of GST-DP4WT and GST-DP4M**

15% SDS PAGE gels were stained with Coomassie. **A)** GST-DP4WT cleavage. Lane 1, 3C protease captured onto glutathione beads (released by x3 SDS sample buffer). Lane 2, GST-DP4WT captured onto glutathione beads, Lane 3, beads post cleavage with 3C captured and the lower band which could either be remaining uncleaved GST-DP4WT or GST and Lane 4 MW markers. **B.** GST-DP4M cleavage. Lane 1, DP4M captured onto GST beads, Lane 2, 3C protease captured onto glutathione beads and Lane 3, beads post cleavage. Sizes are shown on the right (kDa).

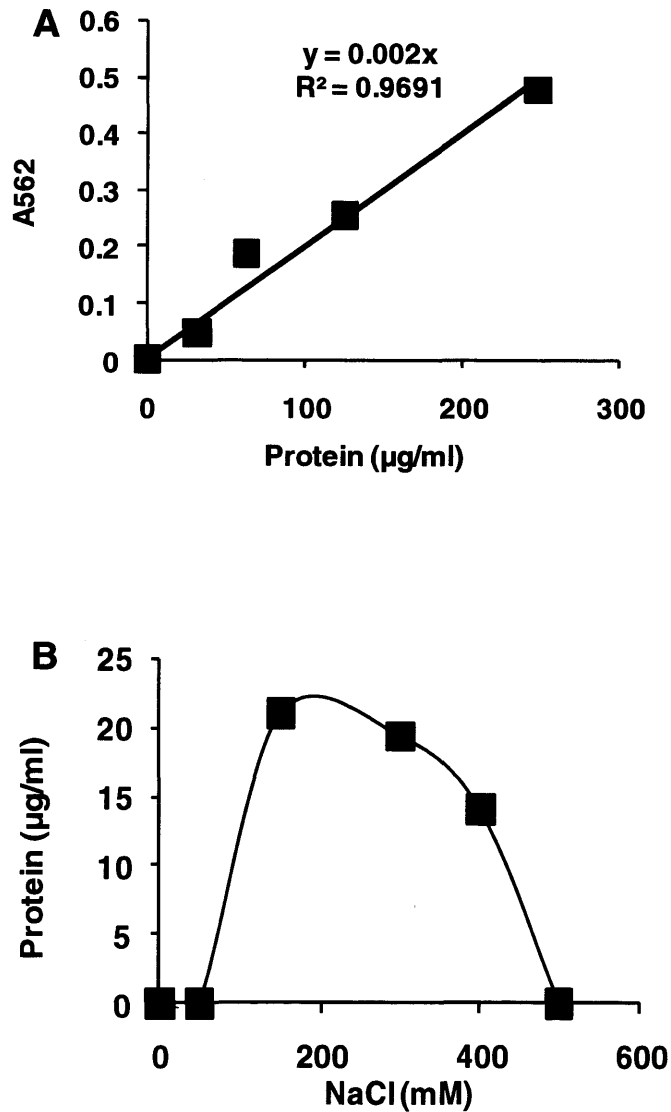


**Figure 5.12 R-DP4WT purification using ion exchange**

**A)** Pierce BCA protein assay was used to measure the absorbance of BSA protein standards. This graph shows the correlation between absorbance at 562 nm and the protein quantity in  $\mu\text{g/ml}$ .

**B)** Cleaved DP4 protein was passed through a Vivapure ion exchange centrifugal spin column at pH 7.0. Elution occurred by passing 2 ml aliquots of increasing NaCl concentration buffer through the column and measuring the absorbance of protein in each eluate fraction. R-DP4WT elution peaked at  $\sim 300$  mM NaCl.

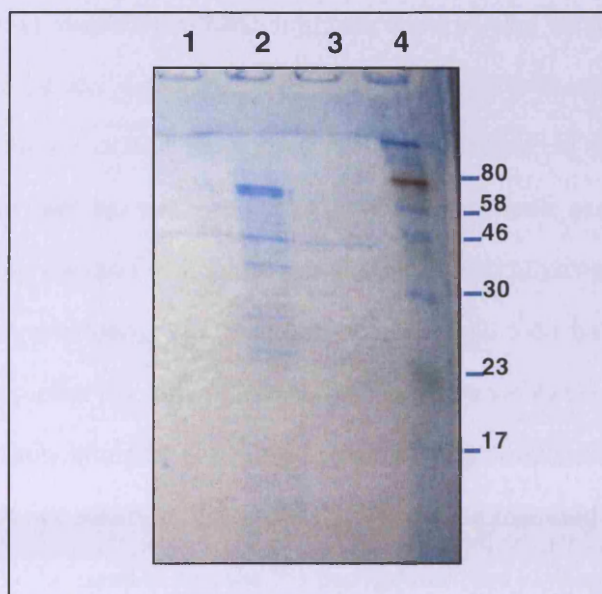


**Figure 5.13 R-DP4WT purification analysis**

Following 3C cleavage, protein was concentrated (section 2.2.5) and the resultant product was run on an 18% SDS PAGE gel to check for contaminating protein. Lane 1, 1xSDS sample buffer. Lane 2, eluate from the 3C cleavage. Lane 3, concentrated DP4 peptide preparation. Lane 4, kaleidoscope protein size marker, sizes are shown on the right (kDa).

#### **5.4 Discussion**

DP4 was cloned into the pGEX-6P-1 vector system and the R2458C mutation was successfully inserted using a Quikchange kit. Expression of protein as a GST tagged (GST-DP4WT/M) construct was optimised and expression levels were high. Cleavage of the R-DP4WT/M peptides from the tag was accomplished using 3C protease, though this resulted in a significant loss of peptide judged by the theoretical yield predicted at this stage. A limited number of experiments were performed using the peptides, both attached to the GST tag and cleaved from it (see chapter 6). There were, however, difficulties in the purification process and in finding a means of concentrating liberated peptide due to its small size. Assessing the purity and tracking the peptide was also problematic due to its unique amino acid composition.

### 5.4.1 Purification of recombinant peptide

The peptides were not amenable to our normal purification protocols post-cleavage as their small size, of ~4 kDa, made them difficult to concentrate using centrifugal concentration before further purification by ion exchange and gel filtration chromatography. Attempts with 3000 MWCO concentrators resulted in no appreciable increase in protein concentration. The theoretical pI of the peptides was calculated as 8.9, which would give it a positive charge at pH 7.0. It was therefore decided to capture the liberated peptide using a Vivapure column IEX S (which is negatively charged). The captured protein could then be thoroughly washed before elution to increase purity. Contamination by other proteins would be reduced by this step as the majority are negatively charged at pH 7.0. This also might represent a potential concentration step if the high salt necessary in the elution buffer can be tolerated in future assays, as a 2 ml elution volume could be used to release the peptide from the ion exchange resin, representing a 27.5 fold concentration from a starting volume of 55 ml. Dialysis with 3000 MWCO, the lowest available size, could not be used to exchange the buffer to a lower NaCl.

The R-DP4WT and R-DP4M were remarkable peptides in that they contained no amino acids that could be used to measure or track the protein through purification protocols.  $A_{260}$ , for example relies upon the UV absorption of the aromatic rings in tryptophan, tyrosine and phenylalanine residues, which were absent in the peptide protein sequences (Figure 5.10). Similarly Coomassie based protein assay is not suitable for small peptides (~3 kDa) and this would also limit detection of peptide on Coomassie-stained SDS gels. BCA protein assay, which measures peptide bonds, was therefore chosen for protein determination.

Yields of cleaved R-DP4WT and R-DP4M were lower than expected from the quantities of GST-DP4WT/M affinity captured by glutathione beads. The yields of GST-DP4WT and GST-DP4M were 3.6 mg/L and 2.5 mg/L respectively. The expected yield of peptide from its GST-peptide upon cleavage would be ~0.5 mg/L. However, the total yield was 0.030 mg/L (of culture) and 0.015 mg/L for R-DP4WT and R-DP4M respectively and thus only 3-6% of the theoretical yield was obtained. It was not easy to ascertain where the loss was occurring. One possibility was poor cleavage, although the batch of 3C protease used for these experiments was one which

was used routinely for a larger recombinant protein (data not shown). It is possible that the protease might be active but the cleavage site was sterically obscured by the peptide. In addition, these peptides were only 4 kDa and it was not clear whether the cleaved GST could be distinguished from uncleaved GST-DP4WT by SDS PAGE in Lane 3 of Figure 5.11, even on a 15% gel. Recombinant GST, run as a control, was not a defining option as it has the multiple cloning site also expressed which adds an additional 18 amino acids between the cleavage site and the first stop codon, making it only 10 amino acids shorter than GST-DP4WT. Thus, the efficiency of cleavage could not be determined from SDS PAGE analysis. It was deduced that the BCA assay was likely to be measuring R-DP4WT and R-DP4M peptides in the concentrated product from elution, due to the low level of contaminants (Figure 5.13), but this assay could not be used to track protein yield in the earlier steps where the eluates were much more dilute. As the protein could not be visualised using SDS PAGE, the purity is unknown. The most important test would be the peptide activity (see chapter 6). Loss of the peptide due to insolubility also has to be considered, although no obvious aggregates or precipitates were seen in the cleavage solution.

For a x10 dilution into an assay for [<sup>3</sup>H]ryanodine binding at a final active concentration of 100  $\mu$ M, a peptide solution of 1 mM would be required which equates to ~4.3 mg/ml. For a 2 ml elution from the Vivapure IEX 8.6 mg would need to be captured. For 8.6 mg to be liberated from the GST fusion the starting mass of GST-DP4WT would need to be 61 mg of protein. The efficiency of the cleavage and capture process to produce the peptides therefore requires more consideration and refinement.

**Chapter 6; Peptide and  
pharmacological regulation of RyR1**



---

## **CHAPTER 6: Peptide and pharmacological regulation of RyR1**

### **6.1 Introduction**

Previous studies have shown there are appreciable differences in the 3D structure of RyR between non-activated and activated states (Orlova, Serysheva et al. 1996; Serysheva, Schatz et al. 1999). In order to understand the mechanism of channel regulation in both normal and diseased states it is important to identify and characterize the domains involved in this conformational control.

Most MH-linked mutations have been found to reside in the N-terminus and central domains of RyR1, whereas those linked to CCD populate the C-terminus, especially the transmembrane domain. MH mutations on these domains cause aberrant channel function, including hyper activation and hyper sensitization of the channel to various physiological and pharmacological agonists, resulting in a leaky calcium channel (Dirksen and Avila 2002). These findings suggest that these MH domains are involved in the conformational control of RyR calcium channels . Domain peptides are useful as functional probes as they are able to maintain their native conformational structure *in vitro* in solution. Clustering of MH mutations to the DP4 region of RyR1 suggests that this region may play a critical role in inter-domain interaction. Domain interactions are proposed to maintain the channel in its closed state but undergo a conformational change as part of the molecular rearrangement of the RyR as it gates from the closed to open conductive state (Yamamoto, El-Hayek et al. 2000; Bannister, Hamada et al. 2007).

The tetragonal symmetry of the RyR provides four identical regulatory sites for every RyR modification or interaction (Orlova, Serysheva et al. 1996). It is not yet known whether they require saturation with all sites occupied or whether there is cooperativity once one subunit is modified. The domain interaction could be intra subunit or between adjacent subunits of the homotetramer. A recent study labelling the N terminus and Central domains with fluorescent peptides and measuring FRET has suggested an inter subunit interaction is likely (Liu, Wang et al. 2010). Some studies have shown that for MH, irrespective of the individual point mutation, the phenotypes were similar. This indicates that mutations in either of these domains make an

equivalent contribution to the abnormal mode of channel regulation regardless of position. Therefore channel disorder may be controlled by a global mechanism involving a domain or domains of the RyR, rather than specific residues (Treves, Anderson et al. 2005).

Initial experiments using the DP4 peptide (Yamamoto, El-Hayek et al. 2000) have shown a calcium biphasic dose response unchanged in the presence of 100  $\mu\text{M}$  DP4, but with a 4 fold increase in the magnitude of binding activity observed in activating calcium concentrations. DP4 was also able to significantly enhance ryanodine binding at 0.01  $\mu\text{M}$  calcium, because this level of calcium is associated with an almost closed channel state this suggests there are calcium dependent and calcium independent activation mechanisms at work in the mode of DP4 activation. [ $^3\text{H}$ ]ryanodine binding experiments were also carried out in the presence of varying magnesium concentrations, the  $\text{EC}_{50}$  with and without DP4 was approximately the same, implying that the magnesium is still able to exert a significant inhibitory effect in the presence of the activatory peptide. An alternative peptide, corresponding to the LCC has also been shown to activate the RyR1 and is proposed by the group to mimic voltage-dependent induction of skeletal muscle type ECC (allosteric activation). DP4 was shown to have an effect additive to this peptide. Polylysine (an RyR-specific ligand) was also tested with DP4, where it was shown to shift the biphasic activation curve to the left. These effects correspond to changes in the activity pattern in MH conditions i.e. Hyperactivation of the release channel activity and the increased affinity to the release triggering reagents. The R to C mutation of DP4 was shown to abolish the activatory effect of the wildtype peptide, as mentioned earlier, indicating the high specificity of amino acid sequence required for this RyR1 domain. The peptide DP1, corresponding to the N-terminal, activated the RyR1 in a similar fashion to the DP4 central domain peptide, however a combination of both resulted in half maximal activation, which was interpreted as a sign that the peptides are competing for a common site of regulation. These observations lead to the N-terminus and central domain interaction hypothesis (Yamamoto, El-Hayek et al. 2000).

DP4 was combined with CHAPs in studies by Murayama et al. as CHAPs was known to override the reduction in CICR gain seen in RyR1 compared to RyR3 in mammalian skeletal

muscle. DP4 was able to activate RyR1 but not RyR3 and the drug Dantrolene, a potent inhibitor of RyR1 used to treat MH, reversed the effects of both DP4 and CHAPs in an identical manner suggesting that activation of RyR1 by DP4 and CHAPs may be through a common mechanism (Murayama, Oba et al. 2005). FKBP12 has been proposed to bind to a region of the central domain inherent to the DP4 sequence (Gaburjakova, Gaburjakova et al. 2001). By incubating SR vesicles with both the peptide and FK506 (to remove all endogenous FKBP12 protein), it was determined whether DP4 resulted in competitive dissociation of FKBP12. DP4 and DP4M had no notable effect. [<sup>3</sup>H]ryanodine binding in the presence and absence of DP4 alongside FK506 also showed the same extent of activation. These results indicate an FKBP12 independent mechanism of activation by both DP4 and CHAPs (Murayama, Oba et al. 2005).

In single channel studies, ATP has been shown to increase the open probability of the channel at least 4 to 8 fold (Laver, Lenz et al. 2001). In most studies using DP4, although activation is seen, this peptide does not increase activity to the same degree as ATP (Murayama, Oba et al. 2005). One [<sup>3</sup>H]ryanodine binding study using the non-hydrolysable ATP analogue (AMPPCP), showed an increase in binding of 7 to 8 fold at all AMPPCP concentrations in the presence of 100  $\mu$ M DP4. There was no significant difference in the activation pattern observed, the EC<sub>50</sub> was approximately the same in both instances, suggesting that DP4 has no additional effect in the presence of ATP (Murayama, Oba et al. 2005). Previous studies carried out in the presence of the DP4 wildtype and mutant peptides have shown it was able to increase spark frequency in permeabilised frog skeletal muscle fibres (Shtifman, Ward et al. 2002). Frog muscle fibres were also assessed for spark generation in the presence of magnesium and DP4 was found to be activatory even in the presence of mM levels of magnesium, although its effect was decreased compared to the control. Frog SR single channel studies have incorporated RyR into lipid bilayers for single channel analysis in the presence of 1 mM magnesium, and 100  $\mu$ M DP4 showed a severe reduction in channel activity in the presence of magnesium, which was mildly overridden by the DP4 addition and a slight increase in opening rate was seen, but was not as dramatic as the effects seen measuring sparks in the muscle fibre preparations. DP4 was shown to have a lower apparent affinity for RyR in the presence of magnesium, suggesting magnesium is able to modulate the ability of DP4 to 'unlock' the channel. This group

hypothesize that it is the low affinity I-binding site for magnesium involved in regulation of DP4 effectiveness (Murayama, Oba et al. 2005).

A combination of experimental data from RyR1 studies incorporating the DP4 peptide and its mutant have contributed to the understanding of RyR modulation in normal and disease (MH and CCD) states. Although the effects of magnesium and ATP have been characterised previously not much is known of the effects of other physiological modulators in addition to one another and, more importantly in an RyR model where phosphorylation and endogenous FKBP levels are controlled and standardised. The latter concept has been addressed in this study to enable a tighter grasp on the modulatory effect of DP4, and to simultaneously assess the region of convergent regulation previously proposed for PKA and FKBP12 modulatory effect (Blayney, Jones et al. 2010).

This chapter will examine the effects of DP4WT and DP4M on isolated RyR1, in the presence of FKBP12, magnesium, ATP, both to characterise these effects on our solubilised RyR1 preparations and to add new insight into whether the effects of RyR modulators are linked to the N-terminus and central domain interaction. Preliminary studies using [<sup>3</sup>H]ryanodine binding will provide valuable information on the activation/deactivation of the channel. Due to the aforementioned effect of the anti-MH drug on DP4WT activation (chapter 5) and previous work done by Blayney et al. showing inhibition of both RyR1 and RyR2 by K201 (Blayney, Jones et al. 2010), there was an initial plan to assess the effects of the anti-arrhythmic drug K201 on DP4WT activation to assess whether this also had an inhibitory effect. However, due to the lack of availability of the benzothiazepine K201, diltiazem, a less specific derivative, was tested instead. The respective structures of these two compounds are shown in figure 6.1. Diltiazem is a broad range calcium channel blocker but has been shown to suppress arrhythmias in isoprenaline perfused mouse hearts in one study, suggesting a role in treatment of  $\beta$ -adrenergic related arrhythmias (Balasubramaniam, Chawla et al. 2004). Given that approximately 50% channel inhibition has been observed in [<sup>3</sup>H]ryanodine binding studies in the presence of K201 (Blayney, Jones et al. 2010), it was of interest to test whether a less specific drug would demonstrate the same inhibition.

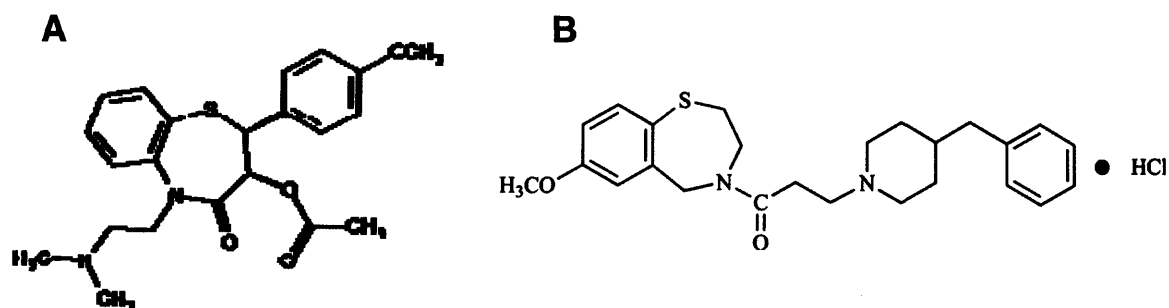


**Figure 6.1 Structures of A) Diltiazem and B) K201**

## **6.2 Results**

### **6.2.1 Effect of synthetic DP4WT and DP4M peptides on RyR1 [<sup>3</sup>H]ryanodine binding**

DP4WT synthetic peptide from Severn Biotech was shown to have the greatest effect on [<sup>3</sup>H]ryanodine binding at 100  $\mu$ M, increasing binding from the control value of 100% to 182.46%  $\pm$  11.66 (Figure 6.1A). DP4M synthetic peptide showed a similar potency to the wildtype, increasing from 100% to 202.1%  $\pm$  15.01 (n=4). DP4WT activation was compared to ATP activation of RyR1, as demonstrated earlier in chapter 4, and it is clear that although the DP4WT peptide is capable of increasing binding, and therefore opening the RyR channel above that caused by calcium alone, ATP is still more activatory, increasing binding to close to 400% (370.77%  $\pm$  32.06) (Figure 6.2). However, the expense of the peptides prevented the extension of the dose response curve to higher concentrations.

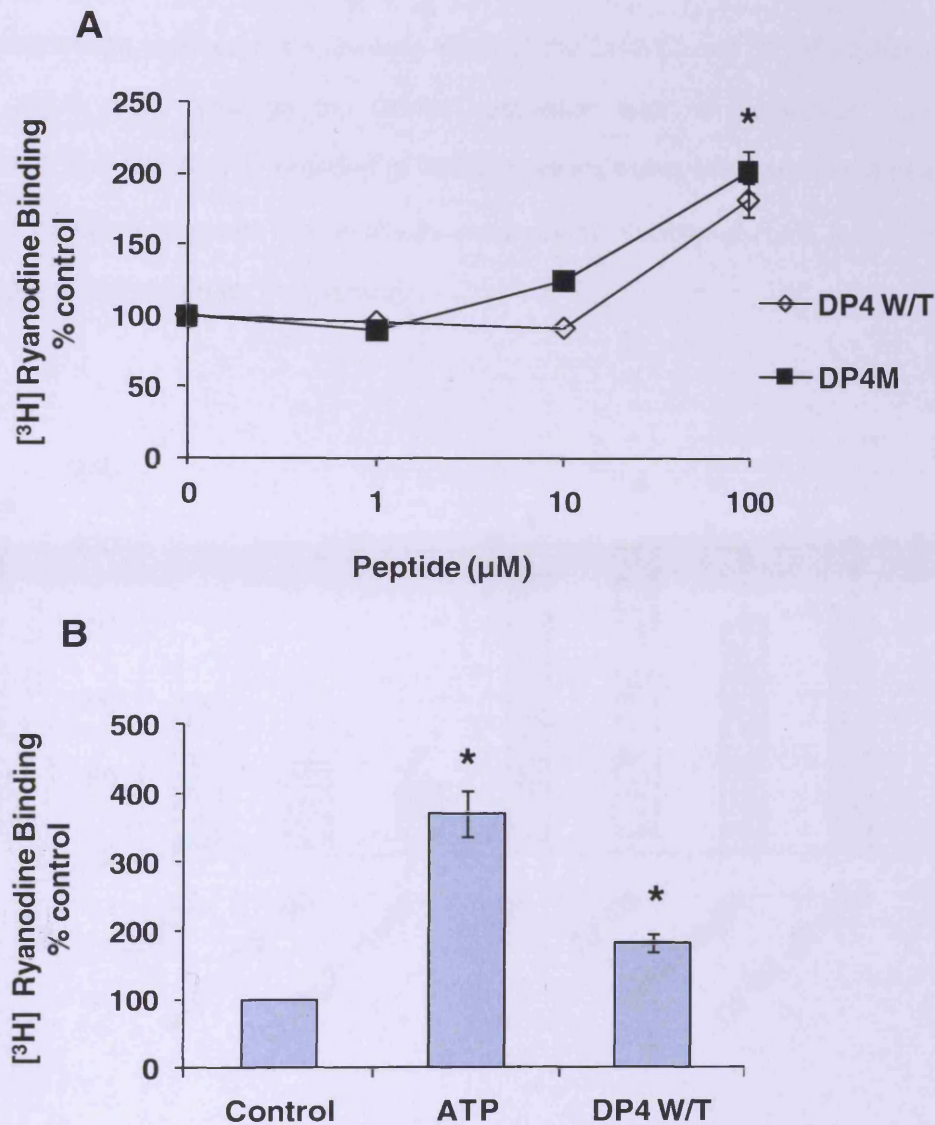


**Figure 6.2 Effect of synthetic DP4WT peptide on RyR1 [ $^3\text{H}$ ]ryanodine binding**

**A)** DP4 dose response is shown for both the wildtype and mutant DP4 peptides. Each point represents the mean of paired data for 1 RyR1 preparation, except for 100  $\mu\text{M}$  of peptide which was the average of 4 RyR1 preparations. (\*) indicates a significant difference ( $p < 0.05$ , students paired t-test) from the control value without peptide addition. (Binding in  $p\text{Ca}4$  is taken as 100%). Bars show standard error.

**B)** Comparison of the effect of 100  $\mu\text{M}$  synthetic DP4WT with ATP activation of RyR1 [ $^3\text{H}$ ]ryanodine binding. Each point represents the mean of 4 RyR1 preparations. (\*) indicates a significant difference ( $p < 0.05$ , students unpaired t-test) from the control value without ATP or DP4 addition. (Binding in  $p\text{Ca}4$  is taken as 100%). Bars show standard error.

## 6.2.2 Effect of inhibitors of RyR1 activity on DP4WT activation of the channel

### 6.2.2.1 Magnesium

0.5 mM magnesium reduced the activatory effect of the DP4WT and DP4M peptides used at 100  $\mu$ M (Figure 6.3). Although the DP4WT activation was not completely reversed by magnesium, it was significantly reduced ( $p < 0.05$ , students t-test) when compared to activation in the absence of magnesium. The results for magnesium inhibition of RyR1 by 0.5 mM and 1 mM magnesium are shown for comparison.

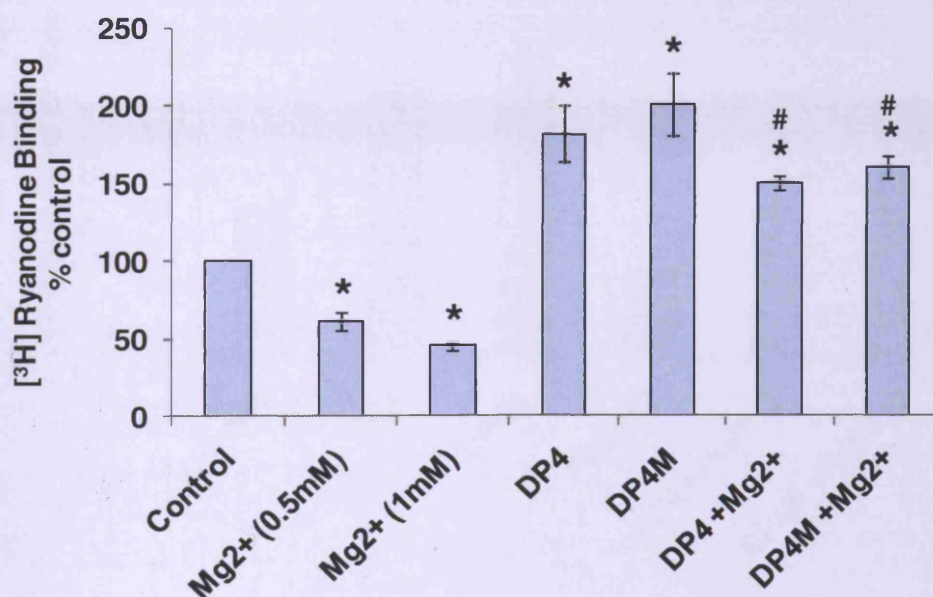


**Figure 6.3 Effect of synthetic DP4WT activation on RyR1 [<sup>3</sup>H]ryanodine binding in the presence of Mg<sup>2+</sup>**

Magnesium (0.5 mM) and DP4WT/M (100  $\mu$ M) effect are shown compared with DP4WT and DP4M (100  $\mu$ M) peptides added in the presence of magnesium. Each point represents the mean of 4 RyR1 preparations. (\*) indicates a significant difference ( $p < 0.05$ , students paired t-test) from the control value without magnesium or peptide addition. (#) indicates a significant difference ( $p < 0.05$ , students paired t-test) from the DP4WT control. (Binding in pCa4 is taken as 100%). Bars show standard error.

### 6.2.2.2 FKBP12

Figure 6.4 shows the effect of 10  $\mu\text{M}$  FKBP12 addition to RyR1 was to reduce the activity of the control by 50%. The addition of 10  $\mu\text{M}$  FKBP12 to DP4WT activated RyR1 also reduced activity to a similar extent, returning the binding to control levels. DP4M activation was also reversed but to a lesser extent.

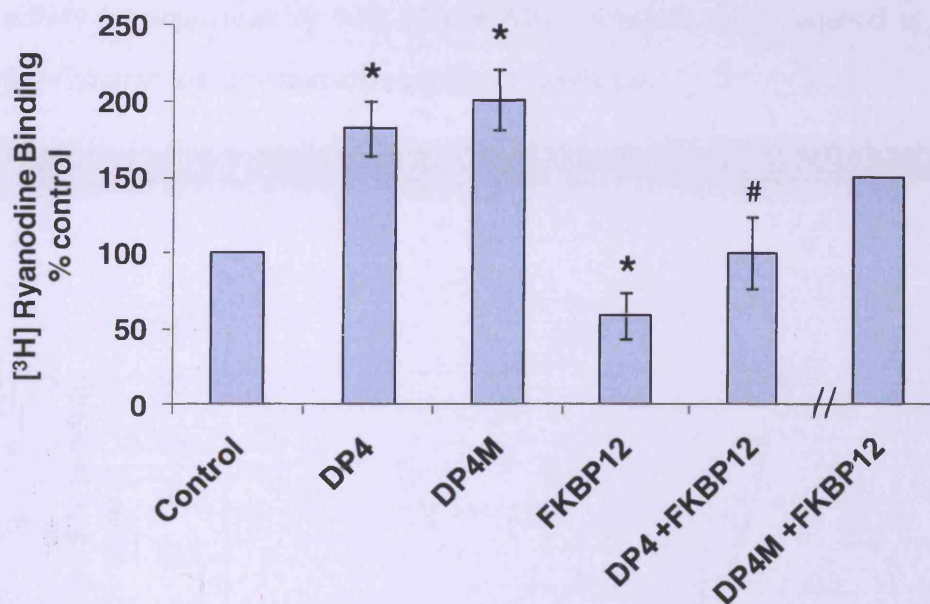


**Figure 6.4 Effect of synthetic DP4WT activation on RyR1 [<sup>3</sup>H]ryanodine binding in the presence of FKBP12.**

FKBP12 (10  $\mu\text{M}$ ) and DP4 (100  $\mu\text{M}$ ) effect are shown compared with DP4WT and DP4M (100  $\mu\text{M}$ ) peptides added in the presence of FKBP12. Each point represents the mean of 3 RyR1 preparations, except for DP4M+FKBP12 which is  $n=1$ . (\*) indicates a significant difference ( $p < 0.05$ , students paired t-test) from the control value without FKBP12 or peptide addition. (#) indicates a significant difference ( $p < 0.05$ , students paired t-test) from the DP4WT control. (Binding in pCa4 is taken as 100%). Bars show standard error.



### 6.2.3 Effect of the original Ikemoto DP4WT peptide

The dose response to the Ikemoto wildtype (IK-DP4WT) peptide (Figure 6.5) was shown to be similar to that for the Severn Biotech wildtype peptide (Figure 6.2A). Used at 100  $\mu\text{M}$  peptide the relative increase in binding compared to the control was approximately 2-fold in both cases. Due to the limited quantity of IK-DP4 available for experiments, an n of 2 was only obtained for the dose response and 100  $\mu\text{M}$  was the chosen concentration for all further experiments. Magnesium and FKBP12 reduced DP4 activation compared with the control DP4 data, magnesium reduced binding to almost control level (without additions), whereas FKBP12 reduced activity by approximately 50% (Figure 6.6). A higher (n) is required to determine whether these differences observed are statistically significant.

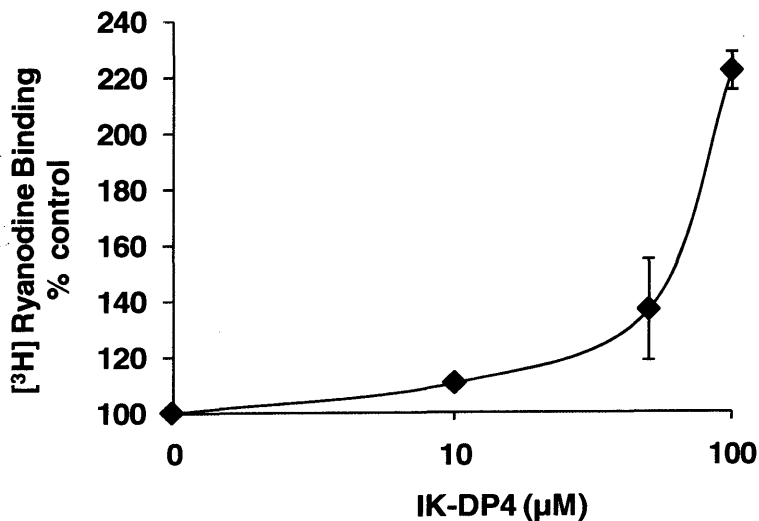


**Figure 6.5 Effect of IK-DP4WT peptide on RyR1 [<sup>3</sup>H]ryanodine binding.**

IK-DP4WT dose response is shown. Each point represents the mean of 2 RyR1 preparations. (Binding in pCa4 is taken as 100%). Bars show standard error.

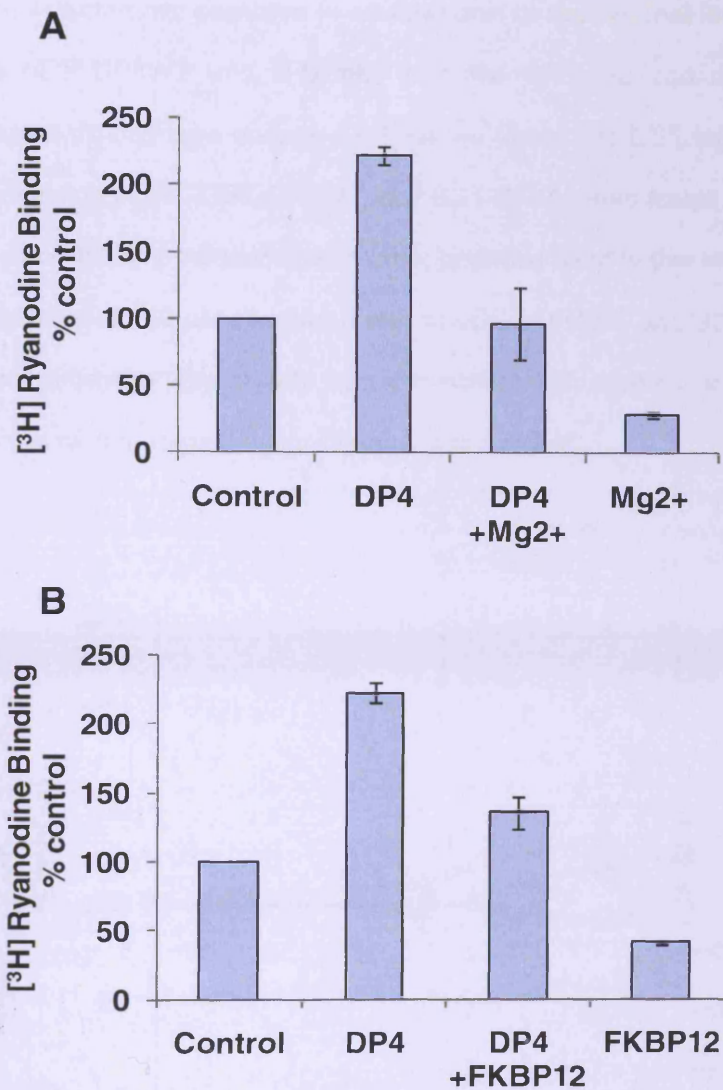


**Figure 6.6** Effect of IK-DP4WT peptide activation on RyR1 [<sup>3</sup>H]ryanodine binding in the presence of magnesium and FKBP12.

**A)** Magnesium (0.5 mM) effect is shown compared to IK-DP4WT (100 μM) and IK-DP4WT added in the presence of magnesium.

**B)** FKBP12 (10 μM) effect is shown compared to IK-DP4WT (100 μM) and IK-DP4WT added in the presence of FKBP12. Each point represents the mean of 2 RyR1 preparations. (Binding in pCa4 is taken as 100%). Bars show standard error.

#### 6.2.4 Effect of recombinant peptides in comparison to the original Ikemoto peptide

The cleavage of R-DP4WT and R-DP4M from the GST tag and particularly subsequent purification proved difficult (see chapter 5). Thus we tested the GST tagged peptides to see if they had an activating effect. GST-DP4WT and GST-DP4M were found to have little activatory effect on ryanodine binding compared with other peptides used in this study. Figure 6.7 shows the IK-DP4 response at 100  $\mu\text{M}$  compared with the GST-DP4WT and GST-DP4M and the latter effects were not shown to vary greatly from the control with no peptide addition. A greater (n) would be required to determine the significance of this result.

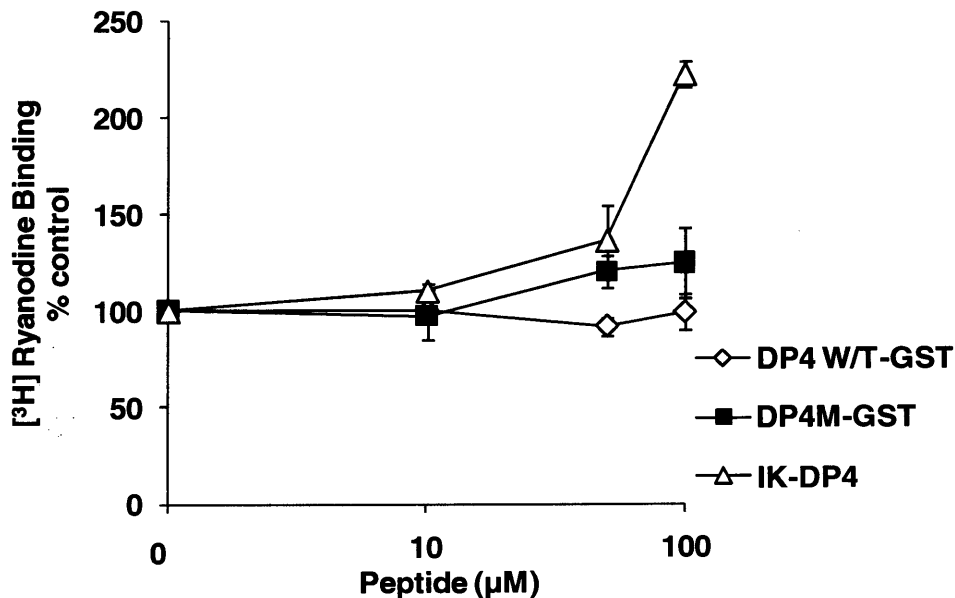


**Figure 6.7** Effect of recombinant GST-DP4WT/M on RyR1 [ $^3\text{H}$ ]ryanodine binding.

GST-DP4WT and GST-DP4M dose responses compared with IK-DP4WT at 100  $\mu\text{M}$ . Each point represents the mean of 2 RyR1 preparations. (Binding in pCa4 is taken as 100%). Bars show standard error.

Figure 6.8 shows the effect of the cleaved DP4 recombinant peptide, without the GST tags and although the maximal concentration available for these peptides was only 10  $\mu\text{M}$ , a comparison with the wildtype IK-DP4 at the same concentration suggests that the recombinant peptide is equally as activatory.

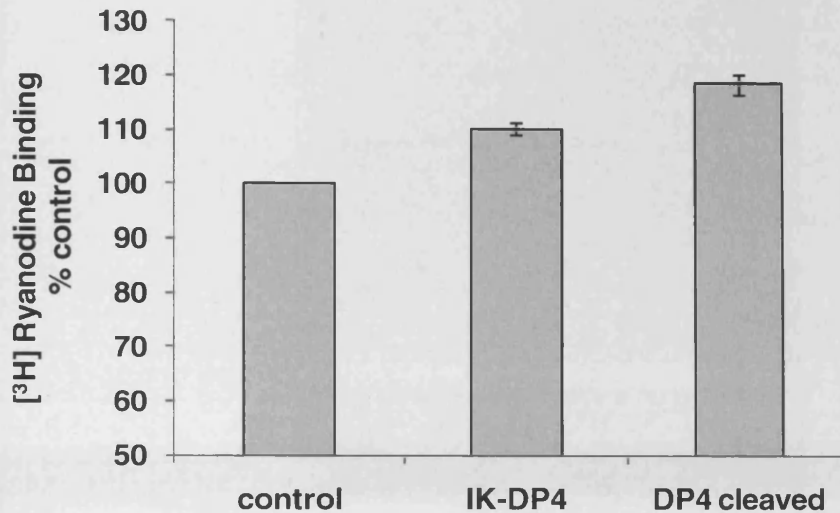


**Figure 6.8** Effect of the recombinant DP4WT peptide on RyR1 [<sup>3</sup>H]ryanodine binding compared with IK-DP4WT peptide.

Binding in the presence of 10  $\mu$ M R-DP4WT (DP4 cleaved) is shown compared with 10  $\mu$ M of IK-DP4WT. Each point represents the mean of 2 RyR1 preparations. (Binding in pCa4 is taken as 100%). Bars show standard error.

### 6.2.5 Peptide interaction with FKBP12 protein

DP4WT and DP4M contain the putative FKBP12 binding motif (Gaburjakova, Gaburjakova et al. 2001; Murayama, Oba et al. 2005), thus the effect of addition of high concentrations of peptide could be to counteract RyR-FKBP12 binding. The GST-DP4WT construct was used in a GST-pull down assay (Figure 6.9). No FKBP12 was detected as being pulled out of solution by GST-DP4WT, as shown by the lack of an FKBP12 band on both the coomassie and the western blot probed with anti-FKBP12 Ab. This indicates that the DP4WT moiety did not interact with FKBP12.

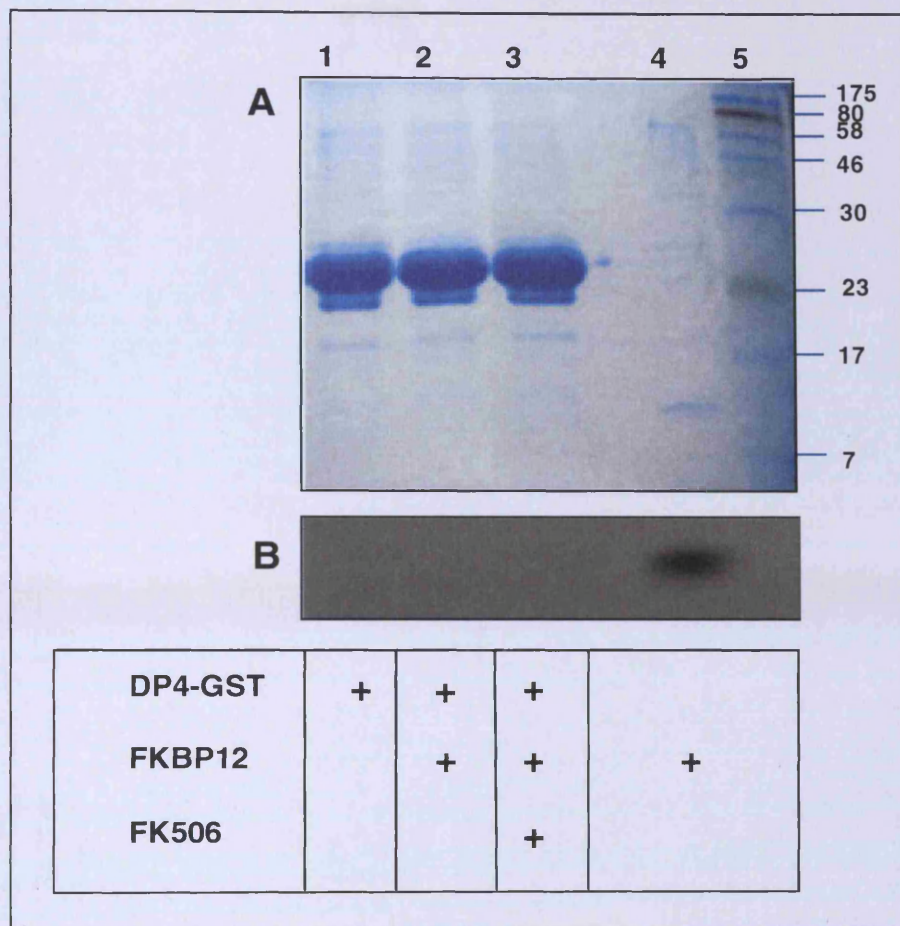


**Figure 6.9 GST-DP4WT pull down assay for FKBP12**

**A)** GST-DP4WT was incubated with FKBP12 for one hour in both the presence and absence of FK506 to determine whether there was any interaction between these proteins. Following incubation, samples were boiled with SDS loading buffer and separated on 15% SDS-PAGE gels **A)** Lane 1, GST-DP4WT control (~30 kDa) without FKBP12 or FK506. Lane 2, GST-DP4WT after incubation with FKBP12. Lane 3, GST-DP4WT after incubation with FKBP12 in the presence of FK506. Lane 4, FKBP12 (10  $\mu$ M) control. Lane 5, kaleidoscope protein size marker, sizes are shown on the right (kDa).

**B)** Samples were also transferred to a PVDF membrane for blotting with anti-FKBP12 specific antibody. Lanes 1-4 contain the same as in **A)**, all were probed with anti-FKBP12 antibody.

### 6.2.6 Pharmacological modulation of RyR1

Previous studies have shown that the anti-arrhythmic drug K201 is able to reduce [ $^3$ H]ryanodine binding by approximately 50%. The initial aim was to incorporate this drug into experiments as part of this investigation however a supply sent to us as a gift and found to be effective previously was exhausted, and we didn't have the rights to use more of this drug. K201 was designed as a diltiazem analogue, so experiments were carried out to determine its effect on

[<sup>3</sup>H]ryanodine binding (Figure 6.10) and if it could be used in a similar way to K201. Diltiazem had no effect at  $\mu$ M concentrations even when increasing the baseline open level of the RyR, by adding 2.5 mM ATP (described earlier in chapter 4). No effect was seen until a concentration of 100 mM, when there was a dramatic decrease in binding. This was a very high concentration for a pharmacological effect so it was concluded that diltiazem could not be used as a surrogate for K201.

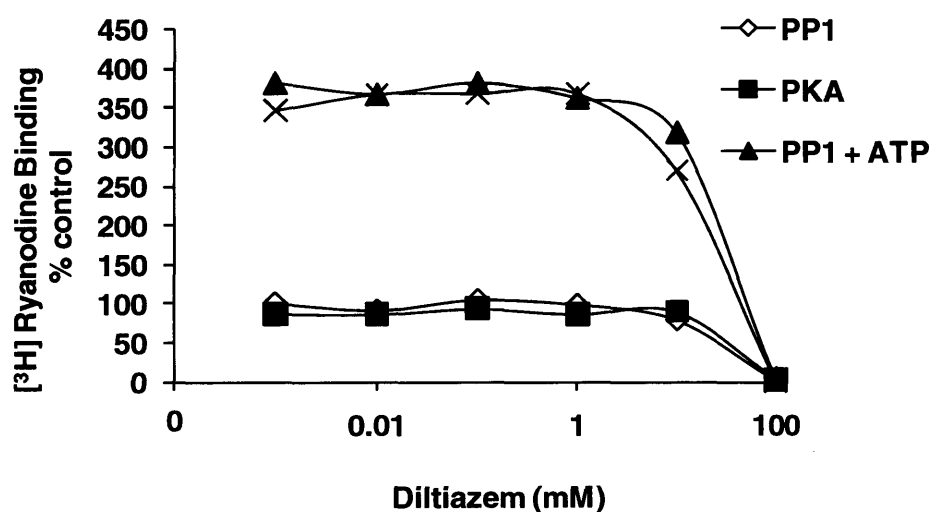


**Figure 6.10 Effect of Diltiazem on RyR1 [<sup>3</sup>H]ryanodine binding.** Diltiazem dose response in the presence and absence of 2.5 mM ATP. Each point represents the mean of paired data for 1 RyR1 preparation. (Binding in pCa4 is taken as 100%). Bars show standard error.

### 6.3 Discussion

The domain peptide DP4 has proved to be a useful tool in the characterisation of the N-terminus/central domain interaction. It was the intention to use DP4 to determine whether the regulation of RyR by phosphorylation and FKBP12 is part of the same interaction. It was first necessary to characterise the effect of DP4WT and DP4M on channel activation using solubilised RyR preparations and [<sup>3</sup>H]ryanodine binding. The initial experiments using peptides chemically synthesised by Severn Biotech showed that the DP4WT and DP4M peptides were equipotent rather than DP4M being an inactive control as described in the literature (Yamamoto,

El-Hayek et al. 2000). This result has necessitated comparison of various sources of the peptides and the functional effects on RyR activity are discussed below.

DP4WT activation was shown to increase up to 100  $\mu$ M, higher concentrations were not tested but this concentration has been used in previous experiments (Yamamoto, El-Hayek et al. 2000). This group found [ $^3$ H]ryanodine binding to increase to 400% of the control value (100%), and an increase to approximately 200% was only ever observed in our investigation, where the two sources of DP4WT peptide were shown to have similar activational curves and one of these peptides was the original IK-DP4WT peptide. For both peptides DP4WT activation was shown to be less than that observed in the presence of 2.5 mM ATP. The assay conditions used for [ $^3$ H]ryanodine binding on SR preparations (Yamamoto, El-Hayek et al. 2000) were very similar to those used in this study so it is interesting that a smaller effect was seen in our experiments. One factor could be the use of solubilised RyR preparations which are different from SR in a number of respects. FKBP12 is stripped off and the preparations were dephosphorylated. This could have contributed to resetting the open closed conformation giving a different 'baseline' from which DP4 has to interact with RyR and this may redefine the ease of opening. RyR within the SR membrane may have a more 'natural' physiological environment but this makes the parameters governing its regulation more difficult to dissect.

Of particular importance was the finding that DP4M had the same activatory effect on [ $^3$ H]ryanodine binding as DP4WT. All of the papers in which DP4WT and DP4M have been used have resulted from collaborations with the Ikemoto Group who have supplied the peptides (Kobayashi, Bannister et al. 2005; Bannister, Hamada et al. 2007; Hamada, Bannister et al. 2007). These were synthesised using Fmoc [N-(9-florenyl)methoxycarbonyl] as the amino protecting group. The peptides were released from the solid support resin and deprotected using 95% trifluoroacetic acid and purified by reverse phase HPLC. The commercial peptides which were synthesised by Severn Biotech were also supplied as a salt of trifluoroacetic acid and these too had been purified by reverse phase HPLC. To solubilise the Severn Biotech peptide we used DMSO. The peptides were then diluted with water to give a 50% DMSO solution of 1 mM final peptide concentration. The dilution into the [ $^3$ H]ryanodine binding assay

was x10 giving a final DMSO concentration of 5% with a maximum active peptide concentration of 100  $\mu$ M. Serial dilutions of DP4WT/M for the assays were always made with 50% DMSO and this maintained a constant 5% DMSO concentration in all assay tubes including the controls. The Ikemoto WT peptide was treated in the same way so that it was strictly comparable to our purchased peptide.

DP4WT activation was shown to increase up to 100  $\mu$ M, higher concentrations were not tested but this concentration has been used in previous experiments (Yamamoto, El-Hayek et al. 2000). This group found [ $^3$ H]ryanodine binding to increase to 400% of the control value (100%), and an increase to approximately 200% was only ever observed in our investigation, where the two sources of DP4WT peptide were shown to have similar activational curves and one of these peptides was the original IK-DP4WT peptide, Although it must be noted that low availability of IK-DP4 has only enabled an n of 2 to be obtained in all experiments, therefore these data cannot be considered statistically significant. For both peptides DP4WT activation was shown to be less than that observed in the presence of 2.5 mM ATP. The assay conditions used for [ $^3$ H]ryanodine binding on SR preparations (Yamamoto, El-Hayek et al. 2000) were very similar to those used in this study so it is interesting that a smaller effect was seen in our experiments. One factor could be the use of solubilised RyR preparations which are different from SR in a number of respects. FKBP12 is stripped off and the preparations were dephosphorylated. This could have contributed to resetting the open closed conformation giving a different 'baseline' from which DP4 has to interact with RyR and this may redefine the ease of opening. RyR within the SR membrane may have a more 'natural' physiological environment but this makes the parameters governing its regulation more difficult to dissect.

The effects of the physiological inhibitors FKBP12 and magnesium were tested to see if they could inhibit RyR activity in the presence of DP4. For DP4 both the Severn Biotech peptide and the IK-DP4WT were ~50% inhibited by 10  $\mu$ M FKBP12. This is the same as the maximal effect of 50% inhibition of [ $^3$ H]ryanodine binding without peptide addition. Unfortunately there was insufficient peptide from any source to obtain a dose response curve for FKBP12 at 100  $\mu$ M



DP4 and determine whether the  $K_i$  for FKBP12 was different from that of the control without peptide.

However, there has been suggestion that DP4 houses an FKBP12 putative binding site (Gaburjakova, Gaburjakova et al. 2001), which may provide an explanation for the inhibitory effect, if the FKBP12 is bound to GST-DP4WT with high affinity and thereby neutralised its binding to the site within the RyR1 molecule. Therefore a GST pull down experiment was carried out where the GST-DP4WT peptide was incubated with FKBP12, both in the presence and absence of FK506 as a control for specificity and with glutathione beads, so that the GST-DP4WT was affinity purified following incubation. The products were run on a gel following wash steps and western blotted with anti-FKBP12 antibody to check for bound FKBP12 'pulled-down' with the affinity purified GST-DP4WT (Figure 6.9). This shows that there was no evident binding of GST-DP4WT with the FKBP12 protein used in these experiments and that the effects seen in [ $^3$ H]ryanodine binding are attributable to an allosteric effect of FKBP12 binding to RyR1 at a different site and probably influencing the conformational change in the DP4 binding domain.

Magnesium significantly reduced the DP4 activation as reported previously (Murayama, Oba et al. 2005). This inhibition appeared to be less potent for the Severn Biotech peptide but equipotent for IK-DP4WT (where despite a low  $n$  the error bars were small) in comparison to the effect of magnesium in the absence of peptide. A higher  $n$  for these experiments and a dose response would be required to see if this was a real difference or the result of insufficient data. It has been shown that magnesium has the same  $EC_{50}$  in the presence and absence of DP4 (Bannister, Hamada et al. 2007).

The majority of previous studies using IK-DP4M have shown very little activation and this is one of the key findings that has led to the domain interaction hypothesis, as the single amino acid change in the mutant peptide mimics an MH mutation which has previously been suggested to be sufficient to disrupt domain interaction and thus RyR stability. It is of note however, that one study (Bannister, Hamada et al. 2007), comparing various DP4M peptides containing other MH or alternative mutations, showed a range of activation by all mutant peptides tested, but the

DP4M R-C mutation had the least effect. At 100  $\mu\text{M}$ , activation by the R-C mutant peptide (DP4M) was comparably less than the wildtype, but still showed activation of the RyR, increasing with concentration.

This leaves us with the question as to why, in these experiments, the synthetic DP4M peptide was as active as DP4WT. NMR data shows the backbone of the WT peptide to consist of two helices connected by a loop (Bannister, Hamada et al. 2007). The MH mutations published to date, in this region, all fall in the loop or in the first helix adjacent to the loop. The position of R2458 is shown in the centre of the loop, which is consistent with interaction with another protein since interaction sites are frequently in such loop regions (Figure 5.1) (Bannister, Hamada et al. 2007). The protein concentration necessary for NMR was 4 mg/ml. The mutant could not have its structure assessed as it was not soluble at this concentration in the desired buffer. One of the disadvantages of the use of these peptides is the apparent very low affinity of the DP4WT for their partner interaction site (30 -100  $\mu\text{M}$   $K_d$ ) and this necessitates using these peptides at very high concentrations (Bannister, Hamada et al. 2007). To achieve the 500  $\mu\text{M}$  concentration of peptide in some of the dose response curves the final assay concentration would need to be 2 mg/ml. Thus even for a 1:1 assembly of an assay mix the starting concentration would need to be 4 mg/ml and even higher if a greater dilution was required to make additions to the assays. Differences in solubility, which limited the concentrations that could be compared for activity, were also noted for DP4 peptides containing R2452W, R2454C and R2458H mutations. These peptides could only be compared up to a maximum final concentration of 200  $\mu\text{M}$  (Bannister, Hamada et al. 2007). This begs the question as to whether the inactivity of the DP4M as a synthetic peptide might be a function of its solubility under some assay conditions, particularly at high concentrations. In this study, it was possible to solubilise the Severn Biotech peptides, both mutant and WT, in 50% DMSO to 1 mM and the IK-DP4WT peptide was treated similarly. The IK-DP4WT was supposed to be soluble in water but in our hands this was not the case.

GST-DP4WT was not found to be an effective substitute for the standard peptides as no increase in [ $^3\text{H}$ ]ryanodine binding was observed. It is possible that the GST tag (26 kDa) prevented interaction. However, larger molecules such as an antibody to DP4 and DP1

peptides have been used to activate RyR, in a similar way to the peptides (Kobayashi, Yamamoto et al. 2004), so access to the interdomain space is not the reason for this observation. Alternatively, perhaps the peptides are sterically prevented from interacting with their binding domain. It was encouraging to observe that once the GST tag was removed, the wildtype peptide appeared to be activatory at the equivalent concentration (10  $\mu\text{M}$ ) to the original IK-DP4, although this was too low a concentration for a definitive result, so it would be interesting to see whether this peptide would be as active at 100  $\mu\text{M}$ . Purification difficulties following 3C cleavage of the GST tag, as discussed in chapter 5, have prevented the development of a more concentrated peptide preparation as yet.

Previous experiments have used K201 as a useful tool in conformational studies. As an alternative to K201, Diltiazem was tested and found to have no significant effect on [ $^3\text{H}$ ]ryanodine binding, and even in the presence of ATP, which is known to open the channel maximally (Meissner 2002), no effect was observed until concentrations of the drug were reached that were unlikely to be pharmacologically useful. This finding suggests that Diltiazem does not serve as a suitable alternative therapy to the anti-arrhythmic drug K201. Perhaps the less specific nature of Diltiazem means that in an SR preparation the apparent effect on RyR might not be due to a direct effect on the RyR molecule. A previous study linking the use of Diltiazem with suppression of  $\beta$ -adrenergic arrhythmia found the drug to be effective at micromolar concentrations on perfused mouse hearts, suggesting a more intact cardiovascular model is required for efficacy of this drug (Balasubramaniam, Chawla et al. 2004). However the isolated channels used in our investigation would require a drug that directly modulates RyR to show any effect on [ $^3\text{H}$ ] ryanodine binding.

Using [ $^3\text{H}$ ]ryanodine binding, the effect of the DP4WT activatory peptide on both magnesium and FKBP12 inhibition of isolated, native RyR1 stripped of endogenous FKBP12 has been demonstrated. It is worth noting that binding in the presence of DP4WT could be reduced by either FKBP12 or magnesium, as seen in the absence of DP4WT, showing that inhibition by these modulators can counter the activatory effect of the DP4WT peptide. The effect of FKBP12 on DP4WT activation was a novel finding and an effect that was attributed to an

allosteric interaction and not competition resulting from FKBP12 binding to the peptide. The data supports the concept that the effects of DP4WT on the central domain interaction and those of magnesium and FKBP12 regulation of RyR activity may be linked. Peptides were of insufficient concentrations to enable paired experiments to be carried out on phosphorylated and de-phosphorylated preparations. For the future it will be of interest to test whether this has any impact on the ability of DP4WT to activate the channel. Given previous findings it may be the case that no difference would be observed with [<sup>3</sup>H]ryanodine binding (Jones, Lai et al. 2006). A more subtle change in affinity for FKBP12 may be measured using the Biacore (Jones, Reynolds et al. 2005). The finding that FKBP12 was unable to bind to the DP4WT peptide is valuable as it enables the Biacore experiments to be carried out in the knowledge that the inclusion of peptide would not result in it binding to the sensor chip and directly competing with RyR binding. This would test the effect of the peptides to alter the kinetics of FKBP12 binding to RyR1 in response to phosphorylation and link the central domain interaction to the conformational change caused by phosphorylation (Blayney, Jones et al. 2010).

## Chapter 7; Modulation of RyR2

## **CHAPTER 7; Modulation of RyR2**

### **7.1 Introduction**

In parallel with the studies on RyR1, it was proposed to examine the effects of the physiological modulators of RyR2 function; calcium, ATP and magnesium and to compare these with the action of the activatory peptide DPc10.

The RyR2 dose response curve to free calcium concentration has been shown to be biphasic suggesting that like RyR1, RyR2 has high affinity activation sites and lower affinity inactivation sites. (Xu, Mann et al. 1996),(Liu, Pasek et al. 1998). These have been labelled A for activation and I for inhibition (Laver 2007). Single channel bilayer studies have demonstrated that calcium alone cannot completely open an RyR2 channel (Sitsapesan, Montgomery et al. 1995),(Laver 2007). ATP at ~2 mM in addition to calcium is necessary to fully activate a channel and the presence of ATP decreases the  $K_a$  for calcium from 6 to 1  $\mu$ M (Laver 2007).

The physiological concentration of free magnesium in the heart is estimated to be ~100mM (Hohl, Garleb et al. 1992), (Koretsune, Corretti et al. 1991), with much of the total magnesium being complexed with ATP. Studies assessing magnesium and ATP effects on RyR2 have yielded similar results to those for RyR1, although Meissner et al have suggested that RyR2 from cardiac muscle is not activated by ATP to the same extent as RyR1 in the absence of calcium (Meissner, Rousseau et al. 1988).

DPc10 peptide (G2460-P2495), a peptide homologous to the RyR2 central domain, is an RyR2 equivalent of DP4, and has been shown to increase the sensitivity of RyR2 to activating calcium and increase [ $^3$ H]ryanodine binding, much like DP4 (Yamamoto and Ikemoto 2002). DPc10 studies are pertinent to arrhythmias linked with the disease CPVT as the mutant of this peptide (DPc10M) includes the R2474S CPVT mutation, and this was found to be inactive compared to the WT DPc10 (Laver, Honen et al. 2008). Single channel studies with RyR2 incorporated from SR preparations have tested the effect of the RyR2 peptide DPc10 and showed that with calcium alone DPc10 caused activation but DPc10M did not. ATP caused an increase in channel activation, but no further increase was observed with DPc10 addition. This implied that ATP had fully opened the channel (Laver, Honen et al. 2008). DPc10 has also been shown to

lower the threshold for spontaneous calcium release in a study using permeabilised rat cardiomyocytes as it increased the number of spontaneous calcium sparks (Yang, Ikemoto et al. 2006).

FKBP12.6 can regulate RyR2 in a similar manner to FKBP12 regulation of RyR1. It binds to the channel and stabilises its activity (see main introduction). The relationship between FKBP12.6, RyR2 and phosphorylation has become an important focus in the mechanism underlying arrhythmia and SCD in HF. The hyperphosphorylation hypothesis suggests that increased sympathetic activity results in persistent phosphorylation of RyR2 and this causes the loss of FKBP12.6 which destabilises channel activity (Marx, Reiken et al. 2000). This results in diastolic leak of calcium resulting in DADs, as described previously (chapter 1). Experiments, mainly using a paced dog model of heart failure, have investigated the underlying mechanisms in respect of the involvement of a faulty domain interaction. In SR preparations from control dogs, DPc10 (but not DPc10M) caused a calcium leak, which could be inhibited by K201 (JTV519). However, DPc10 was shown to have no appreciable effect on dissociation of FKBP12.6 from RyR2 or on the phosphorylation level in the absence of cAMP, suggesting a link to  $\beta$ -AR stimulation. When SR was preincubated with cAMP, FKBP12.6 dissociation occurred in a concentration-dependent manner concurrent with an increase in PKA phosphorylation (Oda, Yano et al. 2005). When similar experiments were performed on SR derived from the paced dogs neither DPc10 nor cAMP caused an increase in calcium leak. Using DPc10 to carry a fluorescently labelled probe into the target domain it was shown that in HF the domains were already 'unzipped' explaining the lack of effect of the peptide and cAMP. The anti-arrhythmic drug, K201 was able to restabilise the domains. Similar experiments using the fluorescence quench method showed that oxidation also unzipped the domain targeted by DPc10. The DPc10 domain peptide (but not DPc10M) was shown to increase the number of spontaneous calcium sparks in permeabilised myocytes and K201 was able to suppress this effect (Tateishi, Yano et al. 2009).

Extending this type of study to look at the CPVT mutation clusters and again using fluorescent quench analysis to determine whether FKBP12.6 mediated stabilization of RyR2 is produced by

abnormal domain interaction with the DPc10 peptide, Hamada et al found K201 (JTV519) almost completely inhibited DPc10 induced calcium leak (Hamada, Gangopadhyay et al. 2009). The amount of FKBP12.6 bound was unchanged in the presence of K201, suggesting inhibition of calcium leak by K201 is not mediated by rebinding of FKBP12.6 to the SR vesicle (see main introduction). However, the group have postulated that destabilisation incurred by DPc10 may result in RyR2 phosphorylation having a greater effect on FKBP12.6 dissociation- suggesting a possible link between the two mechanisms. The affinity of FKBP12.6 for RyR2 has been shown to be reduced when the channel is in the open state, as it is for RyR1 in Biacore affinity studies done by (Blayney, Jones et al. 2010). In the closed channel state, binding affinity to FKBP12.6 was shown to be reduced to the level of the open channel in the presence of PKA phosphorylation, although the binding affinity remained high throughout, suggesting modification of RyR conformation incurred by PKA phosphorylation, which is not observable in [<sup>3</sup>H]ryanodine binding studies.

A more recent study by (Liu, Wang et al. 2010) has involved the use of FRET with CFP and YFP fluorescent probes in RyR2 transfected HEK cells to determine whether the RyR domain interaction occurs between neighbouring subunits (inter-subunit) or remains confined to individual subunits (intrasubunit). Results show that there is in fact evidence of inter-subunit interaction between the N-terminus and central domain. The group postulate that this region of inter-subunit interaction is of critical importance for normal channel function of RyR2 and that mutations in either domain may weaken the normal subunit-subunit interactions, thus altering stability of the channel.

However, no studies have assessed the effect of magnesium inhibition on DPc10 activation, or ATP and DPc10 effects on ryanodine binding, further adding to the validity of pursuing this study on the RyR2 isoform.

This chapter aims to assess the effect of known physiological modulators of RyR2. The FKBP12.6 protein for this study was produced and purified in house using molecular cloning techniques. Initially there was an aim to generate DPc10 peptides with a view to repeat



experiments carried out using the RyR1 isoform with RyR2. This chapter describes the cloning and expression of the DPc10 wildtype peptide, however experiments with this peptide were not realised and the mutant was not developed due to time constraints. This chapter will serve as control data for subsequent studies as proof of effect on RyR2 channel opening due to the specificity of [<sup>3</sup>H]ryanodine binding for the RyR.

## **7.2 Results**

### **7.2.1 Physiological modulators of RyR2**

Purified RyR2 native channels (chapter 3) were shown to exhibit the classic biphasic dose response to calcium using [<sup>3</sup>H]ryanodine binding, thus demonstrating correct functionality of the protein and its suitability for further experiments (Figure 7.1). Phosphorylation and dephosphorylation had little effect on [<sup>3</sup>H]ryanodine binding. pCa4 buffer was shown to have maximal effect on channel opening, therefore this buffer was used for proceeding experiments. ATP was shown to exert maximal effect at 2.5 mM and the total activation observed was 250% in the presence of calcium and ATP (Figure 7.2). Due to the low yield of RyR2 protein obtained after purification, this experiment was only repeated twice, however the values obtained at 0.5 and 1 mM ATP have been shown to be significantly different from the control. A higher (n) number is required to determine whether the overall activation of RyR2 with ATP is consistently lower than for RyR1. The full calcium response was repeated in the presence of 2.5 mM ATP and although these results are not shown to be significantly different from the corresponding values on the calcium curve without ATP, it is clear the ATP is having a notable activatory effect at all calcium concentrations able to open the channel significantly (Figure 7.2 B).

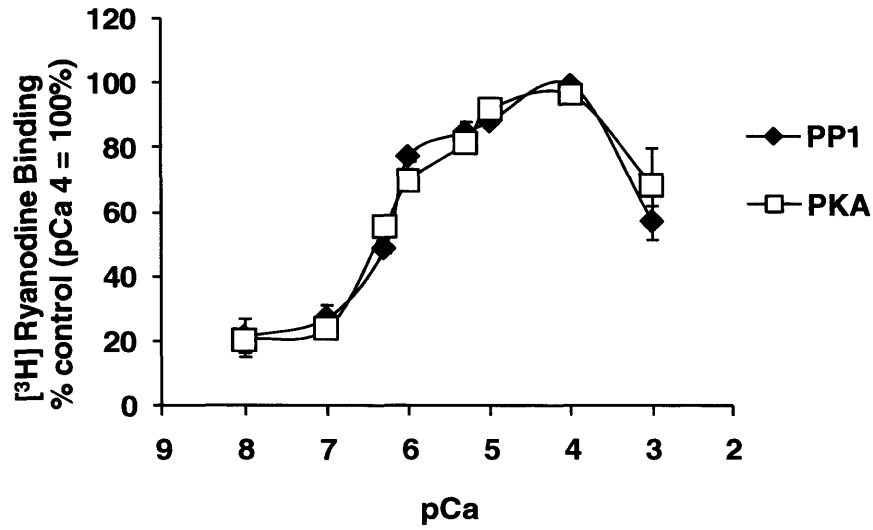


**Figure 7.1 RyR2 biphasic response to varying free calcium (pCa).** Each point represents the mean of 2 RyR2 preparations. (pCa4 is taken as 100%). Bars show standard error.

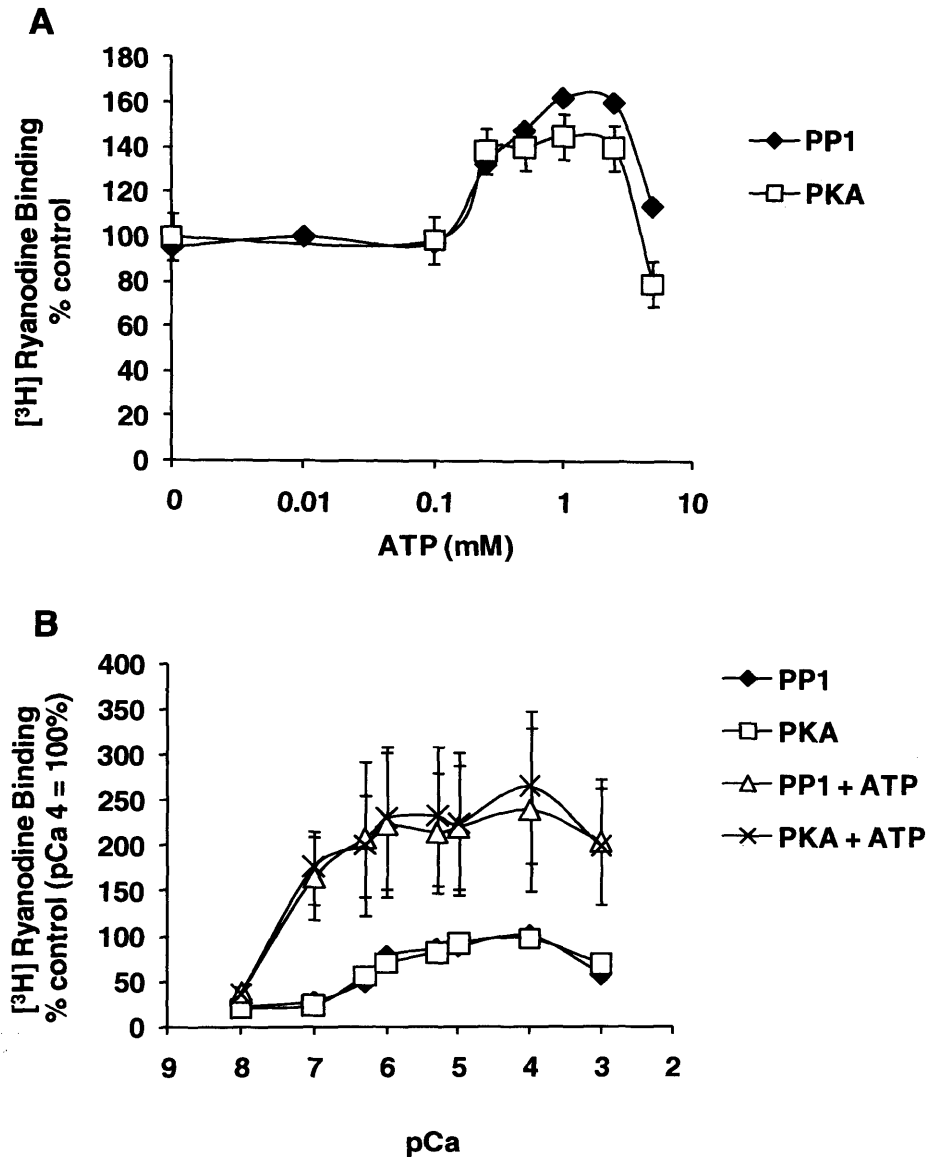


**Figure 7.2 Effect of ATP on RyR2 [<sup>3</sup>H]ryanodine binding.**

A) ATP dose response in the presence and absence of phosphorylation. (\*) indicates a significant difference ( $p < 0.05$ , students paired t-test) from the control without ATP addition.

B) ATP effect on binding across the calcium biphasic response. Calcium response is shown in the presence and absence of 2.5 mM ATP. Each point represents the mean of 2 RyR2 preparations. (\*) indicates a significant difference ( $p < 0.05$ , students paired t-test) from the equivalent value of the calcium dose response without ATP addition. (Binding in pCa4 is taken as 100%). Bars show standard error.

### 7.2.2 Cloning, production and purification of FKBP12.6

FKBP12.6 primers were designed (Figure 7.3) and successfully amplified the FKBP12.6 sequence from cDNA template as shown in figure 7.4 A. The PCR amplicon was digested using BamH1 and EcoR1 restriction endonucleases (section 2.1.2.5) and the PCR clean-up kit (section 2.1.2.3) resulted in sufficient cleaved product for ligation (Figure 7.4 B and section 2.1.2.6). Of 5 minipreps generated from selected colonies (section 2.1.2.9), one was shown to have the correct size insert following restriction digestion with BamH1 and EcoR1 enzymes (Figure 7.5). Subsequent sequencing of this miniprep (Figure 7.6) showed that the insert was correct. The electropherogram confirmed all sequencing was in frame with the 3C restriction site and the BamH1 and EcoR1 sites were present with the stop codon before the EcoR1 site (section 2.1.2.10). The sequence was aligned with the GenBank sequence for FKBP12.6 using BLAST NCBI software, showing 100% match.

The protocol for protein production was assumed to be the same as for FKBP12, due to the high homology of these proteins, therefore protein was induced at 30°C for 3 hours, which was sufficient to generate a high yield of protein. Affinity purification of FKBP12.6 gave excellent results (Figure 7.7 and section 2.2.3), with a very high efficiency of 3C cleavage, shown by SDS-PAGE analysis. Cleaved FKBP12.6 protein quantity was estimated by running a sample alongside known BSA controls (~1 mg/ml) (Figure 7.8A). Protein identity was confirmed by Western blot using an anti-FKBP12.6 specific antibody (Figure 7.8B and section 2.2.1).

**A**

clamp BamH1 hFKBP12.6  
FKBP12.6 F (5'-3') TACTTGGATCCATGGGCGTGGAGATCGAGA

clamp EcoR1 hFKBP12.6  
FKBP12.6 R (5'-3') GCGCGGAATTC~~TCA~~CTCTAAGTTGAGCAGC

**B**

Protein name	Gene of Interest	Genebank Accession Number	Size of Amplicon (bp)
FKBP12.6	hFKBP12.6	BC002614	340

**Figure 7.3 FKBP12.6 forward and reverse primer design**

**A)** Forward and reverse primer sequences. Start codon is highlighted on the forward primer in green and the stop codon on the reverse primer in red. Restriction endonuclease sites were incorporated as shown. GC content is approximately 50%.

**B)** Table demonstrating average primer annealing temperatures- designed to be similar for forward and reverse primers to increase PCR efficiency. Gene sequence was obtained from published GenBank sequence, the accession number for which is provided.

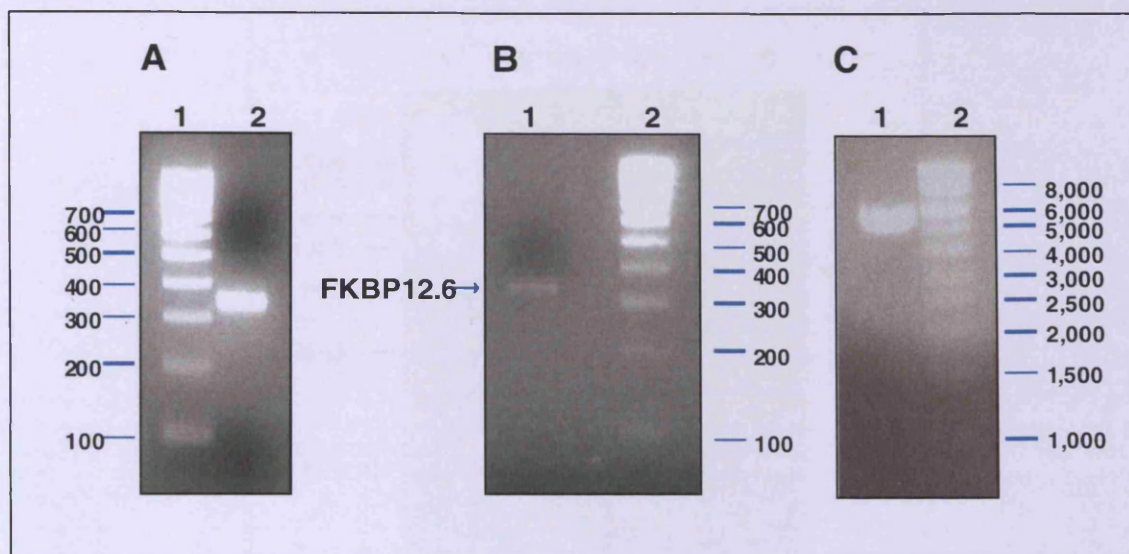


**Figure 7.4 Cloning of FKBP12.6 by PCR and preparation for ligation into pGEX-6P-1 vector**

**A)** PCR was used to generate a 340 bp fragment of FKBP12.6 using the standard PCR cycle. PCR products were separated on a 3% (w/v) TAE agarose gel by gel electrophoresis. Primers used were FKBP12.6F and FKBP12.6R (Figure 7.3) Lane 1, 1 kb DNA marker, sizes are shown on the left in base pairs (bp). Lane 2, FKBP12.6 PCR synthesized DNA product.

**B)** PCR synthesized FKBP12.6 was restriction digested with BamH1 and EcoR1 and PCR cleaned to remove residual enzymes and dNTPs. Product was separated on a 3% w/v TAE agarose gel by gel electrophoresis. Lane 1, FKBP12.6, estimated at ~60 ng/ $\mu$ l. Lane 2, 1 Kb DNA marker with sizes to the right of gel in base pairs (bp).

**C)** Circular vector was subjected to a sequential digest and treatment with alkaline phosphatase to prevent self annealing. Following alcohol precipitation of the digested vector a 10  $\mu$ l sample was separated on 1% w/v TAE agarose by gel electrophoresis. Lane 1, digested pGEX-6P-1 vector, quantity estimated at ~240 ng/ $\mu$ l by UV spectrophotometry. Lane 2, Hyperladder I DNA marker with sizes shown on the right in base pairs (bp).

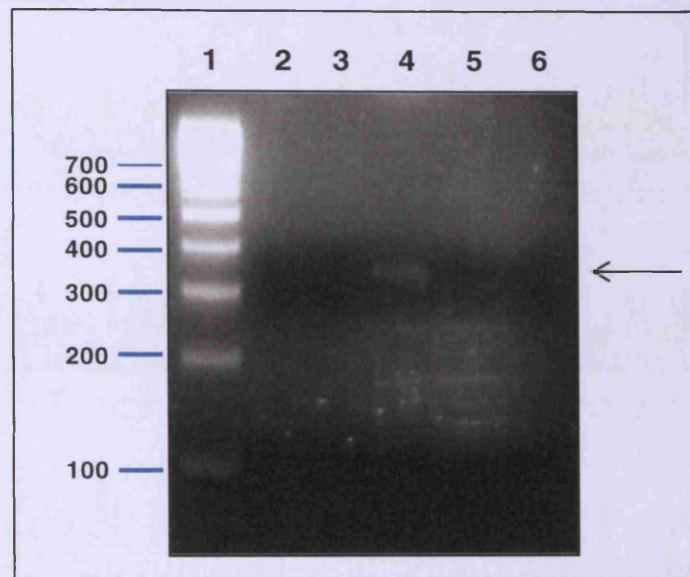
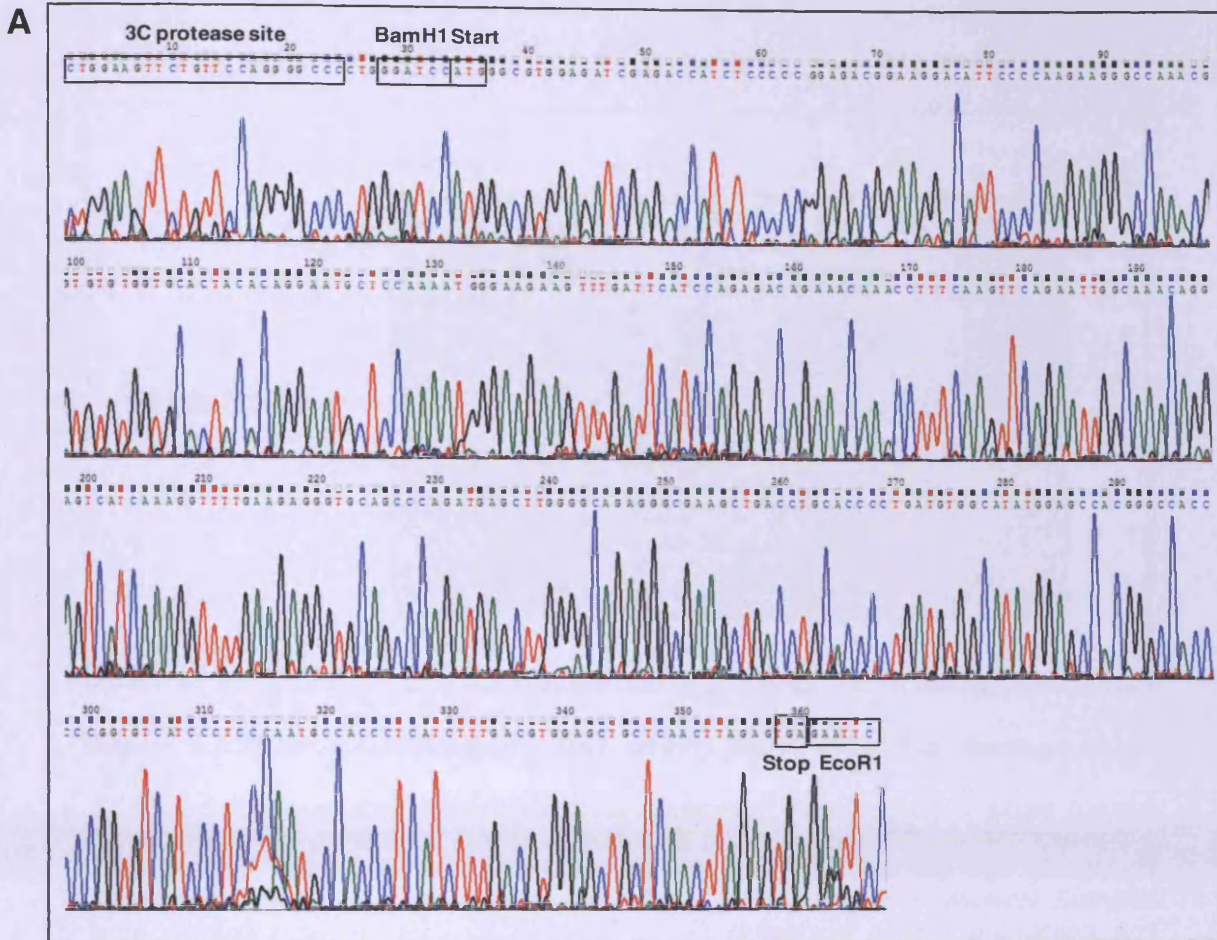


**Figure 7.5 Screening for positive FKBP12.6-pGEX-6P-1 transformed TOP10 colonies**

Of the colonies that grew on LB agar with Ampicillin, 5 were selected and subjected to a plasmid 'mini-prep'. Products were digested with BamH1 and EcoR1 restriction endonucleases and separated on 3% w/v TAE agarose by gel electrophoresis. Lane 1, 1 Kb DNA marker with sizes shown on the left in base pairs (bp). Lanes 2, 3, 5, 6 show minipreps yielding no FKBP12.6-pGEX-6P-1. Lane 4, positive miniprep showing correct sized band following restriction digest.



**B**

FKBP12.6-pGEX-6P-1	TCACTCTAA GTTGAG CAGCTC CACGTC AAAGAT GAGGGT GGCATT GGGAGG GATGAC ACC
BC002614 (463-404)	TCACTCTAA GTTGAG CAGCTC CACGTC AAAGAT GAGGGT GGCATT GGGAGG GATGAC ACC
FKBP12.6-pGEX-6P-1	GGGGTGGCC CGTGGC TCCATA TGCCAC ATCAGGGGTG CAGGTCAGCTTCGC CCTCTGCC
BC002614 (403-344)	GGGGTGGCC CGTGGC TCCATA TGCCAC ATCAGGGGTG CAGGTCAGCTTCGC CCTCTGCC
FKBP12.6-pGEX-6P-1	CAAGCTCAT CTGGGC TGCACC CTCTTCAA AACCTTTGAT GACTTC CTGTTT GCCAAT TCT
BC002614 (343-284)	CAAGCTCAT CTGGGC TGCACC CTCTTCAA AACCTTTGAT GACTTC CTGTTT GCCAAT TCT
FKBP12.6-pGEX-6P-1	GAACTTGAA AGGTTT GTTTCT GTCTCT GGATGAATCAA ACTTCTT CCCATT TTGGAG CAT
BC002614 (283-224)	GAACTTGAA AGGTTT GTTTCT GTCTCT GGATGAATCAA ACTTCTT CCCATT TTGGAG CAT
FKBP12.6-pGEX-6P-1	TCCTGTGTA GTGCAC CACACA CGTTTGGCCCTT CTTGGGGAATGT CCTTCC GTCTCC GGG
BC002614 (223-164)	TCCTGTGTA GTGCAC CACACA CGTTTGGCCCTT CTTGGGGAATGT CCTTCC GTCTCC GGG
FKBP12.6-pGEX-6P-1	GGAGATGGT CTCGAT CTCCAC GCCCAT
BC002614 (163-137)	GGAGATGGT CTCGAT CTCCAC GCCCAT

**Figure 7.6 Sequencing of FKBP12.6-pGEX-6P-1.** **A)** Electropherogram sequencing result. BamH1 and EcoR1 restriction sites are highlighted which flank the FKBP12.6 sequence. C-protease restriction site is shown to be intact. **B)** Sequence identity is confirmed by a BLAST sequence alignment with FKBP12.6 sequence from the GenBank database (Accession number BC002614) showing 100% match.



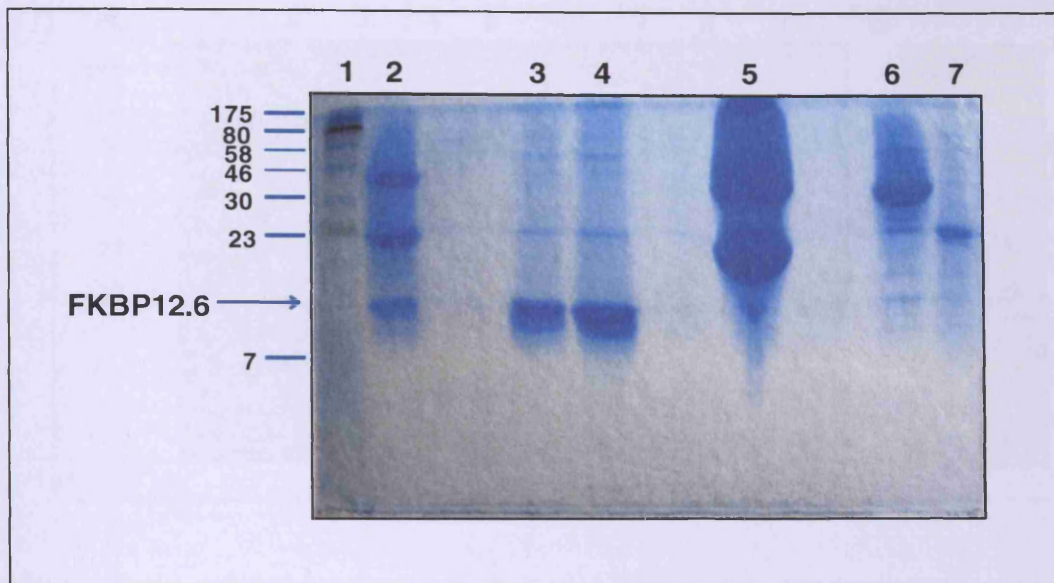


**Figure 7.7 FKBP12.6 expression, GST affinity purification and cleavage of the GST tag**

FKBP12.6 mini-prep was used to transform competent Rosetta cells. A single positive transformant was grown in 1 litre of selective LB broth, protein induced and harvested. The resultant pellet was then lysed and the supernatant combined with glutathione sepharose. The protocol for 3C cleavage of the GST tag was then followed. Samples were analysed on an 18% SDS-PAGE gel to determine protein production and purification efficiency. Lane 1, Kaleidoscope protein size markers with approximate sizes shown on the left (kDa). Lane 2, cleaved FKBP12.6 (12.6 kDa), GST (26 kDa) and 3C-GST (48 kDa) following overnight incubation and prior to separation. Lanes 3 and 4, eluate containing cleaved FKBP12.6 after filtration of the GST beads. Lane 5, washed beads showing GST and 3C-GST but very little FKBP12.6. Lane 6, Uncleaved FKBP12.6-GST (38.6 kDa). Lane 7, GST. It is apparent that all proteins, including the GST control, are running slightly different to their respective marker. As mentioned in chapter 5, the NEB markers used seem to consistently run higher than they should.

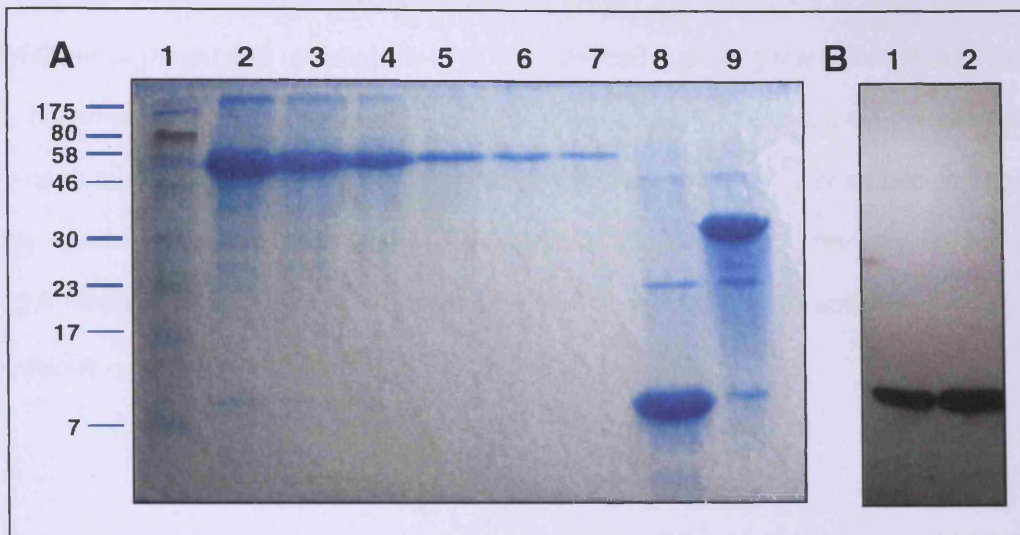


**Figure 7.8 Quantification of purified cleaved FKBP12.6 and FKBP12.6-GST and western blotting**

**A)** Bovine serum albumin (BSA) standards were run alongside FKBP12.6 recombinant proteins to provide an estimate of protein concentration. Samples were run on a 15 % SDS-PAGE gel. Lane 1, Kaleidoscope protein size marker, sizes are given on the left (kDa). Lanes 2-7, serial dilutions of BSA (66 kDa); 2, 20  $\mu$ g, 3, 10  $\mu$ g, 4, 5  $\mu$ g, 5, 2.5  $\mu$ g, 6, 1.25  $\mu$ g, 7, 0.63  $\mu$ g. Lane 8, Cleaved FKBP12.6 (12.6 kDa). Lane 9, FKBP12.6-GST (38.6 kDa). The NEB marker used is shown to run high compared with the BSA standards.

**B)** Neat FKBP12.6 was serially diluted and run on a 15% SDS-PAGE gel. Protein was transferred to a PVDF membrane and incubated with anti-FKBP12.6 antibody for 2 hours at room temperature to confirm that the recombinant protein was correct. Lane 1, FKBP12.6 at approximately 0.25 mg/ml. Lane 2, FKBP12.6 at approximately 0.5 mg/ml.

### 7.2.3 FKBP12.6 effect on RyR2 [<sup>3</sup>H]ryanodine binding

Low RyR2 yields meant that few experiments were carried out using the recombinant FKBP12.6 protein, however, a dose response of FKBP12.6 effect on RyR2 [<sup>3</sup>H]ryanodine binding (section 2.3.2) was obtained and shown to inhibit binding by approximately 50% at a concentration of 10  $\mu$ M. This result was shown to be significantly different (students t-test) from the control without FKBP12.6 addition. This effect was also shown to be specific by the addition of FK506 as a control, which successfully inhibited the FKBP12.6 effect.

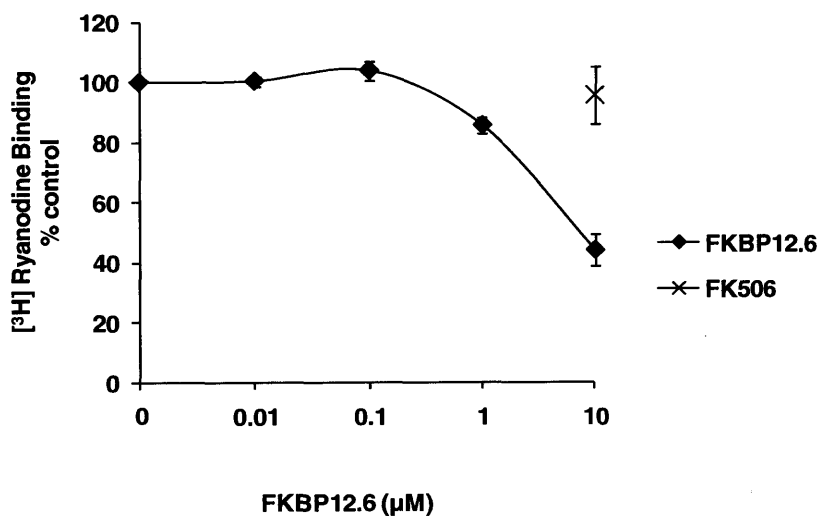


**Figure 7.9 Effect of FKBP12.6 on RyR2 [<sup>3</sup>H]ryanodine binding.** FKBP12.6 dose response. Each point represents the mean of 4 RyR2 preparations. 10  $\mu$ M FK506 was added as a control. (\*) indicates a significant difference ( $p < 0.05$ , students paired t-test) from the control without FKBP12.6 addition (Binding in pCa4 is taken as 100%). Bars show standard error.

### 7.2.4 Cloning of DPc10 into pGEX-6P-1 and optimisation of protein expression.

Primers were designed (Figure 7.10) to amplify the DPc10 sequence from hRyR2 cDNA template at  $\sim 2$  ng/ $\mu$ l using the standard extended PCR cycle (section 2.1.2.2). Figure 7.11A shows the PCR DPc10 amplicon following gel extraction (used instead of PCR clean-up as for

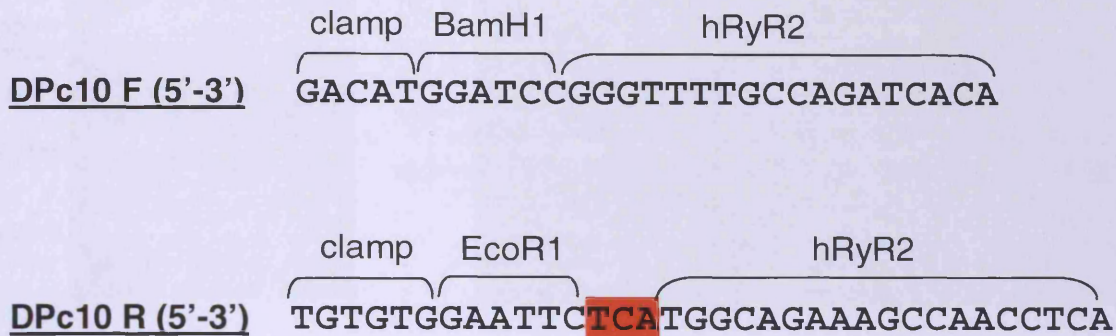
DP4, section 2.1.2.3) and following a restriction digest with BamH1 and EcoR1 enzymes (section 2.1.2.5) to prepare the insert for ligation into pGEX-6P-1 vector (section 2.1.2.6). The vector was prepared as previously and a ligation reaction set-up and incubated overnight at 4°C with an insert to vector ratio of 10:1. Following transformation of TOP10 *E.coli* chemically competent cells (section 2.1.2.7), 9 colonies grown on selective agar were selected for screening by colony PCR (section 2.1.2.8) using the pGEX forward primer and the DPc10 reverse primer which adds (100 bp) to the size of the expected PCR amplicon. The gel shows 4 positive PCR products running at approximately the correct size (Figure 7.11B), although each appears to be different from the next, therefore the brightest band (lane 2) was grown and mini-prepped to extract the plasmid DNA, and this was sent for sequencing (section 2.1.2.10).

The electropherogram (Figure 7.12) shows a correctly in frame DPc10 sequence with BamH1 and EcoR1 and 3C sites intact. Alignment using BLAST 'align two sequences' software confirmed 100% match with RyR2 sequence on GenBank. Although mutagenesis primers were designed to insert the R2474S CPVT mutation into this peptide, time restraints and an inability to obtain sufficient RyR2 for experiments meant that the DPc10 Quikchange mutagenesis was not carried out. Nevertheless, protein expression for the wildtype DPc10 was tested and optimised.

Maxi-prep DNA (section 2.1.2.9) containing the DPc10 insert was used to transform chemically competent Rosetta bacteria. These were grown overnight on selective Amp-Chlor LB agar, then grown in 20 ml of selectable LB broth as a starter culture, before seeding 1 L LB cultures and growing at 37°C. The Optical density (OD) of the culture was tracked at  $A_{600}$  every 30 minutes until an OD of 0.6 was obtained. At this point the culture was transferred to a 30°C incubator for approximately 30 minutes to cool down, before addition of IPTG (final concentration 0.1 mM). 50 ml samples were removed from the culture every hour for 4 hours, from the time of IPTG addition ( $t=0$ ), bacteria were pelleted and frozen at -20°C for further analysis (section 2.2.2).

Following thawing of the pellets, bacteria were sonicated in 3 x 30 second bursts on ice to avoid over heating of cells. Lysed bacteria were centrifuged to remove unlysed bacteria and debris and the supernatant containing protein incubated with PBS washed Glutathione sepharose

beads to capture the GST tagged peptide for 2 hours at 4°C. Beads were then pelleted using an Allegra desk-top centrifuge and washed 3x with 20ml high salt buffer to wash away any excess, non-specifically bound protein. A final wash was done with PBS and a sample of the beads was added to SDS loading buffer and boiled at 100°C for 1 minute to release protein from the beads, before running on a high percentage SDS-PAGE gel (section 2.2.1) for analysis alongside a SIGMA wide-range kaleidoscope marker by coomassie staining. This process was repeated with an induction temperature of 25°C instead of 30°C to determine whether there was any difference in protein expression levels, this was not the case, (Figure 7.11). The coomassie stained gels show substantial protein induction at both temperatures, and the protein appears to be running at the correct size, a GST control has been run alongside although, as suggested for the DP4, the sizes of the GST-DPc10 and the recombinant GST alone will be unresolvable on a coomassie gel. There appears to be a double band forming on both gels, it was assumed that the upper band corresponds to the GST-DPc10 as the lower band seems to be transcribed before the induction period.

**A****B**

Peptide name	Gene of Interest	Genebank Accession Number	Size of Amplicon (bp)
DPc10WT	hRyR2	X98330	133

**Figure 7.10 DPc10 forward and reverse primer design**

**A)** Forward and reverse primer sequences. Start codon is highlighted on the forward primer in green and the stop codon on the reverse primer in red. Restriction endonuclease sites were incorporated as shown. GC content is approximately 50%.

**B)** Table demonstrating average primer annealing temperatures- designed to be similar for forward and reverse primers to increase PCR efficiency. Gene sequence was obtained from published GenBank sequence, the accession number for which is provided.

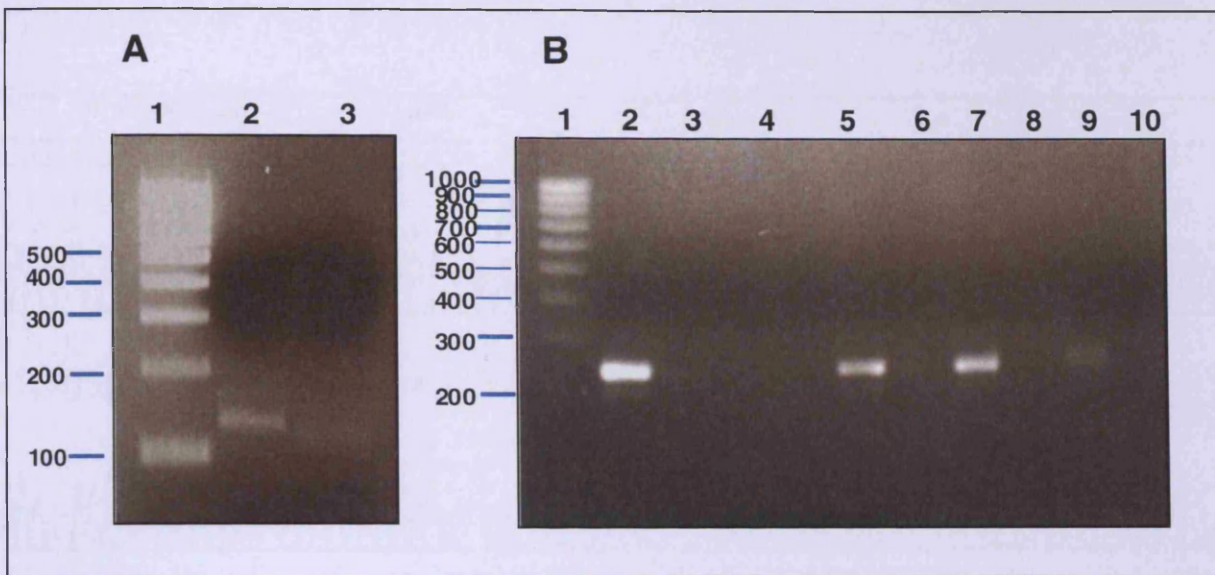


**Figure 7.11 DPc10 cloning into pGEX-6P-1**

**A)** DPc10 forward and reverse primers were used to amplify the desired peptide sequence in a standard PCR reaction. PCR product was then subjected to a restriction double digest with Bam H1 and EcoR1 enzymes and ethanol precipitated. Samples were separated on 3% (w/v) agarose using gel electrophoresis. Lane 1, 1 Kb molecular weight size marker, sizes are shown on the left in base pairs (bp). Lane 2, DPc10 PCR product before restriction digestion. Lane 3, DPc10 post restriction digestion and ethanol precipitation. Quantity estimated at  $\sim 1$  ng/ $\mu$ l.

**B)** 10 colonies grown on selective LB were selected for screening by colony PCR using pGEX-6P-1 forward primer and the reverse DPc10 primer. PCR samples were separated on 3% w/v agarose by gel electrophoresis. Lane 1, 1 Kb molecular weight DNA size marker, sizes are shown on the left in base pairs (bp). Lanes 2, 5, 7 and 10 show positive DPc10-pGEX containing colonies. The pGEX forward primer adds on 100 bp to the amplicon size, meaning that a band is seen between the 200 and 300 bp markers.

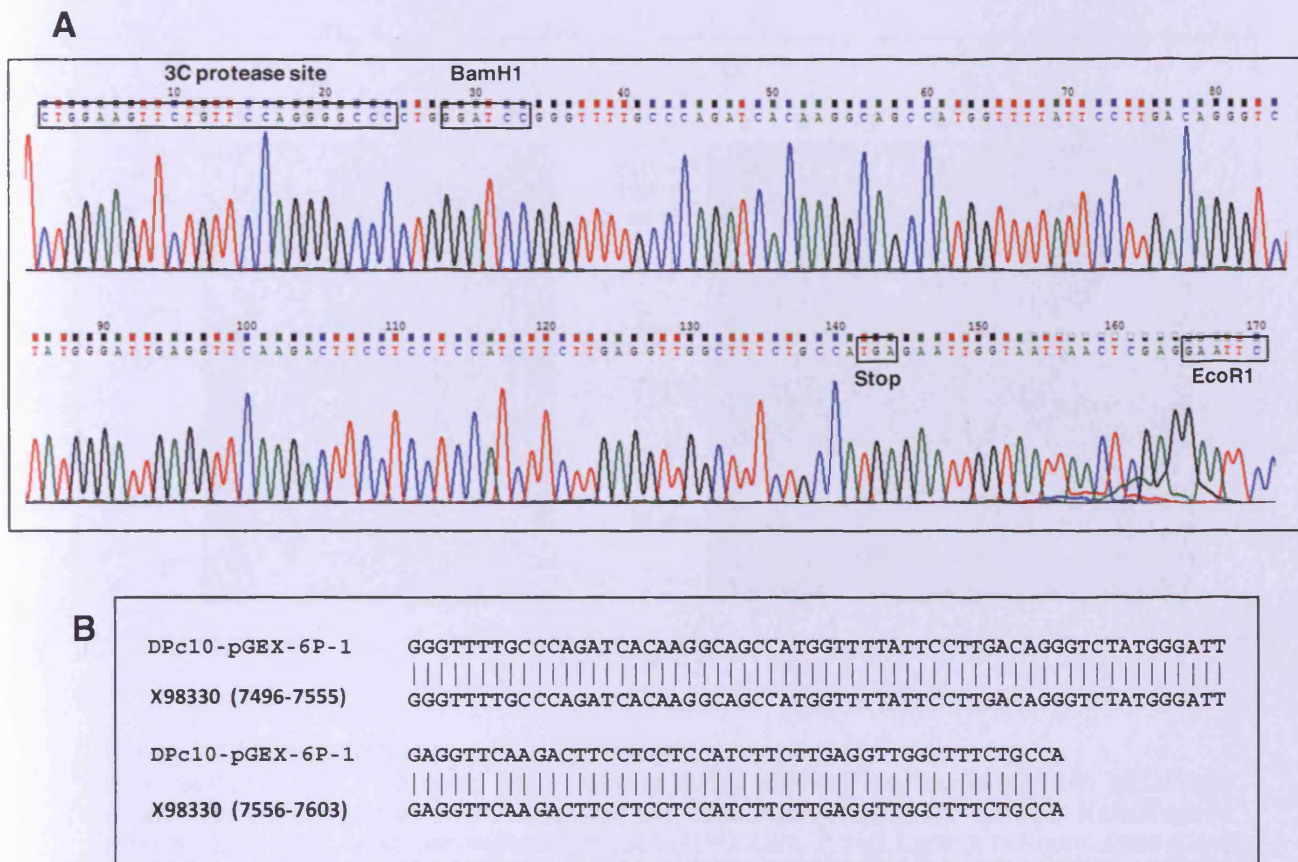


**Figure 7.12 Sequencing of DPc10-pGEX-6P-1.**

**A)** Electropherogram sequencing result. BamH1 and EcoR1 restriction sites are highlighted which flank the DPc10 sequence. C-protease restriction site is shown to be intact.

**B)** Sequence identity is confirmed by a BLAST sequence alignment with RyR2 sequence from the GenBank database (Accession number X98330) showing 100% match.



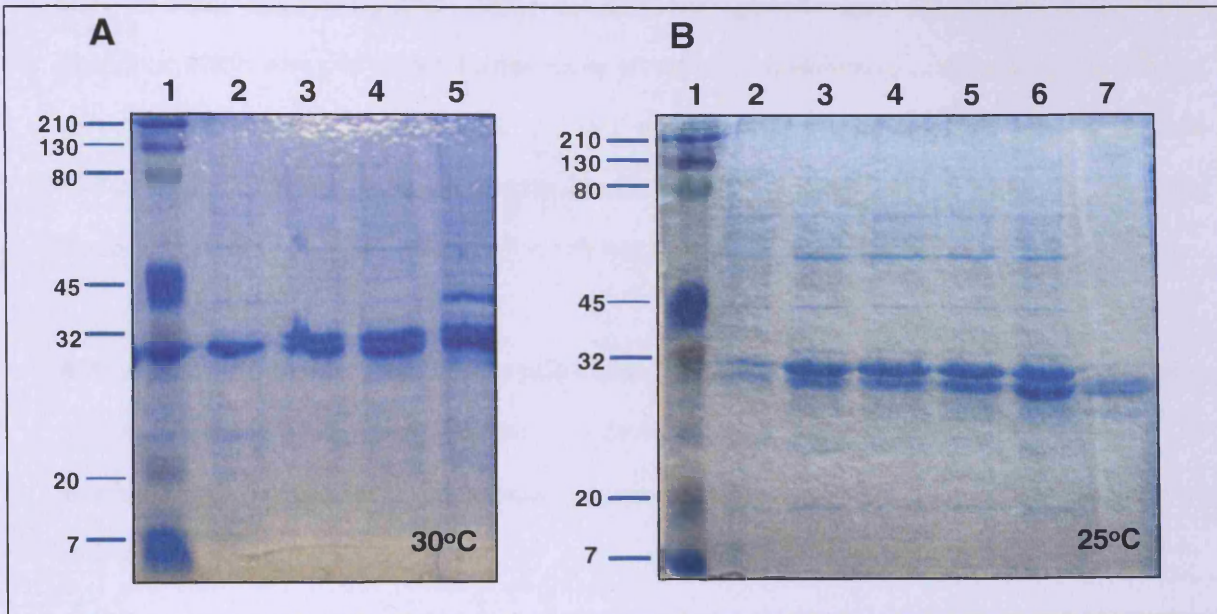


**Figure 7.13 DPc10-GST expression optimisation**

**A)** Induction at 30°C. Samples were taken at hourly intervals and combined with glutathione sepharose. Samples were then separated on 15% SDS-PAGE gels. Lane 1, Kaleidoscope protein size marker, sizes are shown on the left (kDa). Lane 2, t=0, Lane 3, t=1 hour. Lane 4, t=2 hours. Lane 5, t=3 hours. Expected GST-DPc10 size is ~31 kDa.

**B)** Induction at 25°C. Samples were taken at hourly intervals and combined with glutathione sepharose. Samples were then separated on 15% SDS-PAGE gels. Lane 1, Kaleidoscope protein size marker, sizes are shown on the left (kDa). Lane 2, t=0, Lane 3, t=1 hour. Lane 4, t=2 hours. Lane 5, t=3 hours. Lane 6, t= 4 hours. Lane 7, GST (26 kDa).

### 7.3 Discussion

The effects of calcium, ATP and FKBP12.6; physiological modulators of RyR2, on native RyR2 [<sup>3</sup>H]ryanodine binding were examined. The FKBP12.6 protein used was successfully cloned, produced and purified for experiments as a recombinant protein. DPc10 activatory peptide was also generated by molecular biology. DPc10 will serve as a valuable tool in future RyR2 experiments aiming to elucidate the mechanism of modulation involved in aberrant RyR2 function as described for DP4 (chapter 6).

RyR2 channels were found to be functionally active and to respond to calcium in the well documented fashion that is a biphasic dose response. Maximal [<sup>3</sup>H]ryanodine binding was seen in pCa4, with channel inhibition at 1 mM free calcium. ATP activation of [<sup>3</sup>H]ryanodine binding

was found to be maximal at 1- 2.5 mM ATP but was lower than that for RyR1 (~2-fold rather than ~4-fold), suggesting that RyR2 is relatively opened more by calcium than RyR1. Phosphorylation was not shown to have any effect on [<sup>3</sup>H]ryanodine binding, this is consistent with previous findings by Jones et al. who suggest that phosphorylation induced channel conformational change measurable by kinetic binding experiments to FKBP12/12.6 using Biacore, but not seen with [<sup>3</sup>H]ryanodine binding (Jones, Lai et al. 2006).

ATP was able to increase binding at pCa7 to a greater proportion of the maximal binding than calcium alone, consistent with the idea of a calcium independent mode of ATP activation. This activation was not evident at pCa8 however, suggesting ATP required a small level of calcium activation to exert any effect.

Recombinant FKBP12.6 was shown to inhibit the native RyR2 channel (SR preparation) by approximately 50%, reflecting the effect of FKBP12 on RyR1 isolated channels and previous findings by other groups. This also further stresses the importance of RyR1 analysis as a mediator to RyR2 functionality.

The DPc10 mutant peptide still needs to be cloned using site-directed mutagenesis as for DP4M (see chapter 5) and the purification procedure needs to be optimised for both the wildtype and mutant peptides. Given the low yield of cleaved DP4 peptide obtained after treatment with 3C protease, it may be better to modify the purification protocols using the DPc10 peptide, which can be tracked using A<sub>280</sub> as this peptide contains four phenylalanine and one tyrosine residue and therefore the use of FPLC and a UV absorbance monitor can be used. It may also be possible to see a band on SDS PAGE coomassie-stained gels. As the peptides are the same size, they ought to elute at a similar point on a gel filtration column after 3C cleavage, so it may be a case of 'working blind' for the DP4 following optimisation with DPc10. The FPLC fractions found to consistently contain cleaved DPc10 could be quantified using the BCA kit and DP4 presence confirmed using MALDI. The ability to produce significant quantities of DPc10 should therefore, greatly assist DP4 purification optimisation and enable further studies with these peptides and their mutants in the very near future.

## **Chapter 8; Discussion**

## **CHAPTER 8: Discussion**

The domain interaction hypothesis (Yamamoto, El-Hayek et al. 2000) was originally tested using homologous domain peptides. These were proposed to insinuate between the interacting domains and disrupt the natural association, resulting in channel activation. This effect has been observed in a number of experimental models, including single channel studies using artificial lipid bilayers (Shtifman, Ward et al. 2002; Murayama, Oba et al. 2005), SR (Shtifman, Ward et al. 2002; Kobayashi, Yamamoto et al. 2004; Murayama, Oba et al. 2005; Oda, Yano et al. 2005; Bannister, Hamada et al. 2007) and whole cell analysis (Lamb, Posterino et al. 2001; Yang, Ikemoto et al. 2006; Tateishi, Yano et al. 2009). In particular, a domain interaction between the N-terminus and the central domain coincident with disease causing mutation clusters for MH/CCD in skeletal muscle and CPVT/ARVD in cardiac muscle has been described using DP4 and DPc10 peptides respectively.

Our previous work has lead to a hypothesis of convergent regulation where a number of key regulators of RyR function are proposed to act in concert on a defined region of conformational change (Blayney, Jones et al. 2010). Circumstantial evidence suggests that the central domain may participate in the regulatory events described in our studies (Yamamoto, El-Hayek et al. 2000; Kobayashi, Yamamoto et al. 2004; Liu, Wang et al. 2010). To determine whether this is so, this investigation has explored the use of DP4 in our experimental system. This investigation has provided data which further our understanding of the modulation of RyR function in the aberrant calcium handling characteristic of RyR1 (MH and CCD) and RyR2 (CPVT and HF) related disorders.

### **8.1 The domain interaction hypothesis**

The original experiments supporting this hypothesis involved the use of domain peptides and their Abs to activate RyR (Kobayashi, Yamamoto et al. 2004). A recent study using FRET probes has advanced this work further (Liu, Wang et al. 2010). FRET can take place between two fluorescent proteins if they are within ~10 nm of each other. By insertion, through cloning, of the sequence for two probes into the same DNA strand within the N-terminus (YFP- yellow fluorescent protein) and central domains (CFP- cyan fluorescent protein) of recombinant RyR2

and expressing the protein in HEK cells, the proximity of the two domains could be examined under experimental conditions. Using ATP, DPc10, caffeine and DP4 to activate RyR the two domains were 'unzipped' and FRET diminished, whereas dantrolene, which stabilises the domain interaction (Kobayashi, Bannister et al. 2005) could reverse their effects. By cloning the two probes individually and transfecting both into HEK cells, heterologous assembly of RyR tetramers occurred. If it was an intra-domain interaction then no FRET should be visible because the two FRET reporters would not be within the same subunit and thus too far apart. If the natural conformation was the N-terminus of one subunit interacting with the central domain of the next then some of the heterologous tetramers could assemble with a FRET partner in an adjacent subunit and a FRET signal should be visible. The latter was shown to be the case and so an inter-subunit interaction was proposed (Liu, Wang et al. 2010).

This is an exciting prospect in terms of RyR regulation. MH and CPVT are usually heterozygous with one normal and one gene containing the mutation (Lehnart, Mongillo et al. 2008; Grievink and Stowell 2010). If both are expressed at the same time then heterologous assembly of RyR tetramers is a possibility which may explain the RyR instability. If just one mutation failing to interact correctly with a partner domain could cause a perturbation in channel gating then perhaps occupation of one modulator site per sub unit, or one subunit being phosphorylated, could be sufficient to fully modulate a channel. This might explain how the RyR molecule is able to cope with so many modulators and sub optimal occupancy of all four subunits (Blayney and Lai 2009). In this regard, ~10-20% occupancy by FKBP12.6 has recently been suggested to be the physiological norm for RyR2 in mouse and rat hearts (Guo, Cornea et al. 2010). Although the authors suggest this shows that FKBP12.6, despite its high affinity, is not an important regulator of RyR2 function, this could also be interpreted as an indication of the ability of subsaturation FKBP12.6 binding to be sufficient to modulate RyR, especially in light of inter-subunit interactions (Liu, Wang et al. 2010), which may mean one FKBP12.6 molecule bound to one RyR subunit is sufficient to exert effect on not only all 4 subunits of RyR, but also neighbouring RyR channels. An array of RyR molecules which form the functional unit may be made up of two different homotetramers, some WT and the others mutant, where the mutant channels are capable of disrupting the function of neighbouring wildtype channels through inter-

subunit interaction. The role of RyR/RyR molecular interactions, termed coupled gating, may then contribute to the underlying phenotype (Marx, Gaburjakova et al. 2001).

### **8.2 Mode of action of DP4/ DPc10**

The aim of this study was to test known physiological modulators of the RyR1/ RyR2 channel, in the presence of the activatory domain peptides DP4/DPc10 or disease specific mutant forms, with a view to ascertain a potential region of convergent regulation (Figure 1.12).

The key experiment to confirm this idea of convergent regulation would be to test the effect of DP4/DPc10 on the kinetics of FKBP12/12.6 association with RyR1/ RyR2 using SPR as in previous experiments (Blayney, Jones et al. 2010) and under different conditions of channel activation. Before these experiments can be carried out it is necessary to determine the effect of DP4/DPc10 on the open probability of the channel under compatible experimental conditions, for example, the effects of the mutant peptides in the presence of calcium, FKBP12/12.6, magnesium and phosphorylation. Additional experiments using the physiological modulator ATP are included as this, like the DP4 peptide, is able to activate the RyR channel over and above the level achieved by calcium alone (Laver, Lenz et al. 2001). In order to establish these baseline parameters, [<sup>3</sup>H]ryanodine binding experiments were used to measure the open probability, a valuable technique since ryanodine binds to the open state of the channel (Meissner 1992).

This is the first study that has used synthesized DP4 peptides from an independent source, and compared them to those from the Ikemoto group, who first proposed the domain interaction hypothesis (Yamamoto, El-Hayek et al. 2000). The DP4WT peptide synthesized by Severn Biotech and that gifted from Ikemoto both gave the same responses in this study. Both increased open probability by 200% and their effects were inhibited by magnesium, which is supported by the current literature (Yamamoto, El-Hayek et al. 2000; Murayama, Oba et al. 2005). In the presence of DP4WT, inhibition by 10  $\mu$ M FKBP12 was ~50%, which is the maximum effect seen at that concentration in the absence of the peptide. This was observed for both DP4WT peptides used and this is a novel finding. The effect of phosphorylation on these

parameters has yet to be explored. It can be concluded that the peptides are acting, overall, in the manner anticipated by previous experiments. Experiments using the IK-DP4 have a low (n) (Figures 6.5- 6.7) due to limited availability, therefore this data needs to be viewed with caution, but it is encouraging to see similar activation levels to those seen with the Severn Biotech WT peptide where the (n) was higher.

The mutated peptide used in this study activated to the same extent as the wildtype. However, the inhibition of this effect by magnesium and FKBP12 was not as pronounced. This finding has resulted in a detailed examination of the use of these peptides as experimental tools, and the interpretation of the experimental results. The activation seen by DP4WT does not dispute the domain interaction hypothesis. However the validity of the mutant peptide as a mimic of the disease state, and as a necessary control for experiments, is called into question (Yamamoto, El-Hayek et al. 2000). This finding immediately suggests that the single mutation in the corresponding DP4 region of RyR1, is not singly able to prevent RyR stabilisation as a cause of aberrant calcium signalling. This has some implications for interpretation of many of Ikemoto's studies involving the DP4WT and DP4M peptides. The conundrum of the mutant peptide activation has necessitated consideration of a number of factors; source of the peptides, potential effects of the mutation on peptide structure and physical properties, and also the relative physical properties of the DP4WT and DP4M peptides. A number of central domain mutations have been tested in the DP4 peptide in the Ikemoto studies, these have been compared and it is clear that the mutations did not necessarily eliminate the activatory properties of the peptide, but most were less active than the wildtype. However, their relative solubilities have not been compared, though this has been raised as an issue in some papers (Bannister, Hamada et al. 2007) and considered in the discussion of chapter 5.

NMR spectroscopy has provided a backbone structure for the DP4WT peptide but DP4M could not be concentrated sufficiently to obtain similar data (Bannister, Hamada et al. 2007), however, Abs to these peptides do bind to native RyR suggesting that a similar structure is preserved (Kobayashi, Yamamoto et al. 2004). The affinity of DP4 for the RyR1 ( $K_D$  50 – 100  $\mu$ M (Yamamoto, El-Hayek et al. 2000) is considerably lower than, for example FKBP12 affinity for

RyR1 ( $K_D \sim 0.01 \text{ pM} - 1 \text{ nM}$ ) (Jones, Reynolds et al. 2005) as shown by the concentrations required for any observable effect. This low affinity interaction between peptides and their interacting native domain may reflect the necessity of the native domains to move apart and reform rapidly as the channel gates. Perhaps, with this in mind, phosphorylation of the RyR channel would result in lower concentrations of DP4 required to give a comparable effect on channel opening due to the lower threshold that needs to be overcome to push the channel open. The link between the action of DP4 with respect to phosphorylation has not yet been assessed by any other groups but would be especially interesting given the changes in affinity to FKBP noted by Jones et al in their Biacore studies (Jones, Reynolds et al. 2005).

### **8.3 Purified RyR preparations**

This study, using purified RyR preparations, shows a consistently lower activation magnitude by DP4WT peptide compared to previous studies (Murayama, Oba et al. 2005; Bannister, Hamada et al. 2007) using whole SR microsomal preparations (2-fold increase rather than 4-fold). The reason for this difference is not clear. Isolation of the channels from the SR membrane will considerably alter the immediate environment surrounding any one channel. The microdomain environment of the RyR within the SR microsomal membrane maintains the compartmentalisation of cytoplasm and lumen (Meissner 2002). It is possible that the native RyR arrays within the SR environment will contribute to the stability of the channels and provide a more durable backdrop for studies of conformational change. Thus when using the peptides in this environment there may be a greater magnitude of the change. This may be lost for isolated channels. However, to speculate on this point would be to over interpret the difference.

Using SR in experiments means that alteration of one parameter can change others. For example, phosphorylation would upregulate phospholamban and increase SERCA activity and calcium flux. In addition, SR preparations generally include FKBP12/12.6, which binds very tightly to the RyR (Jayaraman, Brillantes et al. 1992). Endogenous phosphorylation is rarely accounted for and nor is the FKBP12/12.6 content of SR preparations. It is not easy to examine differences in terms of the model and the experimental protocols and draw firm conclusions.



The DP4WT peptides (from the two different sources) behaved similarly, both were solubilised in DMSO and the 5% which was carried into the assays was accounted for in the controls. The only difference in the response to the DP4WT is the magnitude and not the dose response characteristics nor characteristics of inhibition, so although the difference was noted, it would appear that the peptide was acting to interfere with the domain interaction in our solubilised preparations in a similar manner to its action in SR preparations.

Bannister et al have shown a significantly reduced level of activation with the R2458C mutant DP4 peptide compared with the wildtype, but this is actually still increasing ryanodine binding by approximately 2 fold (Bannister, Hamada et al. 2007). Given that the magnitude of DP4 activation, seen in our study, at 100  $\mu$ M was only ever 2 fold compared with the control, it is perhaps not surprising that there was no difference in the DP4WT and mutant activation level. If solubilised RyR preparations had shown greater activation by the DP4WT peptide, there would have been a noticeable difference in effect. It may be the case therefore, that the use of DP4M as a control and model of MH in RyR1 is only really revealed using whole SR RyR preparation, as this somehow enables full DP4WT activation.

The intended goal, involving kinetic interactions studies using SPR (Jones, Reynolds et al. 2005), requires a preparation of RyR in solution. The value of this experimental technique is that the biochemical and protein modulators regulating the RyR molecule are limited by isolation, and key modulators of the channel, FKBP12/12.6 and phosphorylation can be carefully controlled. The solubilisation protocol, for example, is used to strip FKBP12/12.6 from the native protein. We have previously characterised these preparations (Jones, Reynolds et al. 2005; Blayney, Jones et al. 2010). The RyR preparations used in this study are similar in that they showed a typical biphasic dose response to free calcium concentration. There were differences in the phosphorylation profile as discussed in chapter 3 but changing the phosphorylation/dephosphorylation protocols enabled phosphorylated and dephosphorylated preparations to be obtained comparable to previous experiments. ATP had not been used in previous [ $^3$ H]ryanodine binding experiments on isolated RyR and we found that the magnitude of activation by ATP (about ~400%) in our preparations was comparable with those in the

literature for SR vesicles (Laver, Lenz et al. 2001). In general the results for DP4WT are as expected in terms of the published concentrations required to activate RyR preparations and the inhibition predicted by the addition of 0.5 mM magnesium (Yamamoto, El-Hayek et al. 2000). In addition we found that DP4WT channel activation was inhibited by the channel modulator FKBP12.6.

Thus we are left to consider whether there is something odd about our batch of DP4M peptide and this requires further experimental investigation by comparison with another source of mutant peptide. The mutant peptide activation was indistinguishable from the wildtype and it was inhibited by magnesium and FKBP12 in the same manner but not to the same extent. As the WT and mutant peptides were synthesized by the same supplier it is unlikely that the process of synthesis would affect the mutant alone. Unfortunately we were unable to obtain any mutant peptide from the Ikemoto group to enable comparison of its effect in our experimental model.

To enable further investigation of the mutant peptide from an alternative source, recombinant peptides were produced 'in house', and although the GST-tagged DP4WT and DP4M peptides had no notable effect on [<sup>3</sup>H]ryanodine binding, the cleaved wildtype peptide (without the GST tag) had an activatory effect equivalent to both the Ikemoto wildtype and the synthetic peptide tested at 10  $\mu$ M. The low (n) obtained for experiments with the recombinant peptide (Figure 6.8) means no strong conclusions can be drawn from this data, however the preliminary results are promising given the similar level of activation to other peptides tested in this study. To further assess this peptide, the purification strategy needs to be refined so greater yields are available for experiments. The DP4M peptide also has a different pI to the DP4WT, and therefore would require a different purification protocol. Solubility of both peptides has yet to be determined but the high concentrations needed for experiments at 100  $\mu$ M (~4 mM stock concentration) may result in solubilisation difficulties (Bannister, Hamada et al. 2007).

The ability to produce this domain peptide in house would greatly increase the opportunities for RyR channel analysis as this would provide a consistent and constant source. In house

purification means the proteins will be fresh and treated as mildly as possible to increase the validity of results generated. It is also important to obtain large yields for future analysis of FKBP12 binding using SPR experiments.

#### **8.4 RyR1 as a surrogate for RyR2**

Our experiments employ a strategy of showing conformational changes and their modulators in RyR1 and using key experiments to show that the mechanism is similar for RyR2. The validity of using RyR1 as a surrogate for RyR2 is supported by the many similarities between the two isoforms. The overall amino acid sequence of the two isoforms share 66% homology. Both isoforms exist as homotetramers and are associated with much smaller accessory proteins such as FKBP12/12.6 and calmodulin present as four molecules per receptor, i.e. one per sub unit (Meissner 2002). Topology models have shown the same overall structure with the cytoplasmic and transmembrane domains and indeed, the mutational clusters found to be associated with the conditions MH and CCD in RyR1 are directly translated into the same clusters for the RyR2-linked pathologies, CPVT and HF (Orlova, Serysheva et al. 1996; Serysheva, Schatz et al. 1999; Lobo and Van Petegem 2009). Most MH carriers exhibit a normal range of skeletal muscle function although patients with the more severe CDD phenotype have some muscle weakness and structural changes in skeletal myocyte contractile protein architecture (Denborough 1998). This range of symptoms is mimicked in CPVT and ARVD with the latter showing fatty streaks in the right ventricle. Both conditions require a trigger to unmask the life-threatening symptoms. For skeletal muscle it is halothane anaesthetics that destabilise RyR1 to trigger MH (Girard, Treves et al. 2002). In cardiac muscle fatal arrhythmias are triggered by physical and emotional stress and the heart performs normally at rest (Brini 2004). The trigger in cardiac myocytes (and also experimentally for RyR1) is linked to phosphorylation (Marx, Reiken et al. 2001).

Mutations manifest in both isoforms as increased sensitivity to calcium and activatory ligands such as polylysine. The DP4 activatory peptide for RyR1, corresponding to a portion of the central domain 'hot spot' for mutations, has also been shown to activate RyR2, suggesting the same regulatory domain interaction (Yamamoto, El-Hayek et al. 2000; Yamamoto and Ikemoto

2002; Liu, Wang et al. 2010). Both channels are also known to be modulated by phosphorylation by both PKA and CaMKII and are responsive to calcium and magnesium ions, although the extent of the sensitivity to these ions has been proposed to differ between the two isoforms in single channel studies (Meissner 2002). Full activation of both RyR1 and RyR2 is also only seen in the presence of ATP. Both channels show sensitivity to the same pharmacological modulators, the plant alkaloid ryanodine binds specifically to the open channel of both isoforms and the antiarrhythmic drug K201 has also been suggested to stabilise both channels (Meissner 2002; Lehnart, Wehrens et al. 2003; Wehrens, Lehnart et al. 2005; Blayney and Lai 2009). In addition, treatment of rodent HF models with the drugs K201 and S107, previously linked to enhanced FKBP12.6 binding to RyR2, has been shown to result in improved skeletal muscle function suggesting a similar mechanism of modulation by these drugs of the binding of FKBP12/12.6 to RyR1/2 (Bellinger, Reiken et al. 2008).

LCCs are voltage sensitive channels present in t-tubules at the junctional face membrane of the SR and communicate with both RyR1 and RyR2, as part of the signal transduction of ECC. However, as mentioned in the introduction, there is a key difference in the way the signal is transmitted to the RyR from the LCC for the two isoforms. RyR1 relies on direct allosteric modulation by the LCC, where RyR2 receives a trigger calcium signal across the dyadic cleft without any direct physical interaction and activation is amplified by CICR. RyR2 may have evolved earlier than RyR1 (Tunwell, Wickenden et al. 1996) so it may be that the allosteric LCC interaction with RyR1 is a later development, particularly as RyR1 can be activated experimentally by cytoplasmic calcium in the same way as RyR2 (Meissner 2002). One other notable difference is the possible reduced affinity of calcium binding to CaM bound to RyR2, compared with CaM bound to RyR1. This was proposed by one group given that the RyR2 inhibition by calcium-CaM was ten-fold lower than that of the RyR1 isoform (CaM acts to both inhibit and activate the RyR channel, with calcium binding turning on the inhibitory mode as cytoplasmic calcium rises) (Rodney, Williams et al. 2000; Puceat 2010).

In terms of RyR structure and conformational regulation the channels, once activated by their respective means, may behave in very similar ways. Using RyR1, which being more abundant,

can be extracted in greater quantities, to establish experimental protocols and explore definitive experimental approaches has been a necessary and valid strategy for our experimental approach to studies aligning function with conformational change. Key experiments have been chosen to establish that the basic concepts apply to both isoforms (Jones, Reynolds et al. 2005; Blayney, Jones et al. 2010). The difficulty in obtaining large yields of purified RyR2 may limit the extent to which those experiments carried out on RyR1 can be repeated on the cardiac isoform in future work. However a different batch of hearts may provide greater RyR2 yields, especially if the source was more controlled. Using the purification protocols tested in this study, enough protein was available to carry out some key experiments once the preliminary data with RyR1 had been obtained. An increased RyR2 yield would be necessary to carry out more thorough analysis of recombinant DPc10 peptide on the native RyR2. To this aim, further purification optimisation is required for the RyR2, perhaps alternative animal sources may generate greater yields or changes in the purification protocol may need to be developed and tested so the ratio of RyR that is extracted from the native tissue is increased compared with that lost in the solubilisation stages.

### **8.5 Do the findings using DP4 peptide support our hypothesis of convergent regulation?**

The model of convergent regulation has been proposed as a unifying idea accounting for the combined regulation of RyR by phosphorylation, FKBP12/12.6, magnesium, K201 and domain interaction. It was the intention to test this model using DP4 and DPc10 peptides to determine whether the conformational change observed previously corresponded to the central domain.

Circumstantial evidence suggests the central RyR domain may be a key site of convergent regulation. DP4 has been shown to reduce magnesium inhibition (Yamamoto, El-Hayek et al. 2000) . This has been demonstrated previously by other groups and also within this investigation. The proposed PKA phosphorylation sites (S2030 and S2808) flank the central domain region (Wehrens, Lehnart et al. 2006; Xiao, Tian et al. 2007), and the K201 binding site coordinate is close to the central domain and proposed to bind to it (Yamamoto, Yano et al. 2008).

The finding that domain activation by DP4 can be inhibited by FKBP12 modulation is particularly interesting. The  $K_i$  needs to be established with a dose response to FKBP12 to determine whether the affinity for FKBP12 is altered by the activatory peptide. Interestingly, the FKBP12 dose response observed with [ $^3$ H]ryanodine binding in the presence of ATP has shown a shift to the right, suggesting FKBP12 is less effective in the presence of ATP. Although 50% inhibition was the maximal effect observed by FKBP12 with ATP, as seen in the presence of calcium alone, the  $EC_{50}$  was shifted from 0.1  $\mu$ M to 1  $\mu$ M, a 10 fold difference. ATP did not feature in the original model, however, it is well known that calcium alone cannot instigate full channel opening (Xu, Mann et al. 1996; Laver, Lenz et al. 2001). Thus it may be that ATP causes a further conformational change from the level of maximal calcium activation. Perhaps DP4 is acting in a similar fashion to ATP in forcing a final conformation movement required for full activation of the channel.

Previous SPR experiments have shown a reduced affinity of RyR for FKBP12 in the presence of ATP, which is consistent with this idea (Jones, Reynolds et al. 2005). Further experiments, using the Biacore technique, as suggested earlier, could be used to measure the affinity of RyR binding to FKBP12, in real time in the presence of the channel modulators DP4 or ATP to see if this conformational change is consistent with a further decrease in FKBP12 affinity.

Another novel finding of this study has shown the effects of magnesium and FKBP12 on channel inhibition to be additive. This could be accounted for by FKBP12 binding to the RyR and inducing a conformational change which closes the channel and in the process revealing the magnesium inhibition site(s) giving magnesium access to its site of regulation, and hence exerting an additional inhibitory effect. This would be consistent with the model and with the findings of others proposing the masking and unmasking of magnesium inhibition sites (Laver, Baynes et al. 1997; Blayney, Jones et al. 2010). It may also be consistent with ATP binding sites being masked as the channel closes, during the same transition (Dias, Szegedi et al. 2006).

PKA phosphorylation had no notable effect on [<sup>3</sup>H]ryanodine binding, apart from on magnesium inhibition. This supports the idea that phosphorylation may poise the channel between the open and closed states (Jones, Lai et al. 2006) to enable faster movement to a fully open state under conditions of  $\beta$ -adrenergic stimulation. These findings all serve to complement and add to the convergent regulation hypothesis, as documented prior to this investigation.

To continue with these experiments it is now necessary to determine the effects of phosphorylation, and with more peptide, proceed to the kinetic measurements. The tools are also now in place to enable parallel experiments with the RyR2 isoform.

### **8.6 Further work**

- Optimise cleavage from the GST tag and improve purification protocols for the cleaved DP4WT and DP4M so that an alternative source of mutant peptide can be tested in our experimental model.
- Ascertain whether the reduced effect of DP4 activation seen in our model is an artefact of the isolated RyR by carrying out parallel experiments with SR preparations from the same source as the isolated channels. These preparations must be stripped of endogenous FKBP12 and dephosphorylated in the same manner as the isolated RyR.
- Generate the DPc10 mutant peptide and optimise purification of the wildtype and mutant peptides, possibly in parallel to DP4 as DPc10 can be tracked more easily.
- Test the peptide effect in relation to phosphorylation, essentially using SPR to assess the affinity for FKBP12 in the presence of DP4 and phosphorylation.
- Test alternative central domain mutations for comparative effects.
- Perform [<sup>3</sup>H]ryanodine binding and SPR experiments to assess DPc10 activation on isolated RyR2.

## **8.7 Conclusion**

In summary, the data provided in this thesis have shown the following;

The DP4 peptide is able to increase RyR1 channel opening above that induced by calcium alone, suggesting interruption of the central and N-terminus interaction does increase the isolated RyR1 channel open probability, but to an amount less than observed by ATP. In addition ATP has been shown to reduce RyR1 sensitivity to FKBP12 inhibition, these findings point to another potential conformational change induced by ATP over and above those proposed in our original model which may be measured as a reduced affinity for FKBP12.

The DP4 activatory effect on RyR1 may be reduced in isolated RyR channels, compared with RyR channels in intact SR membrane preparations, suggesting additional modulation by a factor outside the experimental model used. If this is true then the use of the DP4 mutant peptide as a mimic of the disease state is only valid in an SR experimental model. Alternatively, a single base mutation inserted into the DP4 peptide may not be sufficient to prevent channel activation, and hence is not an accurate interpretation of the disease state.

FKBP12 and magnesium inhibition of RyR1 is reduced by the DP4 peptide, also, FKBP12 and magnesium inhibition of RyR1 are additive, supporting the idea that a conformational change induced by FKBP12 may unmask a magnesium binding site.

In addition, the tools are now in place to enable further assessment of these findings using SPR to assess changes in RyR1 binding affinity for FKBP12 with DP4 and the other modulators tested in this investigation. Subsequent studies can also be pursued using the RyR2 isoform, the DPc10 peptide and its CPVT mutant to ascertain whether the same model of convergent regulation applies to RyR2 modulation. This is of great significance for future studies regarding RyR1/2 dysfunction in arrhythmias linked to MH and CPVT respectively.



## References

**REFERENCES**

Ai, X., Curran, J. W., et al. (2005).  $Ca^{2+}$ /Calmodulin-Dependent Protein Kinase Modulates Cardiac Ryanodine Receptor Phosphorylation and Sarcoplasmic Reticulum  $Ca^{2+}$  Leak in Heart Failure. Circulation Research **97**(12): 1314-1322.

Amador, F. J., Liu, S., et al. (2009). Crystal Structure of Type I Ryanodine Receptor Amino-Terminal  $\beta$ -Trefoil Domain Reveals a Disease-Associated Mutation Hot Spot Loop. Proceedings of the National Academy of Sciences **106**(27): 11040-11044.

Avila, G., Lee, E. H., et al. (2003). FKBP12 Binding to RyR1 Modulates Excitation-Contraction Coupling in Mouse Skeletal Myotubes. Journal of Biological Chemistry **278**(25): 22600-22608.

Balasubramaniam, R., Chawla, S., et al. (2004). Nifedipine and Diltiazem Suppress Ventricular Arrhythmogenesis and Calcium Release in Mouse Hearts. Pflugers Archiv-European Journal of Physiology **449**(2): 150-158.

Balshaw, D. M., Xu, L., et al. (2001). Calmodulin Binding and Inhibition of Cardiac Muscle Calcium Release Channel (Ryanodine Receptor). Journal of Biological Chemistry **276**(23): 20144-20153.

Bannister, M. L., Hamada, T., et al. (2007). Malignant Hyperthermia Mutation Sites in the Leu(2442)-Pro(2477) (DP4) Region of RyR1 (Ryanodine Receptor 1) Are Clustered in a Structurally and Functionally Definable Area. Biochemical Journal **401**: 333-339.

Bassani, J. W., Yuan, W., et al. (1995). Fractional SR  $Ca^{2+}$  Release Is Regulated by Trigger  $Ca^{2+}$  and SR  $Ca^{2+}$  Content in Cardiac Myocytes. Am J Physiol Cell Physiol **268**(5): C1313-1319.

Bellinger, A. M., Reiken, S., et al. (2009). Hypernitrosylated Ryanodine Receptor Calcium Release Channels Are Leaky in Dystrophic Muscle. Nat Med **15**(3): 325-330.

- Bellinger, A. M., Reiken, S., et al. (2008). Remodeling of Ryanodine Receptor Complex Causes Leaky Channels: A Molecular Mechanism for Decreased Exercise Capacity. Proceedings of the National Academy of Sciences **105**(6): 2198-2202.
- Bers, D. M. (2002). Cardiac Excitation-Contraction Coupling. Nature **415**(6868): 198-205.
- Bers, D. M. (2004). Macromolecular Complexes Regulating Cardiac Ryanodine Receptor Function. Journal of Molecular and Cellular Cardiology **37**(2): 417-429.
- Bers, D. M. and Ziolo, M. T. (2001). When Is Camp Not Camp?: Effects of Compartmentalization. Circulation Research **89**(5): 373-375.
- Blayney, L. M., Jones, J. L., et al. (2010). A Mechanism of Ryanodine Receptor Modulation by FKBP12/12.6, Protein Kinase a, and K201. Cardiovascular Research **85**(1): 68-78.
- Blayney, L. M. and Lai, F. A. (2009). Ryanodine Receptor-Mediated Arrhythmias and Sudden Cardiac Death. Pharmacology & Therapeutics **123**(2): 151-177.
- Brette, F. and Orchard, C. (2003). T-Tubule Function in Mammalian Cardiac Myocytes. Circulation Research **92**(11): 1182-1192.
- Brillantes, A.-M. B., Ondrias, K., et al. (1994). Stabilization of Calcium Release Channel (Ryanodine Receptor) Function by FK506-Binding Protein. Cell **77**(4): 513-523.
- Brini, M. (2004). Ryanodine Receptor Defects in Muscle Genetic Diseases. Biochemical and Biophysical Research Communications(322): 1245-1255.
- Bull, R., Finkelstein, J. P., et al. (2007). Effects of ATP, Mg<sup>2+</sup>, and Redox Agents on the Ca<sup>2+</sup> Dependence of RyR Channels from Rat Brain Cortex. Am J Physiol Cell Physiol **293**(1): C162-171.
- Cameron, A. M., Nucifora, F. C., et al. (1997). FKBP12 Binds the Inositol 1,4,5-Trisphosphate Receptor at Leucine-Proline (1400-1401) and Anchors Calcineurin to This FK506-Like Domain. Journal of Biological Chemistry **272**(44): 27582-27588.

- Chelu, M. G., Danila, C. I., et al. (2004). Regulation of Ryanodine Receptors by FK506 Binding Proteins. Trends in Cardiovascular Medicine **14**(6): 227-234.
- Cheng, H., Lederer, M. R., et al. (1996). Calcium Sparks and  $[Ca^{2+}]_i$  Waves in Cardiac Myocytes. Am J Physiol Cell Physiol **270**(1): C148-159.
- Cheng, H., Lederer, W. J., et al. (1993). Calcium Sparks: Elementary Events Underlying Excitation-Contraction Coupling in Heart Muscle. Science **262**(5134): 740-744.
- Cheng, W., Altafaj, X., et al. (2005). Interaction between the Dihydropyridine Receptor  $Ca^{2+}$  Channel  $\beta$ -Subunit and Ryanodine Receptor Type 1 Strengthens Excitation-Contraction Coupling. Proceedings of the National Academy of Sciences of the United States of America **102**(52): 19225-19230.
- Collins, J. H. (1991). Sequence Analysis of the Ryanodine Receptor: Possible Association with a 12K, FK506-Binding Immunophilin/Protein Kinase C Inhibitor. Biochemical and Biophysical Research Communications **178**(3): 1288-1290.
- Currie, S., Loughrey, C. M., et al. (2004). Calcium/Calmodulin-Dependent Protein Kinase  $\delta$  Associates with the Ryanodine Receptor Complex and Regulates Channel Function in Rabbit Heart. Biochem. J. **377**(2): 357-366.
- Denborough, M. (1998). Malignant Hyperthermia. Lancet **352**: 1131 - 1136.
- Dias, J. M., Szegedi, C., et al. (2006). Insights into the Regulation of the Ryanodine Receptor: Differential Effects of  $Mg^{2+}$  and  $Ca^{2+}$  on ATP Binding Biochemistry **45**(31): 9408-9415.
- Dirksen, R. T. and Avila, G. (2002). Altered Ryanodine Receptor Function in Central Core Disease: Leaky or Uncoupled  $Ca^{2+}$  Release Channels? Trends in Cardiovascular Medicine **12**(5): 189-197.

- Duke, A. M., Hopkins, P. M., et al. (2002). Effects of  $Mg^{2+}$  and SR Luminal  $Ca^{2+}$  on Caffeine-Induced  $Ca^{2+}$  Release in Skeletal Muscle from Humans Susceptible to Malignant Hyperthermia. The Journal of Physiology **544**(1): 85-95.
- Duke, A. M., Hopkins, P. M., et al. (2003).  $Mg^{2+}$  Dependence of Halothane-Induced  $Ca^{2+}$  Release from the Sarcoplasmic Reticulum in Rat Skeletal Muscle. The Journal of Physiology **551**(2): 447-454.
- Echt, D. S., Liebson, P. R., et al. (1991). Mortality and Morbidity in Patients Receiving Encainide, Flecainide, or Placebo. New England Journal of Medicine **324**(12): 781-788.
- Eisner, D. A., Kashimura, T., et al. (2009). From the Ryanodine Receptor to Cardiac Arrhythmias. Circulation Journal **73**(9): 1561-1567.
- Erickson, J. R., Joiner, M.-L. A., et al. (2008). A Dynamic Pathway for Calcium-Independent Activation of CaMKII by Methionine Oxidation. Cell **133**(3): 462-474.
- Fabiato, A. and Fabiato, F. (1979). Use of Chlorotetracycline Fluorescence to Demonstrate  $Ca^{2+}$ -Induced Release of  $Ca^{2+}$  from the Sarcoplasmic Reticulum of Skinned Cardiac Cells. Nature **281**(5727): 146-148.
- Farrell, A. (2004). Regulation of Cardiac Excitation-Contraction Coupling by Sorcin, a Novel Modulator of Ryanodine Receptors. Biol Res **37**.
- Farrell, E. F., Antaramian, A., et al. (2003). Sorcin Inhibits Calcium Release and Modulates Excitation-Contraction Coupling in the Heart. Journal of Biological Chemistry **278**(36): 34660-34666.
- Fernandez-Velasco, M., Rueda, A., et al. (2009). Increased  $Ca^{2+}$  Sensitivity of the Ryanodine Receptor Mutant RyR2 R4496C Underlies Catecholaminergic Polymorphic Ventricular Tachycardia. Circulation Research **104**(2): 201-209.

- Ferrero, P., Said, M., et al. (2007).  $\text{Ca}^{2+}$ /Calmodulin Kinase II Increases Ryanodine Binding and  $\text{Ca}^{2+}$ -Induced Sarcoplasmic Reticulum  $\text{Ca}^{2+}$  Release Kinetics During  $\beta$ -Adrenergic Stimulation. Journal of Molecular and Cellular Cardiology **43**(3): 281-291.
- Fleischer, S. (2008). Personal Recollections on the Discovery of the Ryanodine Receptors of Muscle. Biochemical and Biophysical Research Communications **369**(1): 195-207.
- Fleischer, S., Ogunbunmi, E. M., et al. (1985). Localization of  $\text{Ca}^{2+}$  Release Channels with Ryanodine in Junctional Terminal Cisternae of Sarcoplasmic Reticulum of Fast Skeletal Muscle. Proceedings of the National Academy of Sciences of the United States of America **82**(21): 7256-7259.
- Franzini-Armstrong, C., Protasi, F., et al. (1999). Shape, Size, and Distribution of  $\text{Ca}^{2+}$  Release Units and Couplons in Skeletal and Cardiac Muscles. Biophysical Journal **77**(3): 1528-1539.
- Franzini, C. (1970). Studies of Triad .1. Structure of Junction in Frog Twitch Fibers. Journal of Cell Biology **47**(2): 488-497.
- Gaburjakova, M., Gaburjakova, J., et al. (2001). FKBP12 Binding Modulates Ryanodine Receptor Channel Gating. Journal of Biological Chemistry **276**(20): 16931-16935.
- Garrett, R. H. and Grisham, C. M. (1998). Biochemistry, South-Western, Division of Thomson Learning.
- George, C. H., Higgs, G. V., et al. (2003). Ryanodine Receptor Mutations Associated with Stress-Induced Ventricular Tachycardia Mediate Increased Calcium Release in Stimulated Cardiomyocytes. Circulation Research **93**(6): 531-540.
- George, C. H., Jundi, H., et al. (2004). Ryanodine Receptor Regulation by Intramolecular Interaction between Cytoplasmic and Transmembrane Domains. Molecular Biology of the Cell **15**(6): 2627-2638.

- Ginsburg, K. S. and Bers, D. M. (2005). Isoproterenol Does Not Enhance Ca-Dependent Na/Ca<sup>2+</sup> Exchange Current in Intact Rabbit Ventricular Myocytes. Journal of Molecular and Cellular Cardiology **39**(6): 972-981.
- Girard, T., Treves, S., et al. (2002). Phenotyping Malignant Hyperthermia Susceptibility by Measuring Halothane-Induced Changes in Myoplasmic Calcium Concentration in Cultured Human Skeletal Muscle Cells. Br J Anaesth **89**: 571 - 579.
- Grievink, H. and Stowell, K. (2010). Allele-Specific Differences in Ryanodine Receptor 1 mRNA Expression Levels May Contribute to Phenotypic Variability in Malignant Hyperthermia. Orphanet Journal of Rare Diseases **5**(1): 10.
- Grimm, M. and Brown, J. H. (2010).  $\beta$ -Adrenergic Receptor Signaling in the Heart: Role of CaMKII. Journal of Molecular and Cellular Cardiology **48**(2): 322-330.
- Guo, T., Cornea, R. L., et al. (2010). Kinetics of FKBP12.6 Binding to Ryanodine Receptors in Permeabilized Cardiac Myocytes and Effects on Ca<sup>2+</sup> Sparks. Circulation Research **106**(11): 1743-1752.
- Györke, I., Hester, N., et al. (2004). The Role of Calsequestrin, Triadin, and Junctin in Conferring Cardiac Ryanodine Receptor Responsiveness to Luminal Calcium. Biophysical Journal **86**(4): 2121-2128.
- Haarmann, C. S., Dulhunty, A. F., et al. (2005). Regulation of Skeletal Ryanodine Receptors by Dihydropyridine Receptor II-III Loop C-Region Peptides: Relief of Mg<sup>2+</sup> Inhibition. Biochemical Journal **387**: 429-436.
- Hain, J. R., Onoue, H., et al. (1995). Phosphorylation Modulates the Function of the Calcium Release Channel of Sarcoplasmic Reticulum from Cardiac Muscle. Journal of Biological Chemistry **270**(5): 2074-2081.

- Hamada, T., Bannister, M. L., et al. (2007). Peptide Probe Study of the Role of Interaction between the Cytoplasmic and Transmembrane Domains of the Ryanodine Receptor in the Channel Regulation Mechanism. Biochemistry **46**(14): 4272-4279.
- Hamada, T., Gangopadhyay, J. P., et al. (2009). Defective Regulation of the Ryanodine Receptor Induces Hypertrophy in Cardiomyocytes. Biochemical and Biophysical Research Communications **380**(3): 493-497.
- Herzog, A., Szegedi, C., et al. (2000). Surface Plasmon Resonance Studies Prove the Interaction of Skeletal Muscle Sarcoplasmic Reticular Ca<sup>2+</sup> Release Channel/Ryanodine Receptor with Calsequestrin. Febs Letters **472**(1): 73-77.
- Hilliard, F. A., Steele, D. S., et al. (2010). Flecainide Inhibits Arrhythmogenic Ca<sup>2+</sup> Waves by Open State Block of Ryanodine Receptor Ca<sup>2+</sup> Release Channels and Reduction of Ca<sup>2+</sup> Spark Mass. Journal of Molecular and Cellular Cardiology **48**(2): 293-301.
- Hohl, C. M., Garleb, A. A., et al. (1992). Effects of Simulated Ischemia and Reperfusion on the Sarcoplasmic Reticulum of Digitonin-Lysed Cardiomyocytes. Circulation Research **70**(4): 716-723.
- Hudmon, A. and Schulman, H. (2002). Structure-Function of the Multifunctional Ca<sup>2+</sup>/Calmodulin-Dependent Protein Kinase II. Biochem. J. **364**(3): 593-611.
- Hunt (2007). K201 (JTV519) Suppresses Spontaneous Ca<sup>2+</sup> Release and [<sup>3</sup>H] Ryanodine Binding to RyR2 Irrespective of FKBP12.6 Association. J. Biochem **404**: 431-438.
- Ikemoto, N., Nagy, B. L., et al. (1974). Studies on a Metal-Binding Protein of the Sarcoplasmic Reticulum. Journal of Biological Chemistry **249**(8): 2357-2365.
- Inui, M., Saito, A., et al. (1987). Purification of the Ryanodine Receptor and Identity with Feet Structures of Junctional Terminal Cisternae of Sarcoplasmic Reticulum from Fast Skeletal Muscle. Journal of Biological Chemistry **262**(4): 1740-1747.



- Jacob, F. and Monod, J. (1961). Genetic Regulatory Mechanisms in the Synthesis of Proteins. J Mol Biol **3**: 318-56.
- Jayaraman, T., Brillantes, A. M., et al. (1992). FK506 Binding Protein Associated with the Calcium Release Channel (Ryanodine Receptor). Journal of Biological Chemistry **267**(14): 9474-9477.
- Jeyakumar, L. H., Copello, J. A., et al. (1998). Purification and Characterization of Ryanodine Receptor 3 from Mammalian Tissue. Journal of Biological Chemistry **273**(26): 16011-16020.
- Jiang, D., Wang, R., et al. (2005). Enhanced Store Overload-Induced Ca<sup>2+</sup> Release and Channel Sensitivity to Luminal Ca<sup>2+</sup> Activation Are Common Defects of RyR2 Mutations Linked to Ventricular Tachycardia and Sudden Death. Circulation Research **97**(11): 1173-1181.
- Jiang, D., Xiao, B., et al. (2004). RyR2 Mutations Linked to Ventricular Tachycardia and Sudden Death Reduce the Threshold for Store-Overload-Induced Ca<sup>2+</sup> Release (SOICR). Proceedings of the National Academy of Sciences of the United States of America **101**(35): 13062-13067.
- Jiang, M. T., Lokuta, A. J., et al. (2002). Abnormal Ca<sup>2+</sup> Release, but Normal Ryanodine Receptors, in Canine and Human Heart Failure. Circulation Research **91**(11): 1015-1022.
- Jiang, Y., Lee, A., et al. (2002). The Open Pore Conformation of Potassium Channels. Nature **417**(6888): 523-526.
- Jóna, I., Szegedi, C., et al. (2001). Altered Inhibition of the Rat Skeletal Ryanodine Receptor/Calcium Release Channel by Magnesium in the Presence of ATP. Pflügers Archiv European Journal of Physiology **441**(6): 729-738.
- Jones, J. L., D'cruz, L., et al. (2007). Modulation of RyR2 Binding to FKBP12.6 by Phosphorylation and JTV519. Biophysical Journal: 261A-261A.

- Jones, J. L., Lai, F. A., et al. (2006). Phosphorylation by Protein Kinase a Changes the Equilibrium Binding of Ryanodine Receptor  $Ca^{2+}$  Channels for FKBP12. Journal of Molecular and Cellular Cardiology **40**(6): 981-982.
- Jones, J. L., Reynolds, D., et al. (2005). A Surface Plasmon Resonance Study of the Binding of FKBP12 to Open or Closed Ryanodine Receptor Channels. Journal of Molecular and Cellular Cardiology **39**(1): 41.
- Jones, J. L., Reynolds, D. F., et al. (2005). Ryanodine Receptor Binding to FKBP12 Is Modulated by Channel Activation State. Journal of Cell Science **118**(20): 4613-4619.
- Kannankeril, P. J., Mitchell, B. M., et al. (2006). Mice with the R176Q Cardiac Ryanodine Receptor Mutation Exhibit Catecholamine-Induced Ventricular Tachycardia and Cardiomyopathy. Proceedings of the National Academy of Sciences **103**(32): 12179-12184.
- Kentish, J. C., McCloskey, D. T., et al. (2001). Phosphorylation of Troponin I by Protein Kinase a Accelerates Relaxation and Crossbridge Cycle Kinetics in Mouse Ventricular Muscle. Circulation Research **88**(10): 1059-1065.
- Kermode, H., Williams, A. J., et al. (1998). The Interactions of ATP, ADP, and Inorganic Phosphate with the Sheep Cardiac Ryanodine Receptor. Biophysical Journal **74**(3): 1296-1304.
- Kirchhefer, U., Hanske, G., et al. (2006). Overexpression of Junctin Causes Adaptive Changes in Cardiac Myocyte  $Ca^{2+}$  Signaling. Cell Calcium **39**(2): 131-142.
- Kirino, Y., Osakabe, M., et al. (1983).  $Ca^{2+}$ -Induced  $Ca^{2+}$  Release from Fragmented Sarcoplasmic Reticulum:  $Ca^{2+}$ -Dependent Passive  $Ca^{2+}$  Efflux. Journal of Biochemistry **94**(4): 1111-1118.
- Knollmann, B. R. C., Chopra, N., et al. (2006). CASQ2 Deletion Causes Sarcoplasmic Reticulum Volume Increase, Premature  $Ca^{2+}$  Release, and Catecholaminergic Polymorphic Ventricular Tachycardia. The Journal of Clinical Investigation **116**(9): 2510-2520.

- Kobayashi, S., Bannister, M., et al. (2005). Dantrolene Stabilizes Inter-Domain Interactions within Domain Switch of the Ryanodine Receptor. *Biophysical Journal* **88**(1): 484A-485A.
- Kobayashi, S., Bannister, M. L., et al. (2005). Dantrolene Stabilizes Domain Interactions within the Ryanodine Receptor. *Journal of Biological Chemistry* **280**(8): 6580-6587.
- Kobayashi, S., Yamamoto, T., et al. (2004). Antibody Probe Study of Ca<sup>2+</sup> Channel Regulation by Interdomain Interaction within the Ryanodine Receptor. *Biochem. J.* **380**(2): 561-569.
- Kobayashi, S., Yano, M., et al. (2009). Dantrolene, a Therapeutic Agent for Malignant Hyperthermia, Markedly Improves the Function of Failing Cardiomyocytes by Stabilizing Interdomain Interactions within the Ryanodine Receptor. *Journal of the American College of Cardiology* **53**(21): 1993-2005.
- Koretsune, Y., Corretti, M. C., et al. (1991). Mechanism of Early Ischemic Contractile Failure. Inexcitability, Metabolite Accumulation, or Vascular Collapse? *Circulation Research* **68**(1): 255-262.
- Laemmli, U. (1970). Cleavage of Structural Proteins During the Assembly of the Head of Bacteriophage T4. *Nature* **227**(5259): 680-5.
- Lai, F. A., Erickson, H. P., et al. (1988). Purification and Reconstitution of the Calcium Release Channel from Skeletal-Muscle. *Nature* **331**(6154): 315-319.
- Lai, F. A., Erickson, H. P., et al. (1988). Purification, Photoaffinity-Labeling, Structure and Functional Reconstitution of the Ca<sup>2+</sup> Release Channel from Skeletal Sarcoplasmic-Reticulum. *Biophysical Journal* **53**(2): A469-A469.
- Lai, F. A., Misra, M., et al. (1989). The Ryanodine Receptor-Ca<sup>2+</sup> Release Channel Complex of Skeletal-Muscle Sarcoplasmic-Reticulum - Evidence for a Cooperatively Coupled, Negatively Charged Homotetramer. *Journal of Biological Chemistry* **264**(28): 16776-16785.

- Lamb, G. D., Cellini, M. A., et al. (2001). Different  $\text{Ca}^{2+}$  Releasing Action of Caffeine and Depolarisation in Skeletal Muscle Fibres of the Rat. The Journal of Physiology **531**(3): 715-728.
- Lamb, G. D., Posterino, G. S., et al. (2001). Effects of a Domain Peptide of the Ryanodine Receptor on  $\text{Ca}^{2+}$  Release in Skinned Skeletal Muscle Fibers. American Journal of Physiology-Cell Physiology **281**(1): C207-C214.
- Lamb, G. D. and Stephenson, D. G. (1991). Effect of  $\text{Mg}^{2+}$  on the Control of  $\text{Ca}^{2+}$  Release in Skeletal Muscle Fibres of the Toad. The Journal of Physiology **434**(1): 507-528.
- Laver, D., Honen, B., et al. (2008). A Domain Peptide of the Cardiac Ryanodine Receptor Regulates Channel Sensitivity to Luminal  $\text{Ca}^{2+}$  Via Cytoplasmic  $\text{Ca}^{2+}$  Sites. European Biophysics Journal **37**(4): 455-467.
- Laver, D. R. (2005). Coupled Calcium Release Channels and Their Regulation by Luminal and Cytosolic Ions. European Biophysics Journal with Biophysics Letters **34**(5): 359-368.
- Laver, D. R. (2007).  $\text{Ca}^{2+}$  Stores Regulate Ryanodine Receptor  $\text{Ca}^{2+}$  Release Channels Via Luminal and Cytosolic  $\text{Ca}^{2+}$  Sites. Clinical and Experimental Pharmacology and Physiology **34**(9): 889-896.
- Laver, D. R., Baynes, T. M., et al. (1997). Magnesium Inhibition of Ryanodine-Receptor Calcium Channels: Evidence for Two Independent Mechanisms. Journal of Membrane Biology **9156**(3): 213-229.
- Laver, D. R. and Honen, B. N. (2008). Luminal  $\text{Mg}^{2+}$ , a Key Factor Controlling Ryr2-Mediated  $\text{Ca}^{2+}$  Release: Cytoplasmic and Luminal Regulation Modeled in a Tetrameric Channel. Journal of General Physiology **132**(4): 429-446.
- Laver, D. R., Honen, B. N., et al. (2008). A Domain Peptide of the Cardiac Ryanodine Receptor Regulates Channel Sensitivity to Luminal  $\text{Ca}^{2+}$  Via Cytoplasmic  $\text{Ca}^{2+}$  Sites. European Biophysics Journal with Biophysics Letters **37**(4): 455-467.

- Laver, D. R., Lenz, G. K. E., et al. (2001). Regulation of the Calcium Release Channel from Rabbit Skeletal Muscle by the Nucleotides ATP, AMP, Imp and Adenosine. Journal of Physiology-London **537**(3): 763-778.
- Laver, D. R., O'Neill, E. R., et al. (2004). Luminal Ca<sup>2+</sup>-Regulated Mg<sup>2+</sup> Inhibition of Skeletal RyRs Reconstituted as Isolated Channels or Coupled Clusters. Journal of General Physiology **124**(6): 741-758.
- Leenhardt, A., Lucet, V., et al. (1995). Catecholaminergic Polymorphic Ventricular Tachycardia in Children : A 7-Year Follow-up of 21 Patients. Circulation **91**(5): 1512-1519.
- Lehnart, S. E., Mongillo, M., et al. (2008). Leaky Ca<sup>2+</sup> Release Channel/Ryanodine Receptor 2 Causes Seizures and Sudden Cardiac Death in Mice. The Journal of Clinical Investigation **118**(6): 2230-2245.
- Lehnart, S. E., Mongillo, M., et al. (2008). Leaky Ca<sup>2+</sup> Release Channel/Ryanodine Receptor 2 Causes Seizures and Sudden Cardiac Death in Mice. Journal of Clinical Investigation **118**(6): 2230-2245.
- Lehnart, S. E., Wehrens, X. H., et al. (2003). JTV519 Restores Normal Cardiac Ryanodine Receptor Ca<sup>2+</sup> Channel Function in Failing Hearts. Circulation **108**(17): 346.
- Li, L., Desantiago, J., et al. (2000). Phosphorylation of Phospholamban and Troponin I in  $\beta$ -Adrenergic-Induced Acceleration of Cardiac Relaxation. Am J Physiol Heart Circ Physiol **278**(3): H769-779.
- Li, P. and Chen, S. R. W. (2001). Molecular Basis of Ca<sup>2+</sup> Activation of the Mouse Cardiac Ca<sup>2+</sup> Release Channel (Ryanodine Receptor). The Journal of General Physiology **118**(1): 33-44.
- Li, Y., Kranias, E. G., et al. (2002). Protein Kinase a Phosphorylation of the Ryanodine Receptor Does Not Affect Calcium Sparks in Mouse Ventricular Myocytes. Circulation Research **90**(3): 309-316.

- Liu, N., Colombi, B., et al. (2006). Arrhythmogenesis in Catecholaminergic Polymorphic Ventricular Tachycardia - Insights from a RyR2 R4496C Knock-in Mouse Model. Circulation Research **99**(3): 292-298.
- Liu, W., Pasek, D. A., et al. (1998). Modulation of Ca<sup>2+</sup>-Gated Cardiac Muscle Ca<sup>2+</sup>-Release Channel (Ryanodine Receptor) by Mono- and Divalent Ions. Am J Physiol Cell Physiol **274**(1): C120-128.
- Liu, Z., Wang, R., et al. (2005). Localization of a Disease-Associated Mutation Site in the Three-Dimensional Structure of the Cardiac Muscle Ryanodine Receptor. Journal of Biological Chemistry **280**(45): 37941-37947.
- Liu, Z., Wang, R. W., et al. (2010). Dynamic, Inter-Subunit Interactions between the N-Terminal and Central Mutation Regions of Cardiac Ryanodine Receptor. Journal of Cell Science **123**(10): 1775-1784.
- Liu, Z., Zhang, J., et al. (2001). Three-Dimensional Reconstruction of the Recombinant Type 3 Ryanodine Receptor and Localization of Its Amino Terminus. Proceedings of the National Academy of Sciences of the United States of America **98**(11): 6104-6109.
- Lobo, P. A. and Van Petegem, F. (2009). Crystal Structures of the N-Terminal Domains of Cardiac and Skeletal Muscle Ryanodine Receptors: Insights into Disease Mutations. Structure (London, England : 1993) **17**(11): 1505-1514.
- Lodish, H., Berk, A., et al. (2000). Molecular Cell Biology, 4th Edition. New York, W.H. Freeman.
- Lokuta, A. J., Meyers, M. B., et al. (1997). Modulation of Cardiac Ryanodine Receptors by Sorcin. Journal of Biological Chemistry **272**(40): 25333-25338.
- Loughrey, C. M., Otani, N., et al. (2007). K201 Modulates Excitation-Contraction Coupling and Spontaneous Ca<sup>2+</sup> Release in Normal Adult Rabbit Ventricular Cardiomyocytes. Cardiovascular Research **76**(2): 236-246.

- Maclennan, D. H., Duff, C., et al. (1990). Ryanodine Receptor Gene Is a Candidate for Predisposition to Malignant Hyperthermia. Nature **343**: 559 - 561.
- Maclennan, D. H. and Phillips, M. S. (1992). Malignant Hyperthermia. Science **256**: 789 - 794.
- Marks, A. R., Priori, S., et al. (2002). Involvement of the Cardiac Ryanodine Receptor/Calcium Release Channel in Catecholaminergic Polymorphic Ventricular Tachycardia. Journal of Cellular Physiology **190**(1): 1-6.
- Marks, A. R., Tempst, P., et al. (1989). Molecular Cloning and Characterization of the Ryanodine Receptor/Junctional Channel Complex cDNA from Skeletal Muscle Sarcoplasmic Reticulum. Proceedings of the National Academy of Sciences of the United States of America **86**(22): 8683-8687.
- Marx, S. O., Gaburjakova, J., et al. (2001). Coupled Gating between Cardiac Calcium Release Channels (Ryanodine Receptors). Circulation Research **88**(11): 1151-1158.
- Marx, S. O., Reiken, S., et al. (2001). Phosphorylation-Dependent Regulation of Ryanodine Receptors: A Novel Role for Leucine/Isoleucine Zippers. Journal of Cell Biology **153**(4): 699-708.
- Marx, S. O., Reiken, S., et al. (2000). PKA Phosphorylation Dissociates FKBP12.6 from the Calcium Release Channel (Ryanodine Receptor): Defective Regulation in Failing Hearts. Cell **101**(4): 365-376.
- Mayrleitner, M., Chandler, R., et al. (1995). Phosphorylation with Protein Kinases Modulates Calcium Loading of Terminal Cisternae of Sarcoplasmic Reticulum from Skeletal Muscle. Cell Calcium **18**(3): 197-206.
- Mccall, E., Li, L., et al. (1996). Effects of Fk-506 on Contraction and Ca<sup>2+</sup> Transients in Rat Cardiac Myocytes. Circ Res **79**(6): 1110-1121.

Mccarthy, T. V., Healy, J. M., et al. (1990). Localization of the Malignant Hyperthermia Susceptibility Locus to Human Chromosome 19q12-13.2. Nature **343**: 562 - 564.

Meissner (2002). Regulation of Mammalian Ryanodine Receptors. Frontiers in Bioscience.

Meissner, E.-H. (1992). Ryanodine as a Functional Probe.

Meissner, G. (2002). Regulation of Mammalian Ryanodine Receptors. Frontiers in Bioscience **7**: D2072-D2080.

Meissner, G., Darling, E., et al. (1986). Kinetics of Rapid Calcium Release by Sarcoplasmic Reticulum. Effects of Calcium, Magnesium, and Adenine Nucleotides. Biochemistry **25**(1): 236-244

Meissner, G. and Henderson, J. S. (1987). Rapid Calcium Release from Cardiac Sarcoplasmic-Reticulum Vesicles Is Dependent on  $\text{Ca}^{2+}$  and Is Modulated by  $\text{Mg}^{2+}$ , Adenine-Nucleotide, and Calmodulin. Journal of Biological Chemistry **262**(7): 3065-3073.

Meissner, G., Lai, F. A., et al. (1990).  $\text{Ca}^{2+}$  Release Channel of Cardiac Sarcoplasmic-Reticulum. Molecular Biology of the Cardiovascular System. R. Roberts and M. D. Schneider. **131**: 207-214.

Meissner, G., Rousseau, E., et al. (1988). Biochemical-Characterization of the  $\text{Ca}^{2+}$  Release Channel of Skeletal and Cardiac Sarcoplasmic-Reticulum. Molecular and Cellular Biochemistry **82**(1-2): 59-65.

Meyers, M. B., Pickel, V. M., et al. (1995). Association of Sorcin with the Cardiac Ryanodine Receptor. Journal of Biological Chemistry **270**(44): 26411-26418.

Meyers, M. B., Puri, T. S., et al. (1998). Sorcin Associates with the Pore-Forming Subunit of Voltage-Dependent L-Type  $\text{Ca}^{2+}$  Channels. Journal of Biological Chemistry **273**(30): 18930-18935.



- Mickelson, J. R., Litterer, L. A., et al. (1990). Stimulation and Inhibition of [<sup>3</sup>H]Ryanodine Binding to Sarcoplasmic Reticulum from Malignant Hyperthermia Susceptible Pigs. Archives of Biochemistry and Biophysics **278**(1): 251-257.
- Mitchell, R. D., Simmerman, H. K., et al. (1988). Ca<sup>2+</sup> Binding Effects on Protein Conformation and Protein Interactions of Canine Cardiac Calsequestrin. Journal of Biological Chemistry **263**(3): 1376-1381.
- Mochizuki, M., Yano, M., et al. (2007). Scavenging Free Radicals by Low-Dose Carvedilol Prevents Redox-Dependent Ca<sup>2+</sup> Leak Via Stabilization of Ryanodine Receptor in Heart Failure. Journal of the American College of Cardiology **49**(16): 1722-1732.
- Murayama, T., Kurebayashi, N., et al. (1998). Stimulation by Polyols of the Two Ryanodine Receptor Isoforms of Frog Skeletal Muscle. Journal of Muscle Research and Cell Motility **19**(1): 15-24.
- Murayama, T., Kurebayashi, N., et al. (2000). Role of Mg<sup>2+</sup> in Ca<sup>2+</sup>-Induced Ca<sup>2+</sup> Release through Ryanodine Receptors of Frog Skeletal Muscle: Modulations by Adenine Nucleotides and Caffeine. Biophysical Journal **78**(4): 1810-1824.
- Murayama, T., Oba, T., et al. (2005). Postulated Role of Interdomain Interactions within the Type 1 Ryanodine Receptor in the Low Gain of Ca<sup>2+</sup>-Induced Ca<sup>2+</sup> Release Activity of Mammalian Skeletal Muscle Sarcoplasmic Reticulum. Am J Physiol Cell Physiol **288**(6): C1222-1230.
- Murayama, T. and Ogawa, Y. (1996). Similar Ca<sup>2+</sup> Dependences of [<sup>3</sup>H]Ryanodine Binding to α- and β-Ryanodine Receptors Purified from Bullfrog Skeletal Muscle in an Isotonic Medium. Febs Letters **380**(3): 267-271.
- Murphy, E., Steenbergen, C., et al. (1989). Cytosolic Free Magnesium Levels in Ischemic Rat Heart. Journal of Biological Chemistry **264**(10): 5622-5627.

Nagasaki, K. and Kasai, M. (1983). Fast Release of Calcium from Sarcoplasmic Reticulum Vesicles Monitored by Chlortetracycline Fluorescence. Journal of Biochemistry **94**(4): 1101-1109.

Obayashi, M., Xiao, B., et al. (2006). Spontaneous Diastolic Contractions and Phosphorylation of the Cardiac Ryanodine Receptor at Serine-2808 in Congestive Heart Failure in Rat. Cardiovascular Research **69**(1): 140-151.

Oda, T., Yano, M., et al. (2005). Defective Regulation of Interdomain Interactions within the Ryanodine Receptor Plays a Key Role in the Pathogenesis of Heart Failure. Circulation **111**(25): 3400-3410.

Orlova, E. V., Serysheva, I. I., et al. (1996). Two Structural Configurations of the Skeletal Muscle Calcium Release Channel. Nat Struct Mol Biol **3**(6): 547-552.

Otsu, K., Willard, H. F., et al. (1990). Molecular Cloning of cDNA Encoding the Ca<sup>2+</sup> Release Channel (Ryanodine Receptor) of Rabbit Cardiac Muscle Sarcoplasmic Reticulum. Journal of Biological Chemistry **265**(23): 13472-13483.

Padua, R. A., Nagy, J. I., et al. (1994). Ionic Strength Dependence of Calcium, Adenine Nucleotide, Magnesium, and Caffeine Actions on Ryanodine Receptors in Rat Brain. Journal of Neurochemistry **62**(6): 2340-2348.

Pereira, L., Métrich, M., et al. (2007). The Camp Binding Protein Epac Modulates Ca<sup>2+</sup> Sparks by a Ca<sup>2+</sup>/Calmodulin Kinase Signalling Pathway in Rat Cardiac Myocytes. The Journal of Physiology **583**(2): 685-694.

Phrommintikul, A. and Chattipakorn, N. (2006). Roles of Cardiac Ryanodine Receptor in Heart Failure and Sudden Cardiac Death. International Journal of Cardiology **112**(2): 142-152.

Pogwizd, S. M. and Bers, D. M. (2004). Cellular Basis of Triggered Arrhythmias in Heart Failure. Trends in Cardiovascular Medicine **14**(2): 61-66.

- Pogwizd, S. M., Mckenzie, J. P., et al. (1998). Mechanisms Underlying Spontaneous and Induced Ventricular Arrhythmias in Patients with Idiopathic Dilated Cardiomyopathy. Circulation **98**(22): 2404-2414.
- Priori, S. G., Napolitano, C., et al. (2002). Clinical and Molecular Characterization of Patients with Catecholaminergic Polymorphic Ventricular Tachycardia. Circulation **106**(1): 69-74.
- Priori, S. G., Napolitano, C., et al. (2001). Mutations in the Cardiac Ryanodine Receptor Gene (HrYr2) Underlie Catecholaminergic Polymorphic Ventricular Tachycardia. Circulation **103**(2): 196-200.
- Puceat, M. (2010). Calmodulin: A Gatekeeper for Ryanodine Receptor Function in the Myocardium. Cardiovascular Research **87**(4): 587-588.
- Radermacher, M., Rao, V., et al. (1994). Cryo-Electron Microscopy and Three-Dimensional Reconstruction of the Calcium Release Channel/Ryanodine Receptor from Skeletal Muscle. The Journal of Cell Biology **127**(2): 411-423.
- Rafael, R., Jonathan, M. K., et al. (2007). Calcium Channel Blockers and  $\beta$ -Blockers Versus  $\beta$ -Blockers Alone for Preventing Exercise-Induced Arrhythmias in Catecholaminergic Polymorphic Ventricular Tachycardia. Heart rhythm : the official journal of the Heart Rhythm Society **4**(9): 1149-1154.
- Rodney, G. G., Williams, B. Y., et al. (2000). Regulation of RyR1 Activity by  $Ca^{2+}$  and Calmodulin Biochemistry **39**(26): 7807-7812.
- Rodriguez, P., Bhogal, M. S., et al. (2003). Stoichiometric Phosphorylation of Cardiac Ryanodine Receptor on Serine 2809 by Calmodulin-Dependent Kinase II and Protein Kinase A. Journal of Biological Chemistry **278**(40): 38593-38600.
- Rosenberg, O. S., Deindl, S., et al. (2005). Structure of the Autoinhibited Kinase Domain of CaMKII and Saxs Analysis of the Holoenzyme. Cell **123**(5): 849-860.

- Saito, A., Seiler, S., et al. (1984). Preparation and Morphology of Sarcoplasmic Reticulum Terminal Cisternae from Rabbit Skeletal Muscle. The Journal of Cell Biology **99**(3): 875-885.
- Samsó, M. and Wagenknecht, T. (1998). Contributions of Electron Microscopy and Single-Particle Techniques to the Determination of the Ryanodine Receptor Three-Dimensional Structure. Journal of Structural Biology **121**(2): 172-180.
- Scoote, M. and Williams, A. J. (2002). The Cardiac Ryanodine Receptor (Calcium Release Channel). Cardiovascular Research **56**(3): 359-372.
- Serysheva, I. I., Hamilton, S. L., et al. (2005). Structure of Ca<sup>2+</sup> Release Channel at 14 Å Resolution. Journal of Molecular Biology **345**(3): 427-431.
- Serysheva, I. I., Schatz, M., et al. (1999). Structure of the Skeletal Muscle Calcium Release Channel Activated with Ca<sup>2+</sup> and AMP-PCP. Biophysical Journal **77**(4): 1936-1944.
- Shannon, T. R., Ginsburg, K. S., et al. (2000). Reverse Mode of the Sarcoplasmic Reticulum Calcium Pump and Load-Dependent Cytosolic Calcium Decline in Voltage-Clamped Cardiac Ventricular Myocytes. Biophysical Journal **78**(1): 322-333.
- Sharma, M. R., Jeyakumar, L. H., et al. (2006). Three-Dimensional Visualization of FKBP12.6 Binding to an Open Conformation of Cardiac Ryanodine Receptor. Biophysical Journal **90**(1): 164-172.
- Shtifman, A., Ward, C. W., et al. (2002). Interdomain Interactions within Ryanodine Receptors Regulate Ca<sup>2+</sup> Spark Frequency in Skeletal Muscle. Journal of General Physiology **119**(1): 15-31.
- Sitsapesan, R., Montgomery, R. A. P., et al. (1995). New Insights into the Gating Mechanisms of Cardiac Ryanodine Receptors Revealed by Rapid Changes in Ligand Concentration. Circulation Research **77**(4): 765-772.

- Song, L.-S., Wang, S.-Q., et al. (2001).  $\beta$ -Adrenergic Stimulation Synchronizes Intracellular  $\text{Ca}^{2+}$  Release During Excitation-Contraction Coupling in Cardiac Myocytes. Circulation Research **88**(8): 794-801.
- Song, Y. and Belardinelli, L. (1994). ATP Promotes Development of Afterdepolarizations and Triggered Activity in Cardiac Myocytes. Am J Physiol Heart Circ Physiol **267**(5): H2005-2011.
- Sorrentino, V. and Volpe, P. (1993). Ryanodine Receptors: How Many, Where and Why? Trends in Pharmacological Sciences **14**(3): 98-103.
- Stern, M. D., Song, L.-S., et al. (1999). Local Control Models of Cardiac Excitation-Contraction Coupling. The Journal of General Physiology **113**(3): 469-489.
- Sumitomo, N., Harada, K., et al. (2003). Catecholaminergic Polymorphic Ventricular Tachycardia: Electrocardiographic Characteristics and Optimal Therapeutic Strategies to Prevent Sudden Death. Heart **89**(1): 66-70.
- Sun, Q. (2009). Culture of Escherichia Coli in SOC Medium Improves the Cloning Efficiency of Toxic Protein Genes. Anal Biochem **394**(1): 144-6.
- Takeshima, H., Nishimura, S., et al. (1989). Primary Structure and Expression from Complementary DNA of Skeletal Muscle Ryanodine Receptor. Nature **339**(6224): 439-445.
- Tateishi, H., Yano, M., et al. (2009). Defective Domain-Domain Interactions within the Ryanodine Receptor as a Critical Cause of Diastolic  $\text{Ca}^{2+}$  Leak in Failing Hearts. Cardiovascular Research **81**(3): 536-545.
- Terentyev, D., Cala, S. E., et al. (2005). Triadin Overexpression Stimulates Excitation-Contraction Coupling and Increases Predisposition to Cellular Arrhythmia in Cardiac Myocytes. Circ Res **96**(6): 651-658.
- Thomas, L. N., George, C. H., et al. (2004). Functional Heterogeneity of Ryanodine Receptor Mutations Associated with Sudden Cardiac Death. Cardiovascular Research **64**(1): 52-60.

- Thomas, N. L., Lai, F. A., et al. (2005). Differential Ca<sup>2+</sup> Sensitivity of RyR2 Mutations Reveals Distinct Mechanisms of Channel Dysfunction in Sudden Cardiac Death. Biochemical and Biophysical Research Communications **331**(1): 231-238.
- Thomas, N. L., Maxwell, C., et al. (2010). Ryanodine Receptor Mutations in Arrhythmia: The Continuing Mystery of Channel Dysfunction. Febs Letters **584**(10): 2153-2160.
- Trafford, A. W., Diaz, M. E., et al. (2001). Coordinated Control of Cell Ca<sup>2+</sup> Loading and Triggered Release from the Sarcoplasmic Reticulum Underlies the Rapid Inotropic Response to Increased L-Type Ca<sup>2+</sup> Current. Circulation Research **88**(2): 195-201.
- Treves, S., Anderson, A. A., et al. (2005). Ryanodine Receptor 1 Mutations, Dysregulation of Calcium Homeostasis and Neuromuscular. Neuromuscular Disorders **15**(9-10): 577-587.
- Tripathy, A., Xu, L., et al. (1995). Calmodulin Activation and Inhibition of Skeletal Muscle Ca<sup>2+</sup> Release Channel (Ryanodine Receptor). Biophysical Journal **69**(1): 106-119.
- Tunwell, R. E. A., Wickenden, C., et al. (1996). The Human Cardiac Muscle Ryanodine Receptor-Calcium Release Channel: Identification, Primary Structure and Topological Analysis. Biochemical Journal **318**: 477-487.
- Uehara, A., Yasukochi, M., et al. (2002). Gating Kinetics and Ligand Sensitivity Modified by Phosphorylation of Cardiac Ryanodine Receptors. Pflügers Archiv European Journal of Physiology **444**(1): 202-212.
- Uwais, M., Michael, H. G., et al. (2006). Sudden Cardiac Death Despite an Implantable Cardioverter-Defibrillator in a Young Female with Catecholaminergic Ventricular Tachycardia. Heart rhythm : the official journal of the Heart Rhythm Society **3**(12): 1486-1489.
- Valdivia, H. H., Kaplan, J. H., et al. (1995). Rapid Adaptation of Cardiac Ryanodine Receptors - Modulation by Mg<sup>2+</sup> and Phosphorylation. Science **267**(5206): 1997-2000.

Valdivia, H. H., Valdivia, C., et al. (1990). Direct Binding of Verapamil to the Ryanodine Receptor Channel of Sarcoplasmic Reticulum. Biophysical Journal **58**(2): 471-481.

Venetucci, L. A., Trafford, A. W., et al. (2006). Reducing Ryanodine Receptor Open Probability as a Means to Abolish Spontaneous Ca<sup>2+</sup> Release and Increase Ca<sup>2+</sup> Transient Amplitude in Adult Ventricular Myocytes. Circulation Research **98**(10): 1299-1305.

Venetucci, L. A., Trafford, A. W., et al. (2007). Increasing Ryanodine Receptor Open Probability Alone Does Not Produce Arrhythmogenic Calcium Waves: Threshold Sarcoplasmic Reticulum Calcium Content Is Required. Circulation Research **100**(1): 105-111.

Viatchenko-Karpinski, S., Terentyev, D., et al. (2004). Abnormal Calcium Signaling and Sudden Cardiac Death Associated with Mutation of Calsequestrin. Circulation Research **94**(4): 471-477.

Wagenknecht, T., Radermacher, M., et al. (1997). Locations of Calmodulin and FK506-Binding Protein on the Three-Dimensional Architecture of the Skeletal Muscle Ryanodine Receptor. Journal of Biological Chemistry **272**(51): 32463-32471.

Walker, C. A. and Spinale, F. G. (1999). The Structure and Function of the Cardiac Myocyte: A Review of Fundamental Concepts. J Thorac Cardiovasc Surg **118**(2): 375-382.

Watanabe, H., Chopra, N., et al. (2009). Flecainide Prevents Catecholaminergic Polymorphic Ventricular Tachycardia in Mice and Humans. Nat Med **15**(4): 380-383.

Wehrens, X. H., Lehnart, S. E., et al. (2003). FKBP12.6 Deficiency and Defective Calcium Release Channel (Ryanodine Receptor) Function Linked to Exercise-Induced Sudden Cardiac Death. Circulation **108**(17): 704.

Wehrens, X. H. T., Lehnart, S. E., et al. (2003). FKBP12.6 Deficiency and Defective Calcium Release Channel (Ryanodine Receptor) Function Linked to Exercise-Induced Sudden Cardiac Death. Cell **113**(7): 829-840.

---

Wehrens, X. H. T., Lehnart, S. E., et al. (2005). Enhancing Calstabin Binding to Ryanodine Receptors Improves Cardiac and Skeletal Muscle Function in Heart Failure. Proceedings of the National Academy of Sciences of the United States of America **102**(27): 9607-9612.

Wehrens, X. H. T., Lehnart, S. E., et al. (2005). Enhancing Calstabin Binding to Ryanodine Receptors Improves Cardiac and Skeletal Muscle Function in Heart Failure. Proceedings of the National Academy of Sciences of the United States of America **102**(27): 9607-9612.

Wehrens, X. H. T., Lehnart, S. E., et al. (2006). Ryanodine Receptor/Calcium Release Channel PKA Phosphorylation: A Critical Mediator of Heart Failure Progression. Proceedings of the National Academy of Sciences of the United States of America **103**(3): 511-518.

Wehrens, X. H. T., Lehnart, S. E., et al. (2004). Protection from Cardiac Arrhythmia through Ryanodine Receptor-Stabilizing Protein Calstabin2. Science **304**(5668): 292-296.

Wehrens, X. H. T., Lehnart, S. E., et al. (2004). Ca<sup>2+</sup>/Calmodulin-Dependent Protein Kinase II Phosphorylation Regulates the Cardiac Ryanodine Receptor. Circulation Research **94**(6): e61-70.

Wehrens, X. H. T., Lehnart, S. E., et al. (2004). Ca<sup>2+</sup>/Calmodulin-Dependent Protein Kinase II Phosphorylation Regulates the Cardiac Ryanodine Receptor. Circulation Research **94**(6): E61-E70.

Welch, W., Rheault, S., et al. (2004). A Model of the Putative Pore Region of the Cardiac Ryanodine Receptor Channel. Biophysical Journal **87**(4): 2335-2351.

Witcher, D. R., Kovacs, R. J., et al. (1991). Unique Phosphorylation Site on the Cardiac Ryanodine Receptor Regulates Calcium Channel Activity. Journal of Biological Chemistry **266**(17): 11144-11152.

Wu, Y., Aghdasi, B., et al. (1997). Functional Interactions between Cytoplasmic Domains of the Skeletal Muscle Ca<sup>2+</sup> Release Channel. Journal of Biological Chemistry **272**(40): 25051-25061.



- Xiao, B., Sutherland, C., et al. (2004). Protein Kinase a Phosphorylation at Serine-2808 of the Cardiac Ca<sup>2+</sup>-Release Channel (Ryanodine Receptor) Does Not Dissociate 12.6-kDa FK506-Binding Protein (FKBP12.6). Circulation Research **94**(4): 487-495.
- Xiao, B., Tian, X., et al. (2007). Functional Consequence of Protein Kinase a-Dependent Phosphorylation of the Cardiac Ryanodine Receptor. Journal of Biological Chemistry **282**(41): 30256-30264.
- Xiao, B. L., Jiang, M. T., et al. (2005). Characterization of a Novel Protein Kinase a Phosphorylation Site, Serine-2030, Reveals No Hyperphosphorylation of the Cardiac Ryanodine Receptor in Heart Failure. Biophysical Journal **88**(1): 188A-188A.
- Xiao, J. M., Tian, X. X., et al. (2007). Removal of FKBP12.6 Does Not Alter the Conductance and Activation of the Cardiac Ryanodine Receptor or the Susceptibility to Stress-Induced Ventricular Arrhythmias. Journal of Biological Chemistry **282**(48): 34828-34838.
- Xu, L., Mann, G., et al. (1996). Regulation of Cardiac Ca<sup>2+</sup> Release Channel (Ryanodine Receptor) by Ca<sup>2+</sup>, H<sup>+</sup>, Mg<sup>2+</sup>, and Adenine Nucleotides under Normal and Simulated Ischemic Conditions. Circulation Research **79**(6): 1100-1109.
- Yamamoto, T., El-Hayek, R., et al. (2000). Postulated Role of Interdomain Interaction within the Ryanodine Receptor in Ca<sup>2+</sup> Channel Regulation. Journal of Biological Chemistry **275**(16): 11618-11625.
- Yamamoto, T. and Ikemoto, N. (2002). Peptide Probe Study of the Critical Regulatory Domain of the Cardiac Ryanodine Receptor. Biochemical and Biophysical Research Communications **291**(4): 1102-1108.
- Yamamoto, T. and Ikemoto, N. (2002). Spectroscopic Monitoring of Local Conformational Changes During the Intramolecular Domain-Domain Interaction of the Ryanodine Receptor. Biochemistry **41**(5): 1492-1501.

- Yamamoto, T., Yano, M., et al. (2008). Identification of Target Domains of the Cardiac Ryanodine Receptor to Correct Channel Disorder in Failing Hearts. Circulation **117**(6): 762-772.
- Yang, Z., Ikemoto, N., et al. (2006). The RyR2 Central Domain Peptide Dpc10 Lowers the Threshold for Spontaneous Ca<sup>2+</sup> Release in Permeabilized Cardiomyocytes. Cardiovascular Research **70**(3): 475-485.
- Yano, M. (2008). Ryanodine Receptor as a New Therapeutic Target of Heart Failure and Lethal Arrhythmia. Circulation **72**: 509-514.
- Yano, M., Kobayashi, S., et al. (2002). FKBP12.6-Mediated Stabilization of Calcium Release Channel (Ryanodine Receptor) as a Novel Therapeutic Strategy against Heart Failure. Circulation **106**(19): 1129.
- Yano, M., Ono, K., et al. (2000). Altered Stoichiometry of FKBP12.6 Versus Ryanodine Receptor as a Cause of Abnormal Ca<sup>2+</sup> Leak through Ryanodine Receptor in Heart Failure. Circulation **102**(17): 2131-2136.
- Yano, M., Yamamoto, T., et al. (2005). Abnormal Ryanodine Receptor Function in Heart Failure. Pharmacology & Therapeutics **107**(3): 377-391.
- Zhang, G.-X., Kimura, S., et al. (2005). Cardiac Oxidative Stress in Acute and Chronic Isoproterenol-Infused Rats. Cardiovascular Research **65**(1): 230-238.
- Zhang, L., Kelley, J., et al. (1997). Complex Formation between Junctin, Triadin, Calsequestrin, and the Ryanodine Receptor. Journal of Biological Chemistry **272**(37): 23389-23397.
- Zhang, R., Khoo, M. S. C., et al. (2005). Calmodulin Kinase II Inhibition Protects against Structural Heart Disease. Nat Med **11**(43): 409-417.
- Zhang, Y. L., Chen, H. S., et al. (1993). A Mutation in the Human Ryanodine Receptor Gene Associated with Central Core Disease. Nature Genetics **5**(1): 46-50.

Zissimofilos, S., Thomas, N. L., et al. (2009). FKBP12.6 Binding of Ryanodine Receptors Carrying Mutations Associated with Arrhythmogenic Cardiac Disease. Biochemical Journal **419**: 273-278.

Zorzato, F., Menegazzi, P., et al. (1996). Role of Malignant Hyperthermia Domain in the Regulation of Ca<sup>2+</sup> Release Channel (Ryanodine Receptor) of Skeletal Muscle Sarcoplasmic Reticulum. Journal of Biological Chemistry **271**(37): 22759-22763.

**PUBLICATIONS**

**Articles**

Blayney, L. M., Jones, J., **Griffiths, J.**, and Lai, F. A. (2010). A Mechanism of Ryanodine Receptor Modulation by FKBP12/12.6, Protein Kinase A and K201. Cardiovascular Res **85**: 68-78.

**Abstracts**

**Griffiths, J.**, Jones, J., Lai, F. A., and Blayney, L. (2009). Ryanodine Receptor Phosphorylation by Protein Kinase A Alters the Affinity for FKBP12. Biophys J, **96**(3) Supl 1: pp108a

Blayney, L., Nomikos, M., Beck, K., D'Cruz, L., McDonald, E., **Griffiths, J.**, and Lai, F. A. (2010). Distinct Properties of CPVT Mutations Located in the Central Domain of Human RyR2. Biophys J, **98**(3) Supl 1 : pp511a

**Appendix**

**APPENDIX****Expasy Proteomics Results**

<http://www.expasy.ch/tools/protparam.html> - Protein parameter computation tool.

**RyR1. Rabbit skeletal muscle**

**Accession number:** P11716

**Number of amino acids:** 5037

**Molecular weight:** 565252.7

**Theoretical pI:** 5.16

**Amino acid  
composition:**

Ala (A)	394	7.80%
Arg (R)	298	5.90%
Asn (N)	170	3.40%
Asp (D)	254	5.00%
Cys (C)	100	2.00%
Gln (Q)	200	4.00%
Glu (E)	483	9.60%
Gly (G)	367	7.30%
His (H)	132	2.60%
Ile (I)	197	3.90%
Leu (L)	561	11.10%
Lys (K)	227	4.50%
Met (M)	146	2.90%
Phe (F)	207	4.10%
Pro (P)	270	5.40%
Ser (S)	282	5.60%
Thr (T)	223	4.40%
Trp (W)	65	1.30%
Tyr (Y)	142	2.80%
Val (V)	319	6.30%
Pyl (O)	0	0.00%
Sec (U)	0	0.00%

**RyR2. Human cardiac muscle****Accession number:** Q92736**Number of amino acids:** 4965**Molecular weight:** 564741.9**Theoretical pI:** 5.87**Amino acid  
composition:**

---

Ala (A)	304	6.1%
Arg (R)	261	5.3%
Asn (N)	191	3.8%
Asp (D)	279	5.6%
Cys (C)	92	1.9%
Gln (Q)	198	4.0%
Glu (E)	400	8.1%
Gly (G)	302	6.1%
His (H)	144	2.9%
Ile (I)	234	4.7%
Leu (L)	550	11.1%
Lys (K)	318	6.4%
Met (M)	160	3.2%
Phe (F)	225	4.5%
Pro (P)	197	4.0%
Ser (S)	360	7.3%
Thr (T)	221	4.5%
Trp (W)	63	1.3%
Tyr (Y)	166	3.3%
Val (V)	300	6.0%
Pyl (O)	0	0.0%
Sec (U)	0	0.0%

---

**FKBP12. Rabbit****Accession number:** P26943**Sequence:**

GPLGSMGVQV ETISPGDGRT FPKRGQTCVV HYTGMLLEDGK KFDSSRDRNK PFKFMLGKQE

VIRGWEEGVA QMSVGQRAKL TISPDYAYGA TGHPGIIPPH ATLVFDVELL KLE

**Number of amino acids:** 113**Molecular weight:** 12362.1**Theoretical pI:** 8.08

<b>Amino acid composition:</b>		
Ala (A)	5	4.4%
Arg (R)	6	5.3%
Asn (N)	1	0.9%
Asp (D)	6	5.3%
Cys (C)	1	0.9%
Gln (Q)	5	4.4%
Glu (E)	7	6.2%
Gly (G)	15	13.3%
His (H)	3	2.7%
Ile (I)	5	4.4%
Leu (L)	8	7.1%
Lys (K)	8	7.1%
Met (M)	4	3.5%
Phe (F)	5	4.4%
Pro (P)	8	7.1%
Ser (S)	6	5.3%
Thr (T)	7	6.2%
Trp (W)	1	0.9%
Tyr (Y)	3	2.7%
Val (V)	9	8.0%
Pyl (O)	0	0.0%
Sec (U)	0	0.00%

**FKBP12.6. Human**



**Accession number:** P68106

**Sequence:**

GPLGSMGVEI ETISPGDGRT FPKKGQTCVV HYTGMLQNGK KFDSSDRNK PFKFRIGKQE  
VIKGFEEGAA QMSLGQRAKL TCTPDVAYGA TGHPGVIPPV ATLIQDVELL NLE

**Number of amino acids:** 113

**Molecular weight:** 12193.9

**Theoretical pI:** 8.64

**Amino acid  
composition:**

Ala (A)	6	5.3%
Arg (R)	5	4.4%
Asn (N)	4	3.5%
Asp (D)	5	4.4%
Cys (C)	2	1.8%
Gln (Q)	5	4.4%
Glu (E)	7	6.2%
Gly (G)	15	13.3%
His (H)	2	1.8%
Ile (I)	6	5.3%
Leu (L)	8	7.1%
Lys (K)	9	8.0%
Met (M)	3	2.7%
Phe (F)	6	5.3%
Pro (P)	8	7.1%
Ser (S)	5	4.4%
Thr (T)	8	7.1%
Trp (W)	0	0.0%
Tyr (Y)	2	1.8%
Val (V)	7	6.2%
Pyl (O)	0	0.0%
Sec (U)	0	0.0%

**Domain peptide 4 (DP4WT). Rabbit skeletal muscle**

**Sequence:**

GPLGSLIQAG KGEALRIRAI LRSLVPLDDL VGIISLPLQI P

**Number of amino acids: 41****Molecular weight: 4274.1****Theoretical pI: 8.74****Amino acid  
composition:**

Ala (A)	3	7.3%
Arg (R)	3	7.3%
Asn (N)	0	0.0%
Asp (D)	2	4.9%
Cys (C)	0	0.0%
Gln (Q)	2	4.9%
Glu (E)	1	2.4%
Gly (G)	5	12.2%
His (H)	0	0.0%
Ile (I)	6	14.6%
Leu (L)	9	22.0%
Lys (K)	1	2.4%
Met (M)	0	0.0%
Phe (F)	0	0.0%
Pro (P)	4	9.8%
Ser (S)	3	7.3%
Thr (T)	0	0.0%
Trp (W)	0	0.0%
Tyr (Y)	0	0.0%
Val (V)	2	4.9%
Pyl (O)	0	0.0%
Sec (U)	0	0.0%

**Domain peptide 4 mutant (DP4M). Rabbit skeletal muscle**

**Sequence:**

GPLGSLIQAG KGEALRIRAI LCSLVPLDDL VGIISLPLQI P

**Number of amino acids:** 41**Molecular weight:** 4221.1**Theoretical pI:** 6.11**Amino acid  
composition:**

Ala (A)	3	7.3%
Arg (R)	2	4.9%
Asn (N)	0	0.0%
Asp (D)	2	4.9%
Cys (C)	1	2.4%
Gln (Q)	2	4.9%
Glu (E)	1	2.4%
Gly (G)	5	12.2%
His (H)	0	0.0%
Ile (I)	6	14.6%
Leu (L)	9	22.0%
Lys (K)	1	2.4%
Met (M)	0	0.0%
Phe (F)	0	0.0%
Pro (P)	4	9.8%
Ser (S)	3	7.3%
Thr (T)	0	0.0%
Trp (W)	0	0.0%
Tyr (Y)	0	0.0%
Val (V)	2	4.9%
Pyl (O)	0	0.0%
Sec (U)	0	0.0%

**GST-tagged domain peptide 4 (GST-PD4WT). Rabbit skeletal muscle**

**Sequence:**

MSPILGYWKI KGLVQPTRL L LEYLEEKYEE HLYERDEGDK WRNKKFELGL EFPNLPYYID  
 GDVKLTQSMA IIRYIADKHN MLGGCPKERA EISMLEGAVL DIRYGVSRIA YSKDFETLKV  
 DFLSKLPEML KMFEDRLCHK TYLNGDHVTH PDFMLYDALD VVLYMDPMCL DAFPKLVCFK  
 KRIEAIQID KYLKSSKYIA WPLQGWQATF GGGDHPPKSD LEVLFQGPLG SLIQAGKGEA  
LRIRAILRSL VPLDDLVGII SLPLQIP

\* Underlined is DP4 sequence

**Number of amino acids:** 267

**Molecular weight:** 30686.8

**Theoretical pI:** 5.92

**Amino acid  
composition:**

Ala (A)	13	4.9%
Arg (R)	12	4.5%
Asn (N)	4	1.5%
Asp (D)	20	7.5%
Cys (C)	4	1.5%
Gln (Q)	8	3.0%
Glu (E)	18	6.7%
Gly (G)	19	7.1%
His (H)	6	2.2%
Ile (I)	19	7.1%
Leu (L)	38	14.2%
Lys (K)	22	8.2%
Met (M)	9	3.4%
Phe (F)	10	3.7%
Pro (P)	17	6.4%
Ser (S)	12	4.5%
Thr (T)	6	2.2%
Trp (W)	4	1.5%
Tyr (Y)	14	5.2%
Val (V)	12	4.5%
Pyl (O)	0	0.0%
Sec (U)	0	0.0%

**GST-tagged domain peptide 4 mutant (GST-DP4M). Rabbit skeletal**

**Sequence:**

MSPILGYWKI KGLVQPTRLL LEYLEEKYEE HLYERDEGDK WRNKKFELGL EFPNLPYYID  
 GDVKLTQSMA IIRYIADKHN MLGGCPKERA EISMLEGAVL DIRYGVSRIA YSKDFETLKV  
 DFLSKLPEML KMFEDRLCHK TYLNGDHVTH PDFMLYDALD VVLYMDPMCL DAFPKLVCFK  
 KRIEAIPOID KYLKSSKYIA WPLQGWQATF GGGDHPPKSD LEVLFQ**GPLG** SLIQAGKGEA  
LRIRAILCSL VPLDDLVGII SLPLQIP

\* Underlined is DP4M sequence

**Number of amino acids:** 267

**Molecular weight:** 30633.8

**Theoretical pI:** 5.75

**Amino acid  
composition:**

Ala (A)	13	4.9%
Arg (R)	11	4.1%
Asn (N)	4	1.5%
Asp (D)	20	7.5%
Cys (C)	5	1.9%
Gln (Q)	8	3.0%
Glu (E)	18	6.7%
Gly (G)	19	7.1%
His (H)	6	2.2%
Ile (I)	19	7.1%
Leu (L)	38	14.2%
Lys (K)	22	8.2%
Met (M)	9	3.4%
Phe (F)	10	3.7%
Pro (P)	17	6.4%
Ser (S)	12	4.5%
Thr (T)	6	2.2%
Trp (W)	4	1.5%
Tyr (Y)	14	5.2%
Val (V)	12	4.5%
Pyl (O)	0	0.0%
Sec (U)	0	0.0%

**Central domain peptide 10 sequence (DPc10). Human cardiac**

**Sequence:**

GPLGSGFCPD HKAAMVLF LD RYVGIEVQDF LLHLLEVGFL P

**Number of amino acids:** 41**Molecular weight:** 4515.3**Theoretical pI:** 4.80**Amino acid  
composition:**

Ala (A)	2	4.9%
Arg (R)	1	2.4%
Asn (N)	0	0.0%
Asp (D)	3	7.3%
Cys (C)	1	2.4%
Gln (Q)	1	2.4%
Glu (E)	2	4.9%
Gly (G)	5	12.2%
His (H)	2	4.9%
Ile (I)	1	2.4%
Leu (L)	8	19.5%
Lys (K)	1	2.4%
Met (M)	1	2.4%
Phe (F)	4	9.8%
Pro (P)	3	7.3%
Ser (S)	1	2.4%
Thr (T)	0	0.0%
Trp (W)	0	0.0%
Tyr (Y)	1	2.4%
Val (V)	4	9.8%
Pyl (O)	0	0.0%
Sec (U)	0	0.0%

**Sequence:****GPLGSGFCPD HKAAMVLF LD SVYGIEVQDF LLHLLLEVGFL P****Number of amino acids: 41****Molecular weight: 4446.2****Theoretical pI: 4.42****Amino acid  
composition:**

Ala (A)	2	4.9%
Arg (R)	0	0.0%
Asn (N)	0	0.0%
Asp (D)	3	7.3%
Cys (C)	1	2.4%
Gln (Q)	1	2.4%
Glu (E)	2	4.9%
Gly (G)	5	12.2%
His (H)	2	4.9%
Ile (I)	1	2.4%
Leu (L)	8	19.5%
Lys (K)	1	2.4%
Met (M)	1	2.4%
Phe (F)	4	9.8%
Pro (P)	3	7.3%
Ser (S)	2	4.9%
Thr (T)	0	0.0%
Trp (W)	0	0.0%
Tyr (Y)	1	2.4%
Val (V)	4	9.8%
Pyl (O)	0	0.0%
Sec (U)	0	0.0%

\*In relevant sequences, the GPLGS region (residual from MCS of pGEX-6p-1) is highlighted in bold.

---

## **Acknowledgements**

I would like to take the opportunity to thank a number of people, without whom, the work in this thesis would not have been possible.

Firstly I would like to thank Tony Lai, for offering me the opportunity to work in his group, and Lynda Blayney, for all her help and guidance throughout the course of this study. It has been a great experience to be a part of the Lai team, and to work with many fantastic people. I would like to thank Leon D'Cruz for his infectious enthusiasm in the early days of my PhD, and Sarju Patel for his precious words of wisdom and encouragement, as well as everybody else that has offered advice throughout.

In addition, I would like to thank my parents for their amazing and continuous support and for always helping to keep things in perspective when the going got tough. Lastly, I would like to thank Alex Harrison, for putting up with me throughout this emotional rollercoaster, for providing me with a hearty meal every evening and for being a huge help in every possible way.